

DEVELOPMENT AND CHARACTERISATION OF MECHANICAL AND ENZYMATIC MODELS OF CARTILAGE DEGENERATION

Carly Taylor

Submitted in accordance with the requirements for the degree of
Doctor of Philosophy

The University of Leeds
Faculty of Biological Sciences

December 2013

The candidate confirms that the work submitted is her own and that appropriate credit has been given where reference has been made to the work of others.

This copy has been supplied on the understanding that it is copyright material and that no quotation from the thesis may be published without proper acknowledgement.

© 2013 The University of Leeds and Carly Taylor

The Right of Carly Taylor to be identified as Author of this work has been asserted by her in accordance with the Copyright Designs and Patents Act 1988.

Acknowledgements

I would like to thank my supervisors, Joanne Tipper, Eileen Ingham and John Fisher for giving me this opportunity. This PhD has changed my life and has allowed me to develop into someone that I never knew I could be. Additionally I would like to thank you for your support and professional guidance which has been invaluable and without which, this thesis would not have been possible. I would also like to thank the EPSRC for funding my project. Finally I would especially like to thank Joanne and Eileen for being inspirational role models for women in science.

Thanks also to my helpful colleagues (and friends!) who have guided me through my PhD including Dan Thomas for all the help and for never moaning at me even though everyone was always nagging you. I would like to also thank Serena “Eli” Russell, I am not sure I would have even made it past the first year if it weren’t for your helpful, patient and generous guidance. Thanks also to anyone else who assisted me throughout the study with anything from pep-talks to help finding an elusive piece of equipment.

Big thanks to the iMBE technical staff that I pestered relentlessly throughout various stages of my PhD, including Phil, Irvin, Keith, Lee, Jane and Adrian. Also, I want to give special thanks for the times in which you helped me at short notice. Also, thanks to all my friends in the IMBE. I am so lucky to have found myself in such a large friendly institute where there was never a struggle to find a group partaking in some kind of fun Friday drinks.

More specifically thanks to my close friends Carols, Fiona, Hazel and Nic, there were so many times you guys kept me going. I will never forget the times in the “skinny office” and I am so grateful I had you guys there to help me through tough stints and to live it up when times were good... so many funny times including karaoke memories- which really gave me something to look forwards to after hours spent in the basement of engineering in the measurements lab... looking for things... “with my eyes”. I have found friends for life in all of you.

I would like to express my deepest gratitude to my partner Scott, who has been by my side throughout this journey. I am not sure if I can express fully in words what your support has meant, I sometimes wonder if I would have made it without you there. You have been a teacher, a defender and a supporter and without you I would not be the person I am today, lots of love x. Thanks also to Bren, noted inventor of the “broomster” who has been another big supporter throughout!

Finally I would like to thank my parents Heather and Leslie. You have always just let me get on with things while supporting me from the sidelines. You have given me the chance to be independent and find my own path which led to this, which is quite funny really because my doing this was quite a shock to all of us... but I guess it’s all gone pretty well considering! Love you both so so much ☺ and thanks again for EVERYTHING! x

Abstract

Currently, there is a gap between pharmacological treatment and joint replacement for the management of cartilage degradation diseases, such as osteoarthritis. It may be possible to use cartilage substitution materials to treat small defects in cartilage tissues, delaying the need for joint replacements, which have a limited lifetime *in vivo*, so are not suitable for many patients. A major barrier to the use of cartilage substitution materials is suitable *in vitro* testing of cartilage materials. Therefore mechanical and enzymatic models of cartilage degeneration were developed, which may be used to assess novel cartilage substitution materials.

A single station pin-on-plate rig with a variable load was used to degrade the cartilage tissue of osteochondral pins and plates to produce two mechanical models of degradation denoted “mild” and “moderate”. A Ringer’s solution and serum based lubricant were chosen to hydrate cartilage tissues during articulation. The lubricants used during mechanical degradation were collected and analysed quantitatively for glycosaminoglycan (GAG) and collagen content. In addition, a method for isolating and imaging the cartilage wear particles in the lubricant was developed. A chondroitinase ABC enzyme was used to enzymatically degrade cartilage tissues.

The mechanical and enzymatic degradation in the models was characterised using a broad range of mechanical and biological assessment techniques. The mechanical degradation and wear of the tissues created using the pin-on-plate rig was evaluated using cartilage height measurements, friction measurements, surface profilometry, histological and immunohistological staining, and quantitative biochemical assays. The wear on the surface of the tissue was observed using environmental scanning electron microscopy and the tissue ultrastructure was observed using transmission electron microscopy. The tissues degraded using chondroitinase ABC were analysed using indentation testing, histological and immunohistological staining, quantitative biochemical assays, and transmission electron microscopy.

It was determined that an increased load used during pin-on-plate testing resulted in an increase in tissue degradation. Mechanical degradation under the “moderate” loading condition caused the surface of the cartilage tissue to become fibrillated and areas of tissue loss were observed. Under the mild condition the cartilage surface remained relatively smooth however, several small fissures were observed in some specimens. The surface of the tissue degraded under moderate conditions was significantly rougher than that degraded under the mild condition. There was a small loss of GAGs in the mild condition whereas a large volume of GAGs were lost from the tissue under the moderate condition, and the aggrecan network in the tissue was heavily disrupted.

There was no significant difference between the friction measurements or the height measurements recorded for the specimens under the two variable loading conditions. Immunohistochemical staining for minor tissue components showed that collagen VI and cartilage oligomeric matrix protein (COMP) were not altered by the mechanical degradation, whereas a loss in biglycan was observed in specimens loaded under the moderate condition. It was observed that the serum lubricant may protect the cartilage tissue from degradation during articulation. An increased number of wear particles were observed in the lubricants recovered from the moderate loading condition tests. Digestion of tissues with chondroitinase ABC led to an increase in tissue deformation during indentation. The level of GAGs in the tissues was reduced and the GAGs associated with the aggrecan network in the tissue were no longer visible. Collagen VI and COMP were not significantly affected by chondroitinase ABC digestion, however biglycan staining was reduced at the superficial to middle zone of the tissue.

The models produced have potential to be used in the assessment of novel cartilage substitution materials. The parameters used in this study will also be useful in the development of *in vitro* whole joint simulators.

Thesis title page	i
Acknowledgements	ii
Abstract	iii
Table of Contents	v
List of Figures	xviii
List of Tables	xxxv
Abbreviations	xxxvii

Chapter 1 Introduction

1.1 Introduction to cartilage	2
1.2 Joints and joint components	2
1.2.1 The knee joint	2
1.2.1.1 The mechanical environment of the knee	3
1.3 Cartilage structure	4
1.3.1 Surface amorphous layer (SAL)	4
1.3.2 Superficial tangential zone (STZ)	5
1.3.3 Middle zone	5
1.3.4 Deep zone	5
1.3.5 Calcified zone	5
1.3.6 Pericellular, territorial and interterritorial matrices	6
1.4 Cartilage composition	6
1.4.1 Interstitial fluid	6
1.4.2 Collagen	7
1.4.2.1 Collagen II	8
1.4.2.2 Collagen VI	9
1.4.2.3 Collagen IX	9

1.4.2.4 Collagen X	10
1.4.2.5 Collagen XI	10
1.4.3 Cartilage proteoglycans	11
1.4.3.1 Aggrecan	11
1.4.3.2 Small leucine rich proteoglycans	12
1.4.4 Glycosaminoglycans (GAGs)	13
1.4.4.1 Hyaluronan (Hyaluronic acid)	13
1.4.4.2 Chondroitin sulphate	14
1.4.4.3 Keratan sulphate	14
1.4.4.4 Dermatan sulphate (DS)	15
1.4.5 Non-collagenous proteins	15
1.4.6 Chondrocytes	15
1.4.7 Synovial fluid	16
1.6 The Lubrication, wear and mechanical properties of cartilage	17
1.6.1 Tribology	17
1.6.2 Viscoelasticity	18
1.6.2.1 Creep	18
1.6.2.2 Stress relaxation	18
1.6.3 Wear	19
1.6.3.1 Interfacial wear	19
1.6.3.1.1 Adhesive wear	20
1.6.3.1.2 Abrasive Wear	20
1.6.3.1.3 Fatigue wear	20
1.6.4 Cartilage wear particles	20
1.6.5 Cartilage lubrication theories	21

1.6.6 Boundary lubrication	21
1.6.7 Fluid-film lubrication	22
1.6.7.1 Hydrodynamic lubrication	22
1.6.7.2 Squeeze-film lubrication	22
1.6.7.3 Elasto-hydrodynamic lubrication	23
1.6.8 Mixed lubrication	23
1.6.9 Biphasic lubrication	24
1.7 Osteoarthritis and cartilage degeneration	25
1.7.1 Primary and secondary osteoarthritis	25
1.7.2 Early stage osteoarthritis	26
1.7.3 Advanced stage osteoarthritis	27
1.7.4 Chondrocytes in osteoarthritis	28
1.7.5 Collagen in degenerated cartilage	30
1.7.6 Proteoglycans in degenerated cartilage	32
1.7.7 Grading systems for degenerated cartilage tissues	33
1.8 Inflammatory changes in degenerated cartilage	33
1.8.1 Major pro-inflammatory/ catabolic cytokines	34
1.8.1.1 Interleukin-1	34
1.8.1.2 Tumour necrosis factor- α	34
1.8.2 Minor pro-inflammatory/ catabolic cytokines	35
1.8.3 Inhibitory cytokines	37
1.8.3.1 Interleukin receptor antagonist (IL-Ra)	37
1.8.4 Anabolic cytokines	39
1.8.4.1 Insulin like growth factor-1 (IGF)	39

1.8.4.2 Transforming growth factor- β (TGF- β).....	39
1.8.4.3 Bone morphogenic proteins (BMP).....	39
1.9 Matrix metalloproteases (MMPs).....	40
1.9.1 Matrix metalloprotease regulation.....	40
1.9.2 Matrix metalloproteases in osteoarthritis.....	40
1.9.3 MMP subgroups.....	41
1.9.4 Tissue inhibitors of metalloproteinases.....	43
1.9.5 Aggrecanases.....	43
1.9.6 Other molecules found in osteoarthritic cartilage tissue.....	44
1.10 The biotribological properties of degraded cartilage tissues.....	45
1.11 Treatment and management of osteoarthritis.....	46
1.11.1 Drug therapy.....	46
1.11.2 Arthroscopy.....	47
1.11.3 Autologous chondrocyte implantation (ACI).....	48
1.11.4 Marrow stimulation.....	49
1.11.5 Mosaicplasty.....	49
1.11.6 Unicompartmental Knee Arthroplasty (UKA).....	50
1.11.7 Total knee replacement (TKR).....	50
1.11.8 Novel Cartilage replacement therapies.....	51
1.11.9 Preclinical assessment of cartilage substitution materials.....	52
1.12 Models of cartilage degeneration.....	53
1.12.1 <i>In vivo</i> models of cartilage degradation.....	53
1.12.1.1 Spontaneous models of osteoarthritis.....	53

1.12.1.2 Surgical models of osteoarthritis.....	54
1.12.1.3 Intra-articular Injection.....	54
1.12.2 <i>In vitro</i> models of cartilage degradation.....	54
1.13 Rationale.....	57
1.14 Aims and Objectives.....	58
1.14.1 Objectives.....	58
 Chapter 2 Experimental Materials and Methods	
2.1 Materials.....	60
2.1.1 Equipment.....	60
2.1.2 Reagents.....	62
2.1.3 Antibodies.....	64
2.2 Consumables.....	65
2.2.1 Glassware.....	65
2.2.2 Sterile Plasticware.....	65
2.2.3 Dissection Equipment.....	65
2.2.4 Stock Solutions.....	65
2.2.4.1 Ethylenediaminetetraacetic acid (EDTA) solution 12.5% (w/v) at pH 7.....	65
2.2.4.2 Sodium hydroxide solution (6M).....	65
2.2.4.3 Ringer's solution.....	66
2.2.4.4 Phosphate buffered saline (PBS).....	66
2.3 Methods.....	67
2.3.1 pH Measurement.....	67

2.3.2 Microscopy	67
2.3.3 Filter Sterilisation	67
2.4 Tissue Retrieval	68
2.5 Basic histological techniques	69
2.5.1 Decalcification of bovine osteochondral plugs	69
2.5.2 Calcium oxalate test	69
2.5.2.1 Dibasic sodium phosphate solution (0.2M)	69
2.5.2.2 Citrate phosphate buffer, pH 3.4	69
2.5.2.3 Saturated ammonium oxalate solution	69
2.5.3 Paraffin wax embedding of cartilage samples	70
2.5.4 Tissue sectioning	71
2.5.5. Dewaxing and rehydration of paraffin embedded tissue	71
2.5.6 Tissue dehydration and mounting	71
2.5.7 Tissue retrieval for cryoembedding	71
2.5.8 Tissue sectioning and slide preparation of cryoembedded tissues	71
2.6 Histological staining methods	72
2.6.1 Haemotoxylin and eosin staining	72
2.6.2 Alcian blue staining	72
2.6.3 Immunohistochemical staining of bovine osteochondral specimens	73
2.6.3.1 Tris solution (2 M)	73
2.6.3.2 Sodium chloride solution (3 M)	73
2.6.3.3 Tris buffered saline pH 7.6 (TBS)	73
2.6.3.4 Tris buffered saline containing 0.05% (v/v) tween 20 (TBS tween)	73
2.6.3.5 Hydrogen peroxide solution 3% (v/v)	73
2.6.3.6 BSA solution	73
2.6.3.7 Antibody diluent	73
2.7 Microscopy of cartilage specimens	75

2.7.1 Environmental scanning electron microscopy	75
2.7.2 Transmission Electron Microscopy and Cupromeronic Blue Staining	75
2.7.2.1 Monobasic sodium phosphate (0.2M).....	75
2.7.2.2 Dibasic sodium phosphate (0.2M).....	75
2.7.2.3 Phosphate buffer (0.1M).....	75
2.7.2.4 Magnesium chloride hexahydrate (3 M).....	75
2.7.2.5 Aqueous sodium tungstate 0.5% (w/v).....	76
2.7.2.6 Aqueous sodium tungstate 0.5% (w/v).....	76
2.7.2.7 Cupromeronic blue dye solution.....	76
2.7.2.8 Araldite Resin.....	76
2.7.2.9 Saturated uranyl acetate solution.....	76
2.8 Biochemical assays for quantitative assessment of hydroxyproline and glycosaminoglycan content of cartilage tissue	78
2.8.1 Hydroxyproline quantification assay for cartilage tissue	78
2.8.1.1 Assay buffer.....	78
2.8.1.2 Chloramine T solution.....	78
2.8.1.3 Ehrlich's reagent.....	78
2.8.2 Glycosaminoglycan quantification assay for tissue	79
2.8.2.1 Assay buffer.....	79
2.8.2.2 Digestion buffer.....	79
2.8.2.3 Crude papain solution for tissue digestion.....	80
2.8.2.4 DMB dye solution.....	80
2.9 Statistical analysis	81
Chapter 3 Development and Characterisation of a Mechanical Model of Cartilage Degradation	
3.1 Introduction	83

3.1.1 Biglycan	84
3.1.2 Cartilage Oligomeric Matrix Protein	84
3.1.3 Collagen VI	84
3.1.4 Mechanical Degradation Methodologies	85
3.1.5 Lubricants	85
3.2 Aims and objectives	87
3.3 Experimental approach	89
3.4 Methods	91
3.4.1 Lubricants for Mechanical Degradation Regimes	91
3.4.1.1 Serum Lubricant	91
3.4.2 Mechanical degradation of cartilage using a multidirectional pin on plate rig	91
3.4.2.1 Calibration	94
3.4.3 Static loading and deformation assessment of native cartilage	95
3.4.3.1 The six station multi-directional wear rig	96
3.4.3.2 Deformation and Recovery Tests	99
3.4.4 Silicon Mould Surface Replication for Surface Roughness Measurement	99
3.4.4.1 Rationale	99
3.4.4.2 Calibration	100
3.4.4.3 Method	102
3.4.5 Histological assessment of mechanically degraded cartilage tissues	103
3.4.6 Immunohistological assessment of mechanically degraded cartilage tissues	103
3.4.7 Environmental scanning electron microscopy of the mechanically degraded cartilage surface	104
3.4.8 Transmission electron microscopy analysis of mechanically degraded cartilage tissue	104
3.4.9 Quantitative biochemical analysis of degraded cartilage tissue	104
3.4.10 Quantitative analysis of hydroxyproline in lubricants recovered after mechanical degradation of cartilage specimens	104
3.4.10.1 Rationale	104

3.4.10.2 Quantitative analysis of hydroxyproline in Ringer’s solution based lubricants; development steps.....	105
3.4.10.2.1 <i>Sample concentration</i>	105
3.4.10.2.2 <i>Determination of dilution factor</i>	105
3.4.10.2.3 <i>Determination of acid volume</i>	106
3.4.10.3 Quantitative analysis of hydroxyproline in Ringer’s solution based lubricants generated during mechanical degradation regimes.....	108
3.4.10.4 Hydroxyproline quantification assay for serum lubricants.....	108
3.4.11 Quantitative analysis of glycosaminoglycans in lubricants recovered after mechanical degradation of cartilage specimens.....	109
3.4.11.1 Quantitative analysis of glycosaminoglycans in Ringer’s solution based lubricants; development steps.....	109
3.4.11.1.1 <i>Sample concentration</i>	109
3.4.11.1.2 <i>Papain source</i>	109
3.4.11.1.3 <i>Dilution factor investigation</i>	110
3.4.11.1.3 <i>Optimising pure papain concentration for lubricant digestion</i>	111
3.4.11.1.4 <i>Digestion buffer volume</i>	112
3.4.11.2 Quantitative analysis of glycosaminoglycan in Ringer’s solution based lubricants generated during mechanical degradation regimes.....	113
3.4.11.2.1 <i>Pure papain digestion solution</i>	113
3.4.11.3 Quantitative analysis of glycosaminoglycan in serum based lubricants generated during mechanical degradation regimes.....	114
3.4.11.3.1 <i>Dilution Factor Investigation</i>	114
3.4.11.3.2 <i>Papain concentration optimisation</i>	115
3.4.11.4 Quantitative analysis of glycosaminoglycan in serum based lubricants generated during mechanical degradation regimes.....	116
3.5 Results.....	117
3.5.1 Macroscopic evaluation of dynamically mechanically degraded cartilage.....	117
3.5.2 Height loss and recovery of statically loaded cartilage specimens.....	119
3.5.3 Assessment of cartilage height post dynamic mechanical degradation.....	123
3.5.4 Surface roughness measurement of mechanically degraded cartilage replicas.....	127

3.5.5 Friction between pins and plates during mechanical degradation	133
3.5.6 Histological evaluation of mechanically degraded cartilage specimens	135
3.5.7 Qualitative evaluation of GAGs in mechanically degraded cartilage specimens	141
3.5.8 Quantitative evaluation of biglycan in mechanically degraded cartilage specimens	144
3.5.9 Quantitative evaluation of COMP in mechanically degraded cartilage specimens	148
3.5.10 Qualitative evaluation of collagen VI in mechanically degraded cartilage specimens	150
3.5.11 Evaluation of mechanically degraded cartilage tissues using electron microscopy	153
3.5.11.1 Evaluation of the cartilage surface by environmental electron scanning microscopy of the cartilage surface.....	153
3.5.12 Qualitative evaluation of proteoglycans in cartilage tissues stained with cupromeronic blue dye by transmission electron microscopy	156
3.5.12.1 Control cartilage tissue.....	157
3.5.12.2 Mild condition degradation with Ringer’s solution lubricant.....	160
3.5.12.3 Moderate condition degradation with Ringer’s solution lubricant.....	162
3.5.12.4 Moderate condition degradation with serum based lubricant.....	163
3.5.13 Quantitative assessment of hydroxyproline and glycosaminoglycan content of cartilage tissues	165
3.5.13.1 Hydroxyproline content of undegraded and mechanically degraded cartilage tissues.....	165
3.5.13.2 Glycosaminoglycan content of undegraded and mechanically degraded cartilage tissues.....	167
3.5.14 Quantitative assessment of hydroxyproline and glycosaminoglycan content of lubricants recovered from mechanical degradation protocols	169
3.5.14.1 Hydroxyproline content of lubricant recovered from mechanical degradation protocols.....	169
3.5.14.2 Glycosaminoglycan content of lubricant recovered from mechanical degradation protocols.....	170
3.6 Summary of results	171
3.7 Discussion	173
3.8 Conclusion	178

Chapter 4 Development and Characterisation of an Enzymatic Model of Cartilage Degradation

4.1 Introduction	180
4.2 Aims and objectives	183
4.3 Experimental approach	184
4.4 Methods	186
4.4.1 Chondroitinase ABC treatment of cartilage tissue	186
4.4.1.1 Extensive chondroitinase ABC treatment of cartilage tissue	186
4.4.1.2 Antibiotic solution	186
4.4.1.3 Chondroitinase ABC treatment solution	186
4.4.2 Histological assessment of chondroitinase ABC treated cartilage tissues	187
4.4.3 Immunohistological assessment of chondroitinase ABC treated cartilage tissues ..	188
4.4.4 Transmission electron microscopy analysis of chondroitinase ABC treated cartilage tissue	188
4.4.5 Quantitative biochemical analysis of chondroitinase ABC treated cartilage tissue	188
4.4.6 Indentation testing of chondroitinase ABC treated cartilage tissues to derive cartilage deformation properties	188
4.5 Results	190
4.5.1 Histological evaluation of chondroitinase ABC treated cartilage specimens	190
4.5.2 Qualitative evaluation of GAGs in chondroitinase ABC treated cartilage	191
4.5.3 Quantitative evaluation of biglycan in chondroitinase ABC treated cartilage specimens	192
4.5.4 Qualitative evaluation of cartilage oligomeric matrix protein in chondroitinase ABC treated cartilage tissue	194
4.5.5 Qualitative evaluation of collagen VI in chondroitinase ABC treated cartilage tissue	195
4.5.6 Qualitative evaluation of proteoglycans in cartilage tissues stained with cupromeronic blue dye	197

4.5.7 Quantitative assessment of the hydroxyproline and glycosaminoglycan content of untreated control tissue and chondroitinase ABC treated cartilage tissue	200
4.5.7.1 Hydroxyproline content of chondroitinase ABC treated cartilage tissues	201
4.5.7.2 Glycosaminoglycan content of chondroitinase ABC treated cartilage tissues	201
4.5.8 Indentation analysis of chondroitinase ABC treated cartilage specimens	202
4.6 Discussion	204
4.7 Conclusion	207
 Chapter 5 Characterisation of cartilage wear particles generated during mechanical degradation protocols	
5.1 Introduction	208
5.1.1 Rationale	210
5.2 Aims and Objectives	211
5.3 Methods	212
5.3.1 Particle Isolation	212
5.3.2. Investigation into the effects of humidity on particle appearance	213
5.3.3 Imaging of cartilage wear particles using environmental scanning electron microscopy (ESEM).....	213
5.4 Results	216
5.4.1 Study into the effect of humidity on particle appearance	216
5.4.2 Imaging of cartilage wear particles from lubricants using ESEM	218
5.5 Discussion	222
5.6 Conclusion	224
 Chapter 6 General Discussion	
6.1 Discussion	226
6.1.1 Future work	233
6.1.2 Conclusion	236

Chapter Seven

7.1 References	237
-----------------------	------------

List of Figures

Chapter One

- Figure 1.1** **Anterior view of the human knee joint, showing the major ligaments, bony structures and meniscus.** Articular cartilage is shown in purple covering the femur above the menisci. Taken from <http://warwickphysio.com> **3**
- Figure 1.2** **The zonal arrangement of articular cartilage taken from Poole *et al.* (2001).** The image includes details of the territorial and interterritorial regions of the tissue including the proteoglycan arrangements in each zone. The images in the beige boxes highlight the variable collagen morphologies seen through the tissue. **4**
- Figure 1.3.** **The hierarchical structure of a collagen fibre.** Initially, three polypeptide chains form a left-handed triple helix. From there, several triple helices assemble to produce collagen fibrils that in turn align to form a mature collagen fiber. Adapted from Heim *et al.*, 2010. **8**
- Figure 1.4.** **The structure of aggrecan and its interaction with hyaluronan.** **12**
- Figure 1.5** **A typical creep and recovery curve of the cartilage of the superomedial portion of the femoral head with a corresponding curve fit of the creep.** This is the typical response curve of a viscoelastic material in a creep and recovery test showing rapid initial deformation which slows down as it reaches an equilibrium (Athanasίου *et al.*, 1994) **19**
- Figure 1.6.** **Boundary lubrication between opposing articular cartilage surfaces.** **22**
- Figure 1.7.** **Hydrodynamic and squeeze film lubrication in the context of a joint.** Adapted from Nordin and Frankel, 2001. **23**
- Figure 1.8.** **An image taken during arthroscopy of the knee of a patient with cartilage degradation.** Taken from www.icartilage.com. **48**
- Figure 1.9.** **An image showing the surface of the articular cartilage in a knee joint after a moisaiclasty procedure.** Taken from Hangody *et al.*, 2010. **50**
- Figure 1.10.** **The NeoCart[®] matrix used for articular cartilage repair by Histogenics.** **52**

Chapter Two

- Figure 2.1.** Images displaying the areas of the medial condyle and medial patellar groove from which osteochondral pins and plates were dissected. **A.** The medial condyle of the bovine femur showing areas marked for osteochondral pin extraction and a cylindrical void where a pin has been extracted. **B.** A drawing showing the outline of the bovine patellar groove with a shaded region indicating the area from which osteochondral plates were removed. **68**

Chapter Three

- Figure 3.1** The experimental approach taken in the research described in chapter three, which focused on the effects of mechanical degradation on cartilage specimens. The image includes characterisation techniques that were used to analyse specimens and the number of replicates. **90**
- Figure 3.2** The single station multidirectional pin on plate friction rig. **92**
- Figure 3.3** Friction rig components; plate clamp and bath. The components that were used to clamp the osteochondral plate in place on the friction rig. The bath was subsequently screwed to the reciprocating stage of the friction rig. **93**
- Figure 3.4** Equipment and components required for friction rig assembly. **93**
- Figure 3.5** Calibration of the single station multidirectional pin on plate friction rig. **95**
A. The pin holder is suspended in the bridge using a metal ring. A wheel is clamped to the rig. **B.** A thread is looped around the base of the pin holder then around the groove of the wheel before being allowed to hang vertically with the weight holder at the bottom of it.
- Figure 3.6** One of six sets of small components for the six station multidirectional wear rig. **97**

- Figure 3.7** **The plate set up and pin holding assembly.** **A.** The bath well, bath insert and plate were assembled before being placed onto the reciprocating stage. The assembly was then secured with the connecting rod. **B.** The osteochondral pin was placed inside the set up shown with the cartilage surface protruding. **97**
- Figure 3.8** **Small component assembly on the rig.** The bridges were put in place and secured using a clamp. The pin assembly was slotted through the bridge and the ball bearings were placed on top. **98**
- Figure 3.9** **Complete assembly of the six station wear rig.** **98**
- Figure 3.10.** **Microset system equipment and replicas.** **A.** The rubber replicating compound was applied to the cartilage surface from the cartridge in the dispensing gun with the nozzle attached. **B.** The pin and plate moulds after curing was complete. **100**
- Figure 3.11.** **The calibration standard for the Talysurf.** Calibration of the machine with the right hand square is carried out before and after each session to confirm that no damage had taken place to the stylus ensuring correct results are recorded. **101**
- Figure 3.12.** **A typical calibration trace.** Aside from the requirement of an Ra of 0.8, the calibration trace pattern itself was required to appear as in the one shown above with the characteristic “left toe”, one of which is circled on the trace. **101**
- Figure 3.13** **Trace map for cartilage pin and plate replicas.** **A.** Arrows labelled in red indicate traces performed. The P1 trace was used as an undegraded control measurement. The blue line indicates the wear scar which was 18 mm by 9 mm. **B.** Pin traces are shown in red. Pin diameter was 9 mm. The traces are perpendicular to each other and are 8 mm in length. Diagram is not to scale. **103**
- Figure 3.14.** **Standards diluted in assay buffer and standards diluted one to one with assay buffer and neutralised hydrolysed Ringer’s solution.** Black circles represent standards diluted in assay buffer. Green triangles represent known concentrations of hydroxyproline in neutralised hydrolysed Ringer’s solution diluted one to one with assay buffer. Data is presented as the mean (n=3) \pm 95% confidence limits. **106**

- Figure 3.15.** **Effect of acid volume on mild lubricant hydrolysis prior to using the hydroxyproline assay.** The results indicated that 0.5ml of 6M hydrochloric acid was suitable for digestion of 1ml of lyophilised mild Ringer's solution lubricant. Data is presented as the mean (n=3) \pm 95% confidence limits. **107**
- Figure 3.16.** **The absorbance profile of standards diluted in assay buffer and chondroitin sulphate in Ringer's solution that has been digested with 50 U.ml of pure papain.** Green triangles represent digested standards in Ringer's solution that were not diluted in assay buffer. Black circles represent standards in assay buffer. Data is presented as the mean (n=3) \pm 95% confidence limits. **110**
- Figure 3.17.** **The absorbance profile of standards diluted in assay buffer and digested standards in Ringer's solution diluted one to one with assay buffer.** Green triangles represent digested standards diluted one to one with assay buffer. Black circles represent standards in assay buffer. Data is presented as the mean (n=3) \pm 95% confidence limits. **111**
- Figure 3.18.** **Effect of papain concentration on lubricant digestion.** There was no significant difference found in the GAG concentration of specimens digested with the different papain concentrations (One way ANOVA, $P > 0.05$). Data is presented as the mean (n=6) \pm 95% confidence limits. **112**
- Figure 3.19.** **Effect of digestion buffer volume for lubricant digestion.** It was determined that 0.5 ml of 40 $\mu\text{g.ml}$ of pure papain in digestion buffer was sufficient for complete digestion of moderate Ringer's solution lubricant. Asterisks represent a P value of $P \leq 0.01$ determined by one way ANOVA. Data is presented as the mean (n=3) \pm 95% confidence limits. **113**
- Figure 3.20** **The absorbance profile of standards diluted in assay buffer and standards diluted one in five with assay buffer.** Black circles represent standards diluted in assay buffer. Green triangles represent standards in digested lubricant diluted one in five with assay buffer. Data is presented as the mean (n=3) \pm 95% confidence limits. **115**
- Figure 3.21** **Effect of pure papain concentration for serum lubricant digestion.** It was concluded that a 40 $\mu\text{g.ml}^{-1}$ pure papain concentration was suitable for serum lubricant digestion. Data is presented as the mean (n=4) \pm 95% confidence limits. **116**

- Figure 3.22. Osteochondral pin specimens after mild condition degradation in Ringer’s solution.** The pins shown represent the typical damage patterns seen on osteochondral pins after degradation. The third pin has been bisected in preparation for histological analysis. **A.** Specimen A did not appear to have any obvious damage to the surface, however the cartilage did appear swollen. **B.** This pin had a small crack across the surface of the tissue (arrow). The remaining tissue did not appear damaged however the surface did appear to be duller than control specimens. **C.** This pin which has been bisected, shows the most severe type of damage that was observed after mild condition degradation. Several cracks can be seen on the surface of the swollen cartilage (arrow). **117**
- Figure 3.23. Osteochondral pin specimens after moderate condition degradation in Ringer’s solution.** The pins shown are representative of the typical damage patterns observed on osteochondral pins under the moderate degradation conditions. **A.** This specimen was damaged primarily around the circumference of the pin (arrow) which was unusual as the remaining specimens primarily lost tissue from the central region of the pin rather than the edges. The surface of the tissue appeared dull and scratched. **B.** Apart from two cracks across the pin surface (arrows), this pin was not heavily damaged and represented the lower end of the damage scale seen on specimens that underwent moderate condition degradation with Ringer’s solution lubricant. **C.** This specimen was heavily damaged and represented the most severe end of the scale of damage seen on moderate condition pins in Ringer’s solution lubricant. A large volume of cartilage tissue was lost from the pin leaving less than one half of the pin depth remaining. **118**
- Figure 3.24. Osteochondral pin specimens after moderate condition degradation with serum lubricant.** The pins shown here represent the typical damage patterns observed macroscopically on osteochondral pins under the specified loading conditions. The pin to the left of the image had lost a large volume of tissue. The middle pin and right hand pin showed cracks in the surface (arrows). **119**

- Figure 3.25. Osteochondral pin cartilage height recovery post static loading under mild conditions (200 N load applied for 6 hours).** Data is presented as the mean ($n=6$) \pm 95% confidence intervals. The data was analysed by repeated measures analysis of variance followed by determination of significant differences between groups using a Tukey post test; ** equates to $P \leq 0.01$; *** equates to $P \leq 0.001$. **121**
- Figure 3.26. Osteochondral pin cartilage height recovery post static loading under moderate conditions (478 N load applied for 6 hours).** Data is presented as the mean ($n=6$) \pm 95% confidence intervals. The data was analysed by repeated measures analysis of variance followed by determination of significant differences between groups using a Tukey post test; * equates to $P \leq 0.05$; *** equates to $P \leq 0.001$. **121**
- Figure 3.27. Osteochondral plate cartilage recovery post static loading under mild conditions (200 N load applied for 6 hours).** Data is presented as the mean ($n=6$) \pm 95% confidence intervals. The data was analysed by repeated measures analysis of variance followed by determination of significant differences between groups using a Tukey post test; * equates to $P \leq 0.05$; **** equates to $P \leq 0.0001$. **122**
- Figure 3.28. Figure 3.28 Osteochondral plate cartilage recovery post static loading under moderate conditions (478 N load applied for 6 hours).** Data is presented as the mean ($n=6$) \pm 95% confidence intervals. The data was analysed by repeated measures analysis of variance followed by determination of significant differences between groups using a Tukey post test; * equates to $P \leq 0.05$. **122**
- Figure 3.29. Cartilage height of osteochondral pins following mild condition dynamic mechanical degradation in Ringer's solution lubricant.** Data is presented as the mean ($n=6$) \pm 95% confidence intervals. The data was analysed by repeated measures analysis of variance, no significant differences were found. **124**
- Figure 3.30. Cartilage height of osteochondral pins following moderate condition dynamic mechanical degradation with Ringer's solution lubricant.** Data is presented as the mean ($n=6$) \pm 95% confidence intervals. The data was analysed by repeated measures analysis of variance followed by determination of significant differences between groups using a Tukey **124**

post test; * equates to $P \leq 0.05$.

- Figure 3.31. Cartilage height of osteochondral pins following moderate condition dynamic mechanical degradation with serum lubricant.** 125
Data is presented as the mean ($n=6$) \pm 95% confidence intervals. The data was analysed by repeated measures analysis of variance, no significant differences were found.
- Figure 3.32. Height of osteochondral plates following mild condition dynamic mechanical degradation with Ringer's solution lubricant.** 125
Data is presented as the mean ($n=6$) \pm 95% confidence intervals. The data was analysed by repeated measures analysis of variance, no significant differences were found.
- Figure 3.33. Cartilage height of osteochondral plates following moderate condition dynamic mechanical degradation with Ringer's solution lubricant.** 126
Data is presented as the mean ($n=6$) \pm 95% confidence intervals. The data was analysed by repeated measures analysis of variance, no significant differences were found.
- Figure 3.34. Cartilage height of osteochondral plates following moderate condition dynamic mechanical degradation with serum lubricant.** 126
Data is presented as the mean ($n=6$) \pm 95% confidence intervals. The data was analysed by repeated measures analysis of variance followed by determination of significant differences between groups using a Tukey post test; * equates to $P \leq 0.05$.
- Figure 3.35. The mean surface roughness of pin replicas directly after degradation and after 24 and 48 hours of recovery. A.** 129
Post refers to post degradation, 24 denotes 24 hours of recovery, 48 denotes 48 hours of recovery. Data is presented as the mean ($n=6$) \pm 95% confidence intervals. The data was analysed by repeated measures analysis of variance followed by determination of significant differences between groups using a Tukey post test. **B.** The individual R_a measurements for the pins degraded under moderate conditions in serum lubricant immediately after loading, after 2 hours of recovery (**C**) and after 48 hours of recovery (**D**).
- Figure 3.36. The surface roughness of plate replicas directly after degradation and after 24 and 48 hours of recovery.** 131
Post refers to post degradation, 24 denotes 24 hours of recovery, 48 denotes 48 hours of recovery. Data is

presented as the mean ($n=6$) \pm 95% confidence intervals. The data was analysed by repeated measures analysis of variance followed by determination of significant differences between groups using a Tukey post test.

- Figure 3.37. The co-efficient of friction recorded between osteochondral pins and plates during mechanical degradation protocols (N=6). A.** The friction data recorded for all mechanical degradation conditions including error bars. Data is presented as the mean friction coefficient ($n=6$) \pm 95% confidence intervals. The data was analysed by one way analysis of variance which revealed no significant difference in the friction levels at any time point between the three conditions **B.** The friction data recorded for all mechanical degradation conditions excluding error bars **134**
- Figure 3.38. Haematoxylin and eosin stained section of undegraded bovine articular cartilage pin control tissue.** The complete tissue section showing the superficial, middle and deep zones of the tissue. **136**
- Figure 3.39 Haematoxylin and eosin stained section of bovine articular cartilage pins. 137**
A. The superficial zone of the cartilage tissue showing chondrocytes at the surface in flattened lacunae (arrows). **B.** The middle zone of the tissue showing chondrocytes in rough columns. **C.** The deep zone of articular cartilage showing chondrocytes in columnar forms within large irregularly shaped lacunae (arrows).
- Figure 3.40. Haematoxylin and eosin stained section of cartilage pin specimens following mild degradation in Ringer's solution. 138**
 Both images A and B show specimens without visible degradation to the tissue. **C.** This specimen was one of two specimens showing damage to the tissue (arrow). **D.** This specimen contained a fissure in the surface that extended less than 50% of the cartilage height (arrow). Scale bars represent 500 μm .
- Figure 3.41 Haematoxylin and eosin stained section of cartilage pin specimens following moderate degradation in Ringer's solution. 139**
A. This specimen had a relatively smooth superficial zone however the tissue appeared to have become detached at the calcified zone (arrow). **B.** Away from the fissure in the cartilage surface the surface of the tissue remained smooth. **C.** A large volume of tissue loss was observed from this specimen in which the tissue had been lost progressively across the pin resulting in less than

50% of tissue height remaining at the pin edge. **D.** Tissue loss and fibrillation was observed in this specimen (arrows). Scale bars represent 500 μm .

- Figure 3.42. Haematoxylin and eosin stained sections of cartilage pin specimens following moderate degradation with serum lubricant. 140**
A-B. The cartilage surface away from the obvious areas of tissue damage remained smooth. **C.** Severe tissue damage was seen in one specimen in which tissue loss was observed. **D.** Fissures in the tissue were a typical form of damage (arrow). Scale bars represent 500 μm .
- Figure 3.43. Alcian blue stained control cartilage pin section. 141**
 Image shows an undegraded control pin section with superficial, middle, deep and calcified zones.
- Figure 3.44. Alcian blue stained cartilage pin specimens following mild degradation using Ringer's solution lubricant. 142**
A, C. A reduction in staining was observed in the deep zone of some specimens (arrows). **B.** Around areas of tissue damage a reduction in alcian blue staining was seen (arrow head). **D.** An overall loss of staining intensity compared with the undegraded control tissue was evident. Scale bars represent 500 μm .
- Figure 3.45. Alcian blue stained cartilage pin specimens following moderate mechanical degradation in Ringer's solution (N=6). 143**
A. Specimens appeared washed out due to a severe reduction in alcian blue staining. In this specimen the majority of GAG loss appeared to be in the middle to deep zone. **B, C, D.** Specimens with torn or fibrillated areas showed a greater reduction in focal alcian blue staining than areas with a clean fissure as was observed in A (arrows). Scale bars represent 500 μm .
- Figure 3.46. Alcian blue stained cartilage specimens following moderate degradation with serum lubricant (N=6). 144**
A. An overall reduction in alcian blue staining intensity was observed, however it was particularly evident in the superficial zone and in a band through the mid zone. **B.** Specimens showed a reduction in alcian blue uptake across the whole tissue. **C.** A reduction in alcian blue uptake was observed around areas of tissue damage (arrow). **D.** Tissue was seen breaking away from the bone (arrow). Scale bars represent 500 μm .

Figure 3.47.	Biglycan distribution in control cartilage pin specimens. A. Image shows an undegraded control pin section. B. Image shows the isotype control, which was negative.	145
Figure 3.48	A-D. Biglycan distribution in pin specimens degraded under mild mechanical conditions in Ringer's solution. Staining was reduced in the calcified zone of two specimens (B, C). Scale bars represent 500 μm .	146
Figure 3.49	Biglycan distribution in pin specimens degraded under moderate mechanical conditions in Ringer's solution. Scale bars represent 500 μm . Stronger staining was observed in the upper-middle to superficial zone (arrows).	146
Figure 3.50	Biglycan distribution in cartilage pin specimens degraded under moderate mechanical conditions in serum based lubricant. Light staining was observed in the superficial zones of two specimens (arrows). Scale bars represent 500 μm .	147
Figure 3.51.	A. Characterisation of undegraded pin control tissue using a cartilage oligomeric matrix protein antibody. B. Image shows the isotype control, which was negative.	148
Figure 3.52.	COMP distribution in cartilage pin specimens degraded mechanically under moderate conditions with Ringer's solution lubricant. Scale bars represent 500 μm .	149
Figure 3.53.	COMP distribution in cartilage pin specimens degraded mechanically under moderate conditions with Ringer's solution lubricant. Scale bars represent 500 μm .	14*9
Figure 3.54.	COMP distribution in cartilage pin specimens degraded mechanically under moderate conditions with serum lubricant. Scale bars represent 500 μm .	150
Figure 3.55.	Collagen VI distribution in control cartilage pin specimens. A. Image shows an undegraded control pin section. B. Image shows the isotype control, which was negative.	151
Figure 3.56.	Collagen VI distribution in cartilage pin specimens degraded mechanically under mild conditions (N=6). Scale bars represent 500 μm .	152
Figure 3.57.	Collagen VI distribution in cartilage pin specimens degraded mechanically under moderate conditions with Ringer's solution lubricant. Scale bars represent 500 μm .	152

- Figure 3.58. Collagen VI distribution in cartilage pin specimens degraded mechanically under moderate conditions with serum lubricant.** Scale bars represent 500 μm . **153**
- Figure 3.59. Characterisation of undegraded control cartilage pins and mechanically degraded articular cartilage pin surfaces using environmental scanning electron microscopy (ESEM).** **A.** The undegraded control cartilage surface. **B.** The cartilage surface after mild mechanical degradation. **C.** The moderately mechanically degraded surface articulated in Ringer's solution. **D.** The moderate mechanically degraded surface articulated in serum lubricant. **155**
- Figure 3.60. Features of degraded cartilage pin surfaces observed by ESEM.** **A.** The mild surface showing a crack in the surface and increased creasing of the cartilage surface (arrows). **B.** The moderate condition surface articulated in Ringer's solution showing a deep crack in the surface containing protrusions. **C.** The moderate condition surface articulated in Ringer's solution showing a torn area of the cartilage surface (arrow). **D.** The moderate condition surface articulated in serum lubricant showing wear particles accumulating in the edge of a crack in the surface. **156**
- Figure 3.61. Transmission electron microscopy images of the superficial zone of undegraded control cartilage pin tissue stained with cupromeronic blue.** **A.** The superficial zone of the tissue including the surface amorphous layer and a horizontal collagen band (bracket). **B.** Part of the band of fine collagen fibres running parallel to the cartilage surface where small leucine rich proteoglycans were observed (arrows). **C.** The cartilage tissue towards the middle zone of the tissue. **158**
- Figure 3.62. Transmission electron microscopy images of the middle zone of undegraded control cartilage tissue at 11,000 times magnification.** **A.** Aggrecan was observed forming a network within the middle zone of the tissue (arrows). **B.** Proteoglycans were observed interacting with the surface of collagen fibrils (arrow). **159**

- Figure 3.63. Transmission electron microscopy of the deep zone of undegraded control cartilage tissue at 11,000 times magnification (N=3). A.** Thick collagen fibrils were observed behind the dense aggrecan network (arrow). **B.** Patchy dark areas of staining were observed where dense areas of aggrecan appeared (circle). **159**
- Figure 3.64. Transmission electron microscopy of the deep zone in undegraded control cartilage. A.** The image shows the changes in the ultrastructure of the cartilage in the deep zone in close proximity to a chondrocyte (nucleus not visible). To the right hand side of the dashed line the fine parallel collagen fibres that line the perimeter of chondrocytes can be seen **B.** The structure begins to resemble the tissue in the territorial and interterritorial zones as the image is captured further away from the chondrocyte. **160**
- Figure 3.65. Tissues following mild condition mechanical degradation with Ringer's solution lubricant stained with Cupromeronic blue dye for proteoglycans. A.** The superficial zone of the tissue; the surface of the tissue is shown in the bottom left hand corner of the image. **B.** The middle zone of the tissue. **C.** The deep zone of the tissue. **161**
- Figure 3.66. Tissues having undergone moderate condition mechanical degradation with Ringer's solution lubricant stained with cupromeronic blue dye for proteoglycans (N=3). A.** The surface of the degraded tissue specimen possibly showing the hyaluronan network (arrows). **B.** The middle zone of the tissue. **C.** The deep zone of the tissue. **162**
- Figure 3.67. Chondrocyte ultrastructure in the superficial and deep zones of cartilage following moderate mechanical degradation in Ringer's solution lubricant. Stained with Cupromeronic blue A.** A chondrocyte in the superficial zone of the tissue. **B.** A chondrocyte and its nucleus (partially shown ; asterisk) in the deep zone of the tissue. **C.** The transitional zone between the chondrocyte environment and the territorial region of the tissue in the deep zone. **164**
- Figure 3.68. Tissues following moderate condition mechanical degradation with serum solution lubricant stained with Cupromeronic blue dye for proteoglycans. A.** The superficial zone of the tissue showing gaps in the collagen network (arrow). **B.** The middle zone of the tissue. **C.** The deep zone of the tissue. **165**

- Figure 3.69.** The relationship between absorbance at 570nm and the concentration of **trans-4-hydroxy-L-proline (mg.ml⁻¹)**. Data is presented as the mean (n=3) ±95% confidence limits. **166**
- Figure 3.70.** The collagen content of control cartilage and mechanically degraded cartilage. Data is presented as the mean (n=6) ±95% confidence limits. The data was analysed using one way analysis of variance followed by determination of significant differences between groups using a Tukey post test; * equates $P \leq 0.05$. **167**
- Figure 3.71.** The relationship between absorbance at 525nm and the concentration of **chondroitin sulphate B (mg.ml⁻¹)**. Data is presented as the mean (n=3) ±95% confidence limits. **168**
- Figure 3.72.** The GAG content of control cartilage and mechanically degraded cartilage. Data is presented as the mean (n=6) ±95% confidence limits. The data was analysed using one way analysis of variance followed by determination of significant differences between groups using a Tukey post test; *** equates $P \leq 0.001$. **168**
- Figure 3.73.** The collagen content of lubricants recovered after mechanical degradation protocols. Data is presented as the mean (n=6) ±95% confidence limits. The data was analysed using one way analysis of variance followed by determination of significant differences between groups using a Tukey post test; * equates $P \leq 0.05$. **169**
- Figure 3.74.** The GAG content of lubricants recovered from mechanical degradation protocols. Data is presented as the mean (n=6) ±95% confidence limits. The data was analysed using one way analysis of variance followed by determination of significant differences between groups using a Tukey post test; * equates $P \leq 0.05$. **170**
- Figure 3.75.** A summary of the results obtained using a range of methods to characterise cartilage mechanical degradation models. Key: *** indicates strong presence of the feature, ** indicates Presence, * indicates slight presence, - indicates reduction in presence of feature, -- indicates strong reduction, --- indicates complete absence of a feature. **171**

Chapter Four

- Figure 4.1.** **The experimental approach taken in the research described in chapter 4 in which specimens were treated with chondroitinase ABC.** The image includes the characterisation techniques that were used to analyse specimens and the number of replicates. **185**
- Figure 4.2.** **The indentation apparatus used to indent untreated control and chondroitinase ABC treated cartilage specimens.** Image shows the indenter rig and components of the rig required for indentation testing. **189**
- Figure 4.3.** **Representative images of haematoxylin and eosin stained sections of cartilage pin tissue treated with chondroitinase ABC. A.** The untreated control. **B,C,D.** The chondroitinase ABC treated specimens. The pale band of staining has been highlighted (Braces ; N=6). **190**
- Figure 4.4.** **Representative images of alcian blue stained sections of cartilage pin specimens treated with chondroitinase ABC. A.** The untreated control **B,C,D.** The chondroitinase ABC treated specimens. The pale band of staining has been highlighted (Braces ; N=6). **191**
- Figure 4.5.** **Representative images of chondroitinase ABC treated cartilage pin sections labelled with a biglycan antibody (N=6). A.** Untreated control tissue **B.** The surface and upper middle zone of the treated tissue. The arrow shows artifactual staining. **C.** The surface and upper middle zone of the treated tissue, which showed a reduction in haematoxylin staining (brace). **D.** The middle to deep zones of the tissue. **E.** The middle to deep zones of the treated tissue in which some staining was observed (arrows). **193**
- Figure 4.6.** **Chondroitinase ABC treated cartilage pin sections stained with a cartilage oligomeric matrix protein antibody A.** The untreated control tissue. **B-E.** Chondroitinase ABC treated specimens with arrows highlighting artefact staining in the calcified zone of specimens D and E (N=6). **195**
- Figure 4.7.** **Chondroitinase ABC treated cartilage sections labelled with a collagen VI antibody (N=6). A.** The untreated control tissue. **B-E.** The chondroitinase ABC treated specimens (N=6). Interterritorial staining is highlighted (arrow). **196**

- Figure 4.8. Chondroitinase ABC treated and untreated control cartilage specimens stained with Cupromeronic blue dye viewed with TEM. A.** The superficial zone of the chondroitinase ABC treated tissue showing the cartilage surface in the top left corner. **B.** The superficial zone of the untreated negative control cartilage tissue showing the cartilage surface in the top left corner. **198**
- Figure 4.9. Figure 4.9 Chondroitinase ABC treated and untreated control cartilage specimens stained with Cupromeronic blue dye viewed with TEM. A.** The middle zone of the chondroitinase ABC treated tissue where the aggrecan network has been disrupted (circle). **B.** The middle zone of the untreated negative control cartilage tissue with examples of intact areas of the aggrecan network (circles). **198**
- Figure 4.10. Figure 4.10. Chondroitinase ABC treated and untreated control cartilage specimens stained with Cupromeronic blue dye viewed with TEM. A.** The deep zone of the chondroitinase ABC treated tissue. **B.** The deep zone of the untreated negative control cartilage tissue. **199**
- Figure 4.11 TEM images of cartilage tissue treated with chondroitinase ABC and stained with Cupromeronic blue dye to act as negative control images. A.** The superficial zone of the tissue; the surface of the tissue is visible in the top right hand side of the image. **B.** The upper middle zone of the tissue. Hyaluronan was observed in the extensively treated specimens (arrow) **C.** The middle zone of the tissue. **D.** The deep zone of the tissue. **200**
- Figure 4.12. The collagen content of untreated control cartilage and cartilage treated using chondroitinase ABC at a concentration of 0.1U.ml^{-1} for 16 hours.** No significant difference was found between the two values. Data is presented as the mean (n=6) \pm 95% confidence limits. **201**
- Figure 4.13. The glycosaminoglycan content of untreated control cartilage and cartilage treated using chondroitinase ABC.** A significant difference was found between the two values. Data is presented as the mean (n=6) \pm 95% confidence limits. The data was analysed using a Student's t-test; **** equates $P \leq 0.0001$. **202**

- Figure 4.14. The displacement of untreated control tissue and chondroitinase ABC treated cartilage tissue during a 60 minute indentation test. A** The purple line marks the deformation of the chondroitinase ABC treated tissue. The orange line marks the deformation of the untreated control tissue. A significant difference was found between the values at several time points. Data is presented as the mean (n=6) \pm 95% confidence limits. The data was analysed using a Student's t-test; * $P \leq 0.05$, ** $P \leq 0.01$. **B.** The early elastic response region which showed no significant differences between displacement of control and digested tissues. **203**
- Chapter Five**
- Figure 5.1. Apparatus for cartilage wear particle isolation. A.** The vacuum filter holder (composed of a measuring cylinder and filter holder with bung), and filter flask components. The measuring cylinder and filter holder were held together with a clamp. **B.** The case containing 45 mm diameter 10 μ m pore filters and the petri dish. **C.** The electric pump. **213**
- Figure 5.2. A schematic of the filter post filtration, including the area of the filter which was removed using a 6mm diameter biopsy punch for imaging using ESEM. 214**
- Figure 5.3. Calculation of the percentage area of the filter observed during imaging. 215**
- Figure 5.4. The appearances of the cartilage wear particles at a range of humidities. 217**
As the humidity dropped the clarity of the images was improved. Precipitated salt crystals from the Ringer's solution could be seen clearly on the surface of the largest particle in the images taken at 55 and 45 % humidity. There was only one feature that was visible on the lowest humidity image that was not also clearly visible on the highest humidity image (circled).
- Figure 5.5. The average number of particles found in 1 ml of lubricant recovered from mild and moderate mechanical degradation protocols. 218**
The values were normalised to each ml of lubricant. Data is presented as the mean (n=5) \pm 95% confidence limits. The data was analysed using one way analysis of variance followed by determination of significant differences between groups using a Tukey post test; * equates to $P \leq 0.05$; *** equates to $P \leq 0.001$.

- Figure 5.6. A range of images taken of cartilage wear particles in Ringer’s solution lubricant recovered from mild condition mechanical degradation using ESEM. A-F.** Typical images of cartilage particles which were clearly defined. Globular particles with smooth edges (asterisks) were observed alongside fibrillar particles (arrow heads), irregular particles with rough edges (arrow) and irregular shaped particles (crosses). **G-I.** Examples of images that included particles with semi-amorphous boundaries (arrows). Scale bar represents 50 μm . Magnification 1500X. **219**
- Figure 5.7. A range of images taken of cartilage wear particles in Ringer’s solution lubricant recovered from moderate condition mechanical degradation taken using ESEM. A-E.** Typical screenshots showing particles recovered from moderate condition lubricant including globular particles with both smooth (arrow) and rough edges (crosses). **F.** An amorphous globular particle is shown with pores of the filter visible through part of the particle (arrows). **G-I.** Images show screenshots that include examples of diffuse (arrow), globular (cross) and amorphous particles (asterisk). Scale bar represents 50 μm . Magnification 1500X. **220**
- Figure 5.8. Images showing typical contaminants in the control lubricant taken using ESEM. A.** Occasionally, granular particles that appeared similar to the cartilage particles found in the recovered lubricants were observed in the control solutions. **B.** A sharp granular particle. **C.** A small spherical contaminant particle **D.** A straight fibrous hair like particle was observed. Scale bar represents 50 μm . Magnification 1500X. **221**

Chapter Six

- Figure 6.1. Future development of degradation models for assessment of cartilage substitution materials.** It will be possible to use the simple configuration degradation models for assessment of cartilage substitution in a range of formats. **A.** Osteochondral pin against cartilage substitution plate. **B.** Osteochondral pin against osteochondral plate with cartilage substitution material insert. **C.** Cartilage substitution material pin against osteochondral plate. **233**

List of Tables

Chapter One

Table 1.1.	The Outerbridge system for grading of ex vivo cartilage damage severity	29
Table 1.2.	The minor pro-inflammatory cytokines that promote cartilage degradation	36
Table 1.3.	Minor inhibitory cytokines that inhibit catabolic cytokines	38
Table 1.4.	The MMP subgroups implicated in cartilage degeneration	42
Table 1.5	ADAMTs categories, adapted from (Jones and Riley, (2005))	45

Chapter Two

Table 2.1	Equipment that was used in this study	60
Table 2.2.	Reagents that were used in this study	62
Table 2.3.	Antibodies for labelling of cryosections using Immunohistochemical analysis	64
Table 2.4	Tissue Processor programme 9 for processing of bovine osteochondral pins for wax embedding	70

Chapter three

Table 3.1.	The specific composition of the Ringer's solution used in this study	91
Table 3.2.	The different conditions used to generate mechanical degradation in cartilage	94
Table 3.3.	The post lyophilisation weights of 1ml of moderate Ringer's solution lubricant and Ringer's solution	107
Table 3.4.	The significant differences between the surface roughness (Ra) values of pin replicas taken of mechanically degraded and undegraded control specimens	130
Table 3.5.	The significant differences between the surface roughness (Ra) values of plate replicas taken of mechanically degraded and undegraded control specimens	132

Chapter Four

Table 4.1	Antibiotic concentrations in the antibiotic solution	187
------------------	--	------------

Chapter Five

Table 5.1.	The Co-ordinates used when taking images of particles on the filter	215
-------------------	---	------------

List of Abbreviations

ACI	Autologous chondrocyte implantation
ADAMTS	A disintegrin and metalloprotease with thrombospondin type 1 motif
AFM	Atomic force microscopy
ASTM	American society for testing and materials
BMP	Bone morphogenic protein
BSA	Bovine serum albumin
CILP	Cartilage intermediate layer protein
CoCr	Cobalt Chrome
COMP	Cartilage oligomeric matrix protein
DAMPs	Damage associated molecular patterns
DDSA	Dodecyl succinic anhydride
DMB	1,9-Dimethyl-Methylene Blue
EDTA	Ethylenediaminetetraacetic acid
ECM	Extracellular matrix
ESEM	Environmental scanning electron microscopy
FACIT	Fibril associated collagens with interrupted triple helices
BFGF	Basic fibroblast growth factor
FGFs	Fibroblast growth factors
GAG	Glycosaminoglycan
GalNAc	N-acetyl galactosamine
GlcA	Glucuronic acid
HABR	Hyaluronan binding region
HC-gp39	Human cartilage glycoprotein
HCL	Hydrochloric acid
HXP	Hydroxyproline
IGF-	Insulin like growth factor
IGFB	Insulin like growth factor binding protein
IL-	Interleukin growth factor
IL-1RI	Interleukin one receptor type one
IL-1RII	Interleukin one receptor type two
KS	Keratan sulphate

LVDT	Linear variable differential transformer
MMP-	Matrix Metalloprotease
MPa	Mega Pascals
NBF	Neutral buffered formalin
NO	Nitric oxide
NSAIDS	Non-steroidal anti-inflammatory drugs
OA	Osteoarthritis
OCT	Optimal cutting temperature embedding medium
PBS	Phosphate buffered saline
SAL	Surface amorphous layer
SEM	Scanning electron microscope
STZ	Supercial tangential zone
SZP	Superficial zone protein
TBS	Tris buffered saline
TEM	Transmission electron microscopy
TGF-β	Transforming growth factor beta
TKR	Total knee replacement
TNF receptor I	TNF alpha receptor one
TNF receptor II	TNF alpha receptor two
TIMPs	Tissue inhibitor of metalloproteases
TNF-α	Tumour necrosis factor alpha
TSP-	Thrombospondin type domain
UHMWPE	Ultra high molecular weight polyethylene
UKA	Unicompartmental knee arthroplasty

Chapter 1

General introduction

1.1 Introduction to cartilage

Within the body there are three major types of cartilage: hyaline cartilage, elastic cartilage and fibrocartilage. Hyaline cartilage is the most common cartilage found in the body and sub types of hyaline cartilage exist, the most typical sub-type being articular cartilage. Articular cartilage is an aneural and avascular tissue found at the ends of long bones such as the tibia and the femur that contributes to the low friction environment found in synovial joints and helps to distribute loads over a relatively broad area. Articular cartilage consists of an extracellular matrix phase and a small number of sparsely distributed cells called chondrocytes bathed in a fluid phase consisting of water and inorganic salts. Articular cartilage is an anisotropic material due to its zonal structure.

Articular cartilage is a semi-transparent white material with a glossy glass like surface. Articular cartilage, along with synovial fluid and other joint components helps to create an almost friction free, congruent environment for the articulation of adjacent long bones. The coefficient of friction of fully hydrated normal healthy cartilage articulating on cartilage is very low; it is in the range of 0.002-0.02 (Mow & Huijskes 1979). The intrinsic properties conveyed on cartilage by its internal components allow it to withstand substantial loads while it continues to provide a low friction environment (Greenwald & O'Connor, 1971). This ability is reduced in situations where the cartilage has been damaged for example in the disease osteoarthritis.

1.2 Joints and joint components

1.2.1 The knee joint

The knee is the largest and most complex joint in the human body. The hard tissues of the knee joint are comprised of the medial and lateral condyles of the femur, the tibial plateau and the patella (patella not shown; Figure 1.1). The knee is primarily a hinge joint. It allows flexion and extension in addition to some limited rotation during flexion. As the knee undergoes flexion or extension, the femoral condyles roll across the tibial plateau. The menisci found in the knee are important during flexion and extension because they fit between the two articulating bones and provide increased congruity. The knee joint is relatively unstable in comparison with other joints in the body and is heavily supported by the surrounding muscles, tendons and ligaments in the joint.

The joint capsule within the knee consists of an external fibrous layer and an internal synovial membrane. The synovial membrane lines any area of the joint space that is not covered by cartilage and contains synoviocytes which secrete synovial fluid. The menisci are crescent shaped plates of fibrocartilage found on the surface of the tibia that play a role in shock absorption as well as providing a more congruent environment between the femur and tibia. In cross section they appear wedge shaped with their external edges attached to the joint capsule of the knee.

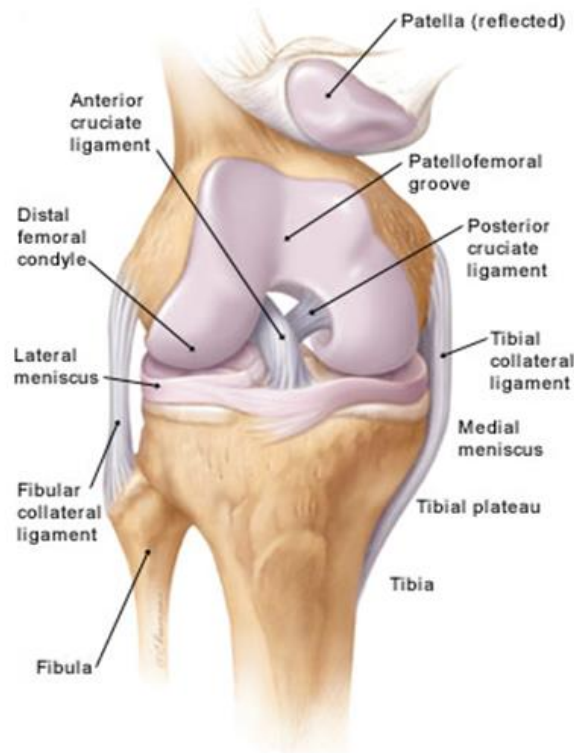


Illustration © 1999 Christy Krames

Figure 1.1. Anterior view of the human knee joint, showing the major ligaments, bony structures and meniscus. Articular cartilage is shown in purple covering the femur above the menisci. Taken from <http://warwickphysio.com>

1.2.1.1 The mechanical environment of the knee

The knee undergoes a large range of stresses during normal physical activity. This can result in the application of a variety of contact stresses on the cartilage which can range from 2.8 MPa during slow walking, 14 MPa during fast walking and 26 MPa during deep flexion of the knee (Thambya *et al.*, 2005 ; Yoshida *et al.*, 2006). The normal range of motion in the knee in women and men is usually 5 to 143 degrees and 6 to 140 degrees respectively. However, hyperextension of the knee is possible which results in a range of motion that includes a

negative value. It has been estimated that to rise from a seated position the knee requires 93 degrees of flexion, while shoelace tying requires 106 degrees of flexion (Laubenthal *et al.*, 1972).

1.3 Cartilage structure

Cartilage tissue has an inhomogeneous structure because the components of the tissue change in quantity, orientation and structure throughout the tissue. The layers or zones are classified into the superficial zone, or superficial tangential zone (10-20% of cartilage depth), the middle zone (40-60% of cartilage depth) the deep zone (30% of cartilage depth) and the calcified zone (Figure 1.2; Wu & Herzog., 2002).

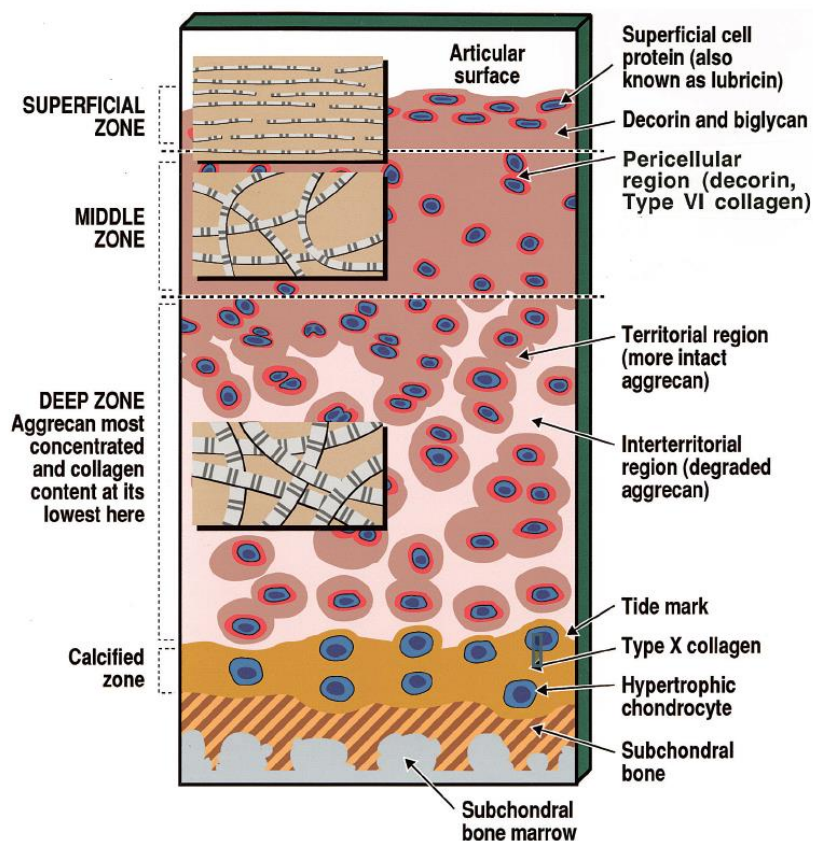


Figure 1.2. The zonal arrangement of articular cartilage taken from Poole *et al.* (2001). The image includes details of the territorial and interterritorial regions of the tissue including the proteoglycan arrangements in each zone. The images in the beige boxes highlight the variable collagen morphologies seen through the tissue.

1.3.1 Surface amorphous layer (SAL)

The superficial zone of cartilage is covered by an amorphous layer thought to be up to 450 μm in thickness (Crockett *et al.*, 2005). The surface amorphous layer (SAL) can be separated into

two zones, the surface laminar layer adjacent to the superficial tangential layer and a boundary layer found above the laminar layer. The SAL contains lipids, proteins and glycosaminoglycans (Graindorge *et al.*, 2006). It does not contain collagen or cells. Treatment of the SAL with α -chymotrypsin has been shown to lead to disruption and thinning of the SAL and an increase in friction (Teeple *et al.*, 2007). The SAL is thought to protect collagen in the tissue from fibrillation and to be responsible for the low coefficient of friction measured on the initiation of motion in load bearing joints after prolonged static periods (Forster & Fisher., 1999; Graindorge *et al.*, 2005).

1.3.2 Superficial tangential zone (STZ)

The superficial layer has a low proteoglycan content, a dense arrangement of fine collagen fibres that lie parallel to the articular cartilage surface and flat disc-shaped chondrocytes (Poole, 1997). It is thought that the fine tightly packed collagen in this zone contributes to reduction of acute mechanical stress by distributing the stresses evenly across the articulating surface. This role seems appropriate due to the high levels of tensile and compressive forces which are found in this zone (Nordin & Frankel, 2001).

1.3.3 Middle zone

In this zone the chondrocytes are spherical in shape and the proteoglycan content is at its highest concentration. The collagen fibres become thicker in diameter and more randomly orientated which creates a transitional layer into the deep zone (Poole, 1997). Cartilage intermediate layer protein (CILP) is found exclusively in this region (Lorenzo *et al.*, 1998).

1.3.4 Deep zone

The deep zone is characterised by rounded chondrocytes arranged in columns and a collagen network that is organised into thick bundles perpendicular to the cartilage surface. The proteoglycan content is higher than in the superficial zone (Poole, 1997).

1.3.5 Calcified zone

The calcified zone has a low concentration of proteoglycans. Here, bunches of collagen fibres anchored perpendicularly to the cartilage surface layer span the tidemark; an undulating line

that marks the separation between the deep and the calcified zones. This arrangement, paired with the border that marks the transition from calcified cartilage to subchondral bone (the cement line) ensures the cartilage is firmly anchored to the bone (Poole, 1997).

1.3.6 Pericellular, territorial and interterritorial matrices

In addition to the layers described above, the circumferential matrix surrounding the chondrocytes within the middle and deep layers can also be divided into zones which are determined by their composition and distance from the chondrocytes (Figure 1.2). These zones are known as the pericellular, territorial and inter-territorial matrices (Poole, 1997). The pericellular matrix is found in the immediate proximity of the chondrocytes and is around 2 μm thick. The territorial matrix is regarded as the transitional cell associated matrix found separating the pericellular and inter-territorial regions. The majority of the cartilage that is not included in the previous two zones that is relatively distant from the chondrocytes is designated as the inter-territorial region (Aigner & Stove, 2003). Within the pericellular region the collagen fibrils range from 10-25 nm in thickness, however in the more distal regions collagen fibres become larger with diameters of up to 300 nm (Mow & Huiskes, 2005). The pericellular region is thought to be very important for the biomechanical transduction and modulation of signals such as lateral and axial strain from the extracellular matrix (ECM) to the chondrocytes. Collagen and proteoglycan content, as well as the fluid volume in the pericellular matrix are important factors influencing how the cell is deformed under pressure. Using a finite element model, Julkunen *et al.* (2009), showed that a loss of collagen from the pericellular matrix and an increased fixed charge density could reduce lateral strains on chondrocytes.

1.4 Cartilage composition

Cartilage is composed of both a fluid and solid phase. Water (interstitial fluid) makes up approximately 75% of the cartilage tissue content. Approximately 25% is made up of the solid part of the tissue (Kheir & Shaw, 2009).

1.4.1 Interstitial fluid

Interstitial fluid is composed predominantly of water, the distribution of which varies throughout the tissue, with water content being most abundant at the articular surface (Mow & Huiskes, 2005). Interstitial water exists internally (intrafibrillarly) and externally

(extrafibrillarly) to the collagen fibres in articular cartilage. The volume of intrafibrillar water is regulated by the fixed charge density generated by the surrounding proteoglycans (Katz *et al.*, 1986). Extrafibrillar water is free to move throughout cartilage tissue due to hydraulic and osmotic pressure gradients, whereas intrafibrillar water is not. The volume of extrafibrillar water varies with age: it has been reported that the volume of extrafibrillar water in the cartilage decreases with age (Torzilli, 1988). It is the internal to external (and vice-versa) movement of the extrafibrillar water that allows reversible cartilage deformation after cartilage has been subjected to loading (Mow & Huijskes, 2005). The ions found most commonly in the interstitial water are sodium, chloride, potassium and calcium (Linn and Sokoloff, 1965; Mow *et al.*, 1999) and for the most part they can participate in un-restricted diffusion between the tissue and its external surrounding environment.

1.4.2 Collagen

Cartilage has a fibrous ultrastructure composed of collagen. The collagen matrix integrity is important for regulation of the structural properties of cartilage, as it provides cartilage with tensile strength. Conversely, collagen has a poor compressive resistance (Bader *et al.*, 1992). Collagen withstands the swelling pressures created by proteoglycans in the cartilage (Mow & Huijskes, 2005). However, this is not the only function of the collagens, which have a broad spectrum of roles. Some types of collagen, as of yet, have undefined functions.

Collagen consists of three left handed helix procollagen peptide chains, which can be heterogeneous or homogeneous. The peptide chains are twisted together to form a tightly wound right handed triple helix (Dejica *et al.*, 2008). The triple helix, is stabilised by hydrogen bonds. The polypeptide chains themselves are formed from a repeating triplet structure in which every third amino acid within the polypeptide chain is glycine. The amino acids, hydroxyproline and proline often constitute the remaining residues within the repeating triplet structure. Glycine is an amino acid with a small side group. The small size of glycine is important for formation of correct collagen structure as it is necessary for the assembly of the tightly wound right handed collagen helix. The triple helix formed from the three peptide chains is known as a micro-fibril and in fibrillar collagens, many micro-fibrils associate to form larger functional collagen fibres which are stabilised by intermolecular cross-links (Figure 1.3 ; Dejica *et al.*, 2008). The triple helix collagen domains are flanked by non-collagenous domains (Gordon & Hahn, 2010). Non-collagenous domains are involved in several processes including alignment, nucleation and folding of the collagen triple helix (Brass *et al.*, 1992).

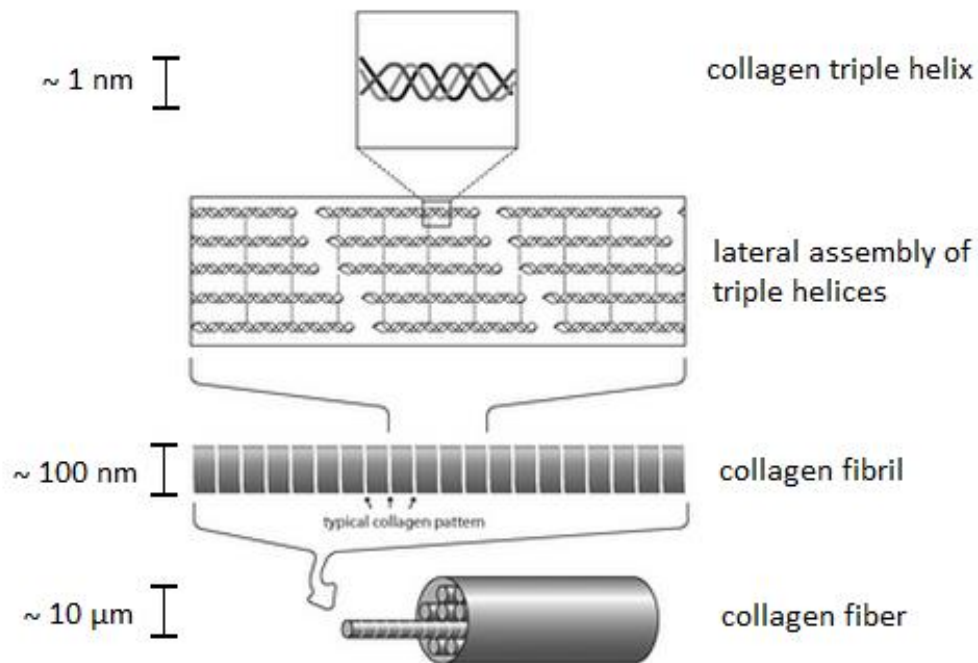


Figure 1.3. The hierarchical structure of a collagen fibre. Initially, three polypeptide chains form a left-handed triple helix. From there, several triple helices assemble to produce collagen fibrils that in turn align to form a mature collagen fibre. Adapted from Heim *et al.*, 2010.

There are over 20 types of collagen all of which contain sequence variations and differ in polypeptide length. Cartilage predominantly contains type II collagen. Other collagens are also present in smaller concentrations, for example types VI, IX, X and XI (Bruckner & van der Rest, 1994; Aigner & Stove, 2003). Collagens do not exist strictly in homogeneous states. In cartilage, fibrils are formed from collagen type II that contain a type XI collagen core. Type IX collagen is found distributed on the fibril surface and is known as a fibril associated collagen (Mendler *et al.*, 1989). Collagen types VI and X form beaded filaments and hexagonal structures, respectively. Collagens are orientated differently throughout the cartilage resulting in anisotropic properties and various zones within the tissue.

1.4.2.1 Collagen II

Collagen II represents the largest percentage of the collagen volume in cartilage, accounting for up to 60% of the tissue dry weight. Collagen II consists of three identical polypeptide α chains. In cartilage it is found associated with collagens IX and XI in an 8:1:1 ratio, respectively (Vaughan *et al.*, 1988). Collagen II is synthesised as procollagen and undergoes post-

translational modification which involves removal of the N and C terminal signal domains, hydroxylation and glycosylation.

Collagen II exists as two different splice variants: collagen IIA and IIB. Collagen IIB is the dominant variant found in mature cartilage. Collagen IIB is produced as a result of differential splicing; the second exon is spliced from the primary COL2A1 gene product, resulting in the absence of a cysteine-rich 69-amino acid domain from the mature protein. Collagen type IIA is present in mature cartilage but in smaller amounts as collagen IIA is usually only produced by immature chondrocytes in developing cartilage (Ryan and Sandell, 1990; Matyas *et al.*, 1997). The two splice variants can have an effect on chondrocyte morphology: the removal of the second exon predisposes cells to a rounded shape. In cells producing collagen IIA, the presence of the second exon results in spindle shaped cells (Sandell *et al.*, 1991). Interestingly, collagen IIB mRNA is co-expressed with aggrecan mRNA supporting the theory that both components are required for a functional extracellular matrix (ECM).

1.4.2.2 Collagen VI

Collagen VI is a trimer composed of three heterogeneous polypeptide α chains. It is a combination of $\alpha 1(VI)$ and $\alpha 2(VI)$, both of which are 140 kDa in size and an $\alpha 3(VI)$ chain which is 260-300 kDa (Lampe & Bushby, 2005; Gordon & Hahn, 2010).

Collagen VI is synthesised as monomers, which aggregate to form tetrameric structures through non covalent interactions. Collagen VI has been observed through transmission electron microscopy as a highly branched fine network that laces in between and around collagen fibrils within tissue (Keene *et al.*, 1988).

1.4.2.3 Collagen IX

Collagen IX is a heterotrimeric molecule composed of three distinct polypeptide chains: $\alpha 1(IX)$, $\alpha 2(IX)$ and $\alpha 3(IX)$, that assemble in a 1:1:1 ratio (Bruckner & van der Rest, 1994). Collagen IX belongs to a group of collagens known as fibril associated collagens with interrupted triple helices (FACIT collagens). Collagen IX contains a glycosaminoglycan side-chain attachment site and is found exclusively in tissues that also contain collagen type II (Myllyharju & Kivirikko, 2001).

Collagen IX contains a chondroitin sulphate GAG binding region that exhibits covalent bonding to chondroitin sulphate (Mendler *et al.*, 1989). Collagen IX binds externally to the collagen fibril network in a regular d-periodic arrangement via its chondroitin sulphate chain (Mendler *et al.*, 1989; Vaughan, 1988). Collagen IX is believed to be important for both

stabilising the collagen network formed from collagen II and XI and increasing the efficiency of fibril formation. Therefore collagen IX assists in resistance to proteoglycan induced swelling and tensile stresses generated in cartilage exposed to loading. However, collagen IX is not essential for fibril formation and other roles for this collagen remain to be elucidated (Blaschke *et al.*, 2000).

1.4.2.4 Collagen X

Collagen X is a network forming collagen like collagen VI. In cartilage, collagen X assembles into hexagonal networks (Kwan *et al.*, 1991). There is only one possible collagen X α -polypeptide chain variation, which naturally results in the ability of this collagen to form homotrimers only. Collagen X is found in hypertrophic cartilage as “filamentous mats”, generally in close proximity to hypertrophic chondrocytes, although it has also been observed in association with collagen II in regions further from chondrocytes. In healthy adult cartilage it is found in the calcified region of the tissue. Collagen X reaches distal zones via diffusion through the extracellular matrix, as a result of its small size (Chen *et al.*, 1990; Gannon *et al.*, 1991).

There is a correlation between the hypertrophic characteristics of chondrocytes and collagen type X production (Gibson and Flint, 1985). Hypertrophic cartilage is observed during endochondral bone formation. Ultrastructural studies have shown that within a hypertrophic environment, collagen II is coated with type X collagen before tissue calcification begins to occur, this leads to a possible role of collagen X in hypertrophic cartilage matrix calcification. Collagen X is increased in chondrocytes of the superficial zone of osteoarthritic cartilage and may also be important for assisting with degradation of the hypertrophic cartilage matrix. This is because collagen X contains collagenase and elastase binding sites. Therefore its presence in the pericellular region may facilitate concentration of collagenases for matrix remodelling activity (Echtermeyer *et al.*, 2009; Schmid *et al.*, 1990). Collagen X may also designate specific collagen fibrils for degradation as bone and marrow replace embryonic cartilage during development (Schmid *et al.*, 1990).

1.4.2.5 Collagen XI

Collagen XI participates in the formation of the fibrous collagen network in conjunction with collagens II and IX. Collagen XI molecules are attached to collagen type II via covalent hydroxylysine-based aldehyde cross links. Collagen XI lies both within and on the surface of collagen II fibres (Cremer *et al.*, 1998; Blaschke *et al.*, 2000). The specific role of collagen XI is to regulate fibril formation by collagen type II, its presence during fibrillogenesis leads to strict

fibril diameter control. In a study by Blaschke *et al.* (2000), it was suggested that the large N-terminal domain found attached to collagen XI can span eight adjacent collagen II molecules. This mechanism leads to a restriction on atypical growth of the collagen II fibre.

1.4.3 Cartilage proteoglycans

Proteoglycans are a group of highly diverse protein polysaccharides synthesised by stromal cells including chondrocytes that account for around a quarter of the dry weight of cartilage.

Proteoglycan macromolecules are negatively charged at physiological pH and consist of a protein core to which many glycosaminoglycans (GAGs), such as chondroitin sulphate and keratan sulphate are attached (Mow and Lai, 1979; Lee *et al.*, 1981).

Proteoglycans are integral for the correct functioning of cartilage because they are responsible for the regulation of its internal fluid transport and therefore its time-dependant viscous properties (Bader *et al.*, 1992). Proteoglycans also confer cartilage with an ability to withstand compressive stresses during loading due to their negative fixed charges. A loss of proteoglycans has been shown to increase friction in joints, this may be due to a reduction in support from the fluid phase during loading (Katta *et al.*, 2007; Naka *et al.*, 2005). Proteoglycans are held in place within the cartilage matrix by the tight meshwork of collagen fibres. Cartilage proteoglycans include aggrecan, biglycan, decorin, fibromodulin and lumican.

1.4.3.1 Aggrecan

The most common proteoglycan found in cartilage is aggrecan (Figure 1.4). Aggrecan constitutes 80-90% of the total proteoglycan content found in cartilage and has a hyaluronan binding region (HABR) that facilitates chondrocyte-aggrecan interactions (Mow & Huiskes, 2005). The bond between hyaluronan and aggrecan is non-covalent and is stabilised by a link protein. It is an important bond because it results in mass immobilisation of aggrecan and provides structural stability and rigidity within the extracellular matrix. The sheer size of aggrecan also helps to retard its movement in situ as it is such a large molecule held in a relatively small space. Up to 100 aggrecan molecules can attach to each hyaluronan chain (Morgelin *et al.*, 1988). Aggrecan has three globular domains, G1, G2 and G3. The G1 domain (HABR) is located at the N terminus. It contains small amounts of keratan sulphate and N-linked oligosaccharides. The G2 region lies in between the HABR and the keratan sulphate rich region found in the G3 domain at the C-terminus (Nordin & Frankel, 2001).

Approximately 150 GAG chains are covalently attached to each individual aggrecan molecule, which are accompanied by O and N linked oligosaccharides all of which are un-

equally distributed resulting in the specific individual GAG rich domains described above (Nordin & Frankel, 2001).

Despite having a generic basic structure, two distinct populations of aggrecans have been identified, one present only in adult cartilage that is rich in keratan sulphate and one present throughout life that is rich in chondroitin sulphate (Nordin & Frankel, 2001). As cartilage ages, its proteoglycan content changes, for example, there is a decrease in chondroitin sulphate concentration. Loss of aggrecan due to disturbances in proteoglycan metabolism leads to a loss of extracellular matrix integrity and consequently results in joint disease (Mow & Huiskes, 2005).

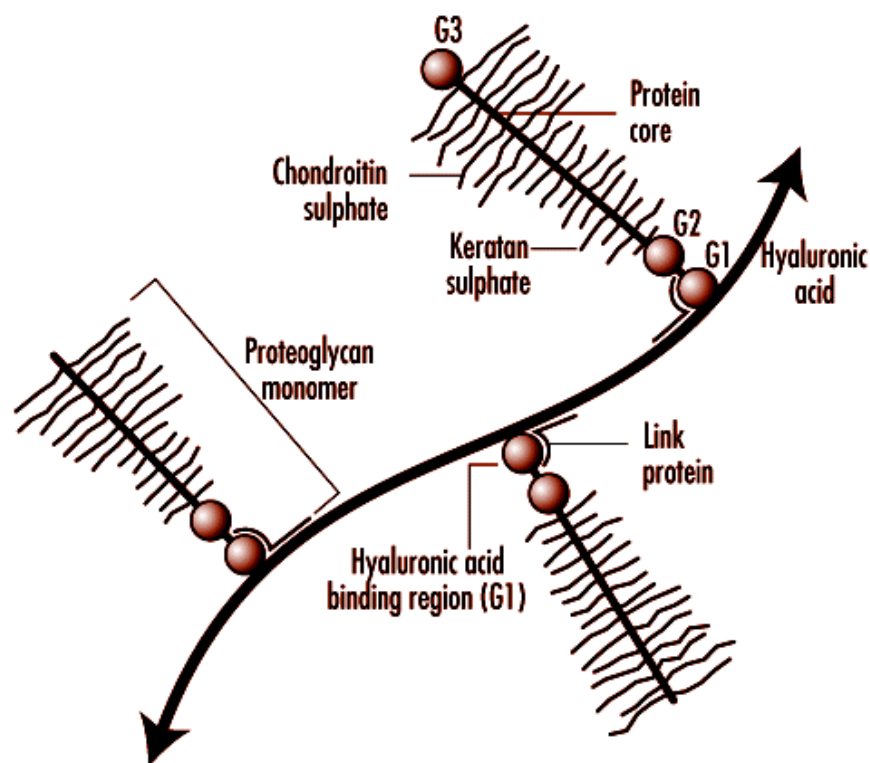


Figure 1.4. The structure of aggrecan and its interaction with hyaluronan.

1.4.3.2 Small leucine rich proteoglycans

Despite appearing in relatively low quantities within cartilage, small leucine rich proteoglycans (SLRPs) are important for the correct organisation and function of cartilage. The SLRP class of proteoglycans includes decorin, biglycan, fibromodulin and lumican. Decorin, fibromodulin and lumican are known to assist with collagen fibril formation, more specifically, regulation of fibril diameter (Danielson *et al.*, 1997; Chakravarti *et al.*, 1998; Svensson *et al.*, 1999). Decorin also interacts with collagen VI and collagen II which may help to bolster interactions between these

two collagens (Bidanset *et al.*, 1992 ; Hedbom, *et al.*, 1993). Biglycan interacts with collagen VI and induces it to form hexagonal networks (Wiberg *et al.*, 2002). Both biglycan and decorin in association with maitrilin-1 have been shown to mediate interactions between collagen VI and both collagen II and aggrecan (Wiberg *et al.*, 2003).

Decorin, fibromodulin and lumican have been reported to protect collagen II from degradation via restriction of access to collagen II fibrils by degradative enzymes such as matrix metalloprotease 13 (MMP-13 ; Geng *et al.*, 2006; Roughley, 2006). In addition to this function, SLRPs can interact with various signalling molecules in the ECM including transforming growth factor- β (TGF- β), which is sequestered by SLRPs to regulate the effects of TGF- β on chondrocytes (Hildebrand *et al.*, 1994). Decorin is also known to down regulate the production of tumour necrosis factor- α (TNF- α ; Yamaguchi *et al.*, 1990). Therefore a loss of small proteoglycans can result in deficiencies in collagen organisation and disruption of normal metabolic processes within the ECM (Merline *et al.*, 2009).

1.4.4 Glycosaminoglycans (GAGs)

GAGs are linear molecules attached to proteoglycan core proteins that contain many negatively charged sulphate and carboxyl groups. The high negative charge of the GAGs in cartilage tissue results in the generation of an electrical potential known as the Donnan potential. To maintain electroneutrality within the tissue, positive counterions move into the cartilage generating a high ion concentration. This draws interstitial fluid into the tissue, causing it to swell. This swelling pressure is known as the Donnan osmotic pressure and it allows the cartilage to maintain a hydrated state. Under physiological conditions, the unequal ion distribution resulting between the cartilage tissue and the external bathing solution, reaches an equilibrium referred to as the Donnan equilibrium. Cartilage swelling is important because it substantially increases the ability of cartilage to withstand physiological loading (Mow & Huiskes, 2005). The various GAGs that are found in cartilage will now be discussed.

1.4.4.1 Hyaluronan (Hyaluronic acid)

Hyaluronan is an unbranched polysaccharide macromolecule found in cartilage and synovial fluid. Hyaluronan differs from other GAGs in that it is not sulphated. It is composed of disaccharide N-acetyl glucosamine units linked to glucuronic acid (Mow & Huiskes, 2005).

Within the synovial fluid, hyaluronan is found twisted into an ellipsoidal configuration. Hyaluronan regulates the viscosity of the synovial fluid through water retention and also

enables it to display non-Newtonian properties. These properties include thixotropy, the property of a fluid becoming less viscous over time when exposed to stresses and elasticity, and the property of becoming less viscous when exposed to shear stress, known as pseudoplasticity. These functions all enable the synovial fluid to protect and lubricate the cartilage.

The other role of hyaluronan in cartilage is to facilitate the formation of immobilised macromolecular aggregates within the collagen network via interaction with aggrecan and the link protein. Additionally, hyaluronan interacts with the cell surface hyaluronan receptor CD44 of chondrocytes to permit synthesis of the pericellular matrix as well as facilitating attachment of chondrocytes to the surrounding extracellular matrix (Knudson & Knudson, 1991; Knudson, 1993; Jiang *et al.*, 2002).

1.4.4.2 Chondroitin sulphate

Chondroitin sulphate is composed of 25-30 disaccharide units of glucuronic acid and N-acetyl galactosamine. Chondroitin sulphate is the most commonly observed GAG found associated with aggrecan. Chondroitin sulphate molecules can be sulphated at either the 4 or 6 position to form chondroitin 4-sulphate and chondroitin 6-sulphate respectively (Baeurle *et al.*, 2009). The species of chondroitin sulphate varies with age and as cartilage ages higher levels of chondroitin 6-sulphate have been observed with reduced levels of chondroitin 4-sulphate (Bayliss *et al.*, 1999).

1.4.4.3 Keratan sulphate

Keratan sulphate (KS) is a linear polymer composed of 13 disaccharide units of galactose and N-acetyl glucosamine. At birth keratan sulphate is present only in small amounts, however its concentration increases with age. There are two classes of KS, known as KSI and KSII which are commonly found in the cornea and cartilage, respectively. KSII is shorter than KSI and is heavily sulphated. The structure of KS can be simplified into three regions: a link region which connects the KS to a core protein (G1). A repeat region composed of the disaccharide unit (G2) and a chain capping region (G3). Most of the KS in cartilage is O-linked to aggrecan between the G2 and G3 regions in a domain characterized by a repeated six-amino acid motif (Flannery *et al.*, 1998)

1.4.4.4 Dermatan sulphate (DS)

Dermatan sulphate is most commonly found in the skin where it is involved in wound repair, it is also present in small amounts in cartilage. Dermatan sulphate is a linear polymer composed of repeated disaccharide units containing a hexosamine, N-acetyl galactosamine (GalNAc) or glucuronic acid (GlcA) motif joined by β 1,4 or 1,3 linkages, respectively. Dermatan sulphate also contains iduronic acid which appears to participate in binding site specificity for GAG-binding proteins.

The length of the DS molecule is variable, as are the location of its sulphation sites and the location of iduronic acid binding, which add to the complex nature of DS and DS-containing proteoglycans (Trowbridge & Gallo, 2002)

Dermatan sulphate accumulation has implications in mucopolysaccharidosis disorders in which there is an absence of lysosomal enzymes or an inability of the enzymes to perform their correct functions, which are required for glycosaminoglycan metabolism. These diseases can lead to a chronic accumulation of dermatan sulphate in cells and cartilage tissue, resulting in severe skeletal dysplasia and short stature.

1.4.5 Non-collagenous proteins

Other minor structural proteins found in the ECM include cartilage oligomeric matrix protein (COMP), fibronectin, cartilage intermediate layer protein (CILP) and matrilins 1 and 3. COMP is involved in extracellular matrix assembly and matrix–matrix protein interactions. It also interacts with fibronectin (Di Cesare *et al.*, 2002). As its name suggests, CILP, is found primarily in the intermediate zone of articular cartilage. Chondrocytes express two isoforms of CILP (Johnson, 2003). The matrilins are involved in the organisation of the extracellular matrix, including the mediation of interactions between ECM components (Wiberg *et al.*, 2003). Matrilins are found associated with collagens and aggrecan (Wagener *et al.*, 2005).

1.4.6 Chondrocytes

Chondrocytes are the only cell type found in cartilage tissue. Chondrocytes are found sparsely distributed through cartilage and account for approximately 3% of the volume of the tissue. Chondrocytes are responsible for the maintenance of the extracellular matrix. They are supplied with nutrients via diffusion through the synovial fluid and underlying bone and do not normally undergo replication after adolescence (Goldring, 2000).

Chondrocytes display both anabolic and catabolic activity, both of which assist the cells in performing their metabolic functions. Anabolic and catabolic activity is necessary for equilibrated matrix turnover and maintenance of ECM integrity. Catabolic enzymes produced by chondrocytes include matrix metalloproteinases and enzymes from the ADAMTS (A disintegrin and metalloproteinase with thrombospondin type-1 motif) family, which includes the aggrecanases (Aigner & Stove, 2003). These enzymes are implicated in the progression of the disease, osteoarthritis.

Chondrocytes are surrounded by a narrow membrane known as the pericellular matrix. Chondrocytes exhibit changes in shape and population number throughout the cartilage resulting in metabolic specialisation which contributes to the depth-related variations in cartilage. Chondrocytes in the calcified layer are rounded, this influences the material properties of the cartilage in relation to the surrounding collagen fibre network (Wu and Herzog, 2002 ; Mow and Huijskes, 2005). Chondrocytes in the superficial layer are less active than those found in the middle and deep layers. In the deeper layers chondrocytes synthesise a matrix with a higher proteoglycan concentration and thicker collagen fibrils.

The distribution of chondrocytes in cartilage, is far from randomised. Chondrocytes have been shown to form four distinct morphological patterns within the tissue depending on their anatomical origin, namely, strings, clusters, pairs of chondrocytes and single chondrocytes. There is usually one dominating pattern of chondrocyte distribution in each cartilage zone. For example in samples of the superficial cartilage of the femoral condyles of the knee joint, over half of the chondrocytes were found in a string formation, whereas over two thirds of cells in the radial head were positioned in clusters (Rolauuffs, *et al.*, 2008). Chondrocyte numbers are specifically adapted to provide optimal conditions within cartilage depending on the zone in which they are found. Chondrocyte populations decrease from the surface to the deep zone and this is thought to provide mechanical stability to the cartilage (Wu and Herzog, 2002)

As chondrocytes age there is an alteration in their metabolic activity. Chondrocytes can undergo senescence which is thought to contribute to the development of osteoarthritis due to alterations in chondrocyte metabolism (Skaalure *et al*, 2012 ; Martin & Buckwalter, 2002).

1.4.7 Synovial fluid

Synovial fluid is secreted by cells known as synoviocytes that are found within the synovium, into the joint cavity. It is an ultrafiltrate of plasma and contains various molecules that are speculated to assist the fluid in its role of contributing towards a friction free environment

within joints. Molecules in synovial fluid include hyaluronan, lubricin, superficial zone protein and surface active phospholipids.

For some time it was believed that hyaluronan was the main lubricating component of synovial fluid however under heavy loads hyaluronan was shown to fail to provide effective boundary lubrication (McCutchen, 1966). This led to the hypothesis that other components of synovial fluid, especially lubricin and superficial zone protein (SZP) could be responsible for the lubricating properties of synovial fluid.

Lubricin is a PRG4 proteoglycan meaning it is synthesised from the proteoglycan 4 gene. Lubricin has been shown to display lubricating properties that are identical to those of synovial fluid as a whole (Swann *et al.*, 1981). However Schwarz and Hills (1998), later published work showing that lubricin is actually a water soluble carrier for surface active phospholipids such as di-palmitoyl phosphatidyl choline, which were responsible for the lubrication abilities of lubricin.

Lubricin is believed to provide lubrication in synovial fluid by depositing hydrophobic surface active phospholipids on the surface of articular cartilage. Lubricin exists in two populations within a synovial joint: both as an unbound molecule in solution and also as a bound molecule, which is attached to the surface of articular cartilage (Gleghorn *et al.*, 2009).

Lubricin has been postulated to partake in various roles aside from lubrication due to its various structural motifs, including cell proliferation and cytoprotection (Flannery *et al.*, 1999).

1.6 The Lubrication, wear and mechanical properties of cartilage

1.6.1 Tribology

The word tribology is used to describe the friction, lubrication and wear properties of a material. Cartilage tribology is interesting because cartilage has various mechanical properties such as viscoelasticity that affect its biotribology and allow it to provide a low friction environment in joints subject to large forces.

1.6.2 Viscoelasticity

The term viscoelasticity is used to refer to materials that undergo a variable time-dependent deformation response followed by recovery when they are exposed to loading and unloading. The specialised properties needed for viscoelastic materials to perform this function arise from the combination of their elastic and viscous properties.

1.6.2.1 Creep

This occurs when viscoelastic solids are subjected to a constant load. Generally, viscoelastic solids initially display a rapid deformation which is followed by a slower (time dependant) progressive response (creep) until a state of equilibrium is reached (Figure 1.5). In simple terms, creep describes deformation of a material at a slow rate after initial rapid deformation.

1.6.2.2 Stress relaxation

This describes the response of a viscoelastic solid exposed to a constant deformation. Generally a viscoelastic solid will initially display a rapid, high initial stress followed by a slower stress that gradually reduces to maintain the deformation.

The extent to which a viscoelastic material is deformed relies on the speed at which the load is applied or removed. In engineering viscoelasticity is represented by two models known as the Kelvin-Voigt and Maxwell models which consist of a spring and a dashpot connected in parallel and a spring and a dashpot connected in series, respectively.

Cartilage is viscoelastic and its response to loading can be represented by the Kelvin-Voigt model. This is due to the elastic properties of cartilage which give it the ability to undergo reversible deformation; internally storing strain energy supplied by an applied load and then consequently being able to return to its original expanded state instantaneously, with some of the strain energy being dissipated as heat. The reason that the response of cartilage is viscoelastic rather than elastic, is due to the involvement of fluid flow in the cartilage tissue. The fluid regulates the return of the cartilage to its pre-loaded state, preventing an instantaneous return. The interstitial fluid in cartilage contributes to a time-dependant response due to frictional drag created between the fluid and the ECM, both when cartilage is being loaded and after the load is removed. Therefore the contribution of this viscous fluid results in viscoelastic properties.

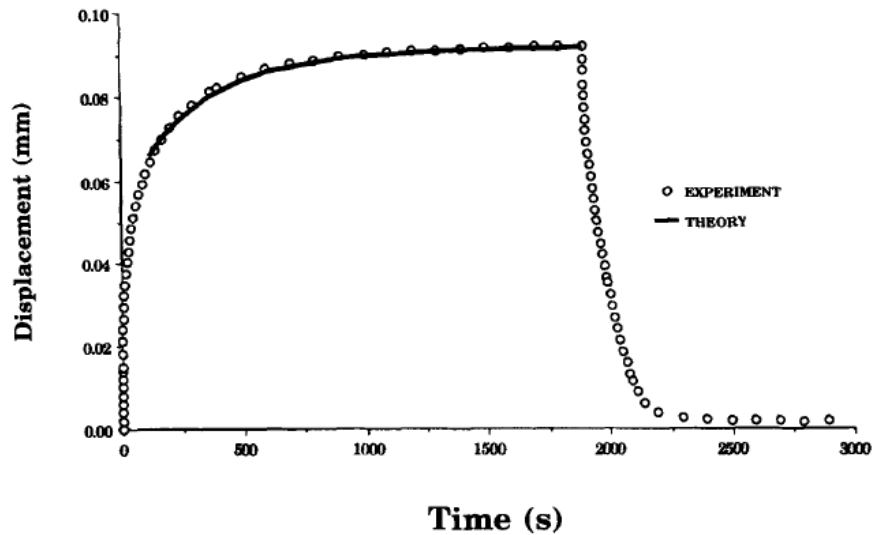


Figure 1.5. A typical creep and recovery curve of the cartilage of the superomedial portion of the femoral head with a corresponding curve fit of the creep. This is the typical response curve of a viscoelastic material in a creep and recovery test showing rapid initial deformation which slows down as it reaches an equilibrium (Athanasίου *et al.*, 1994)

1.6.3 Wear

Wear is the progressive loss of a substance from the surface of an operating body as a result of relative motion at the surface (Jin *et al.*, 2006). Wear is an important factor in the design of joint prosthesis because wear particles that are shed from these replacements are detrimental to the health of the joint. They cause adverse tissue reactions that lead to osteolysis and therefore loosening of the prosthesis (Jin *et al.*, 2006).

Cartilage can become degraded due to wear. In cartilage, wear is caused via mechanical means and is exacerbated by biological degradation. Mechanical wear can be classified into interfacial wear and fatigue wear.

1.6.3.1 Interfacial wear

Interfacial wear occurs as a result of contact between two surfaces in the absence of boundary or fluid-film lubrication mechanisms. It can be further classified into adhesive and abrasive wear.

1.6.3.1.1 Adhesive wear

Adhesive wear occurs when surface protrusions on the bearing surfaces come into contact and attach to each other, followed by movement of the bearing surfaces in opposing directions during which the adhered protrusions are torn from their surfaces.

1.6.3.1.2 Abrasive wear

Abrasive wear is a result of a hard material scraping the surface of a softer material. In a joint this could involve wear particles scratching the cartilage surface. It is thought that in cartilage, there are relatively insignificant levels of interfacial wear taking place because of low occurrences of contact between bearing surfaces, however, in degenerated cartilage the chance of this type of wear may be higher as it may be easier for the fluid film to leak away. This is due to the increased softness and permeability of degenerated cartilage, which is a result of a higher concentration of water in the tissue (Armstrong & Mow, 1982). Abrasive wear can also occur because of loose particles between bearing surfaces, this specific action is known as three-body wear (Nordin & Frankel, 2001 ; Mow & Huiskes, 2005).

1.6.3.1.3 Fatigue wear

This process occurs in bearing materials undergoing repetitive stresses that cause the material to deform and subsequently lead to the production and accumulation of microscopic impairments within it. This can occur under acute and chronic circumstances with repeated short term application of large loads or after repeated application of smaller loads over a long period of time, respectively (Nordin & Frankel, 2001). Within cartilage, fatigue wear could foreseeably accumulate as a result of two mechanisms, the first being through disruption and loosening of the collagen fibres and disruption of proteoglycans and/or the interaction between them and the second through the loss of degraded proteoglycans from the ECM by “wash-out”, where fluid exudation gradually removes the proteoglycans from the ECM.

1.6.4 Cartilage wear particles

When cartilage tissue becomes degraded it can reduce the lubricating ability of the tissue. This means the friction between cartilage interfaces increases resulting in wear particles being created between the two opposing surfaces during loading. It is thought that wear particles can cause inflammation in the joint, therefore augment the progression of degenerative joint

disease (Van den berg, 1999). It has been observed that the shape of wear particles from cartilage tissue varies depending on their zone of origin and on the level of degradation within the tissue (Podsiadlo *et al.*, 1997). For example, as wear increases, wear particles become more complex and less rounded in shape (Graindorge & Stachowiak, 2000). Particles have traditionally been assessed via two dimensional images, however, recently researchers have focused on finding additional useful details about the surface of wear particles that could be added to the list of parameters that are currently considered when grading particles using a numerical system (Tian *et al.*, 2011 ; Tian *et al.*, 2012). The additional features could reveal more information about how cartilage wear progresses and might lead to the establishment of a link between particle surface features and cartilage degeneration.

1.6.5 Cartilage lubrication theories

There is currently no consensus on the definitive lubrication method(s) functioning in synovial joints. Generally it is believed that there is more than one mechanism at work due to the excellent ability of joints to maintain low friction levels under variable conditions (Naka *et al.*, 2005). From an engineering perspective, there are two fundamental types of lubrication: boundary and fluid-film lubrication. Boundary lubrication refers to lubrication caused by a single layer of molecules adsorbed onto bearing surfaces. Fluid-film lubrication consists of a thin fluid film between the two bearing surfaces that leads to a wider separation of the two bearing surfaces so that no boundary lubrication occurs (Nordin & Frankel, 2001).

1.6.6 Boundary lubrication

During boundary lubrication an adsorbed layer of lubricant is found on the surface of each articulating surface (Figure 1.6). The lubricating layer which could be composed of a variety of synovial fluid components including lubricin and surface active phospholipids, prevents direct surface to surface contact (Nordin & Frankel, 2001 ; Schmidt *et al.*, 2007). Boundary lubrication has been proposed as a lubrication method for cartilage because cartilage continues to articulate at low levels of friction in the absence of synovial fluid. Because of the low fluid levels associated with boundary lubrication it is regulated less by fluid viscosity and speed of surface articulation and more by the physiochemical properties of the bearing surfaces (Nordin & Frankel).

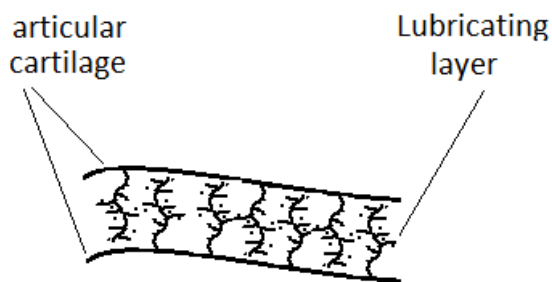


Figure 1.6. Boundary lubrication between opposing articular cartilage surfaces.

1.6.7 Fluid-film lubrication

There are various sub-types of lubrication that involve the use of fluid film lubrication which are discussed below.

1.6.7.1 Hydrodynamic lubrication

This process occurs when two non-parallel rigid surfaces undergoing fluid-film lubrication slide across each other at speed and create a wedge of fluid that produces a lifting pressure. In a synovial joint, the lifting pressure is formed by viscous synovial fluid that is forced between the narrow wedge shaped gap formed by the two bearing surfaces, thereby separating them (Figure 1.7).

1.6.7.2 Squeeze-film lubrication

Squeeze film lubrication is the result of two bearing surfaces travelling perpendicularly towards each other where the fluid film becomes pressurised due to the viscous resistance of the synovial fluid, which delays its exudation from the space between the cartilage (Figure 1.7). This method is likely to occur under heavy loads for short periods of time before boundary lubrication begins to take place as a consequence of asperities present on the cartilage surface (Nordin & Frankel, 2001).

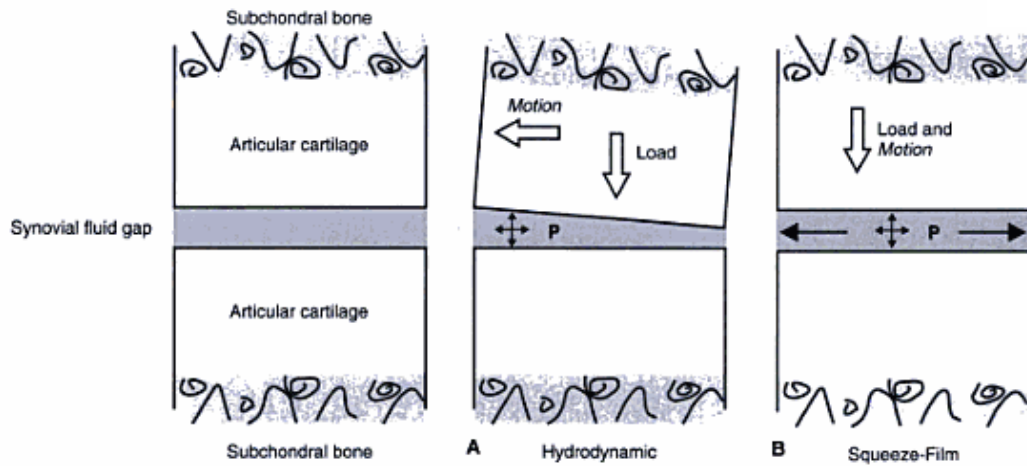


Figure 1.7. Hydrodynamic and squeeze film lubrication in the context of a joint. Adapted from Nordin and Frankel, 2001.

1.6.7.3 Elasto-hydrodynamic lubrication

This type of lubrication can occur during hydrodynamic or squeeze-film regimes. It refers more specifically to the action of the bearing surfaces than that of the synovial fluid because the bearing surfaces must be soft enough to undergo deformation when pressure is exerted on them for elasto-hydrodynamic lubrication to occur. In a synovial joint the deformation works to decrease friction by increasing the surface area of the cartilage while simultaneously decreasing the asperities on its surface thereby creating a more congruent environment. The larger surface area helps to hinder the loss of the fluid from between the surfaces, so the fluid film can persist for a longer period of time (Nordin & Frankel, 2001).

1.6.8 Mixed lubrication

Mixed lubrication is used to describe the combination of boundary and fluid film lubrication regimes that can occur in cartilage. Boosted lubrication is the term used to describe the transient conversion observed as the joint switches from fluid-film lubrication to boundary lubrication at one defined point on the cartilage within the joint. During boosted lubrication, fluid moves from the space between the articulating surfaces into the cartilage followed by small solutes leaving a synovial gel that lubricates the cartilage. Boosted lubrication is most likely to occur during periods of high impact after long exposure time to loading, when fluid-film lubrication is not possible.

The other type of mixed lubrication refers to the temporary existence of both boundary and fluid-film lubrication at “spatially distinct locations” in the joint at the same point in time. For example when fluid-film lubrication is functioning dominantly but a surface asperity on the cartilage causes contact of the two articulating surfaces and boundary lubrication occurs (Nordin & Frankel, 2001).

1.6.9 Biphasic lubrication

Cartilage is a biphasic material in the sense that it is composed of a porous solid phase and an incompressible fluid phase. The fluid phase is composed of water and electrolytes while the solid phase consists of collagen (predominantly type II), proteoglycans, non-collagenous proteins and chondrocytes. The biphasic nature of cartilage partly explains why it is so good at maintaining a low friction environment in the joint.

When cartilage becomes loaded, there is a rapid efflux of interstitial fluid from high pressure regions of the joint, through the solid matrix into the low pressure regions of the joint. The initial rapid fluid flow progressively decreases until the maximum volume of fluid has been squeezed from the matrix. The low permeability of the extracellular matrix to the interstitial fluid is key to the success of initial fluid phase loading because movement of the interstitial fluid through the ECM causes high frictional drag forces within the cartilage which causes compaction or “pressurisation”. As a result the fluid phase supports up to 90% of the load, relieving the solid phase of high loads until all the interstitial fluid has been excluded from the tissue. When the equilibrium strain is reached (this typically takes around 4-6 hours for human cartilage samples with a thickness of 2-4mm) creep ceases and the compressive stress within the ECM is sufficient to allow the solid phase to bear the whole of the applied stress. In these circumstances other lubrication methods such as boundary lubrication must become active to prevent friction in the joint due to the articulating surfaces coming into close proximity of each other (Nordin & Frankel, 2001).

This mechanism of successive loading onto two phases is known as biphasic lubrication. Biphasic lubrication leads to reduced friction between the two articulating surfaces. Experimental data has shown that long loading times are the parameter most likely to cause larger friction coefficients in reciprocating motion simulations inferring that friction increases as the fluid phase depletes (Forster & Fisher, 1999). The frictional drag force created by pressurisation due to loading contributes to the viscoelasticity and energy dissipation functions of cartilage which are essential for its low friction capabilities (Mow & Huiskes, 2005). Additionally, as more pressure is applied to the cartilage over time, it is more difficult to squeeze fluid from it (Mow & Huiskes, 2005). The exudation of fluid from the cartilage also

results in an increased concentration of proteoglycans in cartilage as it becomes compacted, this contributes to the cartilage's ability to resist compression

A triphasic model of cartilage has been developed which includes reference to the monovalent ions found in the interstitial fluid described previously. It was developed to explain the ion-induced swelling effects and other electromechanical behaviours of cartilage (Mow & Huiskes, 2005).

1.7 Osteoarthritis and cartilage degeneration

The avascular and aneural nature of cartilage means it has only a limited ability to repair itself. This inability leads to progressive cartilage damage through acute and chronic injuries and potentially an eventual diagnosis of osteoarthritis. Osteoarthritis (OA), which can occur in primary and secondary forms, is a chronic and debilitating disease primarily characterised by loss of cartilage within the affected joint.

Osteoarthritis is the most common form of joint disease. Approximately 8.75 million people in the UK have sought treatment for OA and more than one million adults consult their GP every year about the disease (arthritisresearchuk.org). OA has a higher prevalence in people over 45 and is more common in women. In the year 2011, over 66,000 primary hip replacements and over 77,000 primary knee operations were performed due to OA in England and Wales (National Joint Registry, 2012).

1.7.1 Primary and secondary osteoarthritis

Primary OA develops progressively over time and has no known cause. It is therefore linked to aging and is usually diagnosed in people aged 60 years old and above. Secondary OA refers to OA caused by damage that is initiated after acute trauma to a specific joint component occurs, for example, the meniscus, ligaments, cartilage and subchondral bone. Various factors are believed to contribute to the progressive biological and mechanical degeneration of articular cartilage such as trauma in the joint, enzymatic degradation and abnormal mechanical forces. The development of OA also has links to age, genetics, gender and environmental factors such as activity levels and the nature of an individual's employment. For example, a common problem for ballet dancers is joint pain in the ankles caused by large and abnormally frequent loads (Mow & Huiskes, 2005). Treatment for both primary and secondary OA is usually the same however joint replacement therapies are less suitable for younger patients with secondary OA due to the limited life span of implants.

Temple-Wong *et al.* (2009) concluded that cartilage degeneration is due to degradation and loss of collagen and proteoglycan matrix components, abnormal collagen network remodelling, consequences of decreased cellularity, and mechanical wear. Consequences of osteoarthritis include joint deformation, cartilage destruction, capsular fibrosis, subchondral bone remodelling and sclerosis and osteophyte formation (Aigner & Stove, 2003).

1.7.2 Early stage osteoarthritis

Early osteoarthritic changes to cartilage include fibrillation at the superficial tangential zone (STZ), cracking and a decreased concentration of proteoglycans through the STZ and middle zones. At this stage, the tidemark becomes enlarged and the subchondral bone begins to penetrate the calcified layer (Nerlich *et al.*, 1993). Morphological changes in osteoarthritic cartilage include softening, discolouration and an irregular surface.

At a molecular level, the ECM shows changes in content compared to healthy ECM. In the early stages of OA there is both a loss of proteoglycans and a decrease in their size. This leads to weakening of the cartilage and a lack of turgor resulting in susceptibility to further mechanical damage and subsequent weakening, resulting in a progressive cycle of damage (L'Hermette *et al.*, 2005). The damage occurs partly because proteoglycan loss reduces the fixed charge density in cartilage, therefore the optimum time-dependant efflux of fluid under loading is diminished (Katta *et al.*, 2007). The disruption of fluid phase loading capabilities could affect the various lubrication methods in action within the joint leading to a reduction in chondrocyte viability resulting in additional damage to the cartilage tissue. Additionally proteoglycan loss and collagen network disruption could result in increased loading on areas of the macromolecular framework, increasing its vulnerability to subsequent mechanical insults.

The collagen network also begins to show signs of deterioration which allows expansion of the proteoglycan network resulting in an increased matrix permeability and increased pore size between collagen fibres. This promotes an increase in water retention that reduces cartilage stiffness (Lorenz & Richter, 2006). This disruption to the collagen component of the tissue could also form part of a cycle of damage leading to further tissue deterioration. Dissociation of collagen-proteoglycan interactions due to cartilage damage could also affect the rate of OA progression. After this primary damage is sustained, chondrocytes react by attempting to repair the damage by increasing production of collagen and proteoglycans. Increased production can continue for several years, until chondrocytes eventually cease to produce elevated levels of these components (Goldring, 2000). Following this, cartilage tissue is lost and osteophytes begin to develop from the subchondral bone.

Osteophytes begin as outgrowths of cartilage which subsequently undergo ossification (Felson, *et al.*, 2005). The exact reason for osteophyte development is not clear however their development is thought to be part of a reparative process (Claassen & Tschirner, 2003). It may be a response to abnormal loading forces experienced by cells in the bone.

Fragments of proteins such as fibronectin found in osteoarthritic joints may aggravate tissue degradation. Fibronectin is elevated in the synovial fluid, on the surface of osteoarthritic cartilage in early osteoarthritis and also within the middle/ deep zones and proximally to OA lesions in late stage OA. The fibronectin is a result of ECM degradation and can enhance synthesis and activation of proteases through interaction with receptors on chondrocytes and synovial fibroblasts. More specifically, stromelysin, gelatinase and collagenase from cartilage which can induce ECM degradation (Homandberg *et al.*, 1992; Yasuda *et al.*, 2003). Additionally, fibronectin expression is increased in osteoarthritic chondrocytes, especially in early degeneration (Aigner *et al.*, 2001).

Damage associated molecular patterns (DAMPs) are tissue damage signals caused by certain molecules that can initiate inflammatory responses. DAMPs can also be known as alarmins (Lukic *et al.*, 2009). DAMPs are thought to initiate inflammatory reactions in tissues through interaction with specific receptors such as toll like receptors 2 and 4 (Kim *et al.*, 2006). DAMP molecules include members of the S100 protein family, such as S100A8, which has been implicated in juvenile idiopathic arthritis (Lukic *et al.*, 2009). It has also been speculated that fibronectin has the potential to be a DAMP. DAMPs are important because it is likely that some DAMPs are involved in the pathogenesis of OA, in addition to certain receptors, including toll like receptors (Scanzello, *et al.*, 2008). Therefore DAMP pathways and receptor interactions are of interest in terms of drug development because inhibition of DAMP pathways may serve to alleviate inflammation in diseases such as OA (Lukic *et al.*, 2009).

Collagen II breakdown products commonly found in osteoarthritic cartilage can lead to the release of a small collagen peptide sequences called CB12-II and CB12-IV. These peptide sequences are capable of increasing collagenase activity and aggrecan cleavage, respectively, as well as promoting an increase in MMP-13 expression by chondrocytes leading to the potential formation of a cycle of catabolism (Yasuda *et al.*, 2006). It is clear however that not all peptide residues contribute to the catabolism of cartilage as some studies have shown that a peptide identical in sequence to the N-terminal of link protein can increase synthesis of proteins including collagen by acting as a growth factor (Liu *et al.*, 2000).

1.7.3 Advanced stage osteoarthritis

In advanced OA, full thickness defects penetrate the whole depth of the cartilage and into the

subchondral bone. Deformation of the bone can be seen in addition to exostotic bone formation and there is a severe loss of proteoglycans. Blood vessels are occasionally observed in highly damaged cartilage that penetrate from the sub-chondral bone through the tidemark (Nerlich *et al.*, 1993).

Full thickness defects unlike partial thickness defects, can initiate a wound healing response by bone marrow progenitor cells that differentiate into chondrocytes to produce ECM. A hematoma is formed within the defect that is replaced by a fibrin clot and finally an ECM that resembles a matrix with elements of both hyaline cartilage and fibrocartilage. Unfortunately however, the resulting repair cartilage has inferior properties compared to native cartilage and can easily become damaged once more (Buckwalter, 1998).

The full thickness cartilage defects seen in advanced osteoarthritic cartilage affect strain distribution over the tissue, with tissue in the proximity of the defects experiencing increased levels of axial lateral and shear strain. In studies in which defects have been loaded in *ex vivo* joints, results have shown collapse of tissue adjacent to the defect, into the defect, with the opposing articulating surface bulging into the void created by the degeneration. Full thickness defects also influence applied normal stress, surface lubrication, friction, sliding path length and the characteristics of the contacting surfaces, all of which influence the rate of wear of the cartilage, this therefore creates a cycle of damage in the tissue. It is also very likely to affect biomechanical transduction to chondrocytes (Gratz *et al.*, 2009). As described above, in advanced stages, chondrocytes are unable to maintain native matrix synthesis indefinitely resulting in total cartilage breakdown and loss (Lorenz & Richter, 2006).

1.7.4 Chondrocytes in osteoarthritis

In the early stages of OA the migratory properties of inflammatory cells through the cartilage tissue are limited. This implies that the source of destructive enzymes found in osteoarthritic tissues, are the chondrocytes. Additionally, it has also been observed that cartilage degeneration originates around chondrocytes in the superficial zone (Hollander & Pidoux, 1995). One obvious stimulus that could explain the catabolic changes to chondrocyte phenotype could be abnormal loading. Various studies have explored the effects of load changes on chondrocyte phenotype and have shown that variable forces can influence either an anabolic or catabolic phenotype of the cells (Smith *et al.*, 2004). In support of this, obesity is a risk factor for osteoarthritis. Increased loading on the joints due to excess body mass may put chondrocytes under abnormal loading conditions which leads to production of catabolic factors that degrade the extracellular matrix.

Degenerative changes to the extracellular matrix induce the chondrocytes to undergo proliferative activities in addition to the synthesis of components to repair the surrounding matrix. However, competent repair is not possible if loss of ECM components occurs more rapidly than the speed at which chondrocytes can replace them and if there is an insufficient number of chondrocytes to perform the reparative processes (Buckwalter, 1998). Overall, the activity of chondrocytes throughout the progression of cartilage degeneration is heterogeneous which is to be expected due to the heterogeneous nature of the cartilage tissue itself. Chondrocyte phenotypes change, and different levels of activity are observed within cells depending on their zonal location. This heterogeneity is reflected by the large variation in the products that chondrocytes synthesise, including variable collagen types. In early OA superficial cells begin producing type III collagen, while deeper cells do not (Aigner *et al.*, 1993). The deeper cartilage layers still contain active chondrocytes while the superficial zone is undergoing degeneration (Aigner and Dudhia, 1997). Adjacent cells in the same environment have been observed to be undergoing variable macromolecule production at the same period in time (Nerlich *et al.*, 1993). Tardif *et al.* (1999), reported on two populations of chondrocytes: H and L chondrocytes, in osteoarthritic cartilage that displayed different response patterns to cytokines. L chondrocytes showed low collagenase 3 (MMP-13) basal synthesis levels and high sensitivity to IL-1 β stimulation and growth factors. H chondrocytes had high collagenase 3 basal synthesis levels and low IL-1 β inducibility with a variable response to growth factors.

At the start of disease progression, chondrocytes in the superficial layer cease to be flattened, become rounded and exhibit hypertrophic activity. Chondrocytes in the medial and deep zones show mild to moderate proliferation leading to hypercellularity, with cells in individual layers producing variable levels of specific collagenases (Fernandes *et al.*, 1998; Lorenz and Richter, 2006). At early stages of OA the synovial membrane also becomes thickened, fibrous and the synoviocytes undergo hyperplasia (Pelletier *et al.* 1985).

The Outerbridge scale is a commonly used grading system for ex-vivo cartilage specimens (Table 1.1). In stage II of OA chondrocytes start to form cell clusters. In the final stages of OA, chondrocyte hypertrophy can be observed in areas with advanced levels of collagen II damage. (Saklatvala, 2003). Chondrocytes also become elongated and fibroblast like, and stain for collagen I and III due to pericellular deposits of these collagens throughout the depth of the cartilage. Levels of these collagens become highest in the latter stages of the disease (Nerlich *et al.*, 1993). Some chondrocytes however continue to produce collagen II at healthy levels during disease progression (Miosge *et al.*, 1998 ; Miosge *et al.*, 2004).

Table 1.1. The Outerbridge system for grading of *ex vivo* cartilage damage severity, (Outerbridge, 1961).

Grade	Distinguishing Features
I	Softening and swelling of the cartilage.
II	Fragmentation and fissuring of cartilage in an area half an inch or less in diameter.
III	Fragmentation and fissuring of cartilage in an area larger than half an inch in diameter
IV	Erosion of cartilage to the bone.

1.7.5 Collagen in degenerated cartilage

Damage to collagen in articular cartilage has been shown to weaken its tensile properties, and stiffness (Bader *et al.*, 1981; Temple-Wong *et al.*, 2009). Although the literature on the role and distribution of collagen in osteoarthritic cartilage still contains certain disparities, there are some trends to be found in the results of different research groups. It is likely that many of the conflicting results could be explained by the heterogeneity of samples and testing methodologies used by different groups and by the largely variable phenotypes of chondrocytes in osteoarthritic cartilage.

Normally in healthy adult articular cartilage, collagen II expression levels are very low and antibody staining reveals an even distribution of type II collagen throughout the ECM. In both early and late OA the levels of collagen II production by the cells is upregulated signified by an increase in collagen II mRNA production (Aigner *et al.*, 1992; Aigner *et al.*, 2001; Grimmer *et al.*, 2006). In stage II of OA, collagen II is upregulated in the middle and deep zones of the cartilage and remains the dominantly produced collagen in degenerating cartilage, despite the increased presence of other collagen types. Despite continued collagen II production the tissue does not become effectively repaired. It may be that the collagen may not sufficiently integrate into the ECM due a loss of other components in the tissue which assist in the integration of collagen into the matrix for example biglycan. Studies that show disparities between collagen expression and actual collagen content observed in tissues stained with collagen antibodies in addition to in situ hybridisation signal experiments support the theory that collagen II is not deposited correctly in the matrix despite increased mRNA levels (Aigner *et al.*, 1992).

Damage to type II collagen has been thought to occur initially around the pericellular region of the STZ and then spread through the cartilage into the deeper zones (Hollander *et*

al., 1995). A study by Saarakkala *et al.* (2010) observed that in early osteoarthritic cartilage collagen fibrils in the STZ show increased disorganisation with the fibres adopting an orientation that was no longer parallel to the cartilage surface. The authors saw no significant decrease in collagen concentrations until the late stages of OA and deduced that the causes of the early fibril disorganisation were mechanical. The same authors also postulated that loss of collagen in very late stages of OA was due to further mechanical wear, reduced lubrication and enzymatic degradation, which leads to a reduction of fibril diameter and the breakdown of fibrils into smaller fragments, allowing them to leach from the tissue. Disruption of fibril orientation was also seen in the deep zones of tissue taken from patients suffering from more advanced stages of the disease.

Increased levels of collagen II have also been found in areas that have suffered from fibrillation, areas that have developed cracks along the cartilage surface or in fibrocartilaginous deposits (Zhang *et al.*, 2007). Subsequent to this damage, the collagen I/III layer in the superficial zone of cartilage becomes thickened and collagen I is deposited primarily in the superficial interterritorial matrix (Nerlich *et al.*, 1993). Miosge *et al.*, (2004), found a 100-fold increase in the amount of collagen I mRNA in stage III OA compared with healthy cartilage. This is significant because type I collagen is not usually present in any great quantity in healthy cartilage.

Osteoarthritic cartilage shows an increase in collagen III, which is not found in healthy cartilage apart from in some occasional small amounts in the superficial layer and as a thin endosteal lining of subchondral bone (Nerlich *et al.*, 1993). These increases occur within the superficial and upper middle zones, in the pericellular matrix of chondrocytes and also in pannus structures that either form over, or within the damaged areas of articular cartilage in the advanced stages of OA. The latter structures may help to provide resistance to mechanical degradation (Aigner *et al.*, 1993 ; Nerlich *et al.*, 1993).

Collagen VI levels are altered during the progression of OA. In healthy cartilage, collagen VI is found concentrated around the pericellular matrix of chondrocytes throughout all of the cartilage zones. Collagen VI can also be found in the interterritorial matrix of the middle and deep zones. In normal cartilage, collagen VI is expressed continuously at a basal rate. In early OA however, collagen VI expression is significantly increased particularly in the deep and middle zones coupled with a decrease in collagen VI mRNA expression in the calcified and superficial zones. In the advanced stages of OA progression, increased collagen VI expression is observed in the matrix and the pericellular regions of chondrocyte clusters. There is also positive staining for collagen VI in the territorial matrix of the deep zone, however this could be due to collagen VI fragments, produced as a result of increased protease presence in the cartilage, that are small enough to diffuse through the matrix into more distal regions. The

physiology of collagen VI is altered during OA. Normally collagen VI is found as fine filaments however a band-like form of type VI collagen has been increasingly observed during disease progression (Aigner *et al.*, 2001; Söder *et al.*, 2002; Pullig *et al.*, 1999).

1.7.6 Proteoglycans in degenerated cartilage

As previously described, proteoglycan loss results in a decrease in the compressive stiffness of cartilage leaving it more susceptible to damage. A decrease in proteoglycan concentration in degenerating cartilage could be due to increased proteoglycan degradation or decreased synthesis, or possibly both. In synovial fluid taken from knee trauma patients and sufferers of OA, large cleaved aggrecan fragments were found which were composed of a short NH₂-terminal stretch of the interglobular domain, the G2 domain, the keratan sulphate domain, and variable lengths of the chondroitin sulphate domain(s) (Sandy *et al.*, 1992). This infers that large pieces of proteoglycan are cleaved and leach out of the tissue. The primary site of cleavage resulting in aggrecan degradation by MMPs is at a Glu 373/Ala 374 motif in the interglobular domain resulting in the removal of the G1 domain from the remaining molecule.

Aggrecan expression is upregulated in the deep zones of osteoarthritic cartilage but a reduction is seen in the STZ when compared to healthy cartilage samples (Aigner *et al.*, 2001). In advanced OA, proteoglycan loss spreads from the superficial zone into the deep zones sometimes resulting in complete proteoglycan loss, shown by a lack of safranin O staining (Lorenz & Richter, 2006).

Lubricin continues to be produced in advanced osteoarthritic cartilage near to the subchondral bone, suggesting that the fibroblast-chondrocytes found here still attempt to provide boundary lubrication in the damaged joint (Zhang *et al.*, 2007).

As cartilage becomes increasingly damaged, levels of decorin and biglycan within different regions of the tissue begin to vary, creating a more heterogeneous distribution than is observed in normal cartilage. However, overall the mean ratio of biglycan and decorin in the tissue remains the same. In healthy cartilage these two small proteoglycans are primarily concentrated in the upper middle zone close to the STZ; the greatest concentration of biglycan has been found in the STZ (Poole, 1996). In osteoarthritic cartilage there is a reduction in biglycan and decorin concentrations in the STZ, which is correlated with collagen degradation observed in this zone (Poole, 1996).

1.7.7 Grading systems for degenerated cartilage tissues

Several grading systems have been developed to assess the extent of cartilage degradation that has occurred in the tissues of patients with osteoarthritis. A commonly used system for grading cartilage tissues *in vivo* via arthroscopy is the Outerbridge system (Table 1.1) which uses simple observations such as swelling and lesions to grade the degradation of cartilage tissues. Recently, the Outerbridge scoring system was incorporated into the International Cartilage Repair Society (ICRS) grading system. The ICRS grading system provides a comprehensive *in vivo* grading system that includes both patients and surgeons, which can determine the extent of degradation in affected cartilage tissues. The ICRS grading system is frequently used to determine whether a patient with osteoarthritis requires surgical intervention to treat their condition. Another frequently used assessment system for *ex vivo* cartilage tissues is the Mankin grading system, which is a histopathological system that grades histological and cellular changes to cartilage tissues affected by osteoarthritis (Mankin *et al.*, 1971).

1.8 Inflammatory changes in degenerated cartilage

Various factors have been reported to contribute to an imbalance of steady state conditions in cartilage leading to its biological degradation. Cytokines play an important role in the progression of healthy cartilage into a degenerated osteoarthritic condition because they can stimulate the production of enzymes such as matrix metalloproteinases (MMPs) by chondrocytes that promote breakdown of cartilage. Catabolic cytokines are those cytokines which stimulate the production of catabolic enzymes cause the breakdown of molecules while anabolic cytokines promote the production of ECM components.

Although many cytokines have been reported to be involved in OA, the primary pro-inflammatory and catabolic cytokines that promote OA progression are interleukin-1 β and TNF- α , with IL-1 β being the most potent of the two. Anabolic activity is promoted by TGF- β , bone morphogenic proteins, fibroblast growth factors (FGFs) 2, 4, 8 and insulin like growth factor (IGF-1) (Sandell and Aigner, 2001). The network of activation created by cytokines is highly convoluted. It includes processes of self activation, activation of other cytokines and synergistic and antagonistic actions between cytokines. The degradation of cartilage tissue that is caused by cytokine and enzyme activity represents the biological axis of cartilage degradation that in combination with the mechanical degradation of cartilage tissues forms the basis cartilage degradation.

1.8.1 Major pro-inflammatory / catabolic cytokines

1.8.1.1 Interleukin-1

The term Interleukin-1 refers to two pyrogenic cytokines known as IL-1 α and IL-1 β . IL-1 α and - β are pro-inflammatory cytokines that are a vital component of the immune defence mechanism that fights infection. IL-1 is produced by a variety of cells but importantly in terms of OA development, by synovial cells and chondrocytes which can result in cartilage breakdown. There is little difference in the biological activity seen between IL-1 α and IL-1 β . For example, they are both able to initiate IL-2 production in activated lymphocytes. Despite this, they only share a 26% sequence homology (March *et al.*, 1985). However, pro IL-1 α is active as a precursor, whereas the IL-1 β precursor is not.

Both IL-1 α and IL-1 β can induce the degradation of proteoglycans in cartilage, for example aggrecan, via the stimulation of aggrecanase production. It is thought that IL-1 α is the most dominant of the two cytokines in terms of aggrecan degradation (Sumer *et al.*, 2006). Work by Williams *et al.* (2000) concluded that IL-1 β was the more dominant of the two IL-1 cytokines concerning the promotion of collagen degradation in OA. IL-1 β is not normally expressed in healthy cartilage tissue, however in osteoarthritic cartilage its expression has been shown to be upregulated (Attur *et al.*, 1998). The activity of IL-1 is transmitted through IL-1 receptors on the chondrocyte cell surface. There are two IL-1 receptors, known as IL-1 receptor type 1 (IL-1RI) and IL-1 receptor type 2 (IL-1RII). IL-1RI is a signal transducer, whereas IL-1RII is a soluble decoy receptor for IL-1 β . IL-1RII together with IL-1 receptor antagonist (IL-1Ra) are inhibitors of IL-1 β , preventing its capability to induce inflammatory responses (Daheshia & Yao, 2008). IL-1 can also induce the production of nitric oxide (NO) (Attur *et al.*, 1998). This is significant because NO is a cytotoxic free radical that has been shown to contribute to cartilage degeneration and chondrocyte apoptosis (Taskiran *et al.*, 1994 ; Blanco *et al.*, 1995).

1.8.1.2 Tumour necrosis factor- α

Tumour necrosis factor- α is a soluble 17 kD protein produced primarily by monocytes and macrophages, however, it is also produced by synovial cells. TNF- α can induce to the cleavage of aggrecan by stimulating the production of A disintegrin and a metalloprotease with thrombospondin motif proteins-4 and -5 (ADAMTs-4 and -5), alongside IL-1 (Tortorella *et al.*, 2001). TNF- α has also been shown to suppress link protein expression preventing stabilisation of the extracellular matrix via in-efficient linking of aggrecan to hyaluronan (Séguin *et al.*, 2003). In mice that over-expressed TNF- α , but not IL-1, inflammation was observed in the

joints, but no cartilage breakdown was seen, suggesting that IL-1 was not essential for inflammatory cell recruitment and that TNF- α mediates the inflammation that can be seen in diseased joints (Milner *et al.*, 2001)

1.8.2 Minor pro-inflammatory/ catabolic cytokines

There are a number of cytokines that have been reported to be involved in cartilage tissue degradation that are not as prolific as IL-1 and TNF- α (Table 1.2). IL-6 has been included in both the catabolic and inhibitory cytokine tables (Table 1.2 and Table 1.3) because of its dual catabolic and inhibitory activity.

Table 1.2. The minor pro-inflammatory cytokines that promote cartilage degradation.

Cytokine	Action	References
IL-6	IL-6 increases inflammatory cell populations in the joint and mediates IL-1 mediated proteoglycan synthesis inhibition in addition to increasing proteoglycan catabolism in cartilage explants. In IL-6 knockout mice, collagen induced arthritis was not observed.	Sui <i>et al.</i> , 2009 ; Nietfeld <i>et al</i> 1990 ; Alonzi, 1998.
IL-8	IL-8 attracts cells of the immune system to sites of inflammation leading to further inflammation and oxidative activity. IL-8 is increased in the synovial fluid of patients with OA.	Henkelsa <i>et al.</i> , 2011 Kaneko, <i>et al.</i> , 2000.
IL-17	Upregulates a number of pro-inflammatory mediators including nitric oxide, MMP-13 and IL-1. IL-17 supresses proteoglycan production.	Jovanovic, 1998. ; Hwang <i>et al.</i> , 2004 ; Attur <i>et al.</i> , 1998 ; Martel-Pelletier <i>et al.</i> , 1999 ; Lubberts, <i>et al.</i> , 2000 ; Benderdour <i>et al.</i> , 2002.
IL-18	IL-18 increases the expression of catabolic gene products such as stromelysin and stimulates nitric oxide production. IL-18 also causes release of proteoglycans from cartilage tissue	Olee <i>et al.</i> , 1999.
Leukeamia Inhibitory factor	LIF inhibits proteoglycan synthesis and promotes proteoglycan release augmented by IL-1 α , IL-1 β and TNF- α .	Carroll & Bell, 1993 ; Hui <i>et al.</i> , 1998.

1.8.3 Inhibitory cytokines

Inhibitory cytokines work to inhibit the activity of catabolic cytokines within the cartilage tissue and the joint. These cytokines therefore help to prevent cartilage degeneration and protect cartilage against osteoarthritic progression.

1.8.3.1 Interleukin receptor antagonist (IL-Ra)

This antagonist is a member of the IL-1 family of cytokines and can be found within the cytoplasm of some cells for example, fibroblasts or can be secreted by cells such as macrophages (Arend *et al.*, 1998). IL-Ra binds competitively to the same receptor as IL-1 to abrogate the effects of IL-1, such as IL-1 mediated tyrosine kinase activity (Dripps *et al.*, 1991). Subsequent to IL-Ra and IL-1 receptor binding, IL-1 receptor accessory protein binds to the complex to complete suppression, which quenches catabolic activity in the tissue.

Research by Economides *et al.* (2003) presented an efficient method of blocking cytokine activity entitled “cytokine trapping”. This system takes into account that initial IL-1 and receptor binding is weak and is reinforced by subsequent receptor accessory protein binding to create a high affinity interaction. Economides *et al.* generated soluble receptors that contained both the receptor and receptor accessory protein components to create potent IL-1 antagonists. This study overcame previous concerns over rapid IL-Ra clearance *in vivo* and inefficient receptor occupancy. A combined IL-4 and IL-13 trap has also now been developed (Economides *et al.*, 2003). In clinical trials on rheumatoid arthritis patients the IL-1 trap has shown promising results and has recently been approved by the American Food and Drug Administration (Guler, *et al.*, 2001; Ratner, 2008).

Table 1.3. Minor inhibitory cytokines that inhibit catabolic cytokines.

Cytokine	Action	References
IL-4	IL-4 and IL-10 can work synergistically to cause potent suppression of IL-1 β , IL-6 and IL-8. IL-4 can also inhibit TNF- α production and induces IL-1Ra production. IL-4 inhibits type 1 helper T cell activation <i>in vitro</i> , which subsequently decreases in IL-1, IFN gamma and TNF- α production.	Van roon <i>et al.</i> , 1995 ; Hamblin, 1993 ; Chomarat <i>et al.</i> , 1995 ; Sugiyama <i>et al.</i> , 1995.
IL-6	IL-6 knock-out mice develop more severe arthritis than wild type mice upon ageing. A lack of IL-6 in mice has also been shown to increase proteoglycan loss compared with wild type mice. Injection of IL-6 into the joint cavity of IL-6 deficient mice has been shown to significantly reduce cartilage destruction. IL-6 can induce TIMP-1 activity which decreases MMP levels.	van de Loo <i>et al.</i> , 1997, Lotz, 1991, de Hooge <i>et al.</i> , 2005.
IL-11	IL-11 inhibits prostaglandin mediated inflammatory activity induced by TNF- α , and reduces cyclooxygenase 2 levels. IL-11 can also work alone or synergistically with IL-10 to inhibit TNF- α and increase TIMP-1 levels.	Hermann <i>et al.</i> , 1998 ; Alaaeddine, 1999.
IL-13	IL-13 has been shown to inhibit nitric oxide production in macrophages via effects on the inducible nitric oxide synthase gene and increases IL-1Ra production in <i>ex vivo</i> synovial membrane fibroblast cells. IL-13 has been shown to inhibit the synthesis of IL-1 β and TNF- α mRNA in addition to inhibiting stromelysin activity.	Jovanovic <i>et al.</i> , 1997 ; Bogdan <i>et al.</i> , 1997.

1.8.4 Anabolic cytokines

These factors promote regeneration of the cartilage tissue, thereby actively ameliorating the degradation that occurs during the progression of OA.

1.8.4.1 Insulin like growth factor-1 (IGF)

IGF exists in two isoforms known as IGF-1 and IGF-2. These two isoforms are functionally different despite being related structurally and immunologically (Blumenfeld & Livne, 1999). IGF-1 is important for cartilage ECM maintenance, for example IGF-1 has been shown to stimulate proteoglycan and collagen synthesis (Guenther *et al.*, 1982 ; Schalkwijk, 1989) in addition to inhibition of IL-1 induced cartilage degeneration via upregulation of the IL-1 decoy receptor (Tyler, 1989 ; Wang *et al.*, 2003).

1.8.4.2 Transforming growth factor- β (TGF- β)

TGF- β has three primary functions: it inhibits cell growth, with chondrocytes and osteoblasts being an exception; it also produces an immunosuppressive effect on cells such as lymphocytes and it promotes deposition of ECM components such as GAGs, proteoglycans and collagen in cartilage ECM (Blumenfeld & Livne, 1999). TGF- β has also been shown to promote proteoglycan synthesis in cartilage tissue, however at excessive concentrations over prolonged time periods TGF- β began to promote degeneration initially within the deeper layers of cartilage, rather than preventing it, suggesting an opposing, detrimental role for this growth factor in some circumstances (van Beuningen, 2000).

1.8.4.3 Bone morphogenic proteins (BMP)

Of the BMP proteins, BMP-7 and BMP-2 appear to afford the most significant protective functions in cartilage tissue. A study by Flechtenmacher *et al.* (1996) showed that BMP-7 increased collagen and proteoglycan production by human articular chondrocytes, particularly collagen II and aggrecan production. BMP-7 is considered to have value as a therapeutic agent to treat osteoarthritis. In combination with microfracture, BMP-7 has been shown to act in a synergistic manner to create cartilage repair tissue that histologically resembles native hyaline articular cartilage. However, the quality of the mechanical and functional properties of this repair tissue remains to be fully characterised (Kuo *et al.*, 2006).

BMP-2 has been shown to stimulate increased collagen II and aggrecan mRNA synthesis in articular cartilage chondrocytes (Grunder *et al.*, 2004). Despite these protective

functions however, some evidence exists that BMPs can initiate production of catabolic MMP-13 (van der Kraan, *et al.*, 2010).

1.9 Matrix metalloproteases (MMPs)

The MMPs are a family of zinc dependent endo-peptidases. They are produced by chondrocytes, although not exclusively, and are key mediators in the turnover of the ECM, facilitating morphogenesis, tissue remodelling and resorption. MMPs exhibit low activity levels in healthy steady-state tissues. They are important factors in the progression of cartilage degradation because they cleave molecules such as proteoglycans and collagens, they also cleave non matrix components (Chakraborti, 2003). The MMP family contains at least 12 enzymes which can be grouped into major sub-categories: collagenases, gelatinases and stromelysins, membrane type MMPs and adamalysins (Bonassar *et al.*, 1996; Koopman & Moreland, 2005).

1.9.1 Matrix metalloprotease regulation

Due to the destructive nature of MMPs, it is important that they are tightly regulated to maintain healthy steady state conditions. Regulation occurs on a multitude of levels that include transcriptional and post transcriptional controls. MMPs are secreted as zymogens which is a factor that contributes to their control. Regulation of the MMP proteins via their inhibitors and activators also occurs and lastly their cell surface localisation is important for their regulation. MMP transcription is primarily regulated by cytokines, growth factors, hormones and cellular transformation. MMP activation pathways are highly complex and include differential regulation, some of which occurs via activation of proteolytic cascades.

1.9.2 Matrix metalloproteases in osteoarthritis

MMPs are major promoters of cartilage degradation, an imbalance of these proteins in cartilage tissue leads to destruction of the ECM. Their levels have been shown to be significantly increased in osteoarthritic cartilage. Their expression is also higher in degenerated areas of cartilage.

Salminen *et al.* (2002) investigated MMP expression in osteoarthritic mouse models and discovered that MMP mRNAs exhibited distinct expression patterns during osteoarthritic disease progression. The most noted increase in mRNA expression was for MMP-13 which was detected at increased levels in the subchondral bone, deep zones of cartilage and in the

synovial membrane. Despite this increase it is thought that MMP-13 does not play a direct role in the initiation of cartilage degeneration, as it has not been found in sites of damage in early stage OA such as fibrillated areas of the superficial zone (Salminen *et al.*, 2002).

Freemont *et al.* (1997) showed, in human knee cartilage, that MMP-1 expression was increased in the superficial zone in early OA and that MMP-3 and -9 were increased in the deeper zones in later stages. MMP-9 and MMP-1 expression were highest in the early stages of the disease and MMP-3 expression was bi-phasic. MMP-1 has also been identified as the most common MMP found in osteoarthritic synovial membranes. This indicates that it could be involved in the initial inflammatory phase of the disease (Koopman & Moreland, 2005). It has been possible to observe co-expression patterns in osteoarthritic development. A study by Aigner *et al.* (2001), observed that MMP-13 appeared to be co-regulated with MMP-2, indicating a synchronised action involving of these both collagenases. It is important to note however that due to the complex heterogeneity of cartilage tissue undergoing degeneration, which could display temporal and spatial variation, that it is difficult to draw conclusions on mRNA expression patterns in reference to whole sections of cartilage tissue in joints.

1.9.3 MMP subgroups

There are several sub-species of MMP thought to be involved in cartilage degeneration, which are described in Table 1.4.

Table 1.4. The MMP subgroups implicated in cartilage degeneration.

Group	MMP	Action	References
Collagenases	MMP-1	Cleaves the α chain of interstitial collagens. Cleaves collagen III preferentially.	Mitchell, 1996; Vankemmelbeke, 1998; Koopman & Moreland, 2005; Tortorella <i>et al.</i> , 2001
	MMP-8	Cleaves the α chain of interstitial collagens. Cleaves collagen I preferentially and can also cleave aggrecan.	
	MMP-13	Cleaves the α chain of interstitial collagens. Cleaves collagen II preferentially.	
Gelatinases	MMP-2	Cleaves collagen via two successive cleavage events. MMP-2 activation is facilitated by membrane type MMP 1 and tissue inhibitor of MMP 2 (TIMP-2).	Patterson <i>et al.</i> , 2001; Sato and Takino, 2010; Kim <i>et al.</i> , 2012.
	MMP-9	Possible role in MMP-13 activation.	
Stromelysins	MMP-3	Broad substrate specificity. The dominant stromelysin in cartilage tissue. Cleaves aggrecan at the Asn341-Phe342 bond found in the interglobular domain. Plays a role in the activation of collagenases.	Flannery <i>et al.</i> , 1992; Murphy <i>et al.</i> , 1987; Knauper <i>et al.</i> , 1993; Koopman & Moreland, 2005; Hooper, 1996
	MMP-10	Broad substrate specificity. Plays a role in activation of collagenases.	
Membrane Type- MMPs	MT- MMPs	Sub-set of the MMP family containing transmembrane C-terminal domains which anchor them to the cell surface. Assist in activation of other MMPs such as MMP-13 and MMP-2.	Mort, 2001; Mort and Billington, 2001; Koopman and Moreland, 2005.

1.9.4 Tissue inhibitors of metalloproteinases

MMPs in healthy cartilage are under strict regulation by endogenous inhibitors known as tissue inhibitors of metalloproteinases (TIMPs), and to a lesser extent α 2-macroglobulin and tissue-factor pathway inhibitor-2 (Brew *et al.*, 2000). TIMPs are produced by chondrocytes and synovial fibroblasts and bind to MMPs with a 1:1 molecular stoichiometry causing their permanent inactivation (Murphy, 2011).

There are four known TIMPs found in humans (TIMPs-1, -2, -3 and -4; Brew *et al.*, 2000). TIMPs are maintained at substantial concentrations in chondrocytes during normal steady-state conditions to prevent aberrant ECM degradation. TIMPs inhibit MMPs via their N-terminal domains while their C-terminal domains determine their MMP binding affinity (Brew and Nagase, 2010).

TIMPs can be specific for certain proteolytic enzymes. For example TIMP-3 inhibits ADAM-TS4 and 5 (Kashiwagi *et al.*, 2001; Isenberg, 2004). TIMP-4 exhibits inhibitory action against MMP-1, MMP-2, MMP-3, MMP-7, and MMP-9 but shows a preferential specificity towards MMP-2 (Liu *et al.*, 1997). TIMPs-2 and -3 are effective inhibitors of the MT-MMPs while TIMP-1 is not (Koopman and Moreland, 2005). TIMP-3 is the only MMP that is bound to the ECM. In early disease states TIMPs have been reported to be down-regulated, tentatively suggesting that a metabolic imbalance begins to occur here which facilitates disease progression however due to variation in the results of different studies, only tentative conclusions may be drawn.

1.9.5 Aggrecanases

Aggrecanases are members of the matrix metalloprotease family and are classified as either ADAMs (a disintegrin and metalloproteinase protein) or ADAMTs (a disintegrin and a metalloprotease with thrombospondin motifs; which are a sub-group of the ADAM family). They are also known as aggrecanases because they facilitate the cleavage of aggrecan into large proteoglycan fragments with MW values of 144000-380000 depending on the cleavage site used (Loulakis *et al.*, 1992 ; Tortorella *et al.*, 2000). Nineteen ADAMTs have been identified to date and can be placed into four categories (Table 1.5).

Table 1.5 ADAMTs categories, adapted from (Jones and Riley, 2005).

Category	ADAMT(s)
Hyalactanases	-1, -4, -5, -8, -9, -15 and -20
Procollagen N-propeptidases	-2, -3 and -14
Von Willebrand factor-cleaving protease	-13
Others	-6, -7, -10, -12, -16, -17, -18 and -19

ADAMs can perform a variety of functions; these include cleavage of proteins using their metalloproteinase domain, adhesion via their disintegrin domain and cell-cell fusion, in addition to cell signalling (Sternlicht & Werb, 2001).

Unlike typical ADAM proteins that are membrane-anchored and have a transmembrane domain and cytoplasmic domain in the C-terminal region, the ADAMTs are secreted and their C terminus contains a varying number of thrombospondin type-1 (TSP-1) motifs. ADAM-TS4 (aggrecanase-1) and ADAM-TS5 (aggrecanase-2) are thought to be the primary aggrecan degrading enzymes in osteoarthritic cartilage, with both ADAMTs cleaving preferentially between the glutamic acid-1667 and glycine-1668 residues of aggrecan (Tortorella *et al.*, 2001; Westling *et al.*, 2002).

Aggrecanase-1 and -2 are not just found in damaged cartilage and can be found degrading aggrecan in healthy tissue helping to maintain a homeostatic balance. Aggrecanase-1 (ADAMTS-4) cleaves aggrecan using its thrombospondin type-1 (TSP-1) motif, it cannot cleave aggrecan that does not contain GAGs (Tortorella *et al.*, 2000). Aggrecanase-2 is the most strongly expressed aggrecanase and has been shown to be the predominant aggrecan degrading protease in murine models of OA. Aggrecanase-1 has been reported to be expressed in small amounts in healthy cartilage and its expression is only slightly elevated in OA (Koopman & Moreland, 2005).

1.9.6 Other molecules found in osteoarthritic cartilage tissue

Tenascin is an extracellular matrix (ECM) glycoprotein whose expression is increased in articular cartilage that has been damaged during OA progression. In human hip tissues, tenascin distribution has been reported to be increased in the superficial and middle zones of the cartilage in very advanced OA, especially in the cellular and pericellular environment, but in mild OA its levels were increased only in central cartilage regions of the superficial zone (Veje *et al.*, 2003). Tenascin has been found in increased quantities in areas of the cartilage tissue that have a significant proteoglycan loss (Pfander *et al.*, 2004). Topographic variation

highlights the importance of accounting for the location of cartilage tissue samples that are removed for use in studies because it is not just in the zonal layers that the biochemical properties change and this could affect the interpretation of results obtained from samples. It could be that the increased tenascin levels reflect a reparative attempt by chondrocytes because tenascin is involved in cell growth and motility and has been localised to areas of cell migration (wound healing) and tissue morphogenesis (Murphy-Ullrich *et al.*, 1996). Interestingly tenascin is one of a few molecules that has been shown to have the potential to be a biomarker of advanced OA (Schmidt-Rohlfing *et al.*, 2002).

Human cartilage glycoprotein-39 (HC-gp39), also known as YKL-40, has been found at increased concentrations in osteoarthritic cartilage, however it is usually not found in healthy cartilage. HC-gp39 has a high sequence similarity with the enzyme family known as the chitinases which are involved in digestion and are used by some organisms to allow remodelling of polysaccharide networks. Therefore it has been speculated that HC-gp39 plays a role in cartilage remodelling potentially via interaction with glycan structures on proteins or the cell surface. Like tenascin, it is a protein that exhibits topographical as well as zonal variations in its distribution in osteoarthritic cartilage. HC-gp39 has been found at increased levels in chondrocytes at points on the femoral head in which there is known to be an increased biomechanical load. Additionally, chondrocytes in the superficial and middle zones of osteoarthritic cartilage showed an increased presence of HC-gp39 compared with chondrocytes in the deep zone and any zone in normal cartilage (Volck *et al.*, 1999).

CD44 is a cell adhesion molecule that is a member of the hyaluronan binding-protein family. Cell adhesion molecules are important mediators in processes such as cell anchorage and matrix metabolism. In normal cartilage CD44 has been shown to be expressed in higher quantities by chondrocytes in the superficial zone compared to those in the deep zone whereas in OA CD44 expression is increased in the deep zone as well as fibrous pannus structures formed at the STZ meaning that the distinct expression pattern of CD44 in normal cartilage is lost as OA progresses (Ostergaard *et al.*, 1997).

1.10 The biotribological properties of degraded cartilage tissues

The tribological properties of cartilage tissues become altered as the tissue becomes increasingly degraded during the osteoarthritic disease process. The friction co-efficient of ex-vivo degenerated human cartilage is higher than that of healthy cartilage tissues and has been shown to increase as degradation of the tissue increases (Pickard and Fisher, 2000; Lee *et al.*,

2013). The increase in friction seen in degraded tissues may result from an increase in the surface roughness of cartilage (Lee *et al.*, 2013). The interest in the surface features of degraded cartilage has culminated in advanced surface characterisation protocols to determine the texture of degraded cartilage (Tian *et al.*, 2011).

Studies of the changes in cartilage surface characteristics as a result of degradation are closely linked with studies that have investigated particles of cartilage that are generated through the wear of the tissue. The numerical descriptors used to characterise the cartilage wear particles have shown that the area and length of particles increases as cartilage in joints becomes increasingly degraded in comparison to controls (Kuster *et al.*, 1998). Since the study by Kuster *et al.* was completed, methodologies to study cartilage wear particles created during cartilage degradation have been developed. This has allowed the surface topography and biomechanical properties of cartilage particles to be determined at the nanoscale using atomic force microscopy (Wang *et al.*, 2013). With further development, it may be possible, in the future, to grade cartilage degradation *in vivo* through examination of cartilage wear particles.

Other mechanical properties of degraded cartilage have been investigated using indentation testing. For example, Wang *et al.* (2012) used micro indentation to investigate various grades of degradation in sheep knee cartilage. The cartilage damage was generated *in vitro*. The study found that the indentation modulus of degraded cartilage was lower in comparison to undegraded controls, which could have been due to collagen disruption (Wang *et al.*, 2012). Indentation testing of human osteoarthritic cartilage on a macroscopic scale has also shown that the properties of degraded cartilage are altered. These alterations include, for example, the permeability of osteoarthritic tissues, which is increased. In addition to this the compressive stiffness and tensile strength of degraded cartilage tissues are reduced (Silver *et al.*, 2001; Kleeman *et al.*, 2005; Boschetti and Peretti, 2008; Marticke *et al.*, 2010). These changes across the cartilage extracellular matrix are reflected in the pericellular matrix surrounding chondrocytes of degraded cartilage tissue, in which the Young's modulus is decreased and the permeability is also increased (Alexopoulos *et al.*, 2005). Interestingly, it has been observed that collagen fibrils from the superficial zone and bone-cartilage interface of patients with early to severe OA (Outerbridge grade) have lower compliance than those with a zero OA grade. The collagen fibres in the middle zone of grade 3 and 4 damaged tissues have also been shown to have reduced compliance (Wen *et al.*, 2012).

1.11 Treatment and management of osteoarthritis

The majority of treatment for OA is palliative in that it attempts to ease pain and temporarily reduce progression of the disease. In some cases it has been observed that certain treatments may aggravate the condition over the long term so there is a lot of interest in development of novel early intervention therapies that could provide effective treatment of the disease and delay the need for total joint replacements.

1.11.1 Drug therapy

Disease modifying drugs are not available for the treatment of osteoarthritis however many OA patients use painkilling drugs to alleviate the painful symptoms of the disease. Non-prescription painkillers may not always be strong enough so many patients are prescribed with strong opiate based medicines or non-steroidal anti-inflammatory drugs (NSAIDs).

Strong prescription pain killers such as Tramadol hydrochloride which are given to OA patients cause a variety of common symptoms such as nausea and dizziness in addition to rarer side effects such as headaches, skin rashes and circulatory problems such as palpitations (www.NHS.uk). These side effects can be especially problematic for patients that are in continued employment, especially for example, those partaking in manual jobs such as those operating machinery in which the side effects might lead to increased risk of accidents.

NSAIDs such as aspirin are prescribed to patients with inflammation and swelling in joints. The most common side effect of NSAIDs after long term use are indigestion and stomach ulcers as they affect the lining of the gastrointestinal tract. NSAIDs also increase the risk of stroke or heart attack in patients so they are not always suitable for smokers or people with conditions such as diabetes. Another major issue with long term use of either prescription or non-prescription painkillers is that they can damage the liver and can increase the risk of some cardiovascular events such as myocardial infarction (Bhala & Emberson *et al.*, 2013).

1.11.2 Arthroscopy

Arthroscopy refers to the use of an arthroscope during surgery to allow examination and/or treatment of damage within joints with minimal invasion (Figure 1.8). Arthroscopic treatments include debridement and lavage of tissue and joint cavities. These two treatments are commonly performed together. The debridement removes loose cartilage while the lavage

flushes out unwanted fluids and debris from within the joint cavity. A recent comprehensive review has shown however that debridement of the knee appears to have a very low potential to improve pain or ability to function compared to placebo via sham surgery. It was also concluded that when compared with lavage, debridement leads to little or no difference in pain or ability to function (Laupattarakasem *et al.*, 2008).



Figure 1.8. An image taken during arthroscopy of the knee of a patient with cartilage degradation. Taken from www.icartilage.com.

1.11.3 Autologous chondrocyte implantation (ACI)

This technique includes an initial procedure where a biopsy of healthy cartilage tissue from a non-load bearing region of the joint is taken. Chondrocytes from the tissue are then isolated and cultured before being implanted at the defect site within the joint to allow their development into new cartilage. They are held in position by a periosteal patch which in the case of the knee joint can be harvested from the proximal tibia. This procedure has been shown to provide a suitable repair of articular cartilage injuries for up to 11 years post operation (Peterson *et al.*, 2002).

Matrix assisted chondrocyte implantation is similar to ACI, however with this technique chondrocytes are cultured on a collagen matrix before being transferred into the defect and subsequent attachment of the matrix with glue and/or sutures. This approach increases the possibility of performing an arthroscopic procedure rather than using open surgery. The membrane is also easier to apply than in ACI (Getgood *et al.*, 2009). There are uncertainties about the effectiveness of this treatment due to heterogeneous results from

studies and there are also risks of side effects such as locking of the knee and periosteal hypertrophy. The treatment is also very expensive, costing at least £2000 per patient for in house chondrocyte expansion alone (NICE Guidelines TA89, 2005). Additionally due to the autologous cellular expansion step, the cells returned into the defect have become aged. This could present problems with the repair of the defect.

1.11.4 Marrow stimulation

This technique utilises the ability of mesenchymal stem cells to produce a fibro-cartilaginous repair tissue within defects created by drilling into the sub-chondral bone plate below the cartilage. The perforations drilled into the bone are 3-4 mm in depth, the holes created are then filled by mesenchymal stem cells, platelets and other chemotactic factors. The fibrocartilage produced is unfortunately mechanically and biochemically inferior to native articular cartilage, however some studies have shown that the technique can provide effective symptom relief for up to two years (Getgood *et al.*, 2009). In the future, marrow stimulation techniques may be supplemented with a collagen membrane composed of collagens I and III, which have shown improved results in filling defects, as a result of the collagen membrane providing a scaffold for cells to reside in (Dorotka *et al.*, 2005).

1.11.5 Mosaicplasty

This technique which is also referred to as osteochondral transplantation, uses osteochondral plugs from non-weight bearing areas of the cartilage to fill defects within a joint (Figure 1.9). The technique can involve the use of allografts or autografts, however autografts are the preferred choice due the lack of immune rejection. The disadvantage of this technique is that the plugs taken from the donor do not perfectly fit the defects within the cartilage. This means that often more than one plug is needed which can present problems due to limitations of donor cartilage availability. This is in addition to donor site morbidity and issues with surface congruency of the repair, due to gaps between the circular plugs (Polster & Recht, 2005). Mosaicplasty has shown mixed success in patients and the quality of the repair may depend on which area of the joint undergoes mosaicplasty (NICE Guidelines IPG162, 2006)



Figure 1.9. An image showing the surface of the articular cartilage in a knee joint after a mosaicclasty procedure. Taken from Hangody *et al.*, 2010.

1.11.6 Unicompartmental Knee Arthroplasty (UKA)

During early stages of osteoarthritis it is often the case that only one component of the knee joint is affected. This means only one joint component needs to be replaced, hence the term unicompartmental knee arthroplasty. In this technique a prosthesis is used to partially replace a joint surface such as the medial femoral condyle as opposed to both the medial and lateral sides (Newman, 2000). The advantages of this technique are that it is less invasive and is accompanied by shorter recovery times than those of total knee arthroplasties. This treatment also leaves the option for revision to total knee replacement open and these follow up operations are often successful. Unfortunately, for this technique to take place early diagnosis is required which is a rare occurrence. It can also lead to increased wear due to inferior lubrication properties of the prosthetic surface in comparison with cartilage. UKA is usually recommended for patients that are over 60 years of age, weighing less than 80 kg that place low activity demands on their knees (Bourne, 1990).

1.11.7 Total knee replacement (TKR)

This technique involves replacement of the diseased knee surfaces with an implant comprised of highly polished metal alloys and an ultra high molecular weight polyethylene tibial tray, which are designed to mimic the shapes of the natural joint components to allow normal

geometric motion. Total knee replacements usually consist of a femoral component, tibial tray and insert and sometimes the patellar component is also replaced (www.orthoinfo.aaos.org). Total knee arthroplasty is usually only considered after other less advanced treatment options are exhausted and the cartilage and subchondral bone are severely damaged.

One of the associated disadvantages with TKR is that its components have inferior frictional properties to cartilage and so produce wear particles which can aggravate certain cells of the immune system (McGloughlin & Kavanagh, 2000). This eventually leads to loosening and failure of the replacement. Once the prosthesis has failed, a revision surgery is required which comes with increased risk of morbidity and complications during surgery. However for many patients TKR significantly reduces pain and improves quality of life for as long as the replacement is viable (0-15years).

1.11.8 Novel Cartilage replacement therapies

Due to the limitations of current treatments for cartilage defects, novel treatments are being developed. These prospective treatments include the use of biomaterials and tissue engineered constructs as early intervention solutions that can be used to repair tissue before joint replacement becomes necessary. Tissue engineering aimed at cartilage tissue regeneration is currently pursued in many research centres across the world

Naturally, engineering cartilage tissue is a complex procedure that involves the use of scaffolds that are seeded with cells, for example chondrocytes, which are placed into defects. The aim is for the scaffold to create a 3D environment for the production of cartilage tissue. Scaffolds can be either synthetic, natural or natural acellular. Growth factors such as TGF- β can be incorporated into the scaffolds to aid ECM regeneration (Chung & Burdick, 2008; Tilwani *et al.*, 2012).

Examples of products that aim to regenerate and repair areas of damaged cartilage include NeoCart[®] (Figure 1.10) which is manufactured by Histogenics and Salubria[®], manufactured by Salumedica. With NeoCart[®], cells from the patient are implanted into a patented 3D matrix and cultured in a bioreactor that mimics conditions found in the body. The cultured matrix is then implanted into the site of cartilage damage. Salubria is a cartilage replacement material that can be implanted into sites of cartilage damage.

Hydrogels are highly hydrated, cross-linked hydrophilic polymers. They have been investigated for use as replacements for damaged articular cartilage, but also have potential for use as scaffolds in tissue engineering. Hydrogels can be natural or synthetic (Cheung *et al.*, 2007). As with tissue engineered cartilage, whether the successful clinical application of hydrogels will occur over the long-term, remains to be seen.



Figure 1.10. The NeoCart® matrix used for articular cartilage repair by Histogenics.

1.11.9 Preclinical assessment of cartilage substitution materials

The recent increase in interest regarding novel cartilage substitution therapies has led to the production of a plethora of different natural and synthetic substitution materials. Part of the problem that arises in engineering tissues is the replication of the anisotropic zonal arrangements that many tissues have, including cartilage. Without replication of zonal regions in tissues, the biomechanical properties of constructs are not likely to be similar to the native tissues. This raises an important question; which of these materials actually provides the best treatment solution for patients with early stage cartilage defects? Many of the materials currently taken forward into animal trials do not undergo rigorous assessment with both biological and mechanical efficacy testing. Often researchers working on substitution materials are predominantly working within either an engineering or biological field and this leads to suboptimal testing of potential biomaterials in the complementary field. With this in mind it is evident that taking materials that have not been thoroughly assessed both biologically and mechanically into animal trials, is a premature step.

In response to this it is apparent that there is a need for the development of an effective *in vitro* system to assess cartilage substitution materials before animal testing to prevent use of animals unnecessarily. An example of an *in vitro* preclinical method to assess novel cartilage substitution materials could be a simulator containing a whole joint running under physiological loading regimes that could be used to determine whether a material has a beneficial or detrimental effect on the surrounding tissues. Given that potential cartilage substitution materials would be used in joints that had been subject to some degree of

degeneration, it would be necessary to test these novel therapies in pre-clinical models that mimic the biotribological conditions of degenerating cartilage.

1.12 Models of cartilage degeneration

A variety of *in vitro* and *in vivo* models have been used in an attempt to replicate the large number of complex changes to joint tissues that take place during the progression of cartilage degeneration. Researchers have attempted to find an ideal model that can reproduce the alterations to tissues that are accumulated over many years, and which will allow investigation into how degenerative changes alter the composition and properties of cartilage tissue. A large variety of animals have been used as models for investigating *in vivo* cartilage degeneration, including mice, rats, guinea pigs, rabbits, dogs, sheep and horses (Smith *et al.*, 2007). The tissues from these, and other animals including cows have also been used to create *in vitro* models of cartilage degeneration.

One reason why it has not been possible to establish a “gold standard” model may be due to the complexity of cartilage degeneration. It is possible that no single model can mimic all of the changes accurately, including the biochemical and mechanical abnormalities that occur, not only in the cartilage but also in the bone and other joint tissues. With this in mind many models have been developed to match the aims of the study as closely as possible and the limitations of the model are taken into account.

1.12.1 *In vivo* models of cartilage degeneration

This section will introduce the different types of *in-vivo* animal models of osteoarthritis including surgery models and spontaneous models.

1.12.1.1 Spontaneous models of osteoarthritis

Hartley Albino guinea pigs are often used in studies regarding OA as this breed of guinea pig begins to develop areas of fibrillation, chondrocyte death in the upper mid region of the cartilage tissue and proteoglycan loss bilaterally in the medial tibial plateau by approximately 6 months of age. By approximately 12 months of age the guinea pigs will have developed osteophytes and profound degenerative changes in all aspects of the medial compartment of the knee including proteoglycan loss and cellular cloning (Bendele & Hulman, 1988). This model is therefore useful for prophylactic testing and assessment of drugs which may potentially be inhibitors of OA.

Mice are also commonly used as spontaneous models of OA as most mice will develop some form of degeneration as they age, which has the potential to develop into OA (Bendele, 2001). Spontaneous OA in primates have also been studied to attempt to elucidate the natural history of OA development. However, due to the difficulties in gaining ethics for primate studies and heterogeneous development of OA in the primates studied they may not be a suitable choice for general study (Carlson *et al.*, 1996).

1.12.1.2 Surgical models of osteoarthritis

One of the most commonly used surgical methods for the study of OA is anterior cruciate ligament transection. The surgery causes instability in the joint which leads to development of OA in a style that aims to mimic OA development after traumatic injury in humans (Pond and Nuki, 1973). One problem with this model is that the animals will tend to decrease loading onto the operated limb by carrying it and loading their remaining limbs. The dogs require large housing areas which is very expensive and not all the lesions developed by the dogs are homogeneous. However the model is useful for studying the development of OA.

Rabbits are also used as animal models, one example being the rabbit partial meniscectomy model. In this model the cartilage begins to degrade represented by loss of proteoglycans, chondrocyte proliferation and osteophyte formation (Moskowitz *et al.*, 1973). The model provides consistent results relatively quickly (within 6 weeks). Due to the rapidity of OA onset the model is more useful for studies of OA pathogenicity.

1.12.1.3 Intra-articular Injection

A variety of substances have been injected into animal joint cavities with the aim of producing tissue degradation. These substances include papain, iodoacetate and IL-1. Iodoacetate injection is commonly used with rats where the iodoacetate inhibits chondrocyte glycolysis and causes cell death. This leads to proteoglycan loss and general cartilage degradation. The chondrocytes in the edges of the joint often survive the injection and begin to form osteophytes (Guingamp *et al.*, 1997).

1.12.2 In vitro models of cartilage degeneration

Several *in vitro* studies have been performed on degraded cadaveric tissues, which have become damaged *in vivo*. For example Wong *et al.* (2008) used human cadaveric lateral

condyle pins to investigate the effects of cartilage degeneration on shear. While, Caligaris *et al.* (2009) used degenerated human cartilage to investigate lubrication mechanisms of cartilage tissue. However, the use of *in vitro* mechanical damage models is relatively unusual.

Researchers have used *in vitro* models to determine the effects of degeneration on cartilage properties with mixed results. For example, crude methods have involved the use of sandpaper to investigate how the friction coefficient is altered in cartilage that has impaired synovial fluid lubrication. In work by Tanaka *et al.* (2005), the friction in porcine temporomandibular joints was measured and compared to the friction in the same group of joints after the joints had been washed in phosphate buffered saline (PBS) and scoured with sandpaper. The authors showed that washing and scouring the cartilage caused an increase in friction of 350%. These authors also concluded that the application of hyaluronic acid to the scratched joint reduced the friction coefficient in the joint. However, the relevance of this work to a physiological environment remains unclear. Other work has involved the use of simplistic methods such as removing full thickness pieces of cartilage from small osteochondral blocks to investigate cartilage contact mechanics and cartilage deformation (Gratz *et al.*, 2009; Wong and Sah, 2009). Again it is questionable whether the methods used in these studies were sophisticated enough to accurately portray scenarios occurring *in vivo*.

Stachowiak *et al.* (2006) developed an automated classification system for cartilage surface wear that they postulated could become a diagnostic tool for assessment of cartilage wear in patients. The wear on the cartilage surface was generated either using a pin on disc system without lubricant, or manually with sandpaper. This raises issues in terms of the relevance of the study because the classification system that was developed was based on wear of the cartilage surface that was not necessarily physiological and therefore may not accurately be able to identify physiological degradation of the cartilage surface. The authors used a physiological sliding speed and contact stress, but it was not clear if the non-reciprocal motion of the pin on disc set up may have also contributed to the generation of cartilage wear which may not represent that observed *in vivo*.

Other more complex studies have investigated the effects of tissue degradation on chondrocyte activity and the initiation of collagen degradation (Quinn *et al.*, 2001; Wilson *et al.*, 2006). In the study by Wilson *et al.* (2006) an indenter tip was used to investigate the effect of mechanical overloading on collagen degradation. The investigators found that "cartilage degradation" was initiated at excessive loads, which caused excessive shear strain along collagen fibrils. However, no attempt was made to investigate how proteoglycans in the tissue had been affected by the indentation. Therefore the conclusion that cartilage degradation was caused by collagen fibre breakdown may only be partly true. In addition to this the loading conditions were not completely physiologically relevant.

Several mechanically based *in vitro* studies have also been conducted in the Institute of Medical and Biological Engineering at the University of Leeds. These studies help to contextualise the work carried out in the current study. Early studies in the Institute focused on investigation of bovine cartilage tribology under variable test conditions using a pin on plate rig. Changes to the conditions included alterations in lubricants, materials articulated and loading times. The studies found that boundary lubrication was important for reducing friction in joints and that the parameter that most affected friction between specimens was the loading time. The authors concluded that the ability of the cartilage to carry loads on its fluid phase was reduced with extended periods of loading (Forster and Fisher, 1996; Forster and Fisher, 1999).

Other *in vitro* studies aimed to assess how proteoglycan depletion changed the biotribological properties of bovine cartilage tissue (Pickard *et al.*, 1998; Katta *et al.*, 2007; Katta *et al.*, 2009). *Ex vivo* tissue from patients has also been investigated using a sliding *in vitro* friction rig which highlighted differences between cartilage tissue degraded *in vivo* and undegraded control tissues; a study by Pickard *et al.* (2000) found that friction was increased in *ex vivo* degraded cartilage tissue in comparison with controls. The cartilage structure of degraded specimens was fibrous and an increase in displacement of cartilage tissue was observed during indentation tests. *In vitro* studies have also been used to investigate how cartilage tribology may be affected *in vivo* following surgery such as hip hemiarthroplasty (McCann *et al.*, 2009; Lizhang *et al.*, 2011). In the study by Lizhang *et al.* (2011) cartilage pins were articulated on cobalt chrome plates under a range of conditions and mechanical characterisation techniques were used to assess the tissues after simulation. It was found that in long term studies (24 hours) with a contact stress equal to or below 4 MPa, the coefficient of friction between bovine osteochondral pins and metal plates remained below 0.35. However, severe damage to the cartilage was observed at a contact stress of 8 MPa and catastrophic damage was observed at contact stresses of 12 MPa and above. In the long term studies, friction was not affected by the contact area of the pin and sliding distances and velocity of articulation only affected the coefficient of friction under contact stresses ranging from 0.5 to 2 MPa. In the short term studies (1 hr) it was observed that the friction coefficient decreased when the contact stress was increased from 0.5 MPa to 2 MPa, but from 2 MPa to 16 MPa the coefficient of friction was increased. Finally an increase in the wear of the cartilage surface, which resulted in a decrease in cartilage height, was observed with increases in contact stress, sliding distance and sliding velocity.

1.13 Rationale

Cartilage degradation has both mechanical and biological origins. The aim of this study was to replicate, *in vitro*, the biotribology of *in vivo* degraded cartilage tissue. Therefore a simple configuration rig was used to create mechanical damage within cartilage specimens. Mechanical degradation was applied using conditions that had been observed *in vivo* e.g. clinically relevant loads and contact stresses were applied in the models. Biological degeneration of cartilage tissue frequently results in loss of GAGs from the tissue. GAG loss was replicated using a chondroitinase ABC in a biological degradation model. The changes that occurred in the cartilage tissue were extensively characterised, which built on the previous work done at Leeds. The study also focused more specifically on the effects of lubricants and loads on cartilage degradation. Finally the study also represents a preliminary step in the development of a natural whole joint simulator for assessment of novel chondroplasty materials, something which has also been investigated previously at Leeds using a pin on plate rig (Northwood and Fisher, 2007).

1.14 Aims and Objectives

The aim of this project was to develop mechanical and biological cartilage degradation methodologies, to replicate the biotribological conditions of degenerated cartilage. A second aim was to assess the degeneration in the models and to collect and analyse wear particles generated by the model.

1.14.1 Objectives

- To characterise healthy bovine articular cartilage from the medial condyle using a range of methodologies, including geometrical height measurements, friction measurements, surface roughness profilometry, histology, immunohistochemistry, electron microscopy, indentation testing and quantitative biochemical assays.
- To generate mechanical degradation models of cartilage using a pin-on-plate friction rig.
- To generate biological degradation models of cartilage using the enzyme, chondroitinase ABC.
- To investigate the characteristics of degenerated cartilage via the methods described previously to determine the alterations that take place in cartilage tissue after mechanical or enzymatic degradation.
- To develop new methodologies to generate, collect and characterise cartilage wear particles and degradation products in the lubricants recovered during mechanical degradation testing.

Chapter 2

Experimental Materials and Methods

2.1 Materials

2.1.1 Equipment

Equipment used during this study is listed in Table 2.1.

Table 2.1 Equipment that was used in this study.

Equipment	Model	Supplier
-25°C freezer	Beko	Jencons
-80°C freezer	Ultralow	Sanyo
Autoclave	PS/MID/C40	Priorclave
Automatic pipettes	Gilson P2-P1000	Anachem Ltd
Balances(4 & 2 Figure)	GR200/GX200	Jencons Plc
Centrifuge	Megafuge 1.0	Heraeus Sepatech
Class II safety cabinet	Herasafe	Heraeus
Copper grids		
Corer- drill bit	Made in house	University of Leeds
Corer- serrated	Made in house	University of Leeds
Corer- smooth	Made in house	University of Leeds
Cryostat	CM1850	Leica
Digital camera	EOS 450D digital SLR	Canon
Disposable vinyl specimen mould	Cryomold standard	Sakura Tissue Tek
Filter (0.2µm)	Minisart	Sartorius stedim biotech
Filter (10µm)	47mm hydrophillic	Whatman
Filtration Kit		Milipore
Freeze dryer	Modulyo	Thermo Fisher Scientific Inc
Fridge	Medicool	Sanyo
Fume Hood	Airone-R	Safe Laboratory Sytems
Hacksaw		
Heated forceps	Speci-ceps System II	Bios Europe
Histology cassettes (plastic)	Histosette	Thermo Fisher Scientific
Hot air oven	Sanyo OMT225	Sanyo Biomedical Europe BV
Hot plate	E18.1 hotplate	Raymond A Lamb
Hot wax dispenser	E66 wax dispenser	Raymond A Lamb
Ice blocks	Medicool MC28	Laminar Medica
Incubator (orbital)	Stuart S150	Scientific Laboratory Supplies
Jig	Made in house	University of Leeds
Magnetic stirrer	Heated Stirrer	Fisher Scientific
Magnetic stirrer Bar		

Microcentrifuge	Microcentaur	MSE
Microplate reader	Multiskan Spectrum	Thermo Fisher Scientific Inc
Microshaker	AM69 Microshaker	Dynatech AG
Microtome	RM 2125 RTF	Leica Microsystems
Orbital shaker	Pos-300	Scientific Laboratory systems Ltd
Paraffin section mounting bath	-	Barnstead Electrothermal
Parafilm	-	Sigma-Aldrich Ltd
pH meter	Jenway 3510	VWR International
Pipette boy	Acu classic	Scientific Laboratory Systems
Plastic sheeting		
Repeat pipetter	AutoRep E	RAININ
Scanning electron microscope	Quanta 200 FEG ESEM	FEI
Shadowgraph		
Shaking table	IKA KS 130 basic	Jencons Plc
Silicone mould kit	50ml system	Microset
Spatula		
Glass Slides	Superfrost Plus	Scientific Laboratory Supplies
Talysurf		Taylor-Hobson
Transmission electron microscope	Spirit G2 12 BioTWIN	FEI
Tissue processor	Leica TP 1020	Leica Microsystems
Ultracut microtome		Reichert-Jung
Upright microscope	Olympus BX51	Microscopes, Medical Diagnostic Systems and Olympus Patient Systems Ltd (Olympus UK Ltd)
Vortexer	MS2 minishaker	IKA
Waterbath	Clifton	Scientific Laboratory Supplies
Wax oven	-	Scientific Laboratory Supplies
Water purifier	Purelab Option	Triple Red Laboratory Technology

2.1.2 Reagents

Reagents used during in this study are detailed in Table 2.2

Table 2.2. Reagents that were used in this study.

Chemical/ reagent	Supplier
Acetic acid	Fisher Scientific
Alcian blue	Raymond A Lamb
Ammonium oxalate	Fisher Scientific
Amphotericin B	
Anhydrous sodium hydrogen phosphate (Na ₂ HPO ₄)	AnalaR
Aprotonin	Nordic Pharma
Araldite CY212	Agar
Bovine serum albumin	Sigma-Aldrich
Chloramine T	Sigma-Aldrich
Chondroitin sulphate B	Sigma-Aldrich
Citric acid	Fisher Scientific
Cupromeronic blue dye	Sigma-Aldrich
DakoCytomation EnVision [®] + Dual Link System-HRP (DAB+)	Dako
Dodeceny succinic anhydride (DDSA)	Agar
1,9 Dimethylene blue	Sigma-Aldrich
Dibasic sodium phosphate	AnaLR
Di-sodium hydrogen orthophosphate	VWR International
Disposable microtome blades	Raymond A Lamb Ltd
DMP30 (2,4,6-tri(dimethylaminoethyl) phenol)	Agar
DPX mountant	Thermo Fisher Scientific Ltd
Dulbecco's PBS with calcium & magnesium	Lonza
Ehrlich's reagent (P-dimethylaminobenzaldehyde)	Sigma Life Science
Eosin	VWR International
Ethanol	
Ethylenediaminetetraacetic acid	Sigma-Aldrich
Formic acid	Sigma-Aldrich
Gentamicin	Sigma-Aldrich
Glacial acetic acid	VWR International
Gluteraldehyde (50%)	Sigma-Aldrich
Haematoxylin (Mayer's)	Raymond A Lamb
Hydrochloric acid	Sigma-Aldrich
Hydrogen peroxide	Sigma-Aldrich
Hydrophobic marker pen (ImmEdge)	Vector Laboratories
Imipenem (Primaxin Intravenous)	Merck Sharpe & Dohme LTD
L-cysteine hydrochloride	Sigma-Aldrich
Magnesium choride hexahydrate	MP
Methylated spirits	Bios Europe Ltd

Monobasic sodium phosphate	AnalR
Neutral buffered formalin (10% w/v)	Genta Medical
Nystatin	Sigma-Aldrich
OCT embedding matrix	Raymond A Lamb
Oxalic acid	VWR International
Papain (crude)	Sigma-Aldrich
Papain (pure)	Sigma-Aldrich
Paraffin wax pellets	Thermo Fisher Scientific Ltd
Phosphate buffered saline tablets	Oxoid
Perchloric acid 60% (w/v)	BDH
Periodic acid shiff kit	Sigma
pH solutions	Scientific Laboratory supplies
Phosphoric acid	
Picric Acid	Sigma-Aldrich
Polymixin B	Fluka Analytical
Potassium permanganate	Thermo Fisher Scientific Ltd
Propan-1-ol	VWR International
Propylene oxide	Agar
Ringer's solution tablets	Oxoid
Sirius red	VWR International
Sodium acetate	AnalaR
Sodium azide 1% (w/v)	Sigma-Aldrich
Sodium chloride	Thermo Fisher Scientific Ltd
Sodium di-hydrogen orthophosphate	VWR International
Sodium formate	VWR International
Sodium hydroxide pellets	Thermo Fisher Scientific Ltd
Sodium tungstate	MP Bio
Trizma base	Sigma-Aldrich
Tween 20	Sigma-Aldrich
Uranyl acetate	Agar
Vancomycin	Sigma-Aldrich
Wax block moulds (base mould)	Fisher Scientific
Wax pellets- Shandon Histoplast	Fischer-Scientific
Xylene	Genta Medical

2.1.3 Antibodies

Antibodies used throughout the study for immunohistochemical analysis of cryosections are detailed in Table 2.3.

Table 2.3. Antibodies for labelling of cryosections using Immunohistochemical analysis.

<i>Antibody</i>	<i>Isotype</i>	<i>Concentration</i>	<i>Dilution</i>	<i>Supplier/ Product code</i>	<i>Incubation time</i>
Primary antibodies					
Biglycan	IgG3	1-10 mg/ml	1/800	AbCam- ab64695	1 hour
Collagen VI	IgG	50 µg	1/500	AbD Serotech- AHP2049	1 hour
Cartilage Oligomeric Matrix Protein	IgG	0.4 mg/ml	1/80	AbCam- ab74524	2 hours
Isotype controls					
IgG3 (Biglycan)	-	0.1 mg/ml	1/8	AbD Serotech- MCA2063	1 hour
IgG (Collagen VI)	-	0.2 mg/ml	1/200	AbCam- ab27478	1 hour
IgG (COMP)	-	0.2 mg/ml	1/200	AbCam- ab27478	2 hours

2.2 Consumables

2.2.1 Glassware

Unless otherwise stated, all laboratory glassware was obtained from Fisher Scientific, Loughborough, UK. Glass ware was cleaned by immersion into a 1% (v/v) solution of Neutracon phosphate free detergent overnight followed by thorough rinsing in tap water. The glassware was then rinsed three times in distilled water before being sterilised using dry heat for 4 hours at 180°C.

2.2.2 Sterile Plasticware

Uncoated Nunc 96 well flat bottomed plates were purchased from Fisher Scientific Loughborough, UK. Disposable pipettes were supplied by Sigma-Aldrich Company Ltd., Poole, Dorset, UK. Pipette tips were purchased from Starlab, Hamburg, Germany. All other sterile plasticware was purchased from Scientific Laboratory Supplies, Hesse, UK.

2.2.3 Dissection Equipment

A size 22 scalpel handle and standard forceps were purchased from Seward Thackray, Gwent, UK and disinfected in 1% (w/v) virkon for 10 minutes at room temperature after each use. Size 22 scalpel blades were purchased from Thermo Fisher Scientific Ltd., Loughborough, UK.

2.2.4 Stock Solutions

2.2.4.1 Ethylenediaminetetraacetic acid (EDTA) solution 12.5% (w/v) at pH 7

Two litres of 12.5% (w/v) EDTA solution were made by adding 250 g of EDTA to 1500 ml of distilled water. The solution was stirred using a magnetic stirrer. Sodium hydroxide pellets were added to bring the pH closer to pH 7 then 1M sodium hydroxide solution was added to bring the pH to 7. Following this distilled water was used increase the solution volume to 2 litres. The solution was stored at room temperature for up to 12 months.

2.2.4.2 Sodium hydroxide solution (6M)

Sodium hydroxide pellets (120 g) were added to 500 ml of distilled water. The solution was stirred using a magnetic stirrer until the pellets had dissolved. This solution was stored at room temperature for up to 12 months.

2.2.4.3 Ringer's solution

Eight Ringer's solution tablets were added to one litre of distilled water and left to dissolve at room temperature. The solution was stored at room temperature until required.

2.2.4.4 Phosphate buffered saline (PBS)

One PBS tablet was added per 100 ml of distilled water and left to dissolve at room temperature. The solution was stored at room temperature for up to 2 weeks.

2.3 Methods

2.3.1 pH Measurement

A Jenway 3510 pH meter was used to measure the pH of solutions. The pH meter was calibrated with premade solutions of pH 7, pH 10 and pH 4. The pH of the solutions was measured using the automatic temperature compensation within the meter. To adjust the pH of solutions, 1-6 M hydrochloric acid or 1-6 M sodium hydroxide was added drop-wise whilst the solution was agitated using a magnetic stirrer.

2.3.2 Microscopy

Bright field microscopy was performed on an Olympus BX51 Microscope. Digital images were captured using an Olympus XC50 camera via Cell B imaging software.

2.3.3 Filter Sterilisation

Filter sterilisation was used to sterilise bovine serum albumin solution for immunohistochemistry. The bovine serum albumin solution in a disposable syringe was passed through a 0.2 µm pore filter into a sterile plastic container in a class II safety cabinet.

2.4 Tissue Retrieval

Femurs from 18 month old cattle were obtained from the local abattoir within 48 hours of slaughter. Before dissection, surfaces were covered in plastic sheeting for cleanliness. The femur was clamped firmly using a vice. Circular osteochondral pins approximately 10-15 mm in length and 9 mm in diameter were taken from the medial condyles of the femur (Figure 2.1). To do this, the surface of the condyle was marked with a smooth 9 mm diameter corer followed by a serrated corer to enhance the impression on the tissue. A drill with a serrated coring attachment was then used to drill around the circumference of the impressions. The smooth corer was then used again to snap the pin from the base and therefore extract the pin from the tissue. A hacksaw was used to extract one osteochondral plate 45 mm in length and 18 mm in width from the medial patellar groove of each of the femurs. The bone at the back of the osteochondral plate was removed using a jig designed and built in house. The plates and pins were stored -25°C in labelled plastic pots containing tissue paper soaked in Ringer's solution before undergoing further processing.

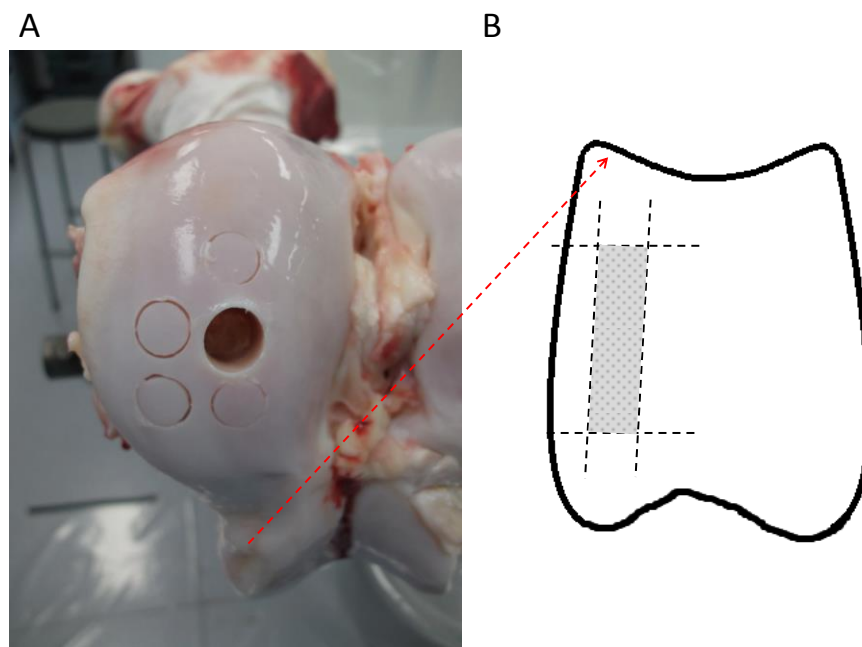


Figure 2.1. Images displaying the areas of the medial condyle and medial patellar groove from which osteochondral pins and plates were dissected. A. The medial condyle of the bovine femur showing areas marked for osteochondral pin extraction and a cylindrical void where a pin has been extracted. **B.** A drawing showing the outline of the bovine patellar groove with a shaded region indicating the area from which osteochondral plates were removed.

2.5 Basic histological techniques

The methods described below were used to prepare the osteochondral specimens for histological examination.

2.5.1 Decalcification of bovine osteochondral plugs

Decalcification of bovine osteochondral pins was carried out in 12.5% (w/v) ethylenediaminetetraacetic acid (EDTA) at pH 7 and at 40°C with gentle agitation in an orbital incubator. Prior to decalcification, each pin was placed into 20 ml of 10% (v/v) NBF for 48 hours. After they had been fixed, each pin was immersed into 20 ml of 12.5% (w/v) EDTA which was changed every 24-48 hours for approximately 2-3 weeks until complete decalcification was confirmed using a calcium oxalate test (Section 2.5.2) and the bone was soft enough to be cut using a scalpel blade.

2.5.2 Calcium oxalate test

2.5.2.1 Dibasic sodium phosphate solution (0.2M)

To 14.1 ml of distilled water, 0.4 g of anhydrous sodium hydrogen phosphate (Na_2HPO_4) was added and dissolved using a magnetic stirrer.

2.5.2.2 Citrate phosphate buffer, pH 3.4

To a volume of 14.1 ml of 0.2 M dibasic sodium phosphate solution, 35.9 ml of citric acid was added. The solution was adjusted to pH 3.4 using citric acid and mixed using a magnetic stirrer. The mixture was then increased to 100 ml with distilled water.

2.5.2.3 Saturated ammonium oxalate solution

Ammonium oxalate powder was added to 80 ml of distilled water in a 100 ml duran bottle until it would no longer dissolve after vigorous shaking by hand for 40-60 seconds.

After specimens had been incubated for approximately 24 hours in fresh EDTA subsequent to the previous EDTA change, 0.5 ml of EDTA was removed from each specimen container and was mixed with 2.5 ml of saturated ammonium oxalate and 1 ml of citrate phosphate buffer. The specimens were placed on a shaking table for 20 minutes after which the formation of a white precipitate confirmed the presence of calcium in the solution. No precipitate formation confirmed an absence of calcium in the solution and indicated that the specimen was ready for processing.

2.5.3 Paraffin wax embedding of cartilage samples

Post dissection, tissue specimens destined for histological examination were stored in 20 ml of 10% (v/v) neutral buffered formalin (NBF) for 48 hours at room temperature prior to decalcification. Following decalcification, specimens were placed into 10% (v/v) NBF for a further 48 hours before being bisected from the cartilage through to the bone with a scalpel blade and placed into plastic cassettes before dehydration in an automatic tissue processor. For histological specimens, the tissue processor was set on programme 9 which had a total duration of 22 hours and involved sequential immersion of tissue samples into various solutions (Table 2.4).

Table 2.4 Tissue Processor programme 9 for processing of bovine osteochondral pins for wax embedding.

Station	Time	Solution
1	1 hour	10% (v/v) NBF
2	1 hour	70% (v/v) Ethanol
3	1 hour	90% (v/v) Ethanol
4	2 hours 20 minutes	100% (v/v) Ethanol
5	3 hours 20 minutes	100% (v/v) Ethanol
6	4 hours 20 minutes	100% (v/v) Ethanol
7	1 hour	Xylene
8	1 hour 30 minutes	Xylene
9	2 hours	Xylene
10	1 hour 30 minutes	Molten wax
11	2 hours	Molten wax
12	2 hours	Molten wax

Once the tissue processing cycle was complete, the specimens were removed from the cassettes one at a time, orientated in wax block moulds with heated forceps and covered in molten wax, they were then left to dry on ice blocks for 1 hour. Once the wax was hardened, the wax blocks were removed from the moulds and excess wax around the block was trimmed away with a spatula.

2.5.4 Tissue sectioning

A microtome was used to section samples embedded in paraffin wax. Sections were cut at 6 μm intervals and floated in a water bath set at 40°C. Sections were then transferred onto Superfrost glass slides that were baked on a hotplate at 55°C for 2 hours. The slides were stored in slide holders for up to 48 hours.

2.5.5. Dewaxing and rehydration of paraffin embedded tissue

Slides were placed into a slide holder and submerged into two successive pots of xylene for 10 minutes each to remove wax. Slides were then placed into three successive pots of 100% (v/v) alcohol for 3, 2 and 1 minutes respectively. Following this slides were submerged into 70% (v/v) alcohol for 30 seconds before being submerged into a pot irrigated by running tap water for 3 minutes.

2.5.6 Tissue dehydration and mounting

Post staining, sections were dehydrated through immersion in 70% (v/v) alcohol for 5 seconds followed by successive immersion into three pots of 100% alcohol for 1 minute each and finally sections were placed into two pots of xylene for 10 minutes each. In a fume hood, slides were mounted one at a time using DPX mountant and a coverslip. Slides were left to dry for a minimum of 4 hours at room temperature before visualisation with a light microscope.

2.5.7 Tissue retrieval for cryoembedding

For cryoembedding, cartilage was removed from the bone of specimens using a scalpel. Cartilage disks cut from the bone were cut in half using a scalpel blade. The flat cut edge of the cartilage disk was placed face down in a disposable vinyl specimen mould. OCT embedding matrix was poured over the sample until it was submerged. The samples were then frozen at -80°C overnight. The samples were then removed from -80°C and placed into -20°C for long term storage in plastic pots.

2.5.8 Tissue sectioning and slide preparation of cryoembedded tissues

Cartilage was sectioned at a thickness of 6 μm using a cryostat set at -21°C. Sections were mounted onto Superfrost Plus slides which were baked on a hotplate at 55°C overnight. After baking, the slides were used within 24 hours.

2.6 Histological staining methods

2.6.1 Haematoxylin and eosin staining

Haematoxylin and eosin staining was used for visualising the architecture of the cartilage tissues in this study. Haematoxylin stains acidic components of tissues such as the cellular nuclei which can be seen at higher magnifications, while eosin which is an anionic dye, stains the basic cellular components, such as the cytoplasm. Haematoxylin requires oxidation to haematin and subsequent attachment to the tissue via a mordant in the stain solution before staining can occur. The eosin counterstain, stains the cytoplasm of the cell and the majority of connective tissues in varying shades of pink and red.

Sections were rehydrated and immersed into haematoxylin solution for 1 minute. Sections were then rinsed in running tap water until the water ran clear and were subsequently immersed into eosin solution for 3 minutes prior to dehydration and mounting followed by microscopic evaluation.

2.6.2 Alcian blue staining

Alcian blue is a cationic dye that stains glycosaminoglycans (GAGs) in tissue samples. It is often counterstained with eosin but can also be counterstained with neutral red. Healthy cartilage contains significant levels of GAGs within its ECM that include chondroitin sulphate and keratan sulphate. The alcian blue dye molecule can be described as a copper phthalocyanin dye which at low pH (<2.5) binds to fixed negative charges found on the carboxyl and sulphate groups in GAG chains via electrostatic bonding.

Specimens were stained using an alcian blue periodic acid schiff kit. Alcian blue dye stains acidic and sulphated mucins. As mucins are heavily glycosylated proteins, GAGs are stained during the alcian blue incubation. The periodic acid and Schiff dyes stain neutral mucins.

Paraffin sections were brought to water before being stained with the Sigma periodic acid Schiff kit. After rehydration slides were immersed in 1% (w/v) alcian blue solution for 15 minutes followed by immersion into a pot of running tap water until the water ran clear, then a rinsing step in distilled water. Slides were immersed into periodic acid for five minutes then rinsed in distilled water. Slides were then immersed into Schiff's reagent for 15 minutes. Slides were then rinsed in a pot of running tap water for five minutes before being immersed into haematoxylin for 90 seconds. Following this, slides were immersed into a pot of running tap

water. Slides remained in the pot until the water in the pot ran clear. This step was followed by dehydration and mounting as previously described in Section 2.5.6.

2.6.3 Immunohistochemical staining of bovine osteochondral specimens.

2.6.3.1 Tris solution (2 M)

In 800 ml of distilled water, 242.26 g of trizma base was dissolved using a magnetic stirrer. The pH was adjusted to pH 7.6 using sodium hydroxide or hydrochloric acid and the solution was increased to one litre using distilled water.

2.6.3.2 Sodium chloride solution (3 M)

To 175.32 g of sodium chloride, one litre of distilled water was added. A magnetic stirrer was used to mix the solution until the sodium chloride had dissolved.

2.6.3.3 Tris buffered saline pH 7.6 (TBS)

To 25 ml of 2 M tris solution, 50 ml of 3 M sodium chloride solution was added. Sodium hydroxide solution at 1M and 1M hydrochloric acid were used to change the pH of the solution to pH 7.6 as the solution was mixed using a magnetic stirrer bar. The solution was made up to 1 litre with distilled water and stored at room temperature until required.

2.6.3.4 Tris buffered saline containing 0.05% (v/v) tween 20 pH 7.6 (TBS tween)

To 9999.5 ml of tris at pH 7.6, 0.5 ml of tween 20 was added and dissolved using a magnetic stirrer.

2.6.3.5 Hydrogen peroxide solution 3% (v/v)

To 90 ml of PBS, 10 ml of 30% (v/v) hydrogen peroxide solution was added and mixed using a magnetic stirrer.

2.6.3.6 BSA solution

To 50 ml of PBS, 2.5g of bovine serum albumin was added and dissolved using a magnetic stirrer. The solution was passed through a filter with a pore size of 0.2 μm into a sterile collection container in a class II cabinet.

2.6.3.7 Antibody diluent

To 50 ml of TBS, 60 μl of 1% (w/v) sodium azide and 300 μl of 5% (w/v) BSA solution was added. The pH of the solution was adjusted to pH 7.6 using hydrochloric acid or sodium

hydroxide and mixed using a magnetic stirrer. The solution volume was increased to 60 ml using TBS.

Ultra V endogenous enzyme blocking kit (Dako Cytomation EnVision Kit)

Labelled polymer horseradish peroxidase (Dako Cytomation EnVision Kit)

Substrate chromagen (Dako Cytomation EnVision Kit)

All of the following steps were performed at room temperature. Prior to staining, cryosections were rehydrated in running tap water for 3 minutes. Following this, sections were immersed in 3% (v/v) hydrogen peroxide for 10 minutes followed by immersion into running tap water for 3 minutes. A hydrophobic marker was used to circle around sections. After the marker ink had dried the slides were rinsed in TBS. One drop of endogenous enzyme block was applied to each section and left to incubate for 10 minutes. The slides were then washed twice in TBS for 10 minutes each. Each section then had 50 µl of primary antibody applied. Before use primary antibodies were diluted accordingly with antibody diluent (Table 2.3). The tissues were incubated with either collagen VI or biglycan antibodies for 1 hour, or with the COMP antibody, for 2 hours. Incubation was carried out in a moist atmosphere. The slides were then washed in TBS Tween twice for 10 minutes each followed by two 10 minute washes in TBS. The sections were then incubated with labelled polymer horseradish peroxidase for 30 minutes in the dark in a humid chamber before undergoing two 10 minute washes in TBS Tween. The slides were then washed twice for 10 minutes using TBS. Fifteen microliters of substrate chromagen was placed on each of the sections for 10 minutes. The slides were then washed four times in distilled water. The slides were immersed into haematoxylin for 10 seconds and then placed into running tap water until the water ran clear. The slides were then dehydrated and mounted as described previously in Section 2.5.6.

2.7 Microscopy of cartilage specimens

2.7.1 Environmental scanning electron microscopy

Samples to be visualised using ESEM were placed onto the Peltier-cooled specimen stage in an FEI Quanta 200F environmental scanning electron microscope. Images of the cartilage surface were taken between 8 and 14 kV at 85-100% humidity. Environmental electron microscopy allowed the samples to remain hydrated. This was through manipulation of the dew point of water in the chamber via chamber pressure alterations and temperature acclimatisation, facilitated by the Peltier-cooled specimen stage. The chamber temperature ranged from 4-5°C with a chamber pressure of approximately 6.5 Torr.

2.7.2 Transmission Electron Microscopy and Cupromeronic Blue Staining

This method was adapted from a method in the series Methods In Cell Biology; Transmission Electron Microscopy of Cartilage and Bone (Keene and Tufa, 2010). This method used the cationic dye Cupromeronic blue to label proteoglycans and produced an image of the supramolecular complex formed by the proteoglycans. Cupromeronic blue was used at a critical electrolyte concentration which resulted in the staining of sulphated proteoglycans only.

2.7.2.1 Monobasic sodium phosphate (0.2M)

To 100 ml of deionised water 2.76 g of monobasic sodium phosphate ($\text{NaH}_2\text{PO}_4\cdot\text{H}_2\text{O}$) was added and stirred using a magnetic stirrer.

2.7.2.2 Dibasic sodium phosphate (0.2M)

To 100 ml of deionised water, 2.839 g of Na_2HPO_4 was added and dissolved using a magnetic stirrer.

2.7.2.3 Phosphate buffer (0.1M)

To 39 ml of 0.2 M monobasic sodium phosphate, 61 ml of 0.2 M dibasic sodium phosphate was added and dissolved using a magnetic stirrer. The pH was adjusted to pH7 using either phosphoric acid or sodium hydroxide. The solution was increased to 200 ml with deionised water.

2.7.2.4 Magnesium chloride hexahydrate (3 M)

To 25 ml of deionised water, 30.5 g of magnesium chloride hexahydrate was added. The solution was mixed using a magnetic stirrer and was finally increased to 50 ml with distilled water.

2.7.2.5 Aqueous sodium tungstate 0.5% (w/v)

To 99.5 ml of deionised water, 0.5 g of sodium tungstate was added. The solution was shaken by hand to dissolve the sodium tungstate.

2.7.2.6 Aqueous sodium tungstate 0.5% (w/v)

To 50 ml of deionised water 50 ml of 100% ethanol was added. Following this 0.5 g of sodium tungstate was added to 99.5 ml of the 50% ethanol solution. The solution was shaken by hand to dissolve the sodium tungstate.

2.7.2.7 Cupromeronic blue dye solution

To 20 ml of 0.1 M phosphate buffer, 5ml of 50% (v/v) glutaraldehyde was added. To the glutaraldehyde phosphate buffer solution, 10 ml of 3 M magnesium chloride hexahydrate was added. Sodium hydroxide or phosphoric acid was used to adjust the pH of the solution to pH 7. The solution was increased to 100 ml using distilled water. To this, 0.05 g of cupromeronic blue dye was added. The solution was mixed using a magnetic stirrer until the dye had dissolved. The solution was stored in the dark at 4°C.

2.7.2.8 Araldite Resin

The following steps were conducted in a fume hood. In a measuring cylinder, 27 ml of Araldite CY212 was added to 23 ml of dodeceny succinic anhydride (DDSA). The solution was poured into a plastic cup. A clamp stand was used to grip the cylinder upside down over the cup to let any of the remaining resin solution drip into the cup. To the resin DDSA mixture, 1 ml of DMP30 was added. A glass rod was used to stir the mixture until the solution became an even golden tan colour. The resin was stored at 4°C for up to 24 hours.

2.7.2.9 Saturated uranyl acetate solution

To 92 ml of distilled water, 8 g of uranyl acetate powder was added.

Cartilage tissue was dissected as previously described (Section 2.4). Cartilage disks were cut from the bone and dissected into blocks approximately 4 mm x 1.5 mm x 2 mm. The tissue was submerged in cupromeronic blue dye solution for 17 hours at 4°C. Specimens were rinsed in

0.02 M phosphate buffer then washed twice in 0.02 M phosphate buffer for 30 minutes. The specimens were placed into aqueous 0.5% (w/v) sodium tungstate for 15 minutes followed by a 15 minute incubation in 0.5% (w/v) sodium tungstate in 50% (v/v) ethanol. The specimens were passed through six ascending alcohol incubations of 20% (v/v), 40% (v/v), 60% (v/v), 80% (v/v) and 100% (v/v), with two 100% (v/v) steps for half an hour each. The samples were then placed into propylene oxide for 20 minutes, this step was repeated before specimens were transferred from the propylene oxide into a 1:1 solution of propylene oxide and Araldite resin solution respectively. The specimens remained in the 1:1 solution overnight before being transferred to a solution of 1:4 propylene oxide to Araldite resin solution for 3 hours. Finally specimens were immersed into 100% Araldite resin for 3 hours. Following this samples were baked in the oven overnight at 60°C.

Resin embedded cartilage specimens were sectioned using glass knives at 90-140 nm using a Reichert-Jung ultracut microtome. Sections were placed onto Formvar resin coated copper grids which were subsequently stained using saturated uranyl acetate for 2 hours. An FEI Spirit G2 12 BioTWIN transmission electron microscope was used to image the specimens at a voltage of 120 kV.

2.8 Biochemical assays for quantitative assessment of hydroxyproline and glycosaminoglycan content of cartilage tissues

2.8.1 Hydroxyproline quantification assay for cartilage tissue

This method was adapted from a method devised by Edwards & O'Brien (1980). In this assay acid hydrolysis was used to release hydroxyproline residues from collagen structures. The hydroxyproline content of a tissue can be used to determine the collagen content of a tissue by multiplying the hydroxyproline content by 7.14. This is possible as hydroxyproline makes up on average every 7.14th residue in collagen II fibrils. The chloramine T oxidised the free hydroxyproline residues inducing formation of pyrrole compounds. The addition of Ehrlich's reagent (p-dimethylaminobenzaldehyde) caused the production of a red chromophore from the pyrrole compounds, which was measured at 570nm.

2.8.1.1 Assay buffer

To 13.3 g citric acid, 3.2 ml glacial acetic acid, 32 g sodium acetate (3 H₂O), 9.1 g sodium hydroxide and 80 ml propan-1-ol (n-propanol) was added. The resulting solution was increased to 300 ml using distilled water and stirred using a magnetic stirrer. The pH of the solution was adjusted to pH 6.0 - 6.5 with 6 M sodium hydroxide, before adjusting the final volume to 400 ml with distilled water. This solution remained stable for up to two months when kept in a dark bottle at 4°C.

2.8.1.2 Chloramine T solution

To 100 ml of water 1.41 g of chloramine T was added and stirred with a spatula until dissolved. This solution was used immediately.

2.8.1.3 Ehrlich's reagent

In a measuring cylinder, 7 ml of distilled water was added to 30ml of propan-1-ol, 13 ml of 62% (v/v) perchloric acid and 7.5 g of p-dimethylaminobenzaldehyde. The cylinder was inverted until the solution was mixed. The solution was used within one hour.

Cartilage was cut from bone plugs with a scalpel blade and weighed. Between 50 and 80 mg of wet tissue from each specimen was placed into glass test tubes and lyophilised to a constant

weight using a freeze dryer at -40°C . Lyophilised tissue was acid hydrolysed by the addition of 5 ml of 6 M HCL to the tissue which was incubated at 120°C for four hours using a bench top autoclave. Once cooled, the hydrolysed samples were neutralised to pH 7 using a range of sodium hydroxide solutions from 12 M to 0.1 M. After neutralisation the volume of the hydrolysed specimens was quantified. The hydroxyproline content of the hydrolysed cartilage tissue was determined using standards made from 4-hydroxy-L-proline in assay buffer that ranged between 1 and $30\ \mu\text{g}\cdot\text{ml}^{-1}$. Specimens and standards were assayed in triplicate, in a clear flat bottomed 96 well plate at a volume of $50\ \mu\text{l}$ per well. A volume of $100\ \mu\text{l}$ of Chloramine T solution was added to the wells and the plate was placed on a shaker for 5 minutes. Finally a volume of $100\ \mu\text{l}$ of Ehrlich's reagent was added to the wells and left to incubate in a water bath for 45 minutes at 60°C with the plate lid on. Parafilm was used to secure the plate lid and to prevent water entering the plate. The absorbance of the specimens was read at 570 nm using a microplate reader and the unknown values were interpolated from the standard curve and multiplied by 7.14 to determine total collagen content.

2.8.2 Glycosaminoglycan quantification assay for tissue

It is possible to use the cationic dye 1, 9-dimethylmethylene blue to stain sulphated proteoglycans. The interaction between the dye and sulphated glycosaminoglycans in cartilage tissue can be measured colorimetrically using a spectrophotometer allowing quantification of the glycosaminoglycans.

2.8.2.1 Assay buffer

To 137 ml of 0.1 M sodium di-hydrogen orthophosphate, 63 ml of 0.1 M di-sodium hydrogen orthophosphate was added and stirred until dissolved using a magnetic stirrer.

2.8.2.2 Digestion buffer

To 900 ml of phosphate buffered saline containing calcium and magnesium 0.788 g of L-cysteine hydrochloride and 1.8612 g disodium ethylenediaminetetraacetic acid were dissolved using a magnetic stirrer bar. The pH of the solution was adjusted to 6.0-6.1 using sodium hydroxide or hydrochloric acid and increased to one litre using phosphate buffered saline containing calcium and magnesium.

2.8.2.3 Crude papain solution for tissue digestion

Fifty units of crude papain were added into each 1 ml of digestion buffer required and dissolved by gentle inversion.

2.8.2.4 DMB dye solution

To 5 ml of ethanol, 2 ml of formic acid and 16 mg of 1, 9- dimethylene blue were added. Two grams of sodium formate were added to the solution and the solution was adjusted to pH 3 using formic acid and increased to 1 litre using distilled water.

Cartilage was cut from bone plugs using a scalpel blade and weighed. Between 50 and 80 mg of wet tissue from each specimen was lyophilised in a plastic bijou to a constant weight using a freeze dryer at -40°C. Lyophilised tissue specimens were added to 5 ml of papain digestion solution and placed in a 60°C incubator for 36-48 hours. Specimens were centrifuged at 1360 g for 5 minutes to sediment the papain particulate. The remaining supernatant was transferred to new bijous. Undegraded control samples were diluted 1/50 with assay buffer. All mechanically and enzymatically degraded samples were diluted 1 in 20 with assay buffer. Standards made from chondroitin sulphate B were prepared in the assay buffer that ranged from 0 µg.ml to 25 µg.ml⁻¹. Digested tissues and standards were pipetted into a 96 well flat bottomed microplate in triplicate at a volume of 40 µl per well. To each 40 µl, 250 µl of DMB dye was added and the plate was placed on a shaker for two minutes. After two minutes the absorbance was measured at 525 nm using a microplate reader. A graph of absorbance was plotted against the standard concentrations and linear regression analysis was used to interpolate the unknowns from the standard curve.

2.9 Statistical analysis

All numerical data was analysed using Graphpad Prism software version 5. All numerical values were expressed as average values \pm 95% confidence limits so *P* values below 0.05 were considered as statistically significant (Sokal & Rohlf, 3rd edition). All data sets with more than two groups were analysed using a one way ANOVA with a Tukey's multiple comparison post-test aside from the data in Sections 3.42 and 3.43 which were analysed using a repeated measures ANOVA with a Tukey's multiple comparison post-test. Data sets with two groups were analysed using a Student's *t* test.

Chapter 3

Development and Characterisation of a Mechanical Model of Cartilage Degradation

3.1 Introduction

The purpose of the study undertaken in this chapter was to investigate the biotribology of cartilage tissue through the development of mechanical degradation models. Previously, many mechanically induced models of cartilage degeneration have focused on examining the chondrocyte response after cyclic, compressive or impact loading regimes (Farquhar *et al.*, 1996 ; Chen *et al.*, 1999 ; Patwari *et al.*, 2001 ; Thibault *et al.*, 2002; Patwari *et al.*, 2003). In contrast, this work aimed to produce a degradation model in which physiological contact stresses were used to produce damage in osteochondral tissues undergoing cartilage on cartilage contact. The purpose of this was to investigate the biotribological changes associated with degraded cartilage tissue including effects of degradation on friction and wear of the cartilage surface.

In order to assess how mechanical degradation processes affected the cartilage tissue, it was necessary to comprehensively characterise the tissue before degradation. Established methods that have previously been used to characterise cartilage tissue include histological staining and biochemical assays to quantify the glycosaminoglycan (GAG) and collagen content of the tissue (Lufti, 1975 ; Tesche and Miosge, 2004 ; Hoemann, 2004). These methods do not allow a full investigation of the changes that may occur in cartilage tissue due to degradation. This is because they are broad and include groups of cartilage components such as “proteoglycans” rather than individual components such as aggrecan and small leucine rich proteoglycans.

To obtain a greater understanding of the effects of a range of mechanical degradation protocols on the tissue, it was necessary to develop a comprehensive range of methods to allow thorough comparisons between degraded and native tissues. Quantitative surface profilometry was used to complement environmental scanning electron microscopy which allowed visualisation of the cartilage surface. Deformation and recovery measurements were obtained to determine the response of the cartilage to static loading and measurements were recorded during mechanical degradation testing to determine how friction changed during dynamic loading protocols. In addition to this, histological stains such as H & E and biochemical assays for determining collagen and GAG content were used. Transmission electron microscopy was used in conjunction with cupromeronic blue staining to examine the structure of both aggregating and small proteoglycans within the tissue. Alcian blue staining was used so that GAGs could be visually assessed; complementing the biochemical GAG assay and TEM analysis. Finally, antibodies to biglycan, cartilage oligomeric matrix protein and collagen VI

were used to label cartilage tissue sections to reveal how mechanical degradation may have affected these components of the tissue.

3.1.1 Biglycan

Biglycan is a small leucine rich proteoglycan. The absence of biglycan from cartilage is thought to increase the rate of cartilage degeneration as shown in a study by Furukawa *et al.* (2011). These authors showed that loss of the “BGN” gene caused significantly increased rates of degeneration of murine intervertebral discs. During osteoarthritic degeneration, biglycan has been shown to become fragmented. It has been suggested that this is caused by catabolic enzymes in the diseased tissue (Melrose *et al.*, 2008). Hence, biglycan fragmentation may have potential as a biomarker for osteoarthritic disease.

Biglycan has been shown to play a role in collagen fibrillogenesis in the mammalian uterus. Here, biglycan has been shown to be associated with thick collagen fibres, while decorin is associated with thin fibres, indicating distinctive roles for these two small leucine rich proteoglycans (SLRP) which may also extend to musculoskeletal tissues such as cartilage.

3.1.2 Cartilage Oligomeric Matrix Protein

Cartilage oligomeric matrix protein (COMP) has been reported to play a role in extracellular matrix assembly and matrix–matrix protein interactions in addition to interaction with fibronectin (Di Cesare *et al.*, 2002). COMP has been shown to be an effective marker for osteoarthritic degeneration in patient serum and synovial fluid making it an interesting subject for a tribological study (Clark *et al.*, 1999; Song *et al.*, 2012). It was of interest to assess whether COMP was affected by *in vitro* mechanical degradation.

3.1.3 Collagen VI

As well as fulfilling a major role as a mediator of cell-matrix interaction and anchoring chondrocytes to the pericellular matrix, collagen VI has also been shown to be involved in cell signalling (Keene *et al.*, 1988; Pfaff *et al.*, 1993; Marcelino and Mcdevitt, 1995; Rühl *et al.*, 1999a). Collagen VI, which is found in relatively small amounts in cartilage, does not participate in the process of fibril formation, associated for example with collagens II and XI. Rather, it is the major component of the beaded filaments which are found in the majority of connective tissues, and in cartilage, in the pericellular environment that surrounds the chondrocytes (Keene *et al.*, 1988; Soder *et al.*, 2002).

Investigating the effects of *in vitro* degradation on collagen VI is important as this collagen is not distinguished from others by the hydroxyproline assay. Additionally, because of the structural differences between collagen II and collagen VI it was of interest to determine whether this collagen was affected in a similar way to collagen II. It would also give an indication of the changes in structure taking place directly adjacent to chondrocytes during degeneration, which could contribute to changes in the mechanical loading experienced by cells *in vivo*.

3.1.4 Mechanical Degradation Methodologies

In order to replicate the biotribological condition of degenerated cartilage tissue *in vitro*, mechanical degradation methodologies were developed. Two physiological contact stresses were chosen as part of the degradation conditions which were designated “mild” and “moderate”. These two conditions were chosen to provide an insight into the tribological condition of cartilage tissue under two distinct degradative conditions. Contact stresses in human cartilage tissues vary widely and under dynamic movement such as deep flexion, they can reach up to 25 MPa. Damage to cartilage is not only observed at high contact stresses for example, chondrocyte death has been measured in impact studies at contact stresses as low as 4 – 4.5 MPa (Hodge *et al.*,1986; Duda *et al.*, 2001; Loening *et al.*,2000). The mild condition contact stress chosen for this study was 3.1 MPa. The moderate condition contact stress chosen was 7.5MPa. Multidirectional motion was chosen to reflect the motion experienced by tissues in an articulating knee joint which includes a small amount of rotation. Finally the sliding distance that was chosen avoided unloading of the tissues in the rig for an unnatural length of time, while the sliding speed was chosen to increase boundary lubrication between specimens.

3.1.5 Lubricants

Two lubricants were chosen for the degradation regimes to allow an investigation of the effects of different lubricants on the cartilage tribology. Ringer’s solution was chosen due to its ability to keep cartilage hydrated and partly due to its simplicity making it easier to analyse. Ringer’s solution was formulated by Sydney Ringer in the 19th century. It is isotonic with bodily fluids and came to recognition after its ability to increase survival times of excised tissues was discovered. Ringer’s solution is a weak buffer due to its bicarbonate content.

A second lubricant was used as part of the degradation methodologies. It was composed of new born calf serum in phosphate buffered saline (PBS). Calf serum is used frequently in cell culture and has a complex list of components including growth factors, amino

acids, hormones, phospholipids and globular proteins including bovine serum albumin. It is not possible to define the exact composition of calf serum comprehensively due to variability between donor animals, which is influenced by many factors including diet and gender (Bryan *et al.*, 2010). This study hypothesised that use of a second lubricant that included calf serum may lead to an interesting variation in results from those observed with Ringer's solution lubricant. This is because components of the serum such as phospholipids have the potential to alter the friction between specimens and therefore could reduce tissue degradation (Forsey *et al.*, 2006). Additionally, as the work completed in this study has the potential to be developed, eventually resulting in a natural whole joint simulator in which living tissues may be used, use of a serum solution to maintain cell viability would be necessary in the latter system.

3.2 Aims and objectives

The overall aim of this part of the study was to develop and characterise a mechanical model of cartilage degradation that replicated the tribological condition of degenerated cartilage. Native bovine cartilage tissues were compared with bovine cartilage tissues that had been subjected to mechanical degradation. The tissues were compared comprehensively using quantitative and qualitative methods.

Objectives:

- To develop a mechanical degradation methodology for bovine cartilage tissue and to record friction during testing using a pin on plate friction rig.
- To assess the deformation and recovery of undegraded control cartilage tissue using static loading methodologies to determine whether loss of tissue height occurs due to loading alone.
- To characterise the changes to the surface roughness of the bovine cartilage tissues post mechanical degradation using contact profilometry.
- To use histological staining to assess the normal histoarchitecture and staining patterns of glycosaminoglycans in undegraded bovine cartilage tissue and mechanically degraded bovine cartilage tissues using haematoxylin and eosin staining and alcian blue staining, respectively.
- To determine the distribution of biglycan, cartilage oligomeric matrix protein (COMP) and collagen VI qualitatively in undegraded and mechanically degraded bovine cartilage tissues
- To use environmental scanning microscopy to observe the undegraded and mechanically degraded bovine cartilage surface in a hydrated state.
- To use transmission electron microscopy with cupromeronic blue dye to examine the bovine cartilage ultrastructure and GAG interactions in mechanically degraded and undegraded tissue.

- To quantitatively determine the glycosaminoglycan and collagen content of healthy and mechanically degraded bovine cartilage tissue.
- To develop methods for quantitatively analysing collagen and GAG content in the lubricants generated during friction testing.

3.3 Experimental approach

The experimental approach that was taken during this study has been summarised in Figure 3.1. A total of six repeats were conducted for each loading condition in the static loading experiments. After the final measurements were taken the tissue was stored in the freezer at -20°C for future use. Six repeats per condition were also performed for the surface roughness measurements. Six repeats per condition were taken for all the histological and immunohistological analysis, each pin was cut in half with one half being used for histology and one half being used for immunohistochemistry. Three repeats were taken for both microscopy techniques with one half of each pin used for ESEM analysis and one half used for TEM analysis. Finally six repeats were conducted for each condition to provide enough tissue for biochemical analysis. Each pin was cut in half with one half being used for the collagen analysis and one half being used for glycosaminoglycan analysis.

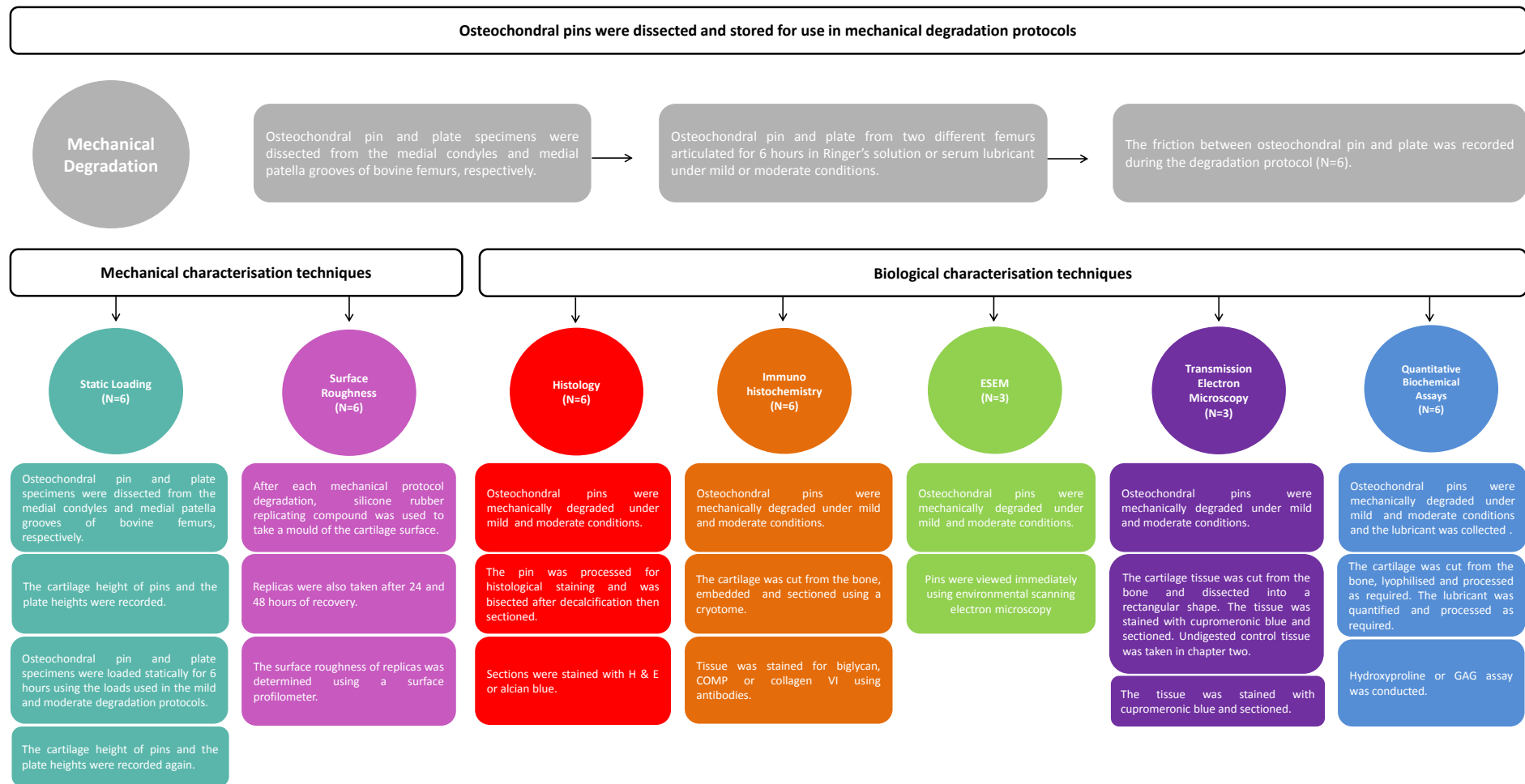


Figure 3.1. The experimental approach taken in the research described in chapter three, which focused on the effects of mechanical degradation on cartilage specimens. The image includes characterisation techniques that were used to analyse specimens and the number of replicates.

3.4 Methods

3.4.1 Lubricants for Mechanical Degradation Regimes

Ringer's solution and newborn calf serum 25% (v/v) in PBS (serum lubricant) were used as lubricants and for irrigation of osteochondral tissues during mechanical degradation. Ringer's solution has previously been described (Section 2.2.1.5). The formula of the Ringer's solution used in this study is shown in Table 3.1.

Table 3.1 The specific composition of the Ringer's solution used in this study.

Formula	Grams Per Litre
Sodium chloride	2.25
Potassium chloride	0.105
Calcium chloride (6H ₂ O)	0.12
Sodium bicarbonate	0.05
pH 7	

3.4.1.1 Serum Lubricant

To 25ml of new born calf serum, 50 ml of PBS (Section 2.2.4.4) was added and mixed by gentle inversion. The pH of the solution was adjusted to pH 7 using 1 M HCl or 1 M sodium hydroxide solution. The solution was topped up to 100 ml with PBS.

3.4.2 Mechanical degradation of cartilage using a multidirectional pin on plate rig

A single station multidirectional pin on plate friction rig was designed and manufactured in the School of Mechanical Engineering at the University of Leeds, UK (Figure 3.2). Osteochondral plates (Section 2.4) were clamped between two opposing stainless steel plates, one of which had a window cut into it in order that the cartilage face of the osteochondral plate was exposed. The opposing steel plates locked the osteochondral plate in place and were held together with plate screws. The plates were fixed into a bath using bath screws. The bath itself was attached securely to the reciprocating plate of the friction rig with clamp screws (Figure 3.3). The various components and equipment required to set up the pin on plate rig are shown in Figure 3.4. A bath was attached to the reciprocating stage and 14ml of lubricant was added to the bath using a syringe. The osteochondral plug (Section 2.4) was placed into the collet with a stainless steel spacer (approximately 7 mm in height) behind it before being placed into

the pin holder and secured with a screw. Care was taken to ensure that at least 5 mm in total of cartilage and bone were left to protrude from the pin holder/collet to prevent the pin holder rubbing against the upper opposing plate during testing.

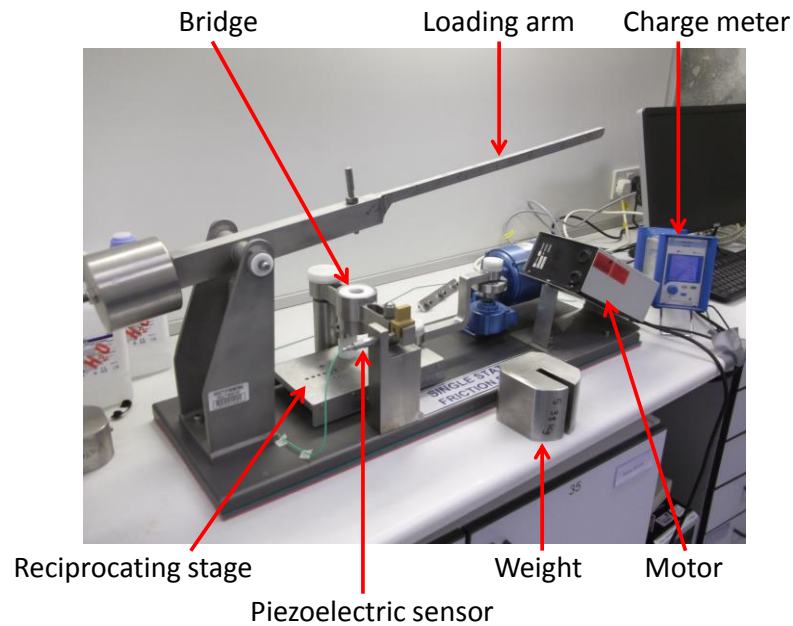


Figure 3.2. The single station multidirectional pin on plate friction rig.

The pin holder was slotted through the bridge of the rig so that the cartilage of the osteochondral pin was contacting the cartilage of the osteochondral plate. Bearings were placed on the top of the pin holder and the loading arm was lowered to contact the bearings. The spirit level was used to check that the loading arm was horizontal when contacting the pin holder (Figure 3.4). The motor and a charge amplifier were switched on. A weight was placed onto the loading arm as the test began. The stage reciprocated over a distance of 9 mm (stroke length) at $4 \text{ mm}\cdot\text{s}^{-1}$ for a total of 6 hours. Three different conditions were used, outlined in Table 3.2. Six repeats were conducted for each condition.

The piezoelectric sensor attached to the bridge of the rig detected the frictional force between the pin and plate which was converted to volts by a data acquisition unit. The voltage was relayed to the charge meter. The forces were recorded by a data acquisition unit and stored on the connected personal computer. The voltages were recorded using Labview 9 software. The co-efficient of friction was calculated from the recorded voltages via a calibration curve.

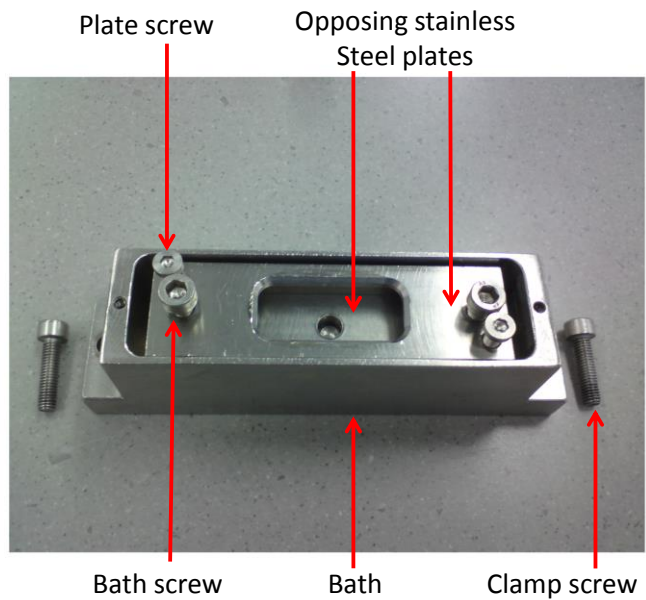


Figure 3.3. Friction rig components; plate clamp and bath. The components that were used to clamp the osteochondral plate in place on the friction rig. The bath was subsequently screwed to the reciprocating stage of the friction rig.

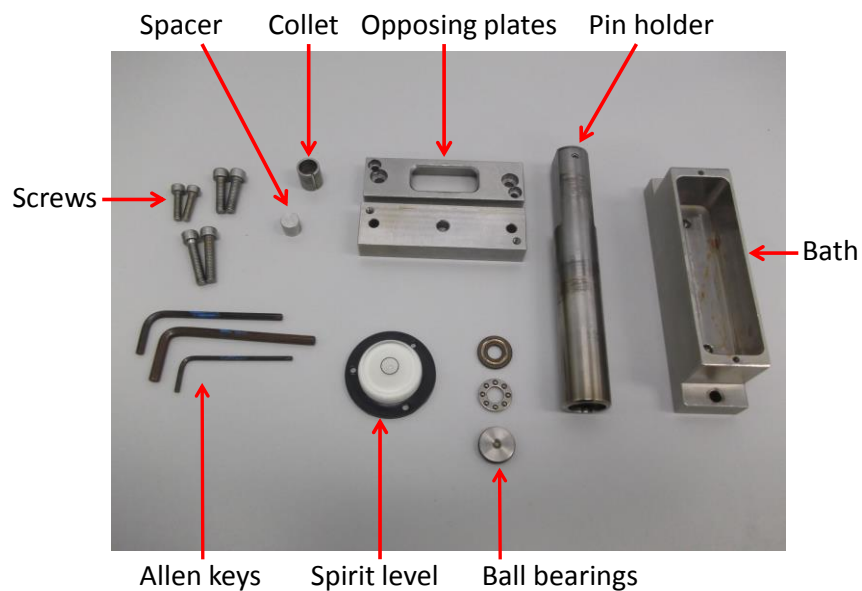


Figure 3.4. Equipment and components required for friction rig assembly.

Table 3.2 The different conditions used to generate mechanical degradation in cartilage specimens.

Condition	Load (N)	Contact Stress (MPa)	Lubricant
Mild	200	3.1	Ringer's solution
Moderate	478	7.5	Ringer's solution
Moderate serum	478	7.5	25% (v/v) Calf serum in PBS

3.4.2.1 Calibration

Calibration was performed so that accurate friction values could be calculated from the recorded voltages taken from the pin on plate friction rig. To calibrate the rig, the pin holder was suspended in the bridge of the rig. A cotton thread with a loop on one end was looped around the base of the pin holder, laid around the wheel and hung vertically with the weight holder attached to the bottom of the thread (Figure 3.5).

Each weight used for the calibration was weighed three times and labelled before the calibration began and the charge meter was turned on. The mean value of the three weight measurements was used as the actual true weight of each weight. When the test had begun, one weight was added to the weight holder every 80 seconds up to a total of 8 weights. One weight was then removed again every 80 seconds until only the weight holder remained. The programme was set to take 4 measurements during the 80 second period. The calibration was repeated three times sequentially. As weights were added and removed, care was taken to keep the movement of the thread to a minimum during the reading to prevent inaccuracies in measurements. A calibration curve was produced from the readings of average voltage against weight in Newtons, which allowed the coefficient of friction to be calculated.

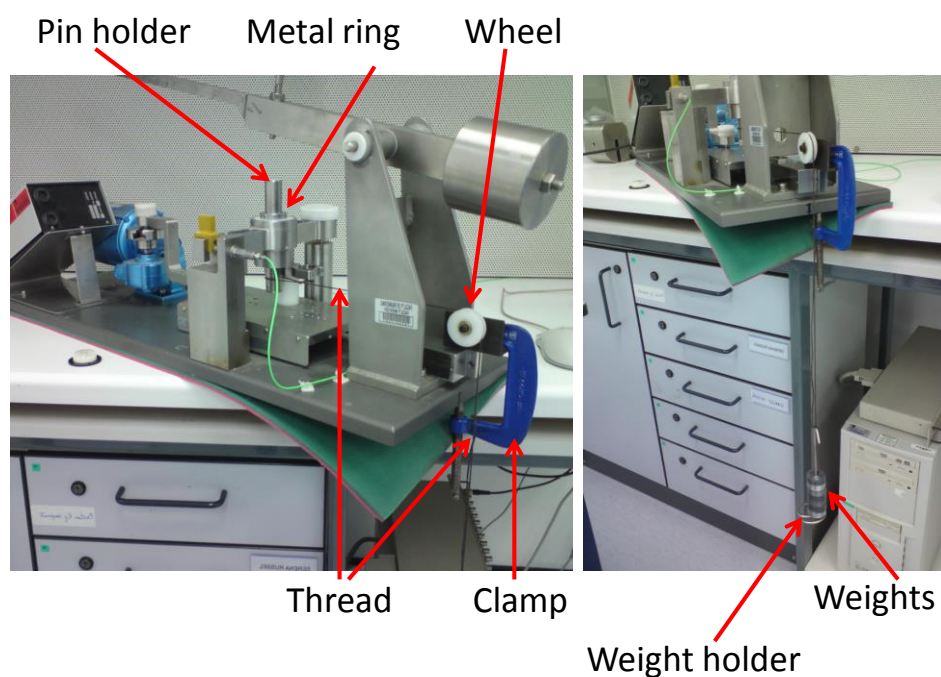


Figure 3.5. Calibration of the single station multidirectional pin on plate friction rig. **A.** The pin holder is suspended in the bridge using a metal ring. A wheel is clamped to the rig. **B.** A thread is looped around the base of the pin holder then around the groove of the wheel before being allowed to hang vertically with the weight holder at the bottom of it.

3.4.3 Static loading and deformation assessment of native cartilage

A six station wear rig and single station multidirectional pin on plate friction rig was used to assess the permanent deformation of the cartilage tissue via static loading of the tissue. This was primarily carried out to determine whether any permanent deformation occurring during mechanical degradation was caused by loading rather than tissue loss. If no loss of height was observed after static loading, any post degradation loss of tissue height could be attributed to tissue degradation alone. A single station rig was used for moderate condition static loading since the six station rig was not able to take a load of 478 N. Details on the set up and use of the single station multidirectional have previously been described in Section 3.4.2. A six station wear rig was used for mild condition static loading, which allowed simultaneous loading of six pin and plate pairs.

3.4.3.1 The six station multi-directional wear rig

The six station multidirectional pin on plate rig was designed and manufactured in the School of Mechanical Engineering at The University of Leeds, UK. The components required for setting up static loading of the six station rig are displayed in Figure 3.6.

To set up static loading conditions, bath inserts were placed into the bath wells and the CoCr plate was secured inside using screws. The well was placed onto the reciprocating stage and attached to the motor using the connecting rods to prevent movement of the stage (Figure 3.7A). An osteochondral plate was then placed onto the CoCr plate. The osteochondral pin was placed inside a small collet, which was then secured into the large collet. A spacer was placed behind the pin within the small collet (Figure 3.7B). A threaded nut was screwed into the large collet/ outer sleeve assembly to secure the pin in place. The bridge sections were placed onto the rig and the large collet/ outer sleeve assembly was slotted into the bridge. The setup was secured in place using clamps (Figure 3.8). Contact between the cartilage of the pin and plate was ensured by adjusting the plate position if necessary. A cantilever arm was placed into the bracket on the rig and secured with a pin. The ball bearings were placed onto the threaded nut. A spirit level was used to check that the lowered arm was horizontal and the weights (200 N) were placed onto the loading arms to produce a contact stress of 3.1 MPa between the pin and plate interface (Figure 3.9). The loading period was for 6 hours to replicate the loading time in the dynamic degradation protocol.

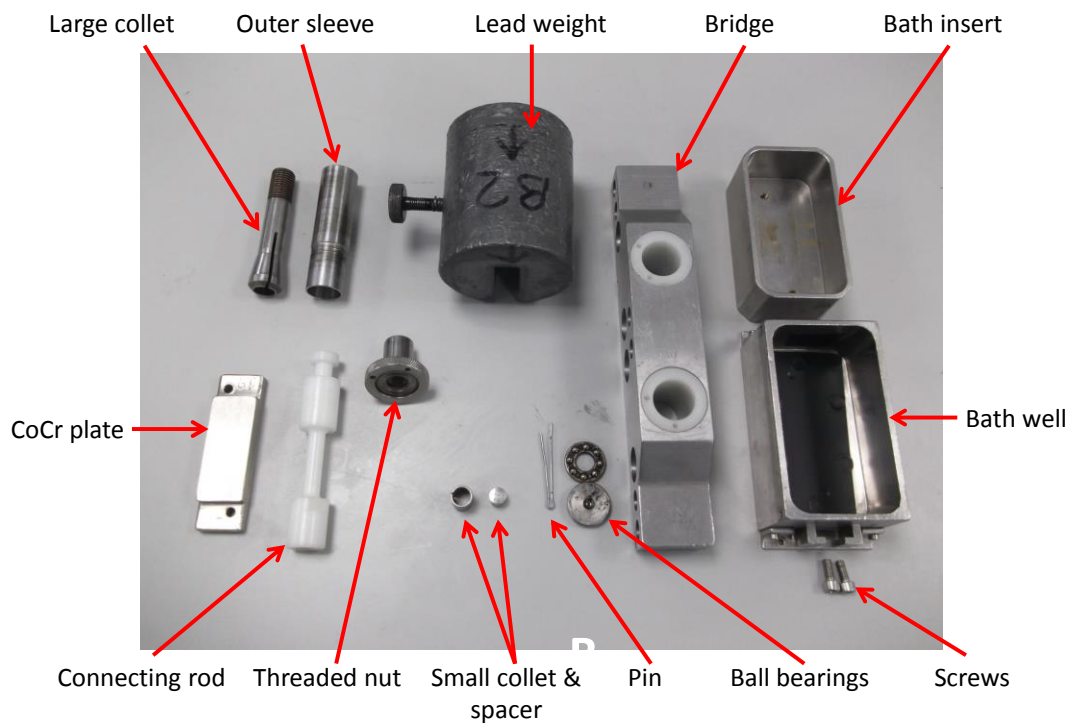


Figure 3.6. One of six sets of small components for the six station multidirectional wear rig.



Figure 3.7. The plate set up and pin holding assembly. A. The bath well, bath insert and plate were assembled before being placed onto the reciprocating stage. The assembly was then secured with the connecting rod. **B.** The osteochondral pin was placed inside the set up shown with the cartilage surface protruding.

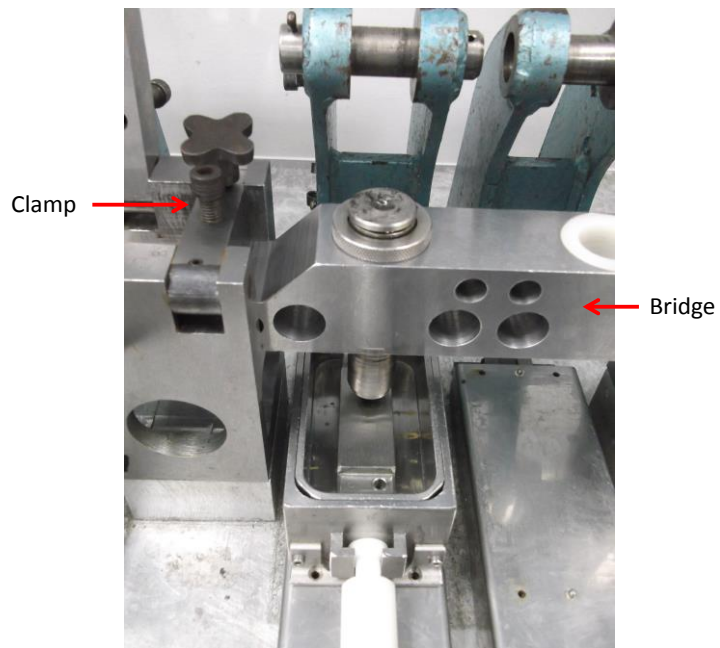


Figure 3.8. Small component assembly on the rig. The bridges were put in place and secured using a clamp. The pin assembly was slotted through the bridge and the ball bearings were placed on top.



Figure 3.9. Complete assembly of the six station wear rig.

3.4.3.2 Deformation and Recovery Tests

To assess changes to cartilage height, a Nikon profile projector was used to measure the cartilage height before loading, directly after loading, after 24 hours recovery from loading and after 48 hours of recovery from loading. The Nikon profile projector was to measure the cartilage height at six points around the circumference of the osteochondral pin. The pins were placed on the specimen platform of the profile projector. The image of the pins on the platform was projected onto a viewing screen which had a set of axis marked on it. The bone-cartilage interface on the osteochondral pin was lined up with the y line on the axis, the specimen platform was then adjusted so that the Y axis line was lined up with the surface of the cartilage tissue. The movement of the platform from the base of the cartilage to the surface was measured by the profile projector in millimetres which allowed the height of the cartilage to be measured. To allow each pin to recover post loading, the pin was placed in a 5 ml bijou containing tissue paper soaked in Ringer's solution and stored 4°C. The measurements on the pin were taken at 6 points around the pin circumference that were approximately equidistant.

Plates were measured using a TRIMOS Vernier height gauge with a dial indicator attached purchased from Draper Expert Middlesex, UK. Three equidistant measurements were taken horizontally across the centre of the pin on plate contact area. The height gauge had a resolution of 1 µm and the dial indicator had a resolution of 10 µm.

3.4.4 Silicon Mould Surface Replication for Surface Roughness Measurement

3.4.4.1 Rationale

Silicon rubber replicas were taken of cartilage specimens post mechanical degradation, after 24 hours of recovery and then again after 48 hours of recovery. The moulds allowed the surface roughness (Ra) of the cartilage surface to be determined using surface profilometry. Replicas of the specimens were taken as a permanent record of the specimens' features, which allowed the Ra to be determined at a later date. If measurements had been taken on the tissue specimens it would have resulted in specimens becoming extensively dried, rendering them useless for further analysis.

A 50 ml Microset system was used to produce the replicas (Figure 3.10). Synthetic rubber replicating compound 101Rf, was used to accurately replicate microstructures on the

cartilage surface. A Talysurf Ultra PGI800 from Taylor & Hobson, UK was used to take Ra measurements on the replicas.

The Ra is a surface roughness parameter that is defined as the arithmetic mean of absolute departures of the roughness profile from the mean line. After the trace had been taken the data was fitted to a line and a Gaussian filter was used to separate the waviness from the surface roughness. The use of this method allowed a quantitative value of roughness to be obtained to complement ESEM studies of the cartilage surface.

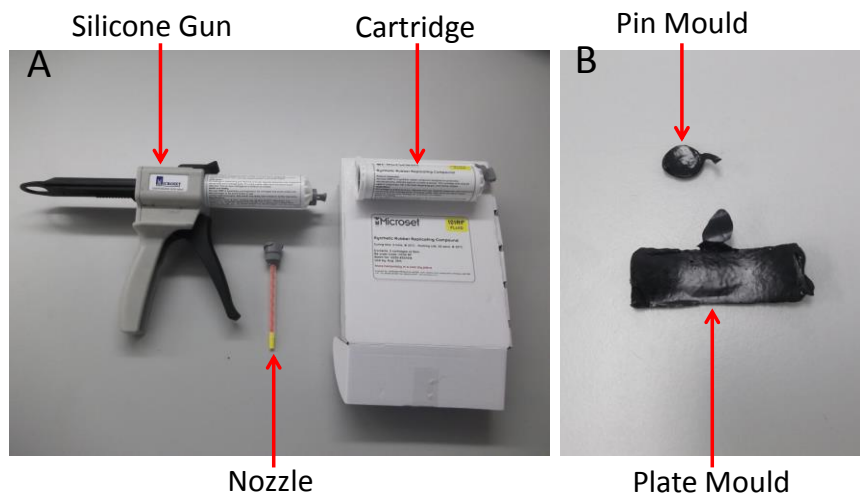


Figure 3.10. Microset system equipment and replicas. A. The rubber replicating compound was applied to the cartilage surface from the cartridge in the dispensing gun with the nozzle attached. **B.** The pin and plate moulds after curing was complete.

3.4.4.2 Calibration

The Talysurf calibration was completed at the beginning and the end of every session. A roughness standard was used to calibrate the machine (Figure 3.11). The stylus was positioned to measure the 0.8 μm line on the standard which resulted in a typical calibration trace and an Ra of approximately 0.8 μm if the tip was functioning correctly (Figure 3.12). Calibration analysis was completed with a least squares line fit, a Gaussian filter with an upper cut off of 0.8 mm and lower cut off of 8 μm .



Figure 3.11. The calibration standard for the Talysurf. Calibration of the machine with the right hand square is carried out before and after each session to confirm that no damage had taken place to the stylus ensuring correct results are recorded.

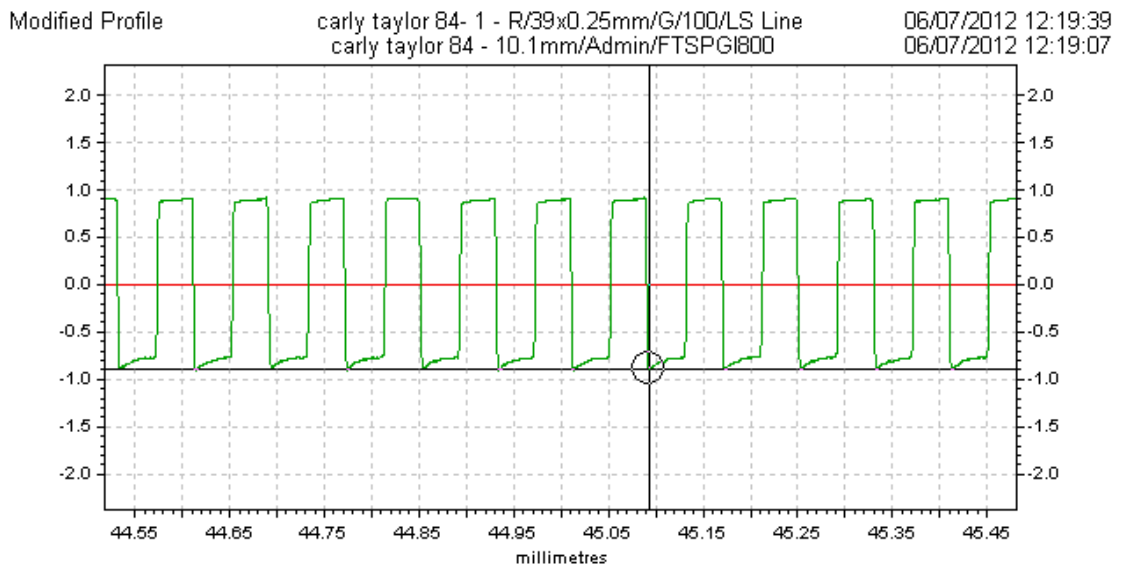
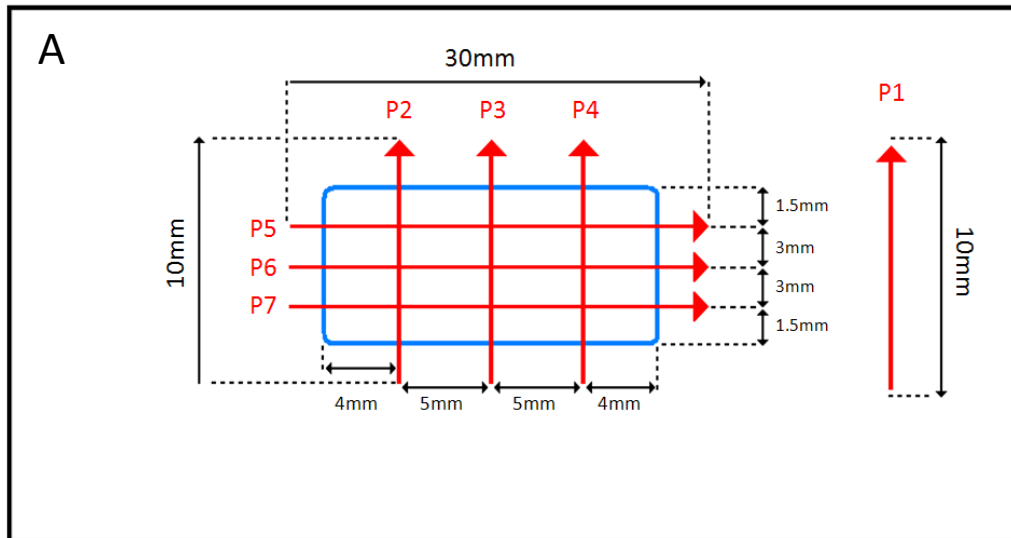


Figure 3.12. A typical calibration trace. Aside from the requirement of an Ra of 0.8, the calibration trace pattern itself was required to appear as in the one shown above with the characteristic “left toe”, one of which is circled on the trace.

3.4.4.3 Method

The specimens were removed from the friction rig and rinsed briefly in Ringer's solution. Specimens were then allowed to air dry for two minutes before the liquid silicone rubber was applied to their surface using the dispensing gun and allowed to cure. Once the silicone rubber had set the moulds were peeled from the cartilage specimens and stored in individual plastic pots at room temperature.

Talysurf measurements were taken as follows; a diamond tip with a radius of $2.5\mu\text{m}$ was used to take traces across the replica surface at 5mm/sec with an applied force on the tip of 0.85 mN (Figure 3.13). As the stylus transversed the replica, vertical movements along the Z axis were recorded as electronic signals which were converted to digital measurements that were used to construct a roughness profile. Analysis of the traces was completed using a Taylor Hobson Ultra software package. Traces were fitted to a least squares line to remove underlying geometries and put through a Gaussian filter with an upper cut off of 0.25 mm and lower cut off of $2.5\ \mu\text{m}$.



B

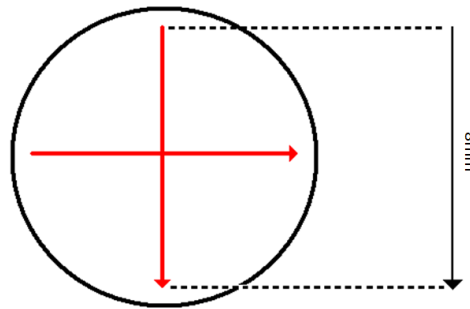


Figure 3.13. Trace map for cartilage pin and plate replicas. **A.** Arrows labelled in red indicate traces performed. The P1 trace was used as an undegraded control measurement. The blue line indicates the wear scar which was 18 mm by 9 mm. **B.** Pin traces are shown in red. Pin diameter was 9 mm. The traces are perpendicular to each other and are 8 mm in length. Diagram is not to scale.

3.4.5 Histological assessment of mechanically degraded cartilage tissues

Specimens were visualised using H & E staining and alcian blue staining as described in sections 2.6.1 and 2.6.2, respectively.

3.4.6 Immunohistological assessment of mechanically degraded cartilage tissues

Immunohistochemical staining for biglycan, collagen VI and cartilage oligomeric matrix protein was carried out as described in section 2.6.3.

3.4.7 Environmental scanning electron microscopy of the mechanically degraded cartilage surface

Scanning electron microscopy was used to assess the alterations to the cartilage surface after mechanical degradation (Section 2.7.1)

3.4.8 Transmission electron microscopy analysis of mechanically degraded cartilage tissue

Ultrastructural changes to the cartilage tissue were assessed using cupromeronic blue staining with transmission electron microscopy previously described in section 2.7.2.

3.4.9 Quantitative biochemical analysis of degraded cartilage tissue

Quantitative biochemical assays for glycosaminoglycans (Section 2.8.2) and collagen (Section 2.8.1) were carried out to assess whether loss of either of these components from the tissue had occurred during mechanical degradation.

3.4.10 Quantitative analysis of collagen in lubricants recovered after mechanical degradation of cartilage specimens

3.4.10.1 Rationale

There is potential in the future for the mechanical model developed and characterised here to be developed into a more complex whole joint simulator model. In a more complex model with extended test times it would be useful to assess the damage to the tissues in the model by analysing the lubricating fluid. With this in mind, the hydroxyproline and glycosaminoglycan assays for tissue (Sections 2.8.1 and 2.8.2 respectively) were developed for use with the lubricants generated during mechanical degradation. Due to the low concentration of collagen and glycosaminoglycans in the lubricants taken from the bath post mechanical degradation (Section 3.4), both the hydroxyproline and glycosaminoglycan assays had to be developed for use with fluids containing small concentrations of these components. In recognition of the differences between the Ringer's solution based lubricant and the serum based lubricant, the assays were optimised separately for each of the lubricants.

3.4.10.2 Quantitative analysis of collagen in Ringer's solution based lubricants; development steps

3.4.10.2.1 Sample concentration

To concentrate the collagen in the Ringer's solution lubricants, 1 ml of each mild and moderate lubricant (n=6 per condition) was pipetted into a sterile glass test tube and evaporated overnight in a dry heat block at 60°C. The dried lubricants were then placed upright in the freeze dryer to remove any remaining water.

3.4.10.2.2 Determination of dilution factor

Before samples were assayed they were diluted in assay buffer. The 1 in 50 dilution factor used for tissue specimens (Section 2.8.1) was too large for the lubricants as it would have resulted in over dilution. In order to prevent over dilution of the samples, a lower dilution factor was investigated.

A range of concentrations of hydroxyproline (standards) were diluted in Ringer's solution then hydrolysed and neutralised to create replicas of lubricant samples with known hydroxyproline concentrations (Section 2.8.1). This range of standards was made so that the standards were double the concentration of the normal range of standards. This was so that when they were diluted in assay buffer they would become the same concentration as the standards in assay buffer alone. The hydrolysed standards in Ringer's solution were diluted 1:1 with assay buffer and the hydroxyproline assay was carried out as in Section 2.8.1. The absorbance readings for both sets of standards were similar and it was concluded that a one to one dilution of specimens with assay buffer could be used in future experiments (Figure 3.14).

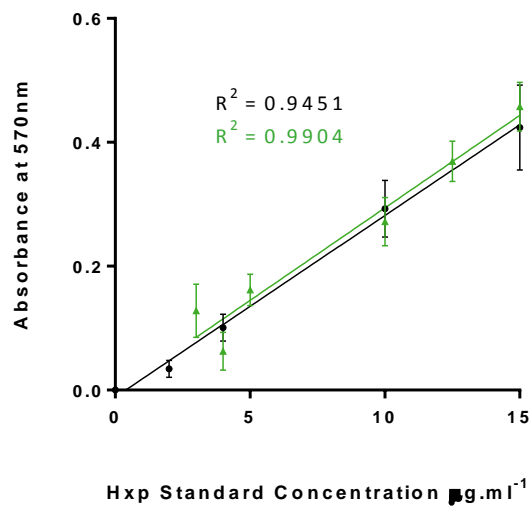


Figure 3.14. Standards diluted in assay buffer and standards diluted one to one with assay buffer and neutralised hydrolysed Ringer's solution. Black circles represent standards diluted in assay buffer. Green triangles represent known concentrations of hydroxyproline in neutralised hydrolysed Ringer's solution diluted one to one with assay buffer. Data is presented as the mean (n=3) \pm 95% confidence limits.

3.4.10.2.3 Determination of acid volume

In the hydroxyproline assay for tissue 5 ml of 6 M HCL was used to hydrolyse each 15 mg of tissue (dry weight) therefore it was reasoned that 2.5ml of 6 M HCL would be suitable for hydrolysing tissue volumes that were less than 7 mg. Six 1 ml samples of lubricant and five 1 ml samples of Ringer's solution were dried and lyophilised. It was found that the major proportion of the dry weight of the lubricants, was made up of the salts from the Ringer's solution (Table 3.3) and on average, less than 0.3 mg of tissue was present in each millilitre of the lubricant. Therefore 2.5 ml of 6 M HCL would be suitable for effective hydrolysis of 1 ml of Ringer's solution lubricant.

After the Ringer's solution lubricant samples had been assayed for collagen, it was found that the mild condition Ringer's solution lubricants required further concentration as the absorbances were close to the lowest standard on the standard curve. To further reduce the dilution of the mild lubricants use of a lower volume of acid could be used to hydrolyse the mild specimens was assessed.

Mild Ringer’s solution lubricant samples (n=3) were dried, and lyophilised. The samples were then hydrolysed with either 0.5 ml 6 M HCL or 2.5 ml of 6 M HCL. The hydroxyproline assay was then carried out on the samples as described in Section 2.8.1. There was no difference in collagen content of the lubricants indicating that 0.5 ml of 6 M HCL was sufficient to hydrolyse the mild Ringer’s lubricants as effectively as 2.5 ml of 6 M HCL (Figure 3.15).

Table 3.3 The post lyophilisation weights of 1ml of moderate Ringer’s solution lubricant and Ringer’s solution.

Sample	Lyophilised moderate condition Ringer’s lubricant (mg).	Lyophilised Ringer’s solution (mg).
1	9.9	10.7
2	9.2	9.6
3	10.6	9.9
4	11.2	8.8
5	9.1	9.6
Average	10.0	9.72

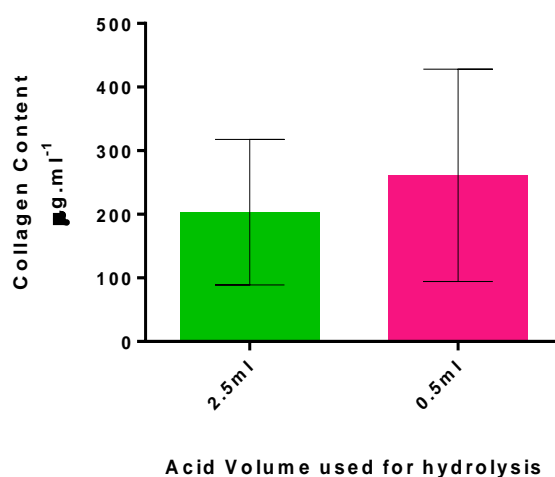


Figure 3.15. Effect of acid volume on mild lubricant hydrolysis prior to using the hydroxyproline assay. The results indicated that 0.5ml of 6M hydrochloric acid was suitable for digestion of 1ml of lyophilised mild Ringer’s solution lubricant. Data is presented as the mean (n=3) ± 95% confidence limits.

3.4.10.3 Quantitative analysis of collagen in Ringer's solution based lubricants generated during mechanical degradation regimes

All reagents used in the assay have been previously described in Chapter 2, Section 2.8.1. Post mechanical degradation, the lubricant bathing the cartilage specimens in the bath was collected and quantified. The lubricant was aliquoted into 1 ml fractions and stored at -25°C until use. To determine the collagen content of the lubricant, 1 ml of each lubricant was pipetted into a test tube and evaporated overnight in a dry heat bath at 60°C. The specimens were then lyophilised using a freeze dryer until specimen weights stabilised. To the moderate condition Ringer's solution lubricants, 2.5 ml of 6 M hydrochloric acid was added. To the mild condition Ringer's solution lubricants, 0.5 ml of 6 M hydrochloric acid was added. The samples were hydrolysed for 4 hours in a bench top autoclave at 121°C, followed by neutralisation with sodium hydroxide solutions that ranged between 12 M and 0.1M. The volume of each sample after neutralisation was quantified and recorded. The neutralised samples were diluted 1 in 2 with assay buffer and 50 µl of each sample, along with a range of hydroxyproline standards, was pipetted into a 96 well flat bottomed microplate in triplicate. Standards were composed of trans-4-hydroxy-L-proline in assay buffer at a range of 0-15 µg.ml⁻¹. Chloramine T solution (100 µl) was added to each of the standards and specimens and the plate was placed on a shaker for 5 minutes. Ehrlich's reagent (100 µl) was then added to the wells and incubated for 45 minutes at 60°C in a waterbath with the plate lid on. Parafilm was used to secure the lid onto the plate and to prevent water entering the plate. The absorbance was read at 570 nm using a plate reader and the unknown values were interpolated from the standard curve.

3.4.10.4 Collagen quantification assay for serum lubricants

Lubricant specimens containing serum were found to undergo caramelisation during acid hydrolysis. It was postulated that the caramelisation was caused by a chemical reaction known as the Maillard reaction between sugars and proteins in both the degradation products and serum. Various methodologies were examined before guanidine extraction was considered including pepsin digestion of cartilage tissues followed by a colorimetric assay using a Sircol kit. Guanidine extraction has been used previously for proteoglycan extraction in many studies (Stanton and Fosang, 2002; Bateman *et al*, 2010). The theory behind the decision to trial this technique lay in the principle that removal of sugars from the lubricants through removal of glycosaminoglycans would prevent the caramelisation reaction occurring. During this study there was insufficient time to complete the development of the hydroxyproline assay for serum lubricants. However it was determined that if cartilage was guanidine extracted for 48

hours before the acid hydrolysis step of the hydroxyproline assay, caramelisation was prevented.

3.4.11 Quantitative analysis of glycosaminoglycans in lubricants recovered after mechanical degradation of cartilage specimens

3.4.11.1 Quantitative analysis of glycosaminoglycans in Ringer's solution based lubricants: development steps

Several development steps were necessary to allow the GAG content of lubricants to be quantified. This was partly due to their low concentration, in addition to other factors including impurities in the papain used for digestion that caused problems with the absorbance readings during the assay.

3.4.11.1.1 Sample concentration

To concentrate the glycosaminoglycan content in the Ringer's solution lubricants, 1 ml of each lubricant was pipetted into a 2 ml eppendorf and then evaporated overnight in a dry heat block at 60°C. The dried lubricants were then placed in the freeze dryer for approximately 24 hours to remove any remaining water content. When the weights of the samples remained stable they were removed from the freeze dryer and digested using papain as described in Chapter 2 Section 2.8.2.

3.4.11.1.2 Papain source

When tissues were analysed using the GAG assay, crude papain was used during the digestion step (Section 2.8.2). The papain enzyme is extracted from papaya fruit and in its crude version contains contaminants and fibrous material that is not removed during its preparation. When lubricants that had been digested with crude papain were assayed with the dimethylene blue dye, the dye turned a yellow/ green colour rather than blue/ pink which resulted in abnormal absorbance readings. This was due to the presence of contaminants in the crude papain used for digestion. To reduce contamination pure papain was used. Pure papain has contaminating particulate matter removed from it resulting in a pure powder with a high concentration of enzyme. This resulted in cleaner digests that did not contain a large amount of particulate contamination. As a result of this, digested lubricant solutions could be diluted less prior to being assayed using DMB.

3.4.11.1.3 Dilution factor investigation

Before the digested samples were assayed in a 96 well plate, they were diluted with assay buffer. Reduced dilution factor volumes were investigated to prevent unnecessary dilution of the lubricants that contained low concentrations of GAGs. A range of concentrations of chondroitin sulphate were diluted in Ringer's solution then digested using 50 U.ml⁻¹ pure papain, to create replicas of lubricant samples with known glycosaminoglycan concentrations. These samples were then assayed as described in Section 2.8.2 against standards diluted in assay buffer alone. The absorbances for the samples that had not been diluted with assay buffer were significantly lower than those in assay buffer. This indicated that dilution in assay buffer was required for samples to allow accurate absorbance readings to be recorded (Figure 3.16).

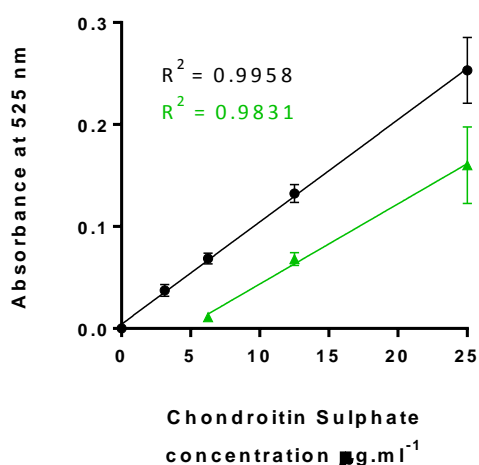


Figure 3.16. The absorbance profile of standards diluted in assay buffer and chondroitin sulphate in Ringer's solution that has been digested with 50 U.ml of pure papain. Green triangles represent digested standards in Ringer's solution that were not diluted in assay buffer. Black circles represent standards in assay buffer. Data is presented as the mean (n=3) \pm 95% confidence limits.

Following this the chondroitin sulphate samples that had been digested with pure papain in digestion buffer were diluted one to one in assay buffer and compared to standards in assay buffer alone (Figure 3.17). The samples diluted one to one with assay buffer did not have a statistically different absorbance to the standards of the same concentration in assay buffer alone. This showed that dilution of digested lubricants one to one with assay buffer before assaying was acceptable as it allowed the standard absorbances and the sample absorbances to be comparable.

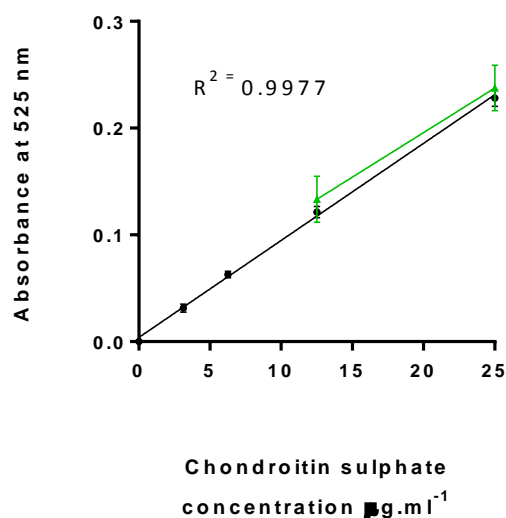


Figure 3.17. The absorbance profile of standards diluted in assay buffer and digested standards in Ringer's solution diluted one to one with assay buffer. Green triangles represent digested standards diluted one to one with assay buffer. Black circles represent standards in assay buffer. Data is presented as the mean (n=3) \pm 95% confidence limits.

3.4.11.1.3 Optimising pure papain concentration for lubricant digestion

To determine whether the concentration of papain used to digest lubricant samples could be reduced, moderate lubricant samples (n=6) were digested with 30, 40 or 50 U.ml⁻¹ of pure papain and assayed using the DMB assay. The GAG content of the lubricants did not differ for samples digested with the different concentrations of papain (Figure 3.18). In light of this 40µg.ml⁻¹ concentration was chosen for future studies.

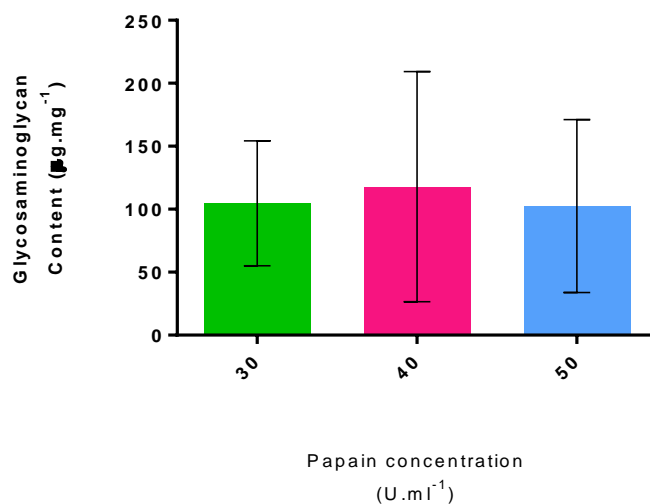


Figure 3.18. Effect of papain concentration on lubricant digestion. There was no significant difference found in the GAG concentration of specimens digested with the different papain concentrations (One way ANOVA, $P > 0.05$). Data is presented as the mean ($n=6$) \pm 95% confidence limits.

3.4.11.1.4 Digestion buffer volume

In the final development step, a smaller volume of digestion fluid was investigated for digestion of lubricant samples. One millilitre aliquots of moderate condition Ringer's solution lubricant were digested with 0.5 ml, 1 ml, 2 ml or 3 ml of 40 U.ml⁻¹ pure papain digestion solution (Figure 3.19).

There was no significant difference between the GAG content of lubricant digested with 0.5 ml, 1 ml and 2 ml of 40 U.ml⁻¹ digestion solution. However, a significantly lower GAG concentration was recorded when a 3ml digestion solution volume was used. Therefore, it was determined that 0.5 ml of 40 U.ml⁻¹ pure papain digestion solution was sufficient to digest 1 ml of lyophilised moderate Ringer's solution lubricant so 0.5ml of digestion solution was used for future experiments.

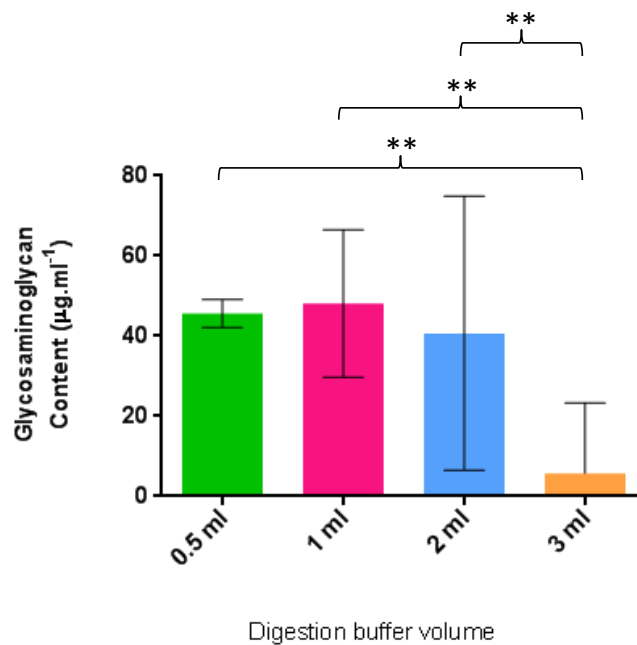


Figure 3.19. Effect of digestion buffer volume for lubricant digestion. It was determined that 0.5 ml of 40 µg.ml of pure papain in digestion buffer was sufficient for complete digestion of moderate Ringer’s solution lubricant. Asterisks represent a P value of $P \leq 0.01$ determined by one way ANOVA. Data is presented as the mean ($n=3$) \pm 95% confidence limits.

The changes described above resulted in the successful quantitation of low GAG concentrations in the mild and moderate condition Ringer’s solution lubricants.

3.4.11.2 Quantitative analysis of glycosaminoglycan in Ringer’s solution based lubricants generated during mechanical degradation regimes

3.4.11.2.1 Pure papain digestion solution

To each 1 ml of digestion buffer, 40 units of pure papain were added and dissolved using gentle inversion by hand. The remaining solutions used in this protocol have previously been described in Chapter 2, Section 2.8.2.

After mechanical degradation was complete, the lubricant bathing the cartilage specimens was collected and the total volume was quantified before being aliquoted into 1 ml fractions and frozen at 25°C. Before use, the lubricant aliquots were defrosted at room temperature. To assay, the Ringer’s lubricants were aliquoted into 2 ml eppendorfs at a volume of 1 ml and placed into a dry heat bath at 60°C overnight to evaporate. Specimens were then lyophilised

until they reached a stable weight. To each of the samples, 0.5 ml of 40 U.ml pure papain solution was added. The specimens were incubated at 60°C for 36 hours then centrifuged for 40 seconds at 1360 G in a minifuge. The supernatant was removed into a clean eppendorf. A range of standards (3.125 to 25 $\mu\text{g.ml}^{-1}$) were made up using chondroitin sulphate B in assay buffer. Standards below 3.125 $\mu\text{g.ml}^{-1}$ were not suitable for this assay due to non-linearity in the standard curve below this concentration. Before assaying, the mild condition samples were diluted 1 in 2 with assay buffer. The moderate samples were diluted 1 in 7 with assay buffer and 40 μl of each specimen and standard was pipetted into a 96 well flat bottomed microplate in triplicate. To each specimen and standard, 250 μl of DMB dye was added using an automatic pipette and the plate was placed on a shaker at 100 rpm. After two minutes the absorbance was determined using a microplate spectrophotometer at 525 nm. A graph of absorbance was plotted against the standard concentrations allowing linear regression analysis to be used to interpolate the unknowns from the standard curve.

3.4.11.3 Quantitative analysis of glycosaminoglycan in serum based lubricants generated during mechanical degradation regimes

Not all of the development steps that were suitable for assaying glycosaminoglycans in the Ringer's solution lubricants were suitable for the serum based lubricant. Unlike Ringer's solution lubricant, serum lubricant was not evaporated and lyophilised prior to digestion. This was due to the formation of an insoluble film around the inside of the eppendorf after evaporation of serum lubricant. The film prevented complete digestion of the lubricant because large particles of the film were still visible after digestion.

3.4.11.3.1 Dilution Factor Investigation

As with the Ringer's solution lubricants, dilution experiments were conducted with the serum lubricants to determine the effects of low dilutions on absorbance readings. A set of chondroitin sulphate concentrations in 25% (v/v) serum in PBS were digested using 60 U.ml⁻¹ pure papain in digestion buffer: 1 ml of each concentration was added to 1ml of pure papain in digestion buffer. The final concentration of the pure papain in the digestion was therefore 30 U.ml⁻¹. The samples were then diluted one in five in assay buffer and compared to standards in assay buffer. There was no difference in absorbance of the standards so it was concluded that a one in ten dilution of digested serum lubricant samples with assay buffer before assaying was appropriate (Figure 3.20).

3.4.11.3.2 Papain concentration optimisation

Finally, it was determined whether a lower concentration of papain could be used to digest serum lubricant samples. The starting concentration for the previous serum lubricant digests had been 60 U.ml⁻¹ so 60 U.ml⁻¹ was compared with 40 U.ml⁻¹. Serum lubricants were digested with either 60 U.ml⁻¹ or 40 U.ml⁻¹ pure papain in digestion buffer and the total GAG content of the lubricants was compared (Figure 3.21). As there was no significant difference between the two values, 40 U.ml⁻¹ of pure papain was used for subsequent assays.

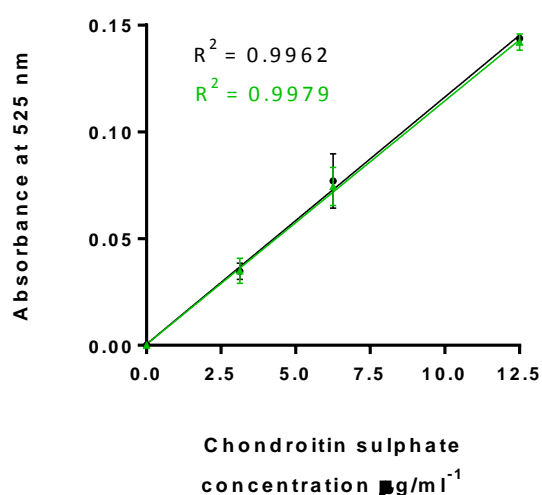


Figure 3.20. The absorbance profile of standards diluted in assay buffer and standards diluted one in five with assay buffer. Black circles represent standards diluted in assay buffer. Green triangles represent standards in digested lubricant diluted one in five with assay buffer. Data is presented as the mean (n=3) ± 95% confidence limits.

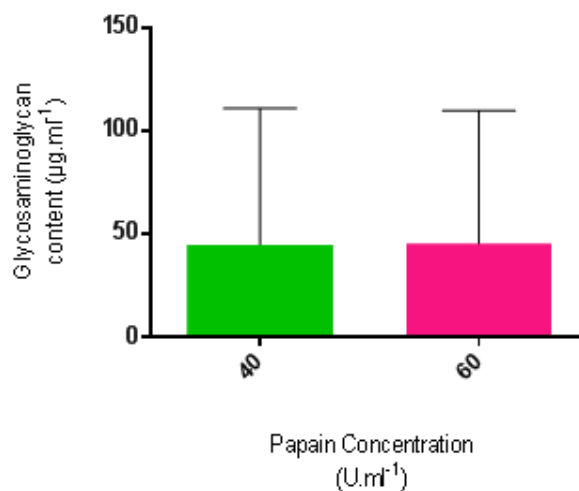


Figure 3.21. Effect of pure papain concentration for serum lubricant digestion. It was concluded that a 40 $\mu\text{g.ml}^{-1}$ pure papain concentration was suitable for serum lubricant digestion. Data is presented as the mean ($n=4$) \pm 95% confidence limits.

3.4.11.4 Quantitative analysis of glycosaminoglycan in serum based lubricants generated during mechanical degradation regimes.

To 1 ml of each serum lubricant sample, 1ml of 40 U.ml pure papain solution was added. The specimens were incubated at 60°C for 36 hours then centrifuged for 40 seconds at 1360 G in a minifuge. The supernatant was removed into a clean eppendorf. The supernatant was diluted 1 in 5 with assay buffer. A 40 μl volume of each sample and standard were pipetted into a 96 well flat bottomed microplate in triplicate. To each 40 μl in the plate, 250 μl of DMB dye was added and the plate was placed on a shaker at 100 rpm. After two minutes the absorbance was determined using a microplate spectrophotometer at 525nm. A graph of absorbance was plotted against the standard concentrations allowing linear regression analysis to be used to interpolate the unknowns from the standard curve.

3.5 Results

3.5.1 Macroscopic evaluation of dynamically mechanically degraded cartilage

Osteochondral pins and plates were degraded using a single station friction rig under varying load and lubricant conditions. The two conditions were classed as mild (3.1 MPa/ 200 N) and moderate (7.5 MPa/ 478 N) which represented two different loading conditions in the knee that have been previously detailed (Table 3.2). A Ringer's based lubricant was used for mild and moderate loading condition, a serum based lubricant was also used with the moderate loading condition. During mechanical degradation osteochondral pins and plates were articulated against each other under load for 6 hours (described in Section 3.4.2). Photographs were taken of specimens allowing assessment of macroscopic damage (Figures 3.22-3.24).

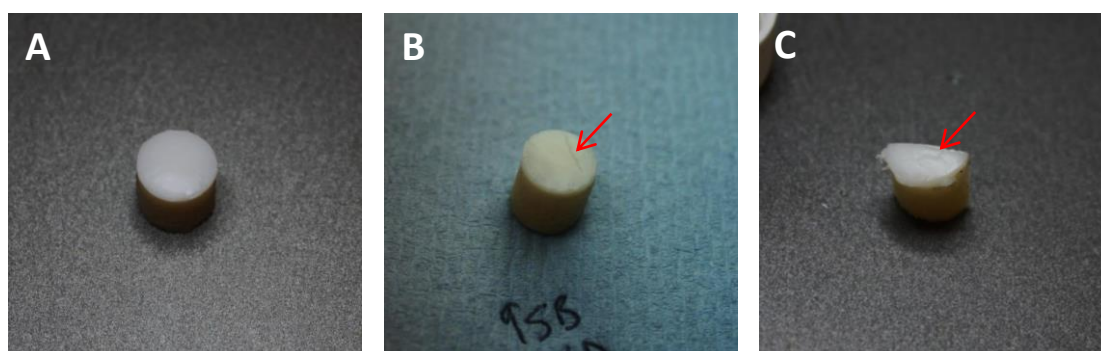


Figure 3.22. Osteochondral pin specimens after mild condition degradation in Ringer's solution. The pins shown represent the typical damage patterns seen on osteochondral pins after degradation. The third pin has been bisected in preparation for histological analysis. **A.** Specimen A did not appear to have any obvious damage to the surface, however the cartilage did appear swollen. **B.** This pin had a small crack across the surface of the tissue (arrow). The remaining tissue did not appear damaged however the surface did appear to be duller than control specimens. **C.** This pin which has been bisected, shows the most severe type of damage that was observed after mild condition degradation. Several cracks can be seen on the surface of the swollen cartilage (arrow).

Mild condition specimens articulated in Ringer's solution demonstrated the least damage of all the conditions and tissue loss was not observed at a macroscopic level (Figure 3.22). The most severe form of macroscopic degradation observed under mild degradation conditions was

cracking at the cartilage surface, four of the specimens had cracks. Two mild condition specimens retained a smooth appearance, however swelling of the tissue was observed. Three specimens had a single fine crack on the surface while one specimen showed several intersecting cracks across its surface (Figure 3.22C).

Moderate condition specimens tested under a 478 N load in Ringer's solution lubricant were highly variable in their macroscopic appearance. Four specimens did not show a large loss of tissue whereas two specimens appeared to have a significant loss of tissue resulting in a loss of over 50% of the cartilage height (Figure 3.23C). Cracking was the most common form of damage under moderate loading conditions in Ringer's lubricant; all of the specimens demonstrated cracking to some degree across the surface.

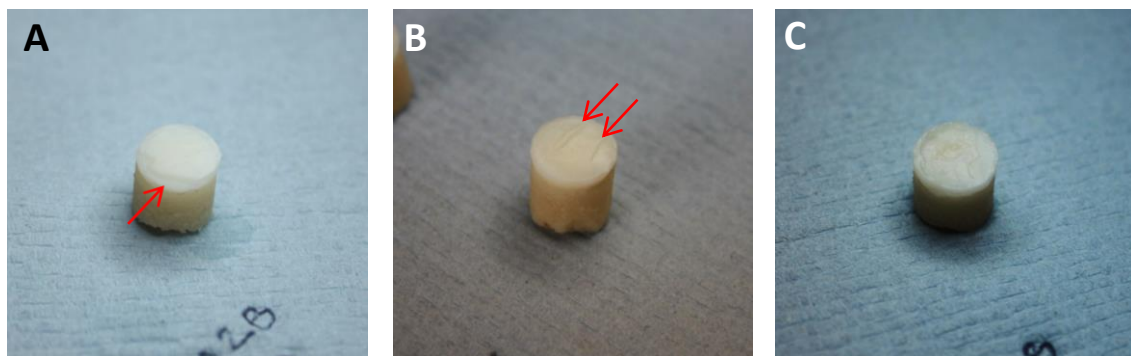


Figure 3.23. Osteochondral pin specimens after moderate condition degradation in Ringer's solution. The pins shown are representative of the typical damage patterns observed on osteochondral pins under the moderate degradation conditions. **A.** This specimen was damaged primarily around the circumference of the pin (arrow) which was unusual as the remaining specimens primarily lost tissue from the central region of the pin rather than the edges. The surface of the tissue appeared dull and scratched. **B.** Apart from two cracks across the pin surface (arrows), this pin was not heavily damaged and represented the lower end of the damage scale seen on specimens that underwent moderate condition degradation with Ringer's solution lubricant. **C.** This specimen was heavily damaged and represented the most severe end of the scale of damage seen on moderate condition pins in Ringer's solution lubricant. A large volume of cartilage tissue was lost from the pin leaving less than one half of the pin depth remaining.

Specimens degraded under moderate conditions with serum lubricant demonstrated similar damage to that observed in the moderate condition specimens in which Ringer's solution lubricant was used (Figure 3.24). Tissue loss that was equivalent to over 50% of the cartilage height was observed in addition to extensive cracking on two specimens. However some

specimens, as was seen with moderate specimens in Ringer's solution, showed only fine superficial cracks.

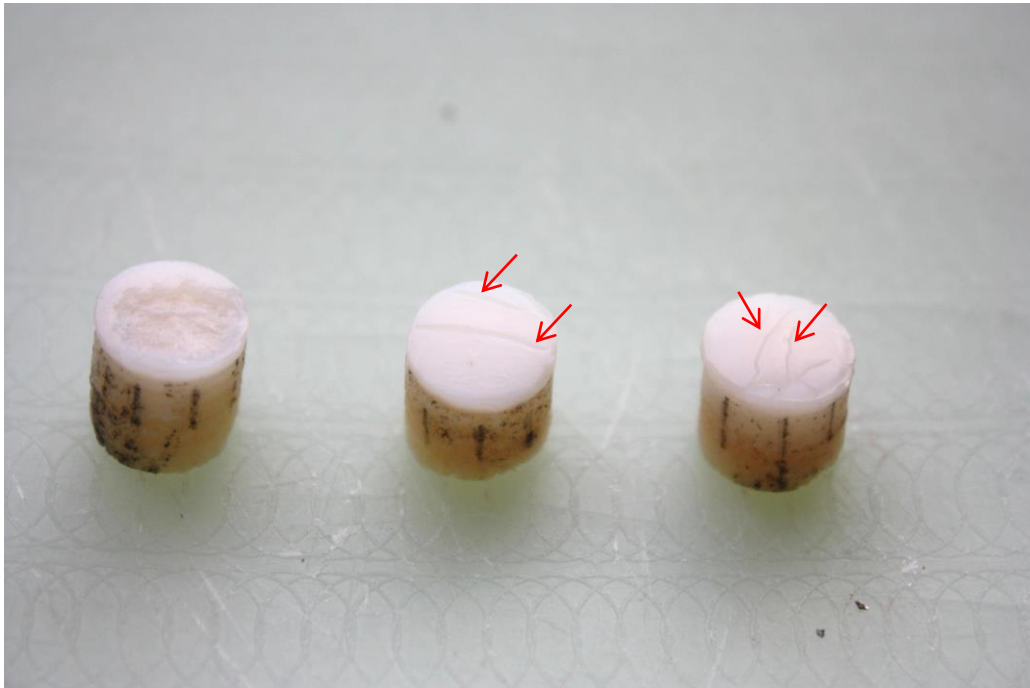


Figure 3.24. Osteochondral pin specimens after moderate condition degradation with serum lubricant. The pins shown here represent the typical damage patterns observed macroscopically on osteochondral pins under the specified loading conditions. The pin to the left of the image had lost a large volume of tissue. The middle pin and right hand pin showed cracks in the surface (arrows).

3.5.2 Height loss and recovery of statically loaded cartilage specimens

To confirm that tissue loss from the osteochondral specimens was due to articulation during degradation rather than permanent deformation and to determine the recovery time of the tissue post degradation, static loading assessments were conducted. The loading protocol and the equipment used to assess the height of the specimens have previously been described (Section 3.4.3). In brief, the osteochondral pins and plates were loaded statically using either a six station wear rig or single station multidirectional friction rig to determine how loading affected cartilage height via permanent deformation. Changes to the height of the cartilage on osteochondral pins was measured using a Nikon profile projector, while changes in the height of the cartilage on the osteochondral plates was measured using a Vernier height gauge. The

tests were conducted in Ringer's solution. A repeated measures ANOVA was used to statistically analyse the static loading data followed by a Tukey's multiple comparison post test.

For the pins loaded statically under mild conditions (3.1MPa) the post loaded cartilage height was significantly lower than the pre loading cartilage height. After 48 hours of recovery, the cartilage height was significantly higher than the post loading height, indicating that recovery had taken place (Figure 3.25). Pins loaded statically under moderate loading conditions had a significant drop in cartilage height directly after loading compared with pre-loading height. A significant difference was also observed between cartilage height prior to loading and heights after 48 hours of recovery (Figure 3.26).

The cartilage height of the plates loaded statically under mild loading conditions dropped significantly between pre and post loading (Figure 3.27). A significant difference was also seen between post loading heights and both the 24 hour and 48 hour recovery specimens, indicating that cartilage recovery was complete within 24 hours.

The cartilage height of plates loaded statically under moderate loading conditions dropped significantly between pre and post loading time points. A significant difference was also observed between post loading heights and both the 24 hour and 48 hour recovery heights, indicating cartilage recovery had taken place by 24 hours (Figure 3.28).

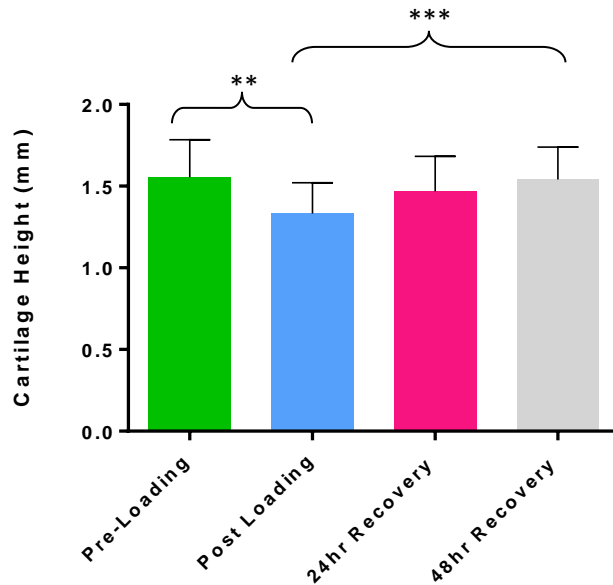


Figure 3.25. Osteochondral pin cartilage height recovery post static loading under mild conditions (200 N load applied for 6 hours). Data is presented as the mean (n=6) ± 95% confidence intervals. The data was analysed by repeated measures analysis of variance followed by determination of significant differences between groups using a Tukey post test; ** equates to $P \leq 0.01$; *** equates to $P \leq 0.001$.

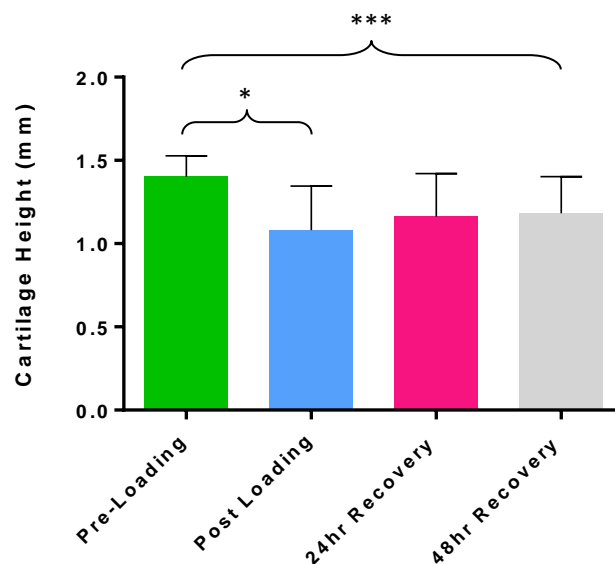


Figure 3.26. Osteochondral pin cartilage height recovery post static loading under moderate conditions (478 N load applied for 6 hours). Data is presented as the mean (n=6) ± 95% confidence intervals. The data was analysed by repeated measures analysis of variance followed by determination of significant differences between groups using a Tukey post test; * equates to $P \leq 0.05$; *** equates to $P \leq 0.001$.

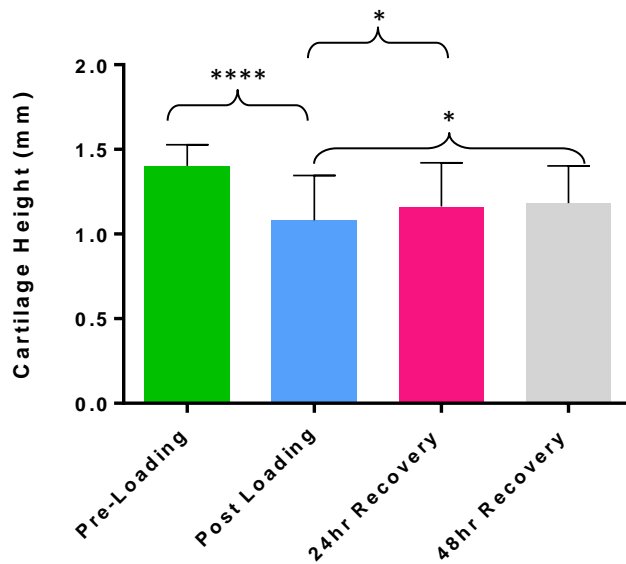


Figure 3.27. Osteochondral plate cartilage recovery post static loading under mild conditions (200 N load applied for 6 hours). Data is presented as the mean (n=6) ± 95% confidence intervals. The data was analysed by repeated measures analysis of variance followed by determination of significant differences between groups using a Tukey post test; * equates to $P \leq 0.05$; **** equates to $P \leq 0.0001$.

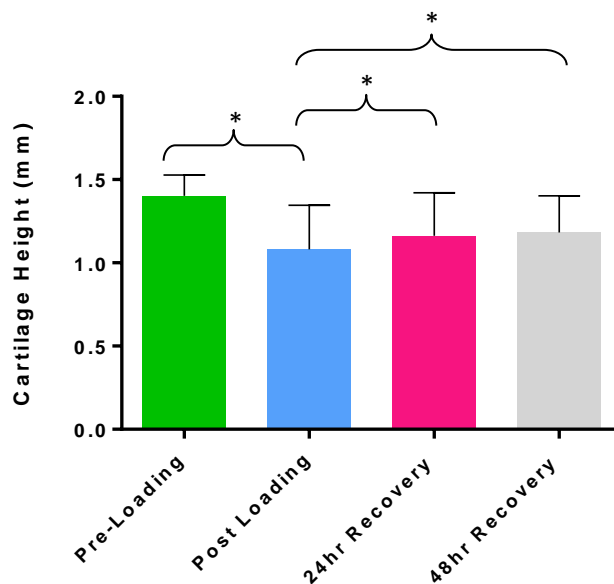


Figure 3.28. Osteochondral plate cartilage recovery post static loading under moderate conditions (478 N load applied for 6 hours). Data is presented as the mean (n=6) ± 95% confidence intervals. The data was analysed by repeated measures analysis of variance followed by determination of significant differences between groups using a Tukey post test; * equates to $P \leq 0.05$.

These results indicated that the cartilage on the osteochondral plates loaded under either the mild or moderate conditions was completely recovered to its original height after 24 hours. The cartilage of the pins that underwent mild condition static loading was recovered after 24 hours. The cartilage of the pins that underwent moderate condition static loading appeared to have recovered at 24 hours as there was no significant difference between the pre loading and 24 hour recovery heights. However, at 48 hours the difference in heights became significant implying that the tissue was not recovered. Due to the conflicting nature of this result, all tissues were allowed to recover for 48 hours after mechanical degradation, before further analysis or freezing was carried out.

3.5.3 Assessment of cartilage height post dynamic mechanical degradation

To assess if tissue loss was occurring during dynamic mechanical degradation, the height of osteochondral plates and the height of the cartilage of the osteochondral pins was recorded using a vernier height gauge and Nikon shadowgraph, respectively. Three measurements were taken equidistantly across the deformed area of the plate using the height gauge (Section 3.4.3.2). Six measurements were taken around the circumference of the pin using the profilometer (Section 3.4.3.2).

The height of the cartilage on the pins that underwent mild condition dynamic loading with Ringer's solution were not significantly different from each other (Figure 3.29). There was a significant difference in the cartilage height of the pins loaded dynamically under moderate conditions in Ringer's solution at the pre-loading and post loading time points (Figure 3.30). There was no significant difference between the cartilage heights of the pins loaded under moderate dynamic conditions with serum based lubricants at any time point (Figure 3.31). There was no significant difference between any of the heights recorded at the different time points, for the plates under mild or moderate conditions with Ringer's solution lubricants (Figures 3.32 and 3.33). There was a significant drop in cartilage height of the plates loaded dynamically under moderate conditions with serum based lubricant at the pre-loading and post loading time points but no difference was seen between the 24 and 48 hour times points (Figure 3.34).

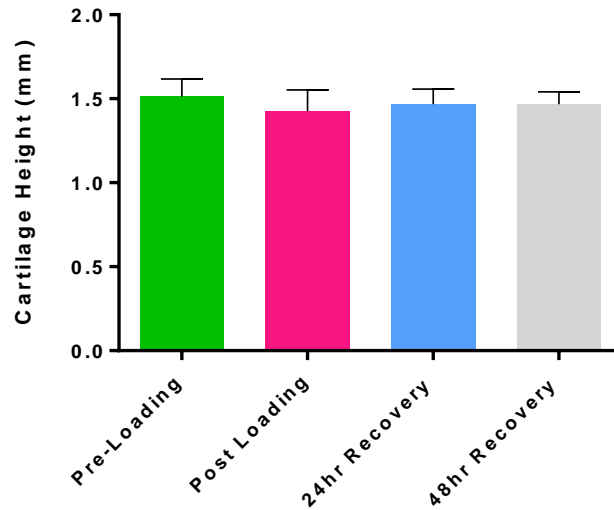


Figure 3.29. Cartilage height of osteochondral pins following mild condition dynamic mechanical degradation in Ringer’s solution lubricant. Data is presented as the mean (n=6) ± 95% confidence intervals. The data was analysed by repeated measures analysis of variance, no significant differences were found.

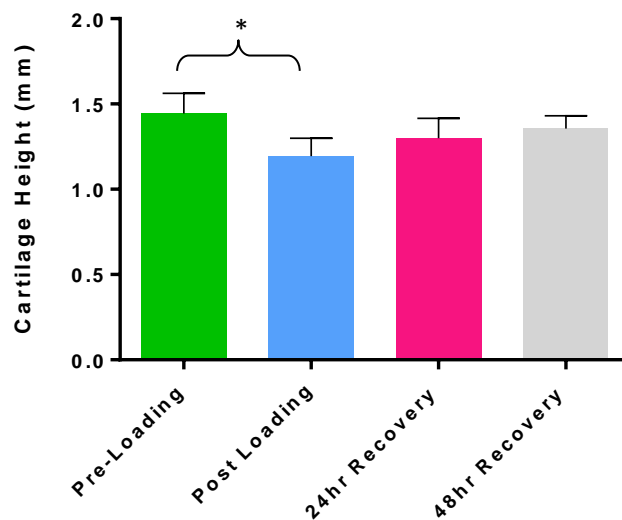


Figure 3.30. Cartilage height of osteochondral pins following moderate condition dynamic mechanical degradation with Ringer’s solution lubricant. Data is presented as the mean (n=6) ± 95% confidence intervals. The data was analysed by repeated measures analysis of variance followed by determination of significant differences between groups using a Tukey post test; * equates to $P \leq 0.05$.

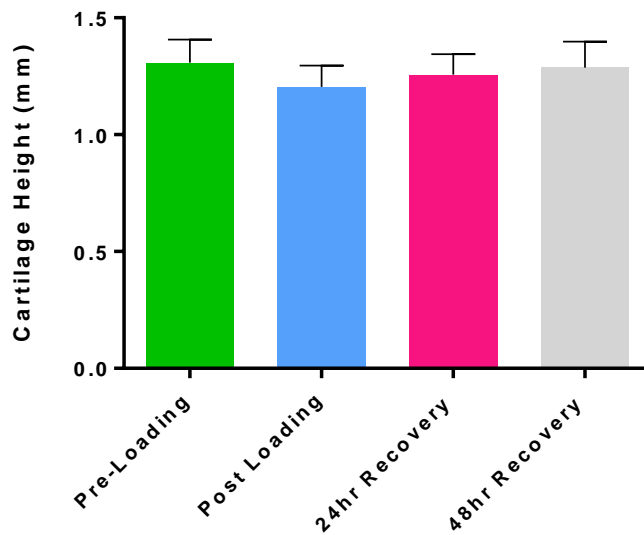


Figure 3.31. Cartilage height of osteochondral pins following moderate condition dynamic mechanical degradation with serum lubricant. Data is presented as the mean (n=6) \pm 95% confidence intervals. The data was analysed by repeated measures analysis of variance, no significant differences were found.

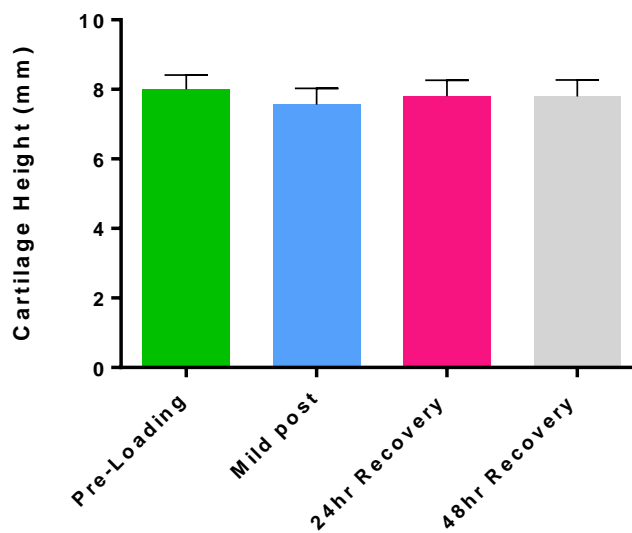


Figure 3.32. Height of osteochondral plates following mild condition dynamic mechanical degradation with Ringer's solution lubricant. Data is presented as the mean (n=6) \pm 95% confidence intervals. The data was analysed by repeated measures analysis of variance, no significant differences were found.

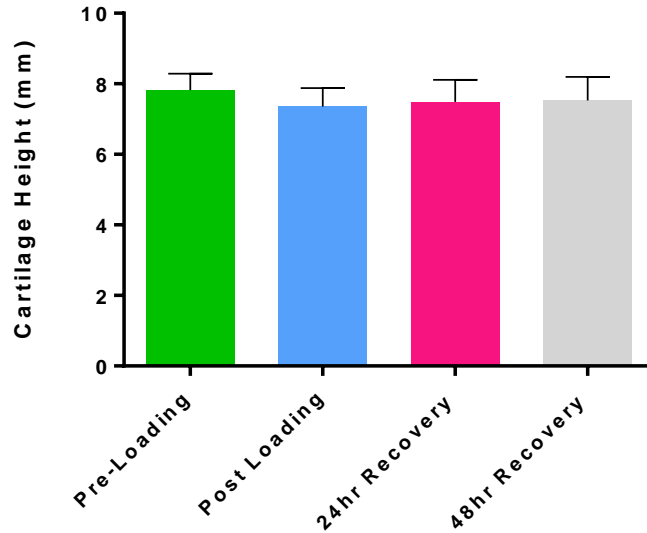


Figure 3.33. Cartilage height of osteochondral plates following moderate condition dynamic mechanical degradation with Ringer’s solution lubricant. Data is presented as the mean (n=6) ± 95% confidence intervals. The data was analysed by repeated measures analysis of variance, no significant differences were found.

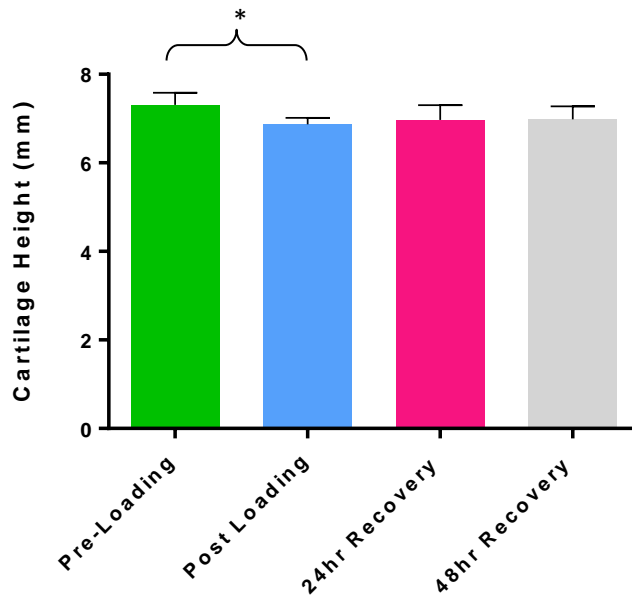


Figure 3.34. Cartilage height of osteochondral plates following moderate condition dynamic mechanical degradation with serum lubricant. Data is presented as the mean (n=6) ± 95% confidence intervals. The data was analysed by repeated measures analysis of variance followed by determination of significant differences between groups using a Tukey post test; * equates to $P \leq 0.05$.

It was concluded from these results that tissues were recovered after 48 hours and that there was no significant loss of tissue from the osteochondral pins and plates due to mechanical degradation.

3.5.4 Surface roughness measurement of mechanically degraded cartilage replicas

To allow quantitative evaluation of the roughness of the cartilage tissue after mechanical degradation had taken place, Ra values were determined using surface profilometry of silicone replicas of the cartilage surface (Section 3.4.4). A Talysurf PGI 800 profilometer was used to perform the measurements. The silicone replicas of the mechanically degraded pin and plate surfaces were taken immediately after mechanical degradation, after 24 hours of recovery and after 48 hours of recovery.

No significant differences in surface roughness was found between the control pin tissue replicas and the replicas of the mild degradation condition pin tissue in Ringer's solution lubricant and the moderate condition pin tissue replicas in serum lubricant (Figure 3.35 / Table 3.4). The surface roughness of the control pin replicas was significantly lower than the replicas of the moderate degradation condition pin tissue in Ringer's solution at the 24 and 48 hour recovery time points. The surface roughness of the pins subjected to moderate degradation conditions in Ringer's solution was significantly higher at the 24 hour and 48 hour recovery time points compared to the surface roughness of the pins subjected to mild degradation conditions in Ringer's solution at all three time points tested (Figure 3.35 / Table 3.4). It was observed that both the pin and plate specimens that underwent moderate degradation conditions had a greater variability in their surface roughness values than the control tissue and the tissues that underwent mild degradation conditions. In addition to this, it was clear that pin specimens that underwent moderate degradation with serum lubricant had greater variability than pins that underwent mild or moderate degradation protocols with Ringer's solution lubricant (Figure 3.35B/C/D.)

The surface roughness of the control plate replicas was significantly lower than the surface roughness of the replicas from plates tested under moderate conditions using Ringer's solution lubricant at all of the time points. A significant increase in surface roughness was also seen between the control plate replicas and the moderate plate replicas with serum lubricant at the 24 hour and 48 hour recovery time points (Figure 3.36 / Table 3.5). A significant increase in Ra was found between the mild condition replica plates at the post, 24 hour recovery and 48 hour recovery time points and the moderate condition plate replicas articulated with Ringer's solution lubricant at the post, 24 hour and 48 hour recovery time points (Figure 3.36 / Table 3.5).

These results indicated that the roughness of mild condition pin and plate tissue did not increase during mechanical degradation as the tissue on both pins and plates that underwent mild condition degradation showed no change in surface roughness compared to the undegraded control. Degradation of pins and plates under moderate conditions in Ringer's solution lubricant increased the surface roughness of the tissue. The results also indicated that the surface roughness of plates increased when they were articulated under moderate conditions with serum lubricant however, the surface roughness of the pins did not.

The moderately degraded pin specimens that were articulated in Ringer's solution were the roughest specimens of the three conditions. The moderate condition pin specimens articulated in serum based lubricant also became rough. However, high variability was observed under this condition, as some specimens became very rough while some remained smooth. The results indicated that a higher load and therefore an elevated contact stress was more likely to produce a rougher surface on the cartilage tissue. The roughness of the pins was more variable than the roughness of the plates, implying that the use of specimens with a smaller surface area led to an increase of variability in the experimental conditions.

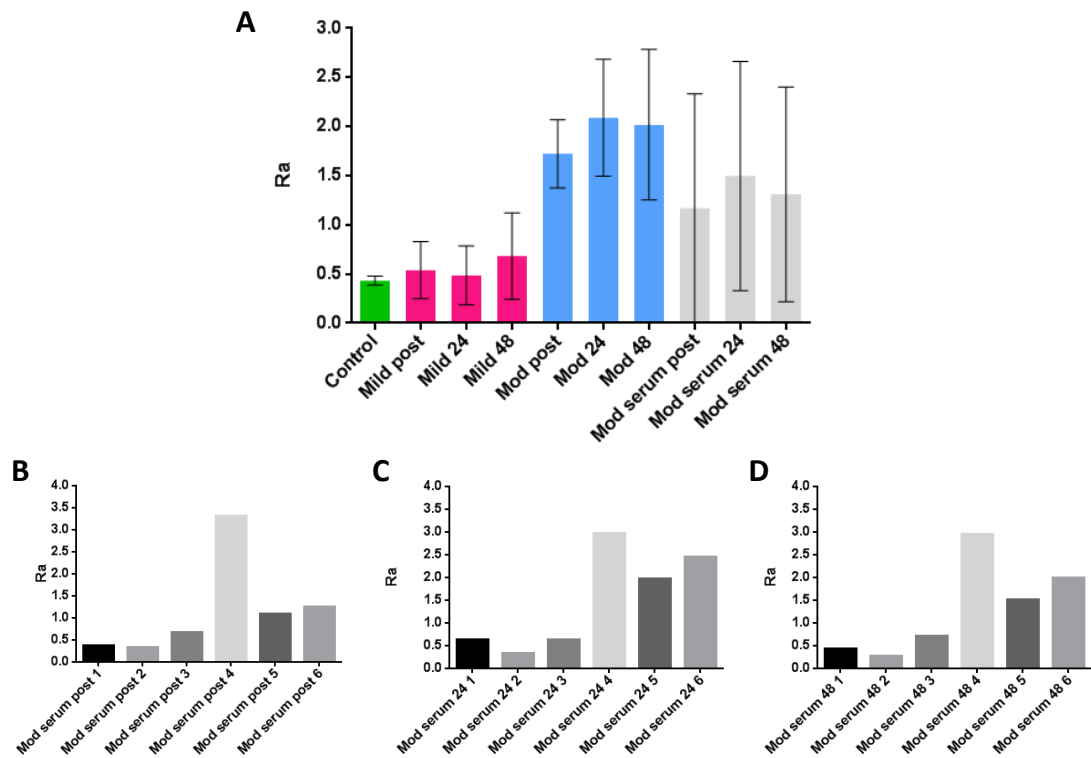


Figure 3.35. The mean surface roughness of pin replicas directly after degradation and after 24 and 48 hours of recovery. A. Post refers to post degradation, 24 denotes 24 hours of recovery, 48 denotes 48 hours of recovery. Data is presented as the mean ($n=6$) \pm 95% confidence intervals. The data was analysed by repeated measures analysis of variance followed by determination of significant differences between groups using a Tukey post test. **B.** The individual Ra measurements for the pins degraded under moderate conditions in serum lubricant immediately after loading, after 2 hours of recovery (**C**) and after 48 hours of recovery (**D**).

Table 3.4 The significant differences between the surface roughness (Ra) values of pin replicas taken of mechanically degraded and undegraded control specimens. Asterisk represents level of significance: one asterisk equates to $P \leq 0.05$, two asterisks equate to $P \leq 0.01$, three asterisks equate to $P \leq 0.001$, four asterisks equate to $P \leq 0.0001$.

	Control	Mild post	Mild 24	Mild 48	Mod post	Mod 24	Mod 48	Mod serum post	Mod serum 24	Mod serum 48
Control	-	ns	ns	ns	ns	**	**	ns	ns	ns
Mild post	ns	-	ns	ns	ns	*	*	ns	ns	ns
Mild 24	ns	ns	-	ns	ns	**	*	ns	ns	ns
Mild 48	ns	ns	ns	-	ns	*	*	ns	ns	ns
Mod post	ns	ns	ns	ns	-	ns	ns	ns	ns	ns
Mod 24	**	*	**	*	ns	-	ns	ns	ns	ns
Mod 48	**	*	*	*	ns	ns	-	ns	ns	ns
Mod serum post	ns	ns	ns	ns	ns	ns	ns	-	ns	ns
Mod serum 24	ns	ns	ns	ns	ns	ns	ns	ns	-	ns
Mod serum 48	ns	ns	ns	ns	ns	ns	ns	ns	ns	-

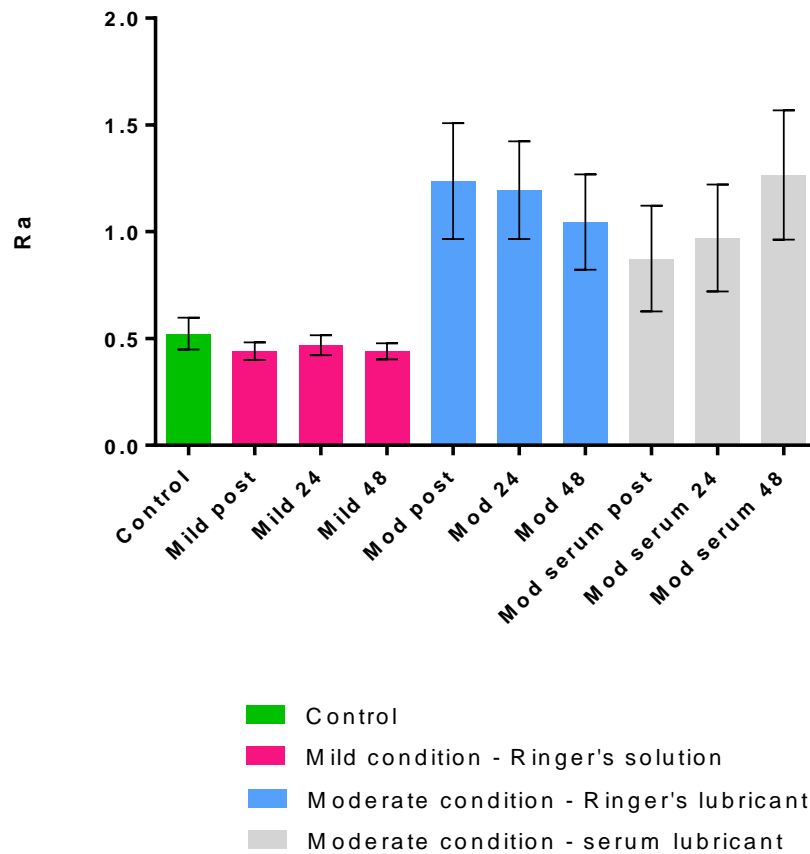


Figure 3.36. The surface roughness of plate replicas directly after degradation and after 24 and 48 hours of recovery. Post refers to post degradation, 24 denotes 24 hours of recovery, 48 denotes 48 hours of recovery. Data is presented as the mean (n=6) \pm 95% confidence intervals. The data was analysed by repeated measures analysis of variance followed by determination of significant differences between groups using a Tukey post test.

Table 3.5 The significant differences between the surface roughness (Ra) values of plate replicas taken of mechanically degraded and undegraded control specimens. Asterisk represents level of significance: one asterisk equates to $P \leq 0.05$, two asterisks equate to $P \leq 0.01$, three asterisks equate to $P \leq 0.001$, four asterisks equate to $P \leq 0.0001$.

	Control	Mild post	Mild 24	Mild 48	Mod post	Mod 24	Mod 48	Mod serum post	Mod serum 24	Mod serum 48
Control	-	ns	ns	ns	****	****	**	ns	*	****
Mild post	ns	-	ns	ns	****	****	***	ns	**	****
Mild 24	ns	ns	-	ns	****	****	**	ns	*	****
Mild 48	ns	ns	ns	-	****	****	***	ns	**	****
Mod post	****	****	****	****	-	ns	ns	ns	ns	ns
Mod 24	****	****	****	****	ns	-	ns	ns	ns	ns
Mod 48	**	***	**	***	ns	ns	-	ns	ns	ns
Mod serum post	ns	ns	ns	ns	ns	ns	ns	-	ns	ns
Mod serum 24	*	**	*	**	ns	ns	ns	ns	-	ns
Mod serum 48	****	****	****	****	ns	ns	ns	ns	ns	-

3.5.5 Friction between pins and plates during mechanical degradation

The friction that occurred between the osteochondral pins and plates during the mechanical degradation regimes was recorded via a piezoelectric sensor (Section 3.4.2). Six repeats were taken for each condition. Data was recorded every 15 seconds for five minutes, subsequently a measurement was taken every 5 minutes for up to 6 hours. There was no significant difference between the co-efficient of friction measurements recorded for any of the degradation conditions, which were taken at each time point up to the 5 minute point and then each hour up to 6 hours, (determined by one way ANOVA; Figure 3.37A).

The co-efficient of friction recorded for the mild conditions was 0.051 at the start of the test which dropped to 0.042 within 3 minutes. From the 3 minute point the friction co-efficient gradually increased for the first hour and plateaued at approximately 0.05 for the remaining five hours of the test. The co-efficient of friction recorded for the moderate condition with Ringer's solution at the start of the test was 0.04, the friction then immediately dropped to 0.038 after the first 15 seconds then increased to 0.041 after the first five minutes. The friction then dropped resulting in a co-efficient of 0.036 at the 20 minute point. From here the friction gradually increased to 0.048 over the remainder of the test (Figure 3.37B).

The co-efficient of friction recorded for the moderate degradation condition with serum lubricant was initially 0.04. The co-efficient dropped to 0.034 by two minutes and fifteen seconds, rose to 0.037 by three minutes and thirty seconds then dropped again to 0.033 at four and a half minutes. By the ten minute time point the friction had increased to 0.037, it then dropped to 0.034 again by the fifteen point minute. From this point the friction gradually increased to 0.048 by the 6 hour time point of the test (Figure 3.37B).

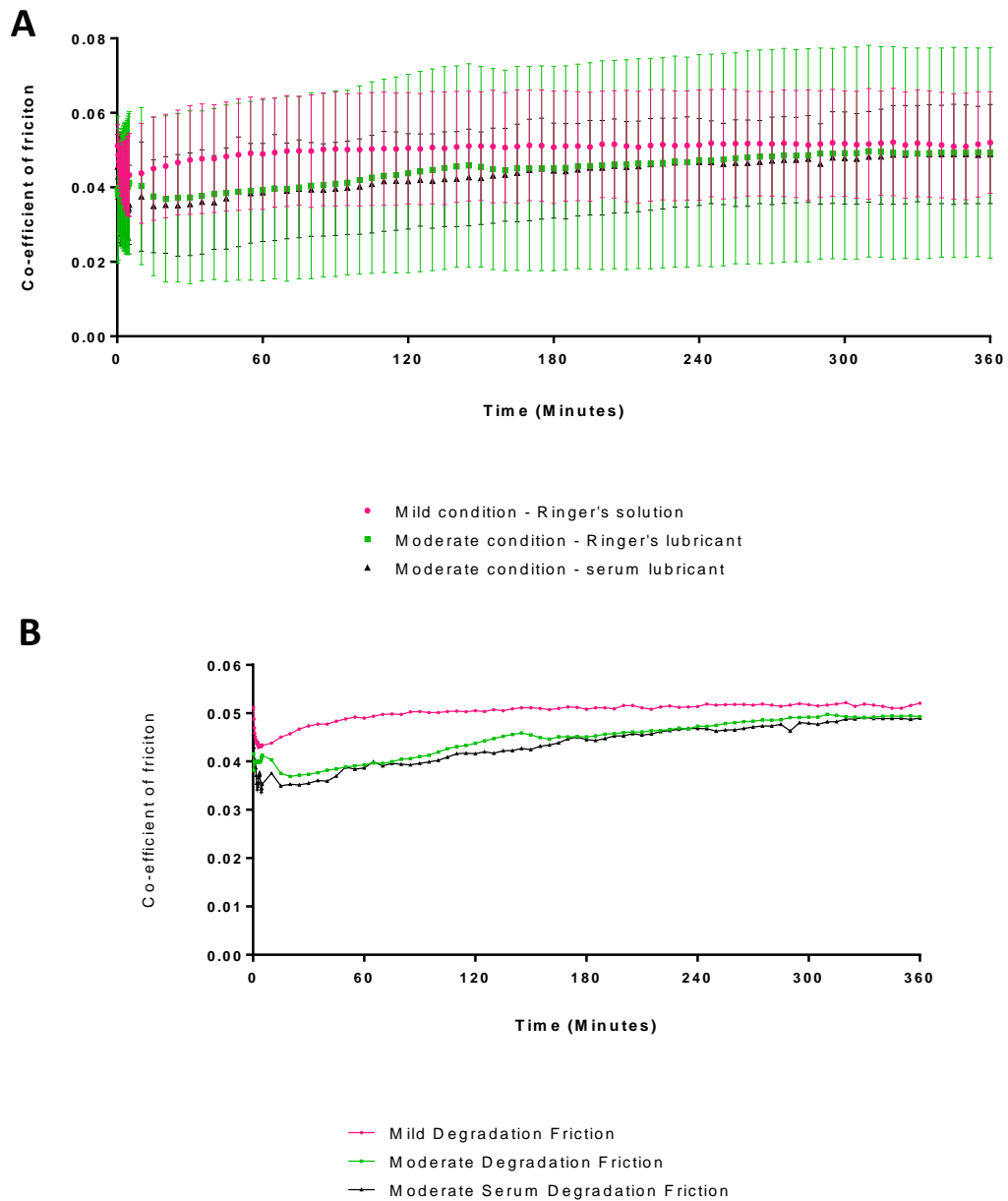


Figure 3.37. The co-efficient of friction recorded between osteochondral pins and plates during mechanical degradation protocols (N=6). A. The friction data recorded for all mechanical degradation conditions including error bars. Data is presented as the mean friction coefficient ($n=6$) \pm 95% confidence intervals. The data was analysed by one way analysis of variance which revealed no significant difference in the friction levels at any time point between the three conditions **B.** The friction data recorded for all mechanical degradation conditions excluding error bars

3.5.6 Histological evaluation of mechanically degraded cartilage specimens

The histo-architecture of the mechanically degraded cartilage tissue was assessed using H & E staining (Section 2.61) This was carried out on six specimens from each condition. The morphology of chondrocytes varied throughout the superficial, medial and deep zones of the undegraded control tissue (Figure 3.38). In the superficial zone chondrocytes contained dark purple stained nuclei, the lacunae containing the chondrocytes were flattened compared with the rounded lacunae observed in the medial zone (Figure 3.39A/B). In the deep zone the lacunae did not have a fixed shape and ranged from circular to elongated and angular shapes. The distribution of chondrocytes varied throughout the tissue; chondrocytes in the superficial zone were not grouped together. In the middle zone it was common to see groups of three or four chondrocytes forming columns (Figure 3.39B). In the deep zone the linear grouping of chondrocytes was again evident as in the middle zone, however some chondrocytes lay next to each other within columns resulting in a less regimented appearance and some of the lacunae appeared to be larger than those in the superficial and middle zones (Figure 3.39C). Some lacunae did not contain chondrocytes. The surface of the cartilage was very smooth. Eosin staining was stronger in the deep zone of the tissue. The images shown (Figure 3.38-3.39) are representative of the six control specimens.

Four of the six specimens that had undergone mild mechanical degradation in Ringer's solution lubricant were observed to have a smooth surface (examples shown in Figures 3.40A/B). Two of the six specimens had obvious tissue damage (Figure 3.40C/D). One of the damaged specimens had a tear through the middle zone that did not extend to the superficial zone. The other damaged specimen had a fissure in the cartilage that extended from the surface into the middle zone of the tissue. No fibrillation was seen on any of the specimens however, small fissures in the superficial zone were observed in the specimen that had internal tearing (Figure 3.40C).

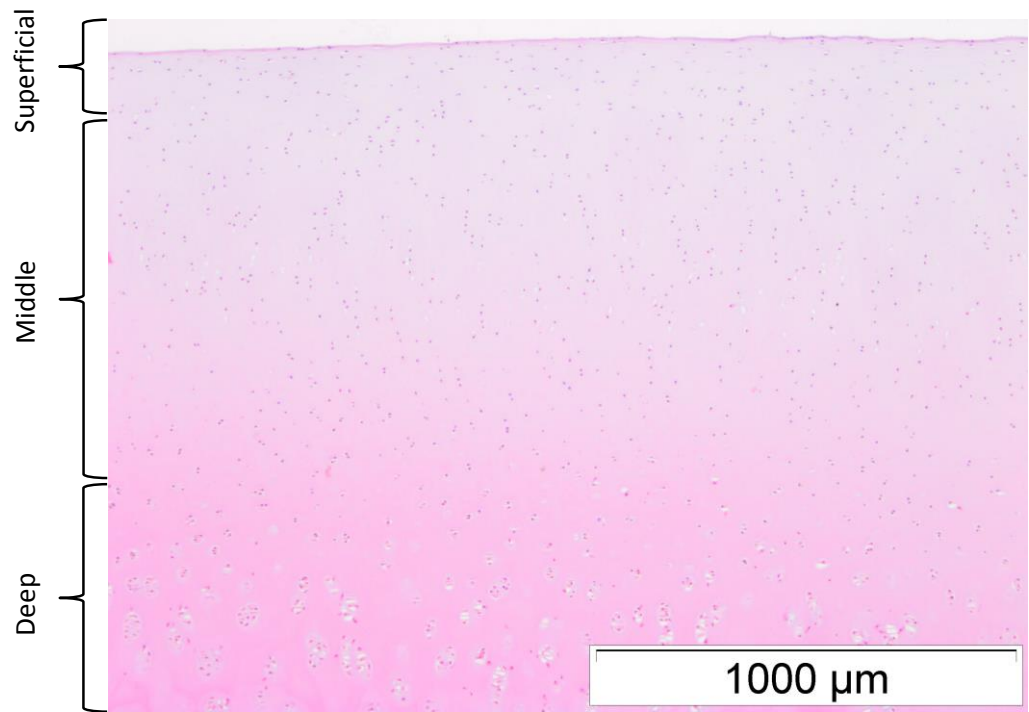


Figure 3.38. Haematoxylin and eosin stained section of undegraded bovine articular cartilage pin control tissue. The complete tissue section showing the superficial, middle and deep zones of the tissue.

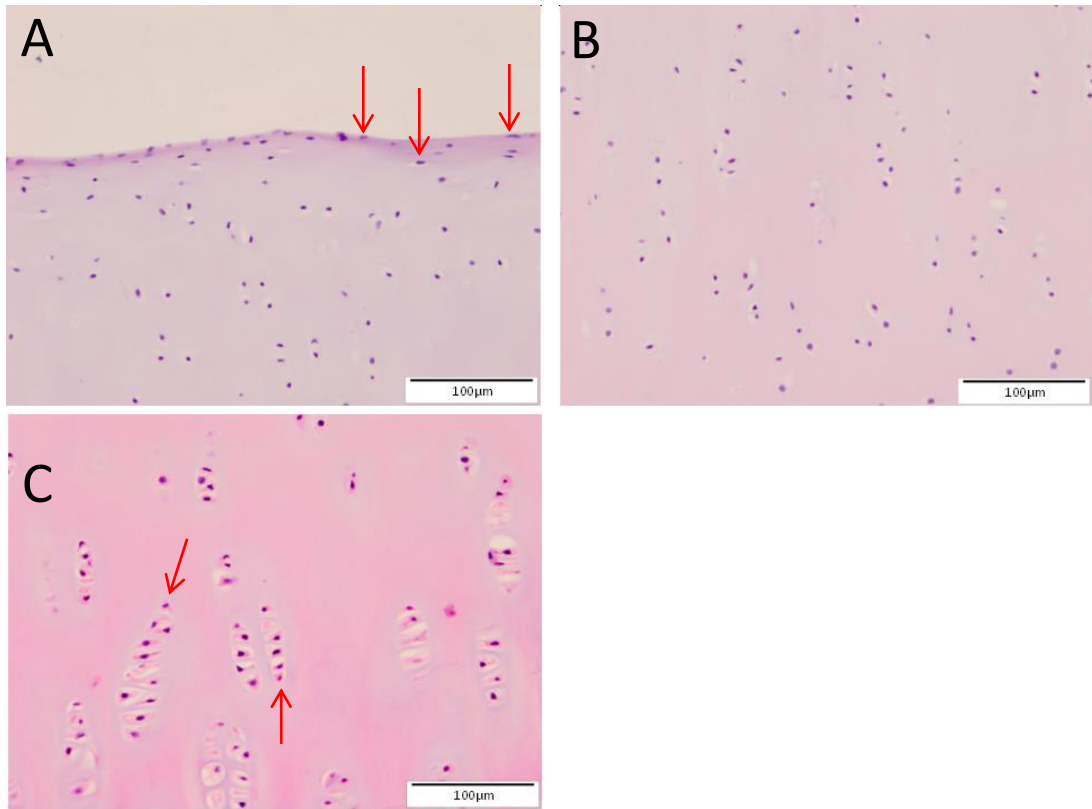


Figure 3.39. Haematoxylin and eosin stained section of bovine articular cartilage pins. A. The superficial zone of the cartilage tissue showing chondrocytes at the surface in flattened lacunae (arrows). **B.** The middle zone of the tissue showing chondrocytes in rough columns. **C.** The deep zone of articular cartilage showing chondrocytes in columnar forms within large irregularly shaped lacunae (arrows).

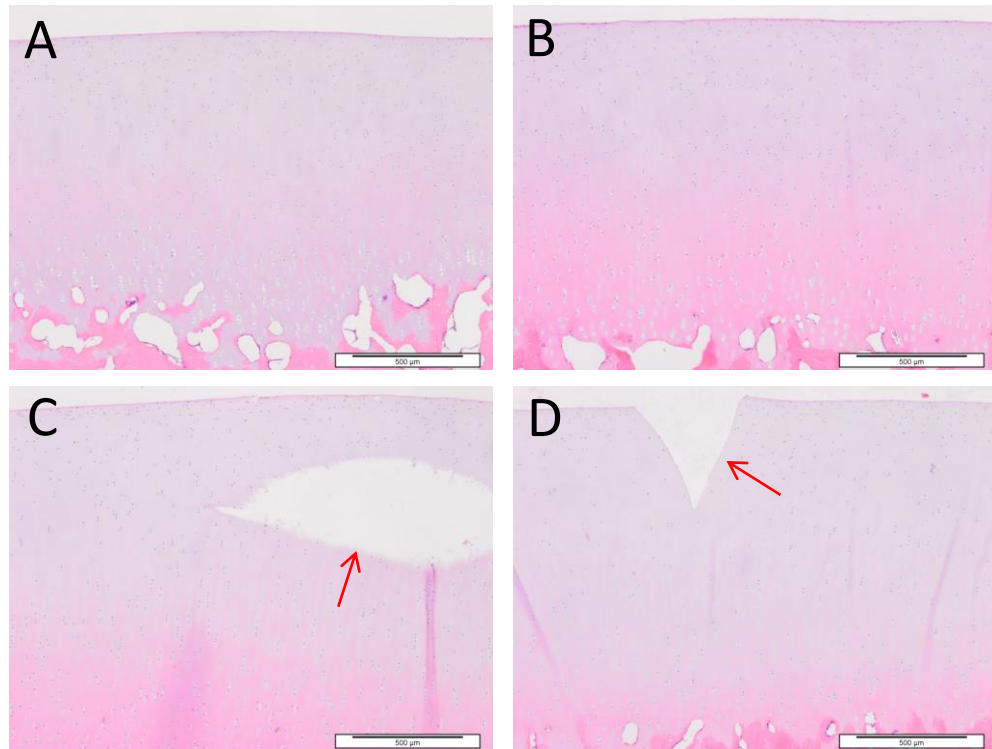


Figure 3.40. Haematoxylin and eosin stained section of cartilage pin specimens following mild degradation in Ringer’s solution. Both images A and B show specimens without visible degradation to the tissue. **C.** This specimen was one of two specimens showing damage to the tissue (arrow). **D.** This specimen contained a fissure in the surface that extended less than 50% of the cartilage height (arrow). Scale bars represent 500 µm.

Various grades of degradation were observed in tissues degraded under moderate mechanical degradation conditions in Ringer’s solution lubricant. One of the six specimens had a relatively smooth surface, however the tissue appeared to be becoming detached from the bone at the deep / calcified zone (Figure 3.41A). Four of the remaining specimens showed focal areas of tissue loss and one specimen had a large volume of tissue loss across a large area of the pin (Figure 3.41C). Fibrillation of the cartilage surface was often observed adjacent to and within areas of tissue loss (Figure 3.41D). Some specimens showed tissue loss that extended deeper than 50% of the tissue height, with one specimen showing extensive tissue loss into the deep zone.

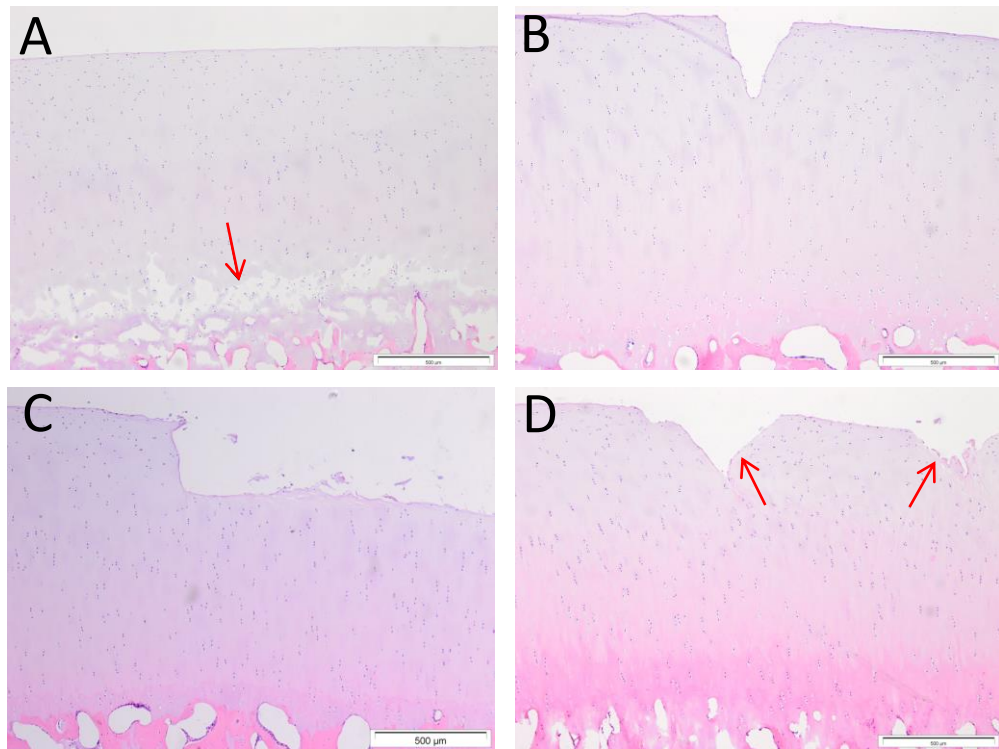


Figure 3.41. Haematoxylin and eosin stained section of cartilage pin specimens following moderate degradation in Ringer’s solution. A. This specimen had a relatively smooth superficial zone however the tissue appeared to have become detached at the calcified zone (arrow). **B.** Away from the fissure in the cartilage surface the surface of the tissue remained smooth. **C.** A large volume of tissue loss was observed from this specimen in which the tissue had been lost progressively across the pin resulting in less than 50% of tissue height remaining at the pin edge. **D.** Tissue loss and fibrillation was observed in this specimen (arrows). Scale bars represent 500 µm.

The cracks seen at the surface of some tissue specimens that had undergone moderate mechanical degeneration in serum lubricant did not extend beyond 50% of the tissue height (Figure 3.42B/D). Away from the areas of focal damage observed, the surfaces of specimens remained smooth. One specimen did not appear to have any signs of degradation (Figure 3.42A). The most severe volume of tissue loss observed in the specimens articulated in serum was similar to that seen in the most severe loss in moderately degraded specimens in Ringer’s lubricant. Fibrillation was not typically observed at the surface of the tissues with the serum based lubricant, however it was observed in one specimen in which the superficial zone had been lost (Figure 3.42C).

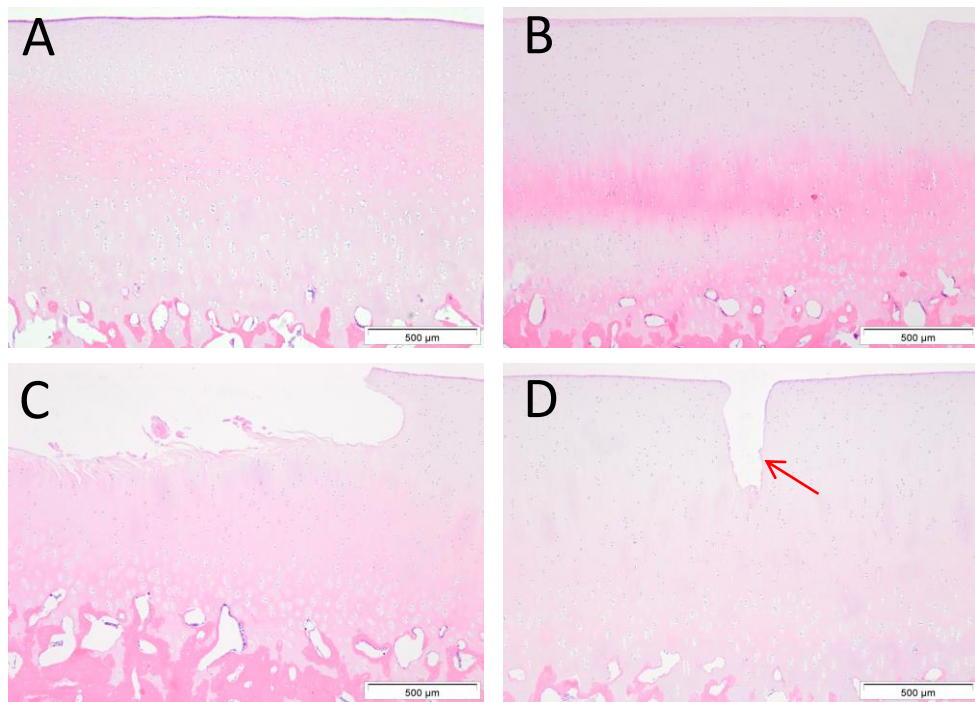


Figure 3.42. Haematoxylin and eosin stained sections of cartilage pin specimens following moderate degradation with serum lubricant. A-B. The cartilage surface away from the obvious areas of tissue damage remained smooth. **C.** Severe tissue damage was seen in one specimen in which tissue loss was observed. **D.** Fissures in the tissue were a typical form of damage (arrow). Scale bars represent 500 µm.

Overall the specimens subjected to mild degradation conditions showed the lowest amount of damage and the majority of the surfaces remained smooth. The specimens that were degraded under moderate conditions in Ringer’s solution had the greatest amount of damage. The specimens degraded under moderate conditions in serum lubricant had the highest variability of damage with some specimens exhibiting signs of severe damage and some specimens retaining a smooth undamaged surface. Therefore a higher contact stress led to an increase in damage to the tissue and the serum lubricant in some cases appeared to protect the surface of the cartilage tissue from the severe damage observed in the specimens degraded in Ringer’s solution under moderate conditions.

3.5.7 Qualitative evaluation of GAGs in mechanically degraded cartilage specimens

Alcian blue was used to stain the glycosaminoglycans (GAGs) in sections of the mechanically degraded specimens. The stain was chosen as the GAGs in the cartilage tissue are integral to its function. The staining procedure has been described previously (Section 2.6.2). Six samples of cartilage were evaluated. Staining in the superficial and upper middle zone of undegraded specimens was even and an intense blue. A patchy reduction in staining was observed from the deep zone to the calcified zone resulting in purple areas where the alcian blue had not been taken up. The areas surrounding these patches showed alcian blue staining that appeared darker than in the middle and superficial zones (Figure 3.43). Patchy alcian blue staining was observed in the transitional zone from cartilage to bone. The subchondral bone did not stain heavily for alcian blue, haematoxylin staining was observed with patches of alcian blue. In general there was high repeatability of staining for the six tissue samples, however in two of the specimens, haematoxylin staining in the mid-deep zones was less visible. Staining in the calcified and subchondral bone was similar across all specimens.

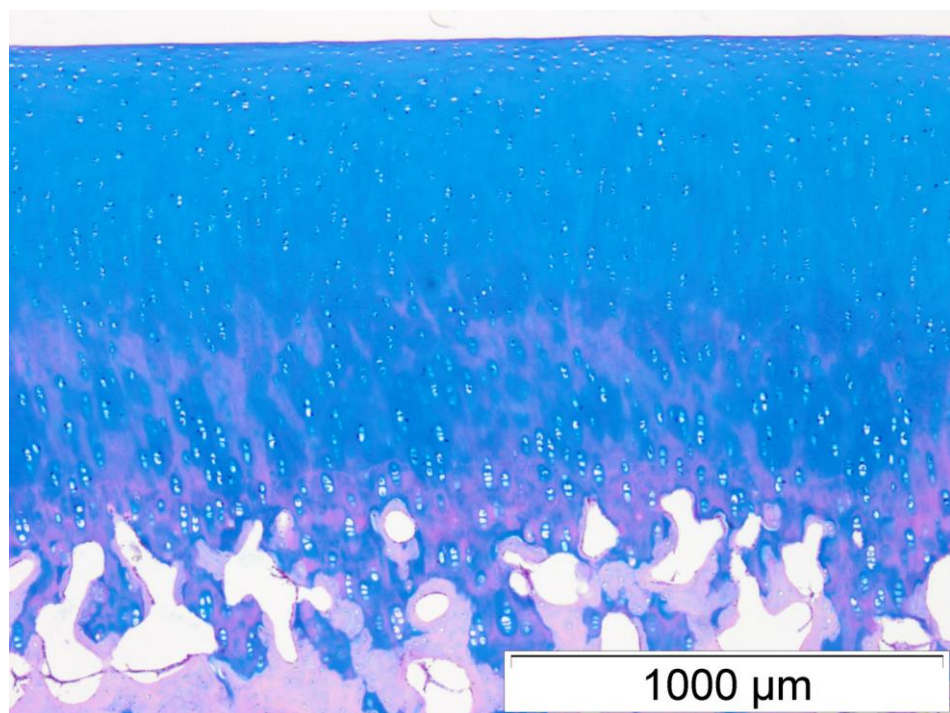


Figure 3.43. Alcian blue stained control cartilage pin section. Image shows an undegraded control pin section with superficial, middle, deep and calcified zones.

Alcian blue staining intensity was reduced in mild mechanically degraded specimens articulated in Ringer's solution. At the superficial zone, the alcian blue was not taken up resulting in a pink region approximately 12 μm deep and a light blue region approximately 50-100 μm thick. The stain was also not taken up as strongly adjacent to some areas of tissue damage, for example torn regions within the tissue (Figure 3.44B). Half of the mechanically degraded mild condition specimens had a significant reduction in alcian blue staining in the deep zone of the tissue, resulting in increased pink staining in this region (Figure 3.44C).

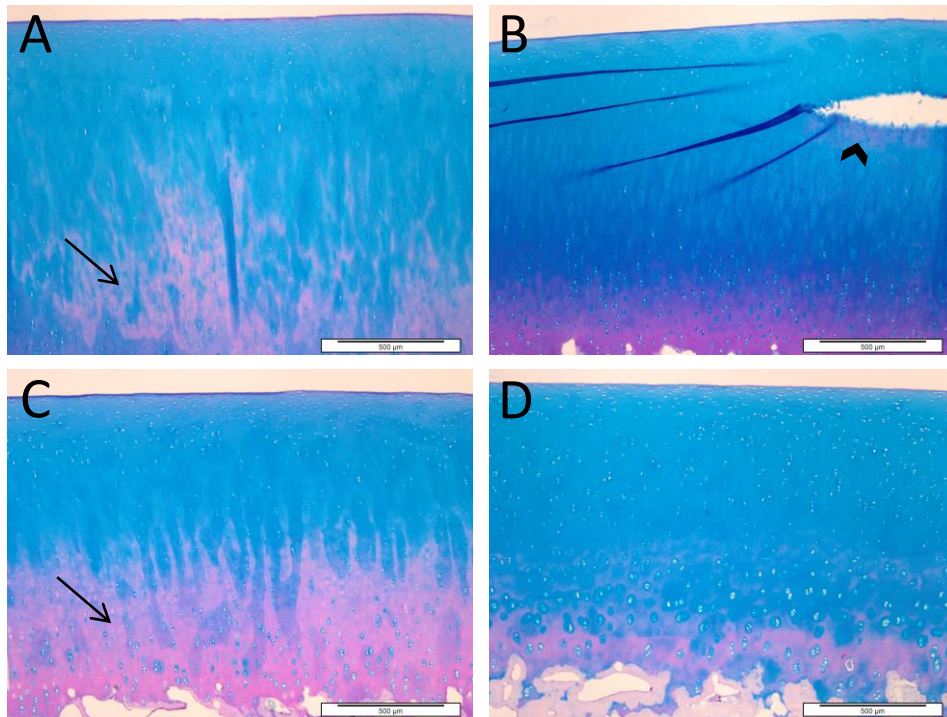


Figure 3.44. Alcian blue stained cartilage pin specimens following mild degradation using Ringer's solution lubricant. A, C. A reduction in staining was observed in the deep zone of some specimens (arrows). **B.** Around areas of tissue damage a reduction in alcian blue staining was seen (arrow head). **D.** An overall loss of staining intensity compared with the undegraded control tissue was evident. Scale bars represent 500 μm .

A large reduction in alcian blue staining intensity was observed in moderate mechanically degraded specimens articulated in Ringer's solution resulting in sections that appeared to be washed out (Figure 3.45). As with mild condition specimens, alcian blue was not taken up at the superficial zone, there was also a lack of alcian blue staining in areas of tissue damage (Figure 3.45B). The alcian blue was especially reduced in areas where tissue had become torn during the degradation protocol (Figure 3.45C).

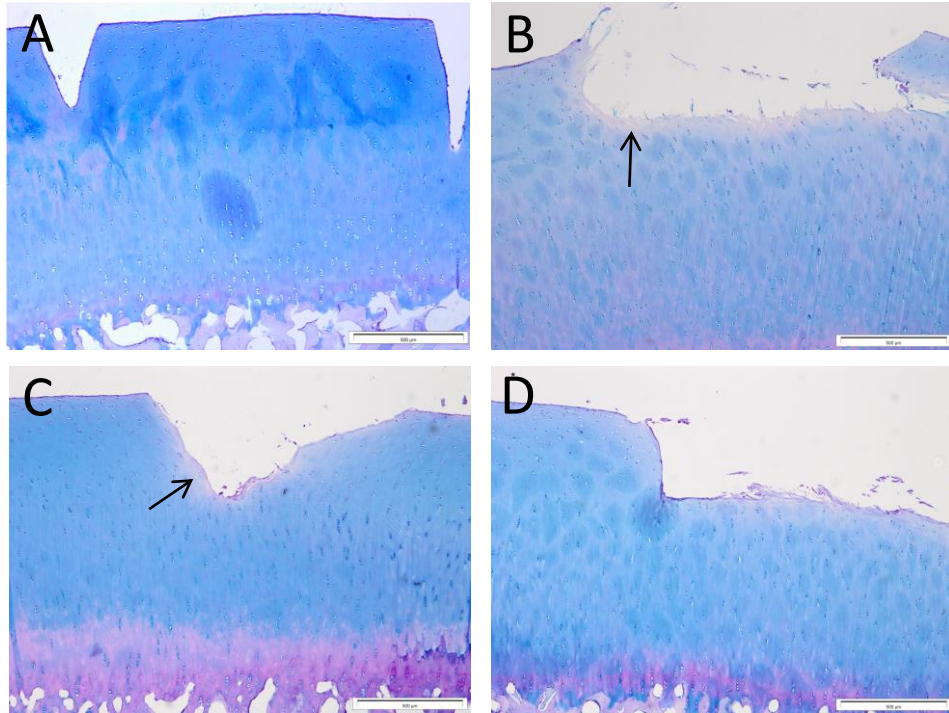


Figure 3.45. Alcian blue stained cartilage pin specimens following moderate mechanical degradation in Ringer’s solution (N=6). A. Specimens appeared washed out due to a severe reduction in alcian blue staining. In this specimen the majority of GAG loss appeared to be in the middle to deep zone. **B, C, D.** Specimens with torn or fibrillated areas showed a greater reduction in focal alcian blue staining than areas with a clean fissure as was observed in A (arrows). Scale bars represent 500 μm .

Moderate condition specimens articulated in serum lubricant showed similar staining patterns to the moderate condition specimens articulated in Ringer’s solution lubricant. Specimens appeared washed out and had reduced alcian blue staining intensity. Overall staining was heterogeneous and specimens showed a net loss of colour across different regions of the tissue (Figure 3.46).

It appeared that the moderate degradation condition led to the largest loss of GAGs as a lower intensity of alcian blue staining was observed in these specimens compared to the undegraded control tissues and the tissue treated under mild mechanical degradation conditions. The largest loss of alcian blue staining intensity was observed in the moderately degraded specimens in serum lubricant.

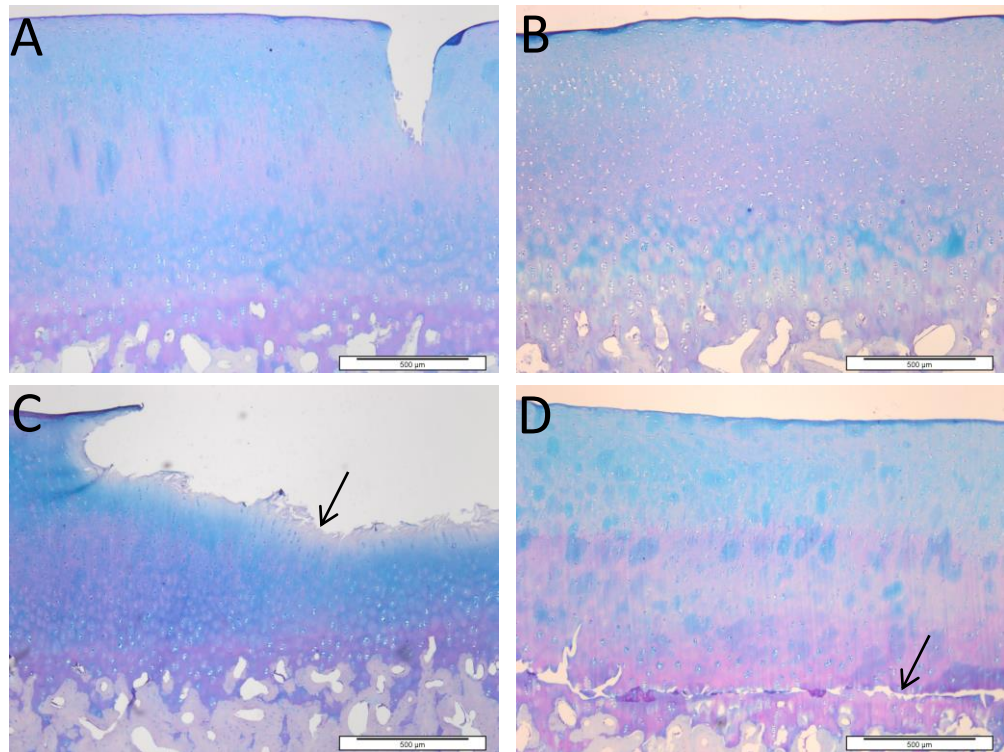


Figure 3.46. Alcian blue stained cartilage specimens following moderate degradation with serum lubricant (N=6). **A.** An overall reduction in alcian blue staining intensity was observed, however it was particularly evident in the superficial zone and in a band through the mid zone. **B.** Specimens showed a reduction in alcian blue uptake across the whole tissue. **C.** A reduction in alcian blue uptake was observed around areas of tissue damage (arrow). **D.** Tissue was seen breaking away from the bone (arrow). Scale bars represent 500 µm.

3.5.8 Quantitative evaluation of biglycan in mechanically degraded cartilage specimens

A biglycan antibody was used to identify changes in the presence of this proteoglycan due to mechanical degradation (Section 2.6.3). In undegraded control specimens, biglycan was present in the superficial and middle zones of the cartilage tissue and was not present in the deep zone of the tissue (Figure 3.47). Biglycan was expressed in the calcified region of the tissue. Antibody labelling of biglycan in control tissues was highly repeatable.

A heterogeneous presence of biglycan was observed in the specimens that had been degraded under mild conditions in Ringer's solution lubricant. One specimen had retained

biglycan in the deep/calcified zone deep/calcified zone and had light staining in the upper middle zone but no staining was seen in the superficial zone (Figure 3.48A). One specimen retained biglycan in the superficial/ upper middle zone and staining in the calcified zone was only visible in the pericellular region (Figure 3.48B) Two specimens appeared to have lost biglycan from the calcified zone and retained it in the superficial and upper middle zone (Figure 3.48C/D).

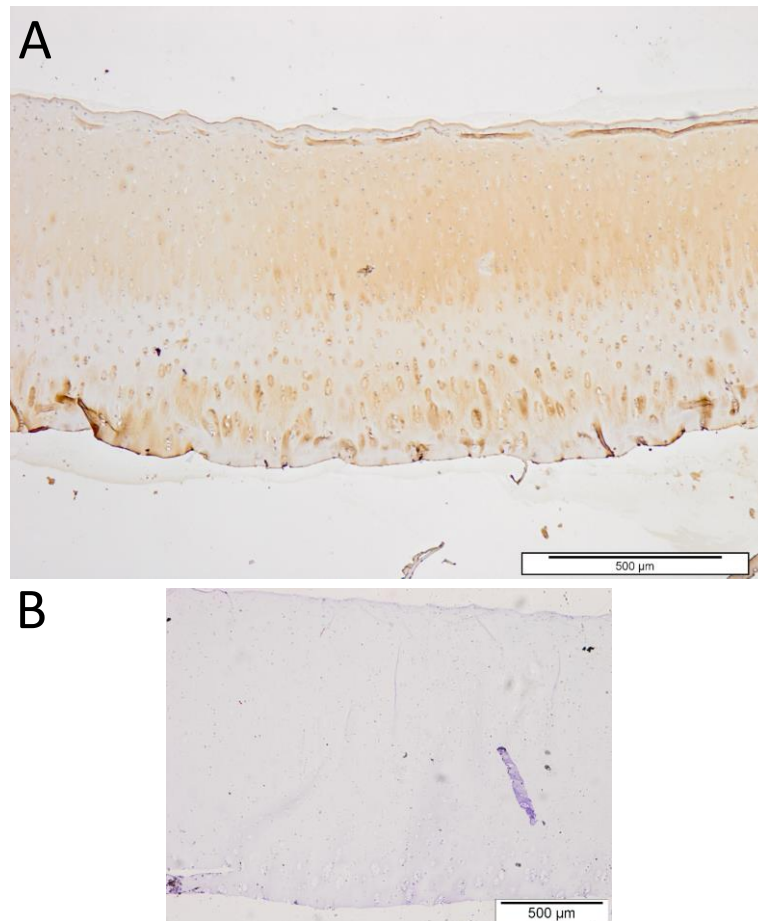


Figure 3.47. Biglycan distribution in control cartilage pin specimens. A. Image shows an undegraded control pin section. **B.** Image shows the isotype control, which was negative.

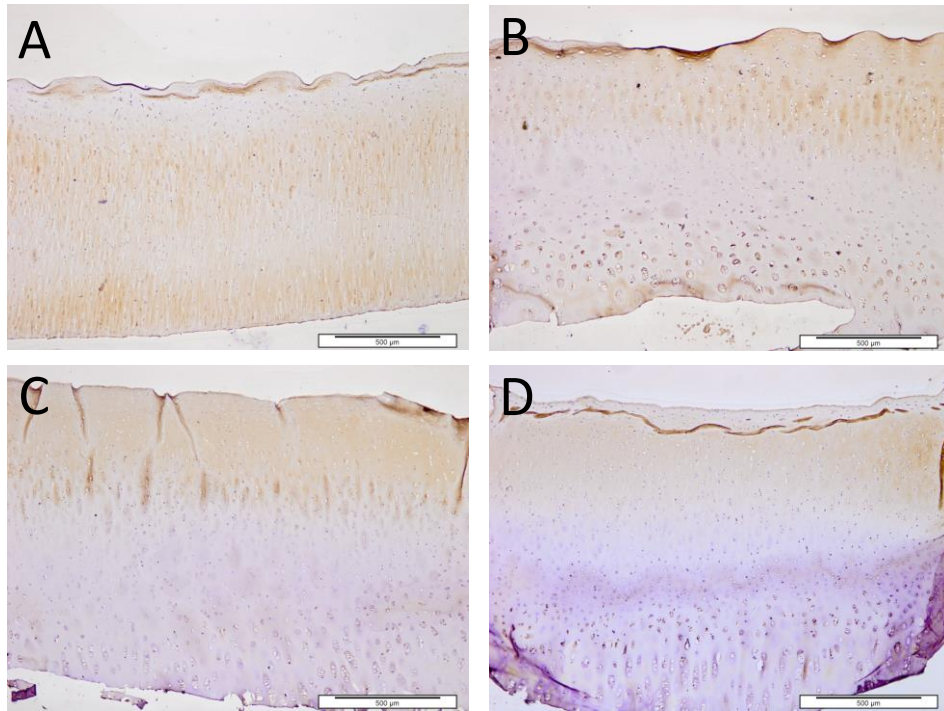


Figure 3.48. A-D. Biglycan distribution in pin specimens degraded under mild mechanical conditions in Ringer's solution. Staining was reduced in the calcified zone of two specimens (B, C). Scale bars represent 500 µm.

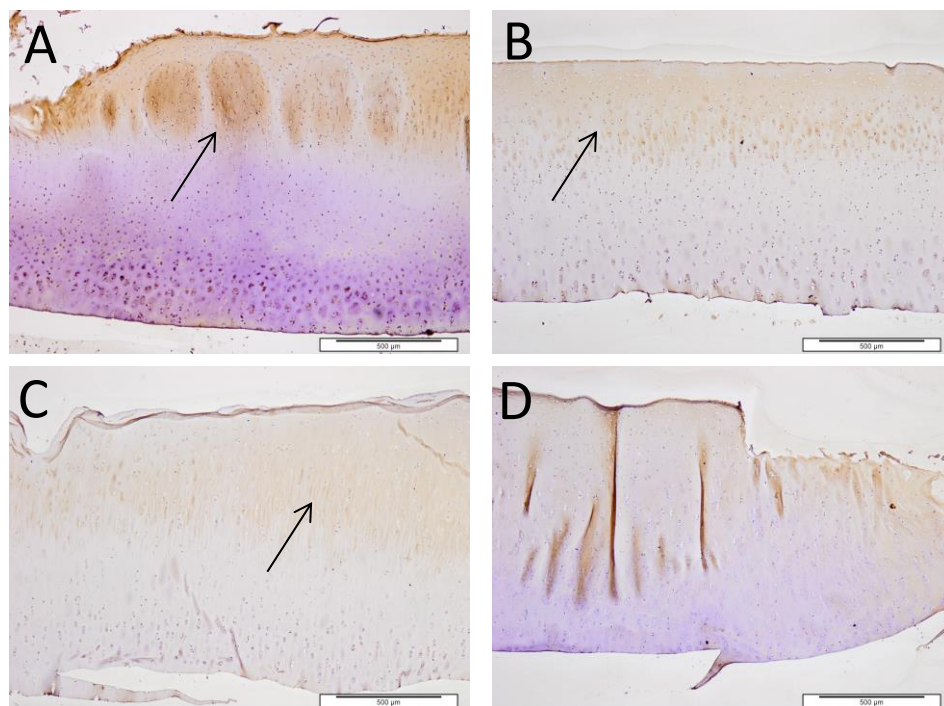


Figure 3.49. Biglycan distribution in pin specimens degraded under moderate mechanical conditions in Ringer's solution. Scale bars represent 500 µm. Stronger staining was observed in the upper-middle to superficial zone (arrows).

Decreased staining for biglycan was seen in the specimens degraded under moderate conditions with Ringer's solution lubricant, when compared with the undegraded control tissue (Figure 3.47). None of the specimens retained the stain in the deep/calcified zone as was observed with the undegraded controls. Strong staining for biglycan was observed in the superficial/upper middle zone (Figure 3.49A).

As with many of the results for the specimens degraded under moderate conditions in serum lubricants, there was a large amount of variation in the biglycan staining observed, however, overall there did appear to be a loss of biglycan in the tissues caused by the mechanical degradation protocol. Two specimens retained light staining in the superficial zone of the tissue (Figure 3.50A/B). One specimen was observed to have light staining in the deep and middle zones but had lost staining intensity at the superficial zone (Figure 3.50C). Two of the specimens were void of any particular staining pattern and showed very little biglycan presence overall (example specimen shown in Figure 3.50D).

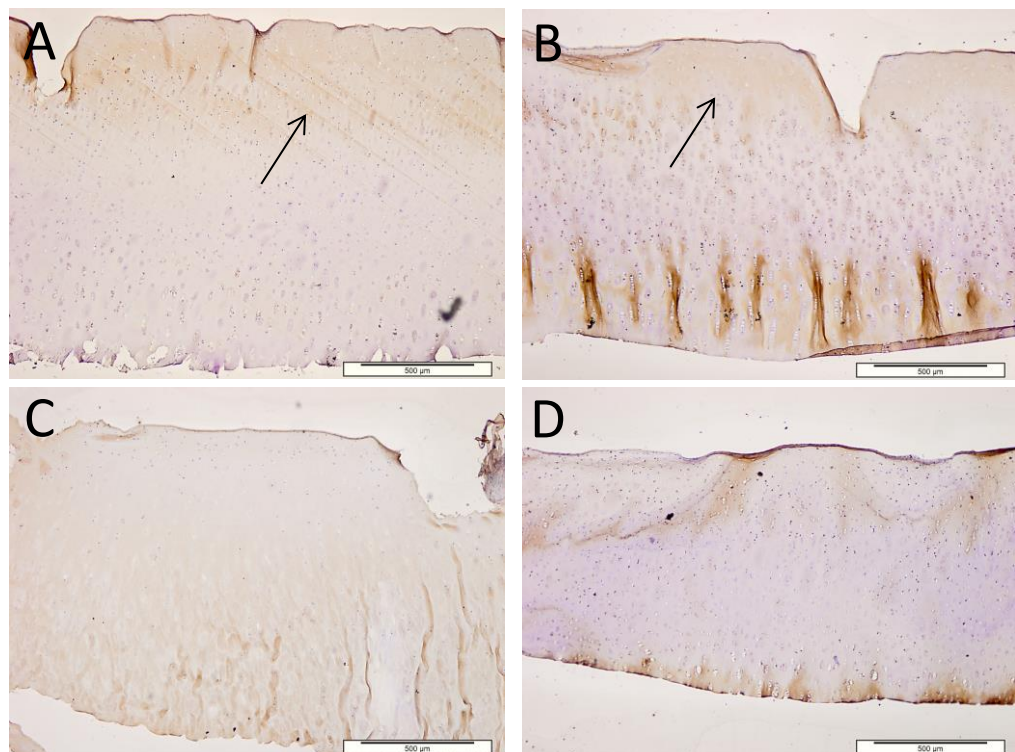


Figure 3.50. Biglycan distribution in cartilage pin specimens degraded under moderate mechanical conditions in serum based lubricant. Light staining was observed in the superficial zones of two specimens (arrows). Scale bars represent 500 µm.

Overall, despite the heterogeneity of the results, mechanical degradation was observed to have an effect on biglycan distribution and presence leading to a reduction in staining and also changes in the location of biglycan throughout the tissue.

3.5.9 Quantitative evaluation of COMP in mechanically degraded cartilage specimens

Undegraded control specimens assessed using immunohistochemical staining for cartilage oligomeric matrix protein (COMP) showed uniform staining across the superficial and middle zones (Figure 3.51). Lighter staining was observed in the deep to calcified zone. A dark band of staining was seen at the superficial zone. The staining pattern was repeatable across all six specimens assessed however, occasionally staining appeared less intense in colour.

Specimens degraded under mild mechanical conditions did not have any reduction in COMP staining intensity or any changes to the staining pattern when compared with undegraded controls (Figure 3.52). Specimens degraded under moderate conditions in either the Ringer's solution or serum based lubricant did not appear to have a reduction in COMP staining intensity or any changes to the staining pattern (Figure 3.53 and 3.54). Overall the staining intensity and the pattern of COMP staining was not affected by any of the mechanical degradation regimes or variations in lubricants.

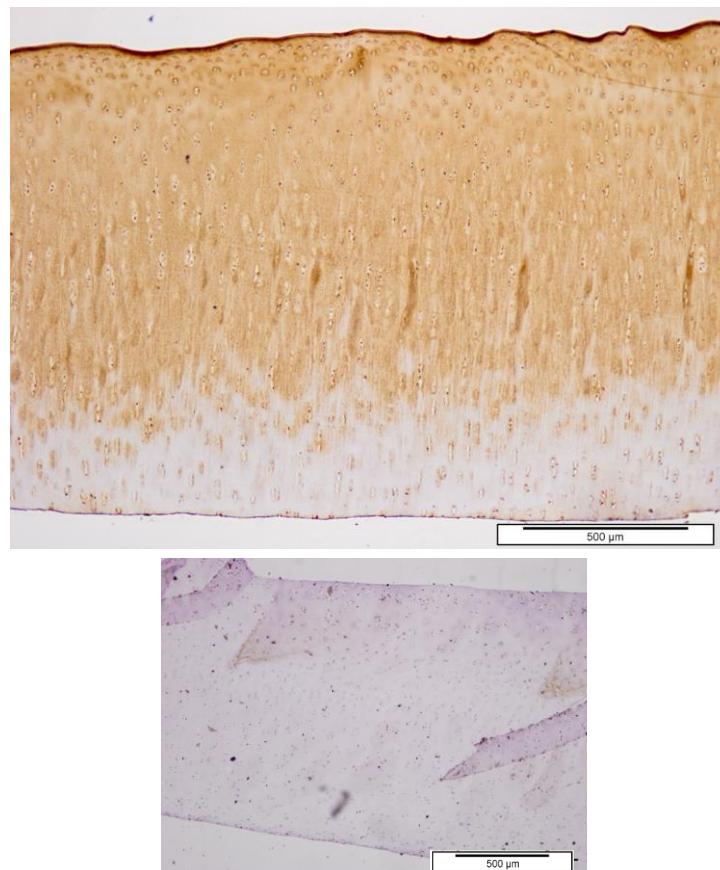


Figure 3.51. A. Characterisation of undegraded pin control tissue using a cartilage oligomeric matrix protein antibody. B. Image shows the isotype control, which was negative.

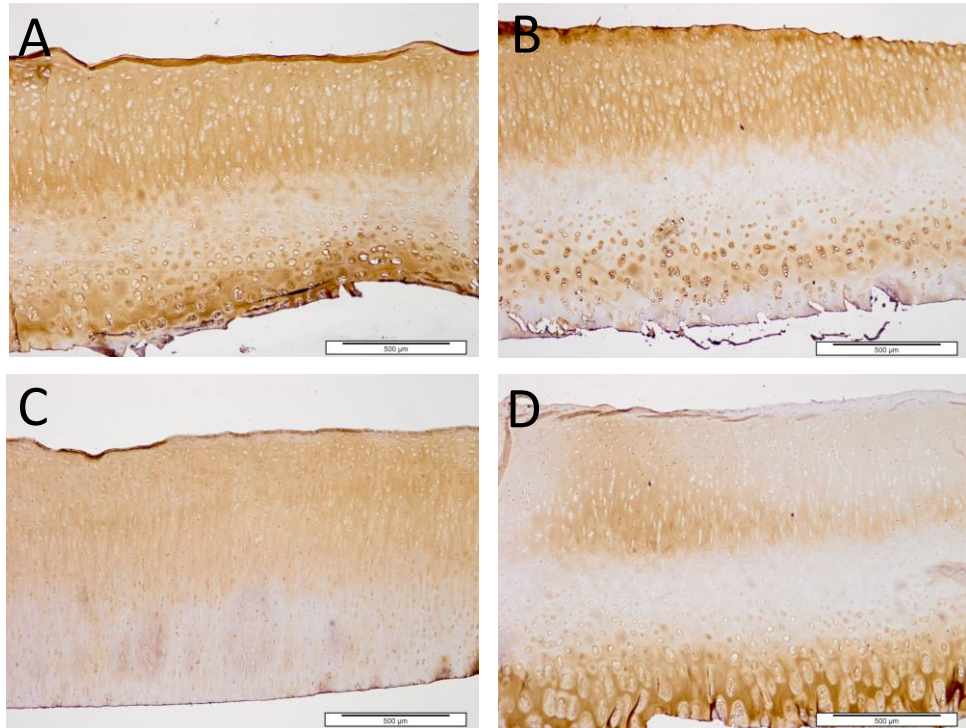


Figure 3.52. COMP distribution in cartilage pin specimens degraded mechanically under mild conditions with Ringer's solution lubricant. Scale bars represent 500 μm .

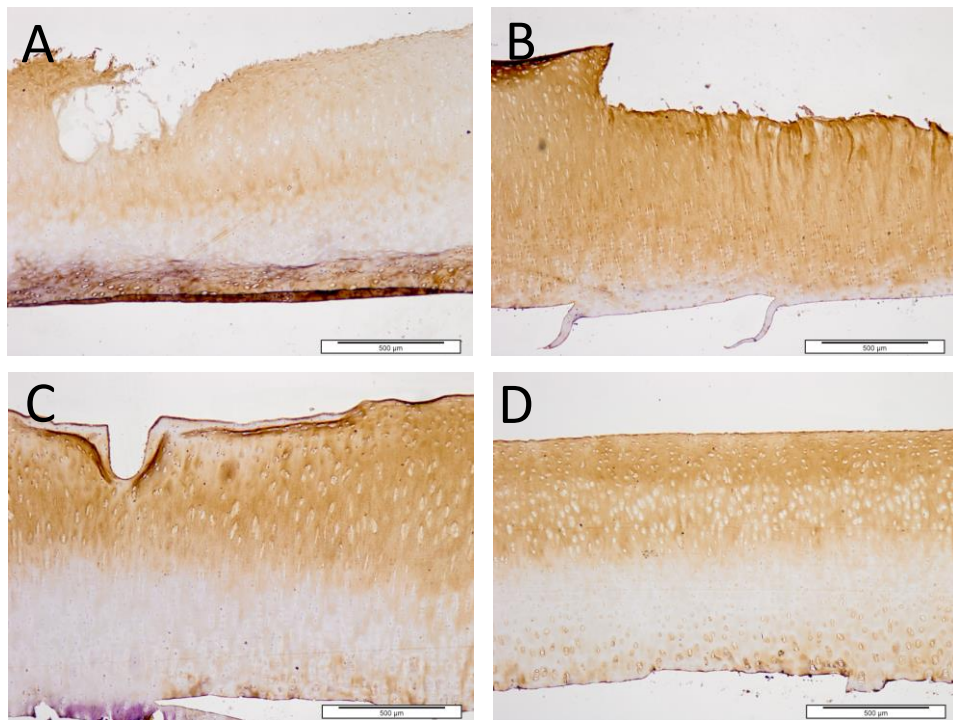


Figure 3.53. COMP distribution in cartilage pin specimens degraded mechanically under moderate conditions with Ringer's solution lubricant. Scale bars represent 500 μm .

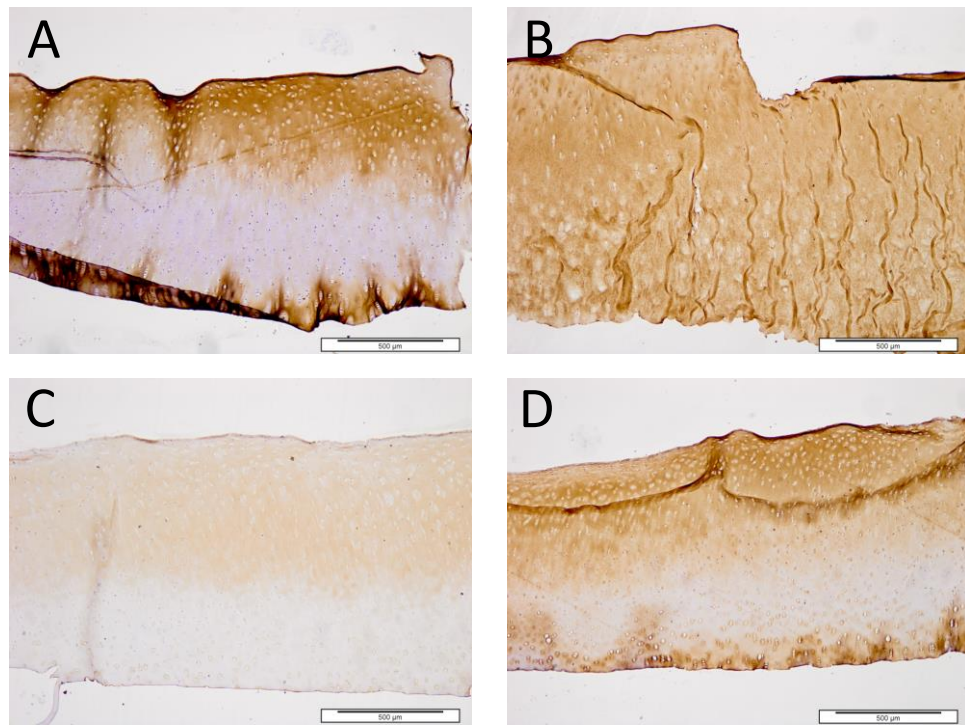


Figure 3.54. COMP distribution in cartilage pin specimens degraded mechanically under moderate conditions with serum lubricant. Scale bars represent 500 µm.

3.5.10 Qualitative evaluation of collagen VI in mechanically degraded cartilage specimens

Heavy staining for collagen VI was observed in the pericellular regions of the cartilage tissue. Interterritorial and territorial staining was also observed in the superficial to mid zones of the tissue (Figure 3.55). Some light staining was observed in the deep-calcified zone. Collagen VI staining was highly repeatable in the six control specimens.

Specimens that were degraded under mild mechanical degradation conditions did not show any reduction in staining intensity for collagen VI or changes to staining pattern when compared to the staining observed in undegraded control specimens (Figure 3.56). Staining was observed in the pericellular regions of chondrocytes in all zones in addition to the territorial and interterritorial regions of the upper middle zone and superficial zones. The same trend was also seen in specimens degraded under moderate mechanical degradation conditions in Ringer's solution lubricant, where the collagen VI staining remained similar to the staining seen in the undegraded tissues (Figure 3.57).

The results for specimens degraded under moderate mechanical degradation conditions in serum were heterogeneous (Figure 3.58). Many of the specimens appeared to have lighter staining in the upper mid and superficial zones, however one specimen had staining similar to that of the controls (Figure 3.58B).

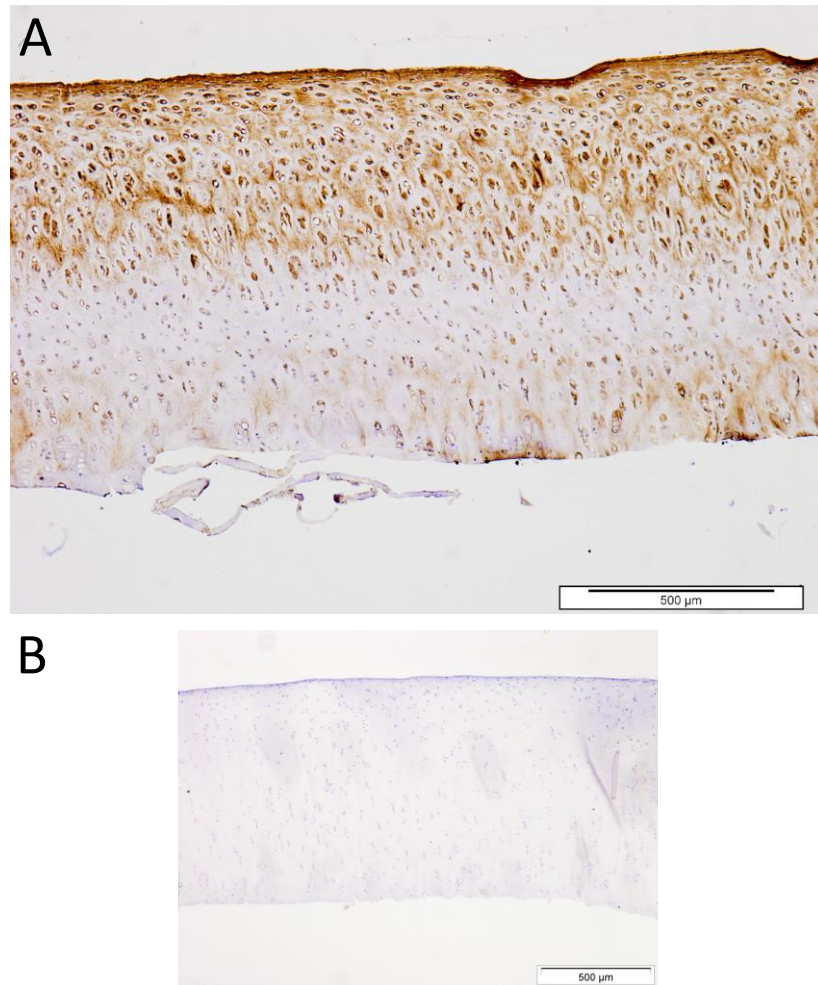


Figure 3.55. Collagen VI distribution in control cartilage pin specimens. A. Image shows an undegraded control pin section. **B.** Image shows the isotype control, which was negative.

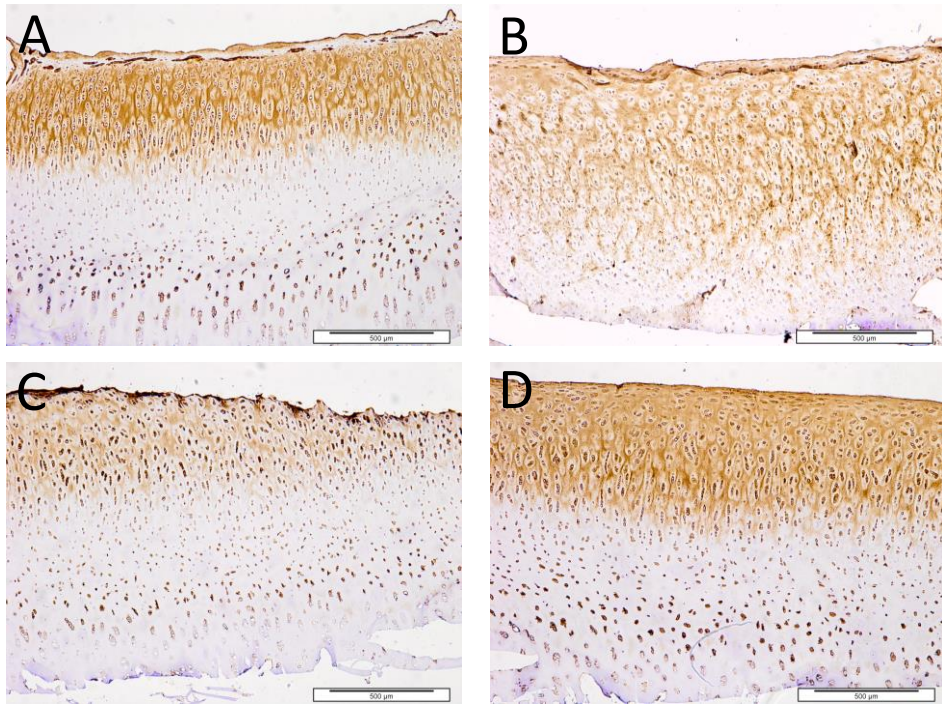


Figure 3.56. Collagen VI distribution in cartilage pin specimens degraded mechanically under mild conditions in Ringer's solution lubricant (N=6). Scale bars represent 500 µm.

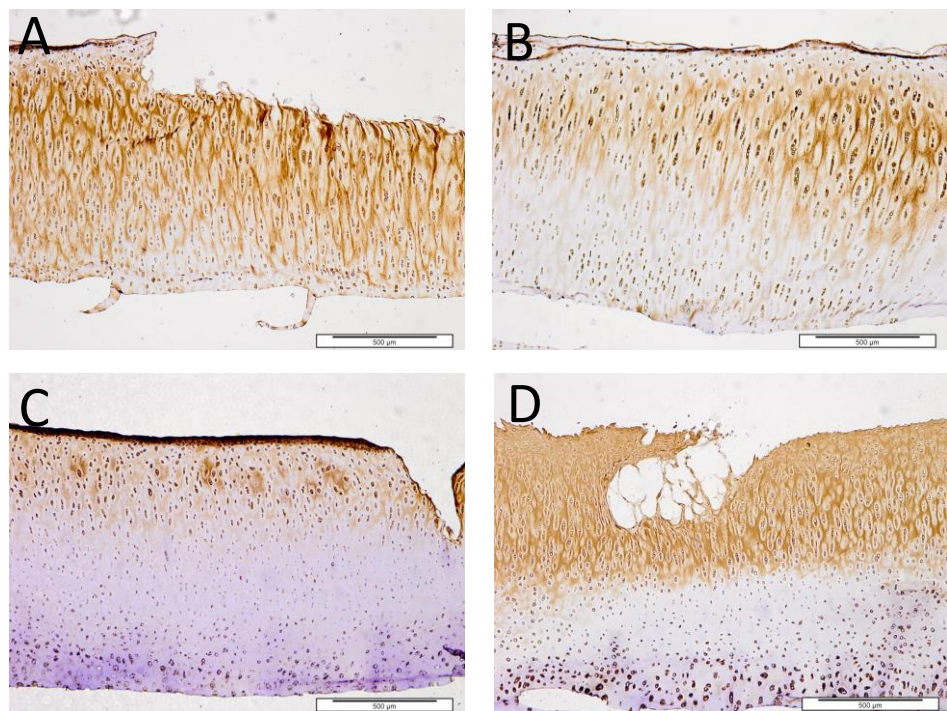


Figure 3.57. Collagen VI distribution in cartilage pin specimens degraded mechanically under moderate conditions in Ringer's solution lubricant. Scale bars represent 500 µm.

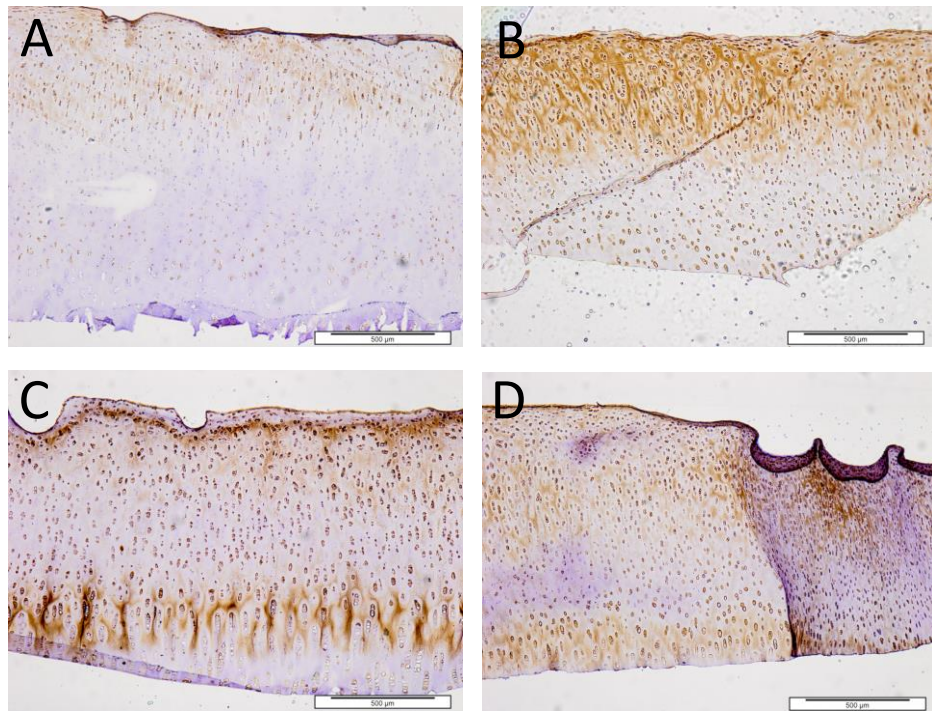


Figure 3.58. Collagen VI distribution in cartilage pin specimens degraded mechanically under moderate conditions in serum lubricant. Scale bars represent 500 µm.

The mechanical degradation protocols did not overtly deplete the collagen VI in the tissue specimens. In both the mild and moderate degradation condition specimens articulated in Ringer's solution, the collagen VI was retained within the pericellular environment of the chondrocytes and in interterritorial regions of the upper middle to superficial zones of the tissue. In the moderately degraded specimens articulated in serum lubricant, the collagen VI was retained in the pericellular environment, however, in one specimen collagen VI appeared to stain more lightly within the interterritorial regions of the superficial and upper middle zones of the tissue (Figure 3.58A).

3.5.11 Evaluation of mechanically degraded cartilage tissues using electron microscopy

3.5.11.1 Evaluation of the cartilage surface by environmental electron scanning microscopy of the cartilage surface.

Environmental scanning electron microscopy (ESEM) was used to image the surfaces of the undegraded pin control tissues and the mechanically degraded pin tissues in a hydrated natural state. Three specimens were analysed using ESEM per condition. The qualitative results gained from the ESEM imaging complemented quantitative surface roughness measurements of

the cartilage tissue taken using a surface profilometer. The methods of imaging the cartilage surfaces have been previously described (Section 2.7.1).

The control cartilage was free from fissuring. Some small particles were seen on the cartilage surface (Figure 3.59A). Overall the surface was observed to be smooth and undulating with some light creasing. The creasing of the surface increased in the mechanically degraded mild condition specimens (Figure 3.59B). Creasing of the tissue was most severe in the moderately degraded specimens that were articulated in Ringer's solution lubricant (Figure 3.59C). The moderate specimens that were articulated in serum lubricant remained relatively smooth and were similar in appearance to the undegraded controls. (Figure 3.59D)

Other interesting features were observed on the surfaces of the degraded cartilage specimens (Figure 3.60). These included fissures in the surface and wear particles. In the moderate mechanically degraded specimens, deep fissures were observed with extensions of cartilage crossing over the fissure remaining attached at each side (Figure 3.60B). A commonly observed macroscopic feature on the degraded cartilage plates was a fibrous gelatinous mass around the edge of the wear scar. In some cases wear particles could be observed accumulating in the fissures in the cartilage surface (Figure 3.60D).

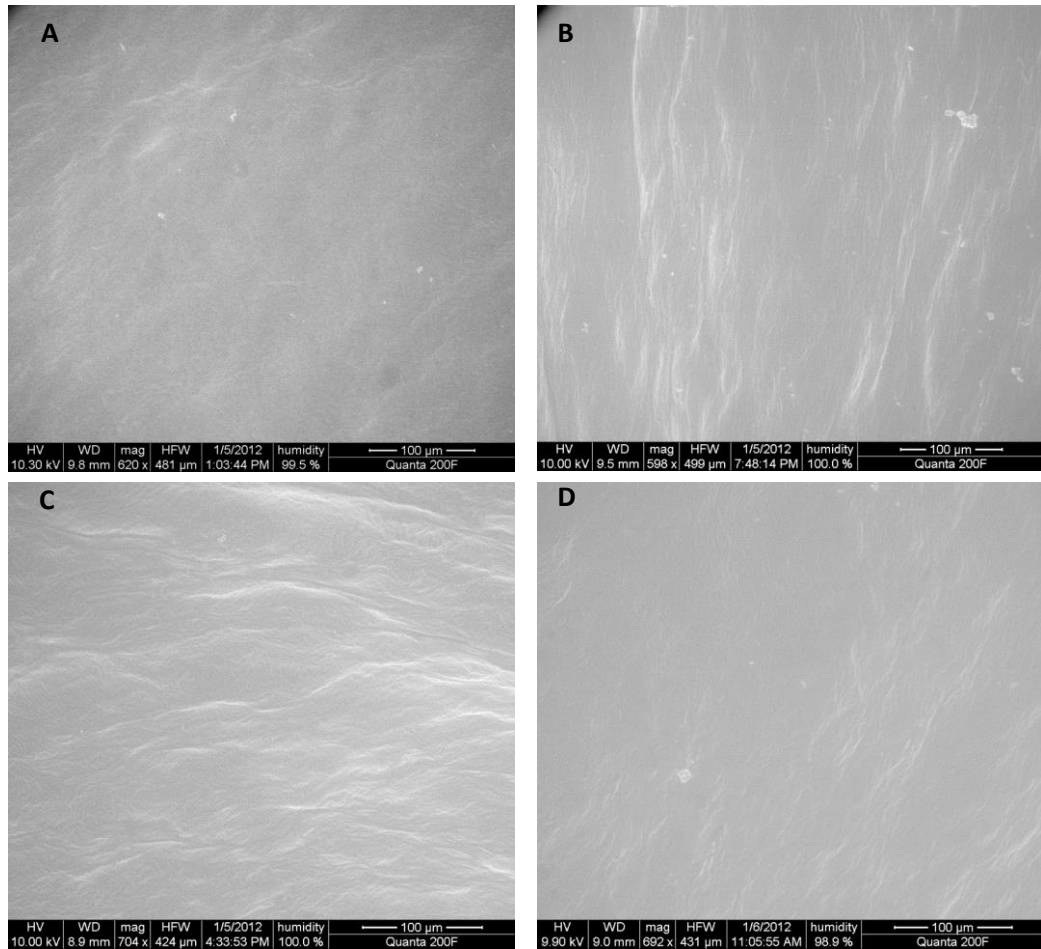


Figure 3.59. Characterisation of undegraded control cartilage pins and mechanically degraded articular cartilage pin surfaces using environmental scanning electron microscopy (ESEM). A. The undegraded control cartilage surface. **B.** The cartilage surface after mild mechanical degradation. **C.** The moderately mechanically degraded surface articulated in Ringer's solution. **D.** The moderate mechanically degraded surface articulated in serum lubricant.

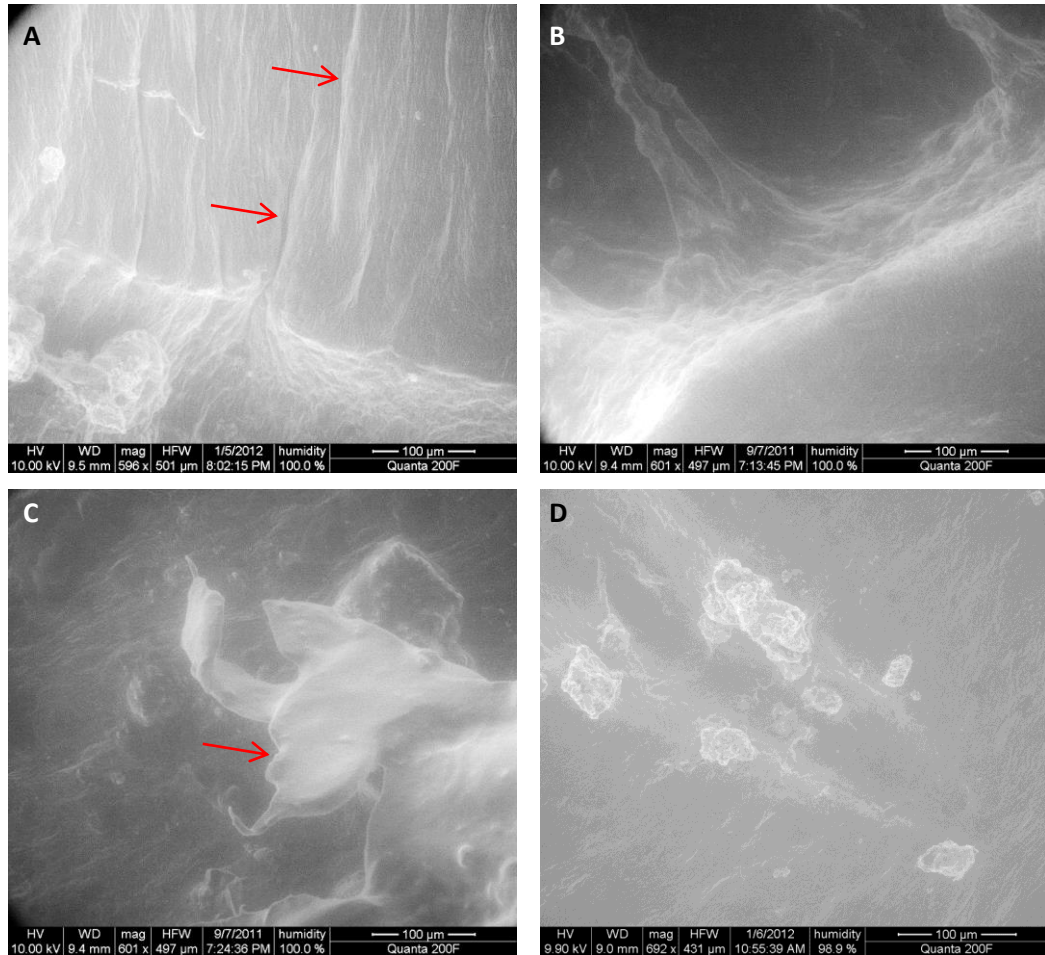


Figure 3.60. Features of degraded cartilage pin surfaces observed by ESEM. A. The mild surface showing a crack in the surface and increased creasing of the cartilage surface (arrows). **B.** The moderate condition surface articulated in Ringer's solution showing a deep crack in the surface containing protrusions. **C.** The moderate condition surface articulated in Ringer's solution showing a torn area of the cartilage surface (arrow). **D.** The moderate condition surface articulated in serum lubricant showing wear particles accumulating in the edge of a crack in the surface.

3.5.12 Qualitative evaluation of proteoglycans in cartilage tissues stained with cupromeronic blue dye by transmission electron microscopy

Transmission electron microscopy of ultrathin sections following treatment with cupromeronic blue dye which stains glycosaminoglycans was used to investigate the ultrastructural changes that took place in the cartilage tissue due to mechanical degradation. Three specimens were examined per condition. Three sections were taken from each specimen; one in the superficial

zone, one in the middle zone and one in the deep zone so that changes throughout the zones of the tissue could be observed. The procedure for preparing and imaging specimens has been described previously (Section 2.7.2).

3.5.12.1 Control cartilage tissue

At the superficial zone of the cartilage tissue there was a region approximately 500 nm thick that was characterised by an absence of collagen fibrils (Figure 3.61A). Below this band was another distinctive region which contained a small number of fine collagen fibrils. There was a small amount of staining for GAGs in this region. Below this region fine collagen fibres approximately 21 nm thick formed a thick band approximately 3 μm in width which could be seen crossing the tissue in parallel to the tissue surface. Below this band, the densely packed collagen fibres were randomly organised. Small proteoglycans could be seen interacting with collagen fibrils in some parts of this zone (Figure 3.61B/C).

Collagen fibrils in the middle section of the tissue had no fixed orientation and were highly visible. The fibres were observed crossing through the tissue without any dominating direction. Round features were observed in the tissue sections, where collagen fibres had been cut transversely, in addition to long fibres where the fibre had been sectioned through the sagittal plane. The distinctive D-band pattern associated with collagen could be seen along the sagittally sectioned fibres (Figure 3.62). Collagen fibres in the middle zone were approximately 52 nm in diameter. Aggrecan was present throughout the middle zone as small black flecks (Figure 3.62). In some areas of the tissue, aggrecan could be seen connecting where it formed a loose honeycomb like structure (Figure 3.62). The aggrecan could also be seen interacting with collagen fibres and spanning gaps between collagen fibres (Figure 3.62).

Collagen fibrils were less visible in the deep zone of the cartilage tissue. Collagen fibres that were thicker than the fibres seen in both the superficial and middle zones of the tissue were observed in the deep zone however some fibrils that were similar in diameter to the middle zone were observed. This resulted in a mixture of fibres ranging from approximately 50-100 nm. Collagen fibres appeared to be loosely aligned in one direction however it was sometimes possible to see collagen fibres in alternative directions to the general direction (Figure 3.63). The aggrecan staining was increased in the deep areas of the tissue and sections appeared darker with amorphous clouds of patchy dark staining. The aggrecan network also appeared to become more densely packed (Figure 3.63). The structure of the tissue changed in the proximity of chondrocytes. Collagen fibres were thinner than those in the interterritorial and territorial regions. The collagen fibres were also arranged in a roughly parallel manner that created a ring around the chondrocyte which can partially be seen in Figure 3.64.

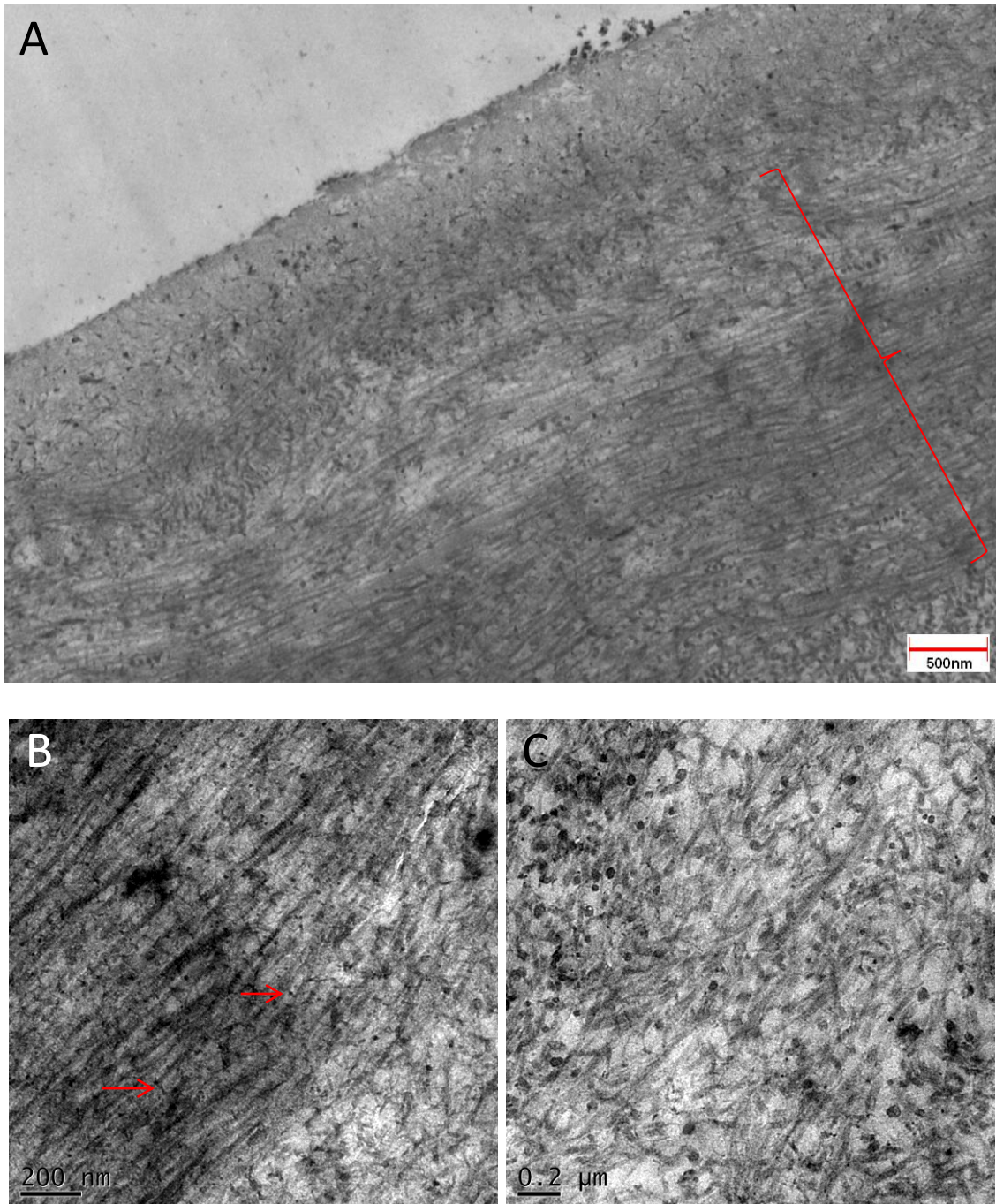


Figure 3.61. Transmission electron microscopy images of the superficial zone of undegraded control cartilage pin tissue stained with cupromeronic blue. A. The superficial zone of the tissue including the surface amorphous layer and a horizontal collagen band (bracket). **B.** Part of the band of fine collagen fibres running parallel to the cartilage surface where small leucine rich proteoglycans were observed (arrows). **C.** The cartilage tissue towards the middle zone of the tissue.

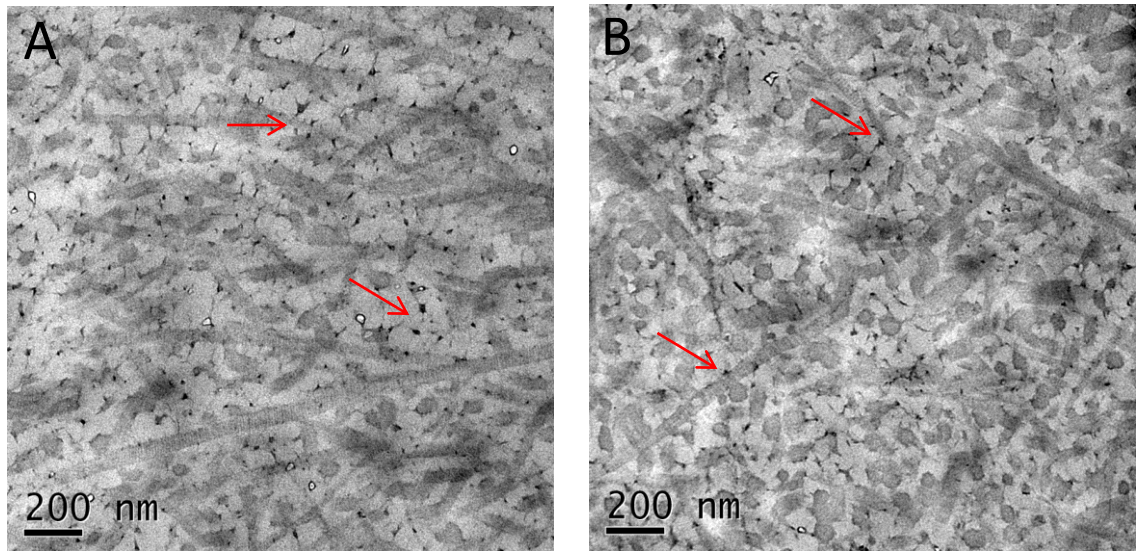


Figure 3.62. Transmission electron microscopy images of the middle zone of undegraded control cartilage tissue at 11,000 times magnification. **A.** Aggrecan was observed forming a network within the middle zone of the tissue (arrows). **B.** Proteoglycans were observed interacting with the surface of collagen fibrils (arrow).

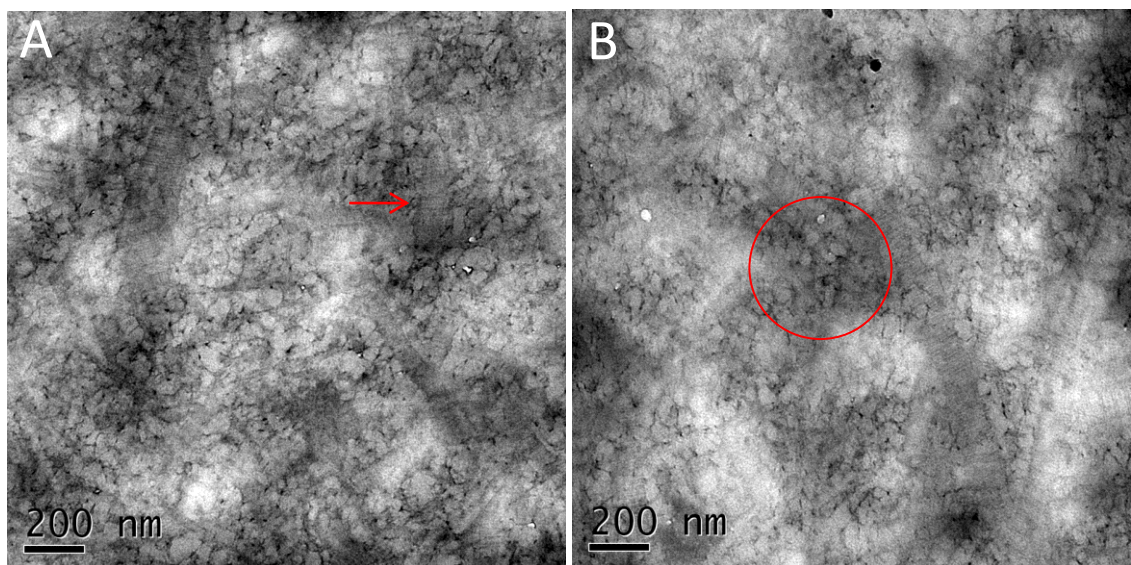


Figure 3.63. Transmission electron microscopy of the deep zone of undegraded control cartilage tissue at 11,000 times magnification (N=3). **A.** Thick collagen fibrils were observed behind the dense aggrecan network (arrow). **B.** Patchy dark areas of staining were observed where dense areas of aggrecan appeared (circle).

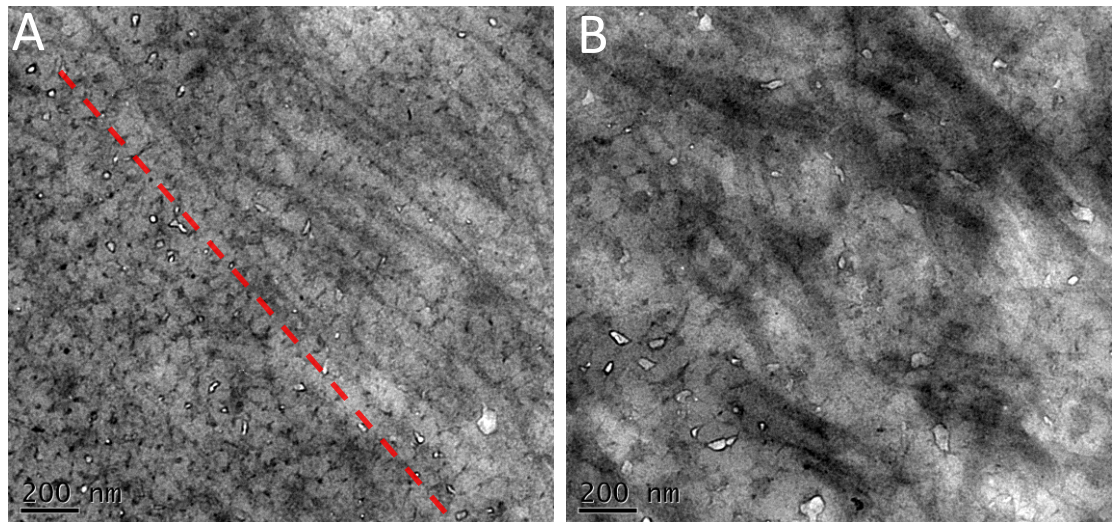


Figure 3.64. Transmission electron microscopy of the deep zone in undegraded control cartilage. **A.** The image shows the changes in the ultrastructure of the cartilage in the deep zone in close proximity to a chondrocyte (nucleus not visible). To the right hand side of the dashed line the fine parallel collagen fibres that line the perimeter of chondrocytes can be seen **B.** The structure begins to resemble the tissue in the territorial and interterritorial zones as the image is captured further away from the chondrocyte.

3.5.12.2 Mild condition degradation with Ringer's solution lubricant.

The tissue that had been degraded under mild mechanical conditions appeared lighter in colour than the undegraded control tissue. The horizontal collagen fibres in the superficial zone were not as tightly packed as they were in the control tissue which meant that many of the fibres did not lie in the same straight and horizontal manner.

The structure of the cartilage at the tissue surface did not appear to be different to the undegraded tissue however the sections appeared lighter and there was a light band that extended approximately 2 μm into the tissue from the surface (Figure 3.65A). In the middle zone of the tissue degraded under mild degradation conditions, collagen fibres were not observed to be different to those in the undegraded control tissues. However, the overall staining intensity of the section was lower and the aggrecan network was fragmented (Figure 3.65B). In the deep zone of the tissue the sections were stained at a lower intensity than those in the undegraded control tissue sections however, a large volume of aggrecan was observed in the tissue. The aggrecan network was more fragmented than the network observed in the undegraded control tissue (Figure 3.65C).

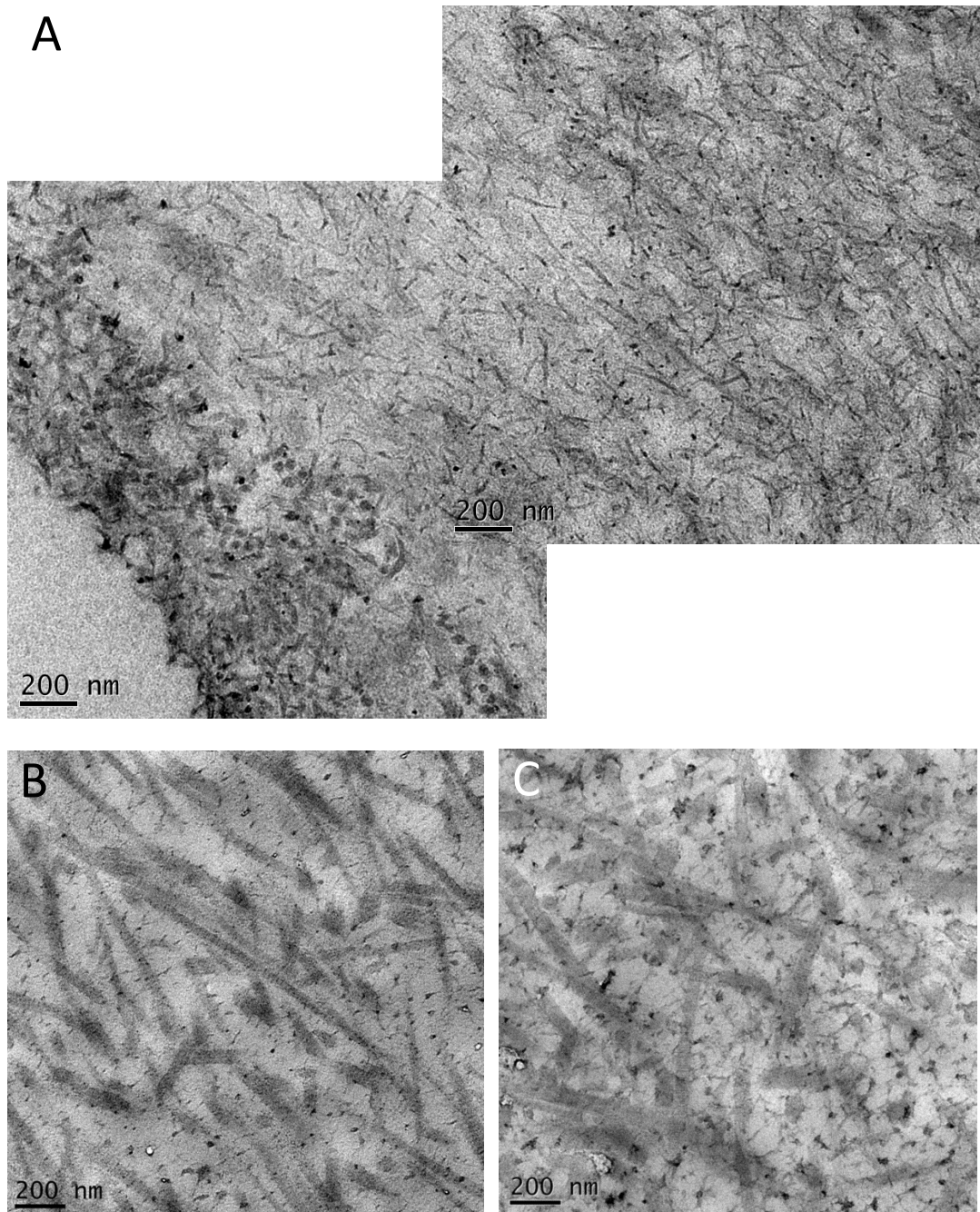


Figure 3.65. Tissues following mild condition mechanical degradation with Ringer's solution lubricant stained with Cupromeronic blue dye for proteoglycans. A. The superficial zone of the tissue; the surface of the tissue is shown in the bottom left hand corner of the image. **B.** The middle zone of the tissue. **C.** The deep zone of the tissue.

3.5.12.3 Moderate condition degradation with Ringer's solution lubricant

In the specimens that had undergone moderate degradation in Ringer's solution, it was not possible to image the superficial zone, as it had been removed during mechanical degradation. It was possible to image the transitional zone between the superficial zone and the upper middle zone in which aggrecan staining was extremely fragmented, with only some small parts of the network remaining. There was also a clear network of what was assumed to be hyaluronan as the reduction in GAG staining intensity allowed other ultrastructural components to be visualised more easily (Figure 3.66A).

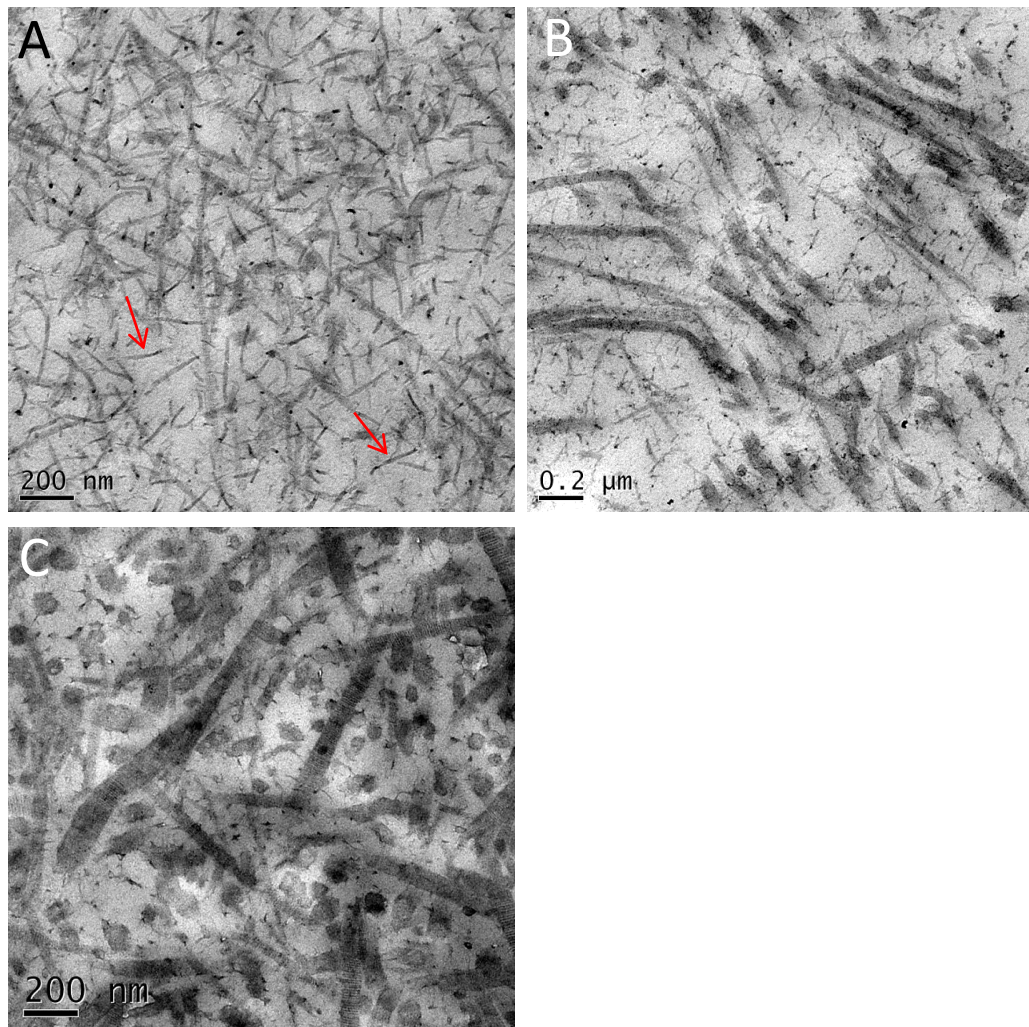


Figure 3.66. Tissues having undergone moderate condition mechanical degradation with Ringer's solution lubricant stained with cupromeronic blue dye for proteoglycans (N=3). A. The surface of the degraded tissue specimen possibly showing the hyaluronan network (arrows). **B.** The middle zone of the tissue. **C.** The deep zone of the tissue.

The collagen fibres in the middle zone of the tissue degraded under moderate conditions in Ringer's solution lubricant were less tightly packed than the fibres in the undegraded control tissue (Figure 3.66B). There was a reduction in aggrecan staining in both the middle and deep zones and the aggrecan network had been destroyed leaving some fragments within the tissue (Figure 3.66B/C).

It was possible to observe the ultrastructure of the tissue surrounding the chondrocytes in the superficial and deep zones of the cartilage tissue that had undergone moderate condition degradation in Ringer's solution lubricant (Figure 3.67). As with the undegraded control tissue, fine collagen fibres lined the perimeter of the chondrocyte then became more randomly orientated as their distance from the chondrocyte increased (Figure 3.67A/C). It was possible to see the chondrocyte nucleus in addition to short fibres which may have been hyaluronan or collagen VI (Figure 3.67B).

3.5.12.4 Moderate condition degradation with serum based lubricant

All of the tissues that were degraded under moderate conditions with serum lubricant showed large gaps in the collagen fibre network in the superficial zone (Figure 3.68A). The middle zone of the tissue had lost a large amount of aggrecan, however some fragments were still visible (Figure 3.68B). The collagen network through the middle zone of the tissue was looser in some areas however in other regions of the tissue a close network of collagen fibres was observed, similar to that seen in undegraded control tissue. In the deep zone of the tissue that had undergone moderate condition mechanical degradation in serum lubricant, there were a variety of changes to the cartilage ultrastructure. Two specimens appeared to have lost their aggrecan network and there was very minimal staining of the fragments that remained (Figure 3.68C). One specimen however, retained more aggrecan despite the fact that the aggrecan network was extremely fractured.

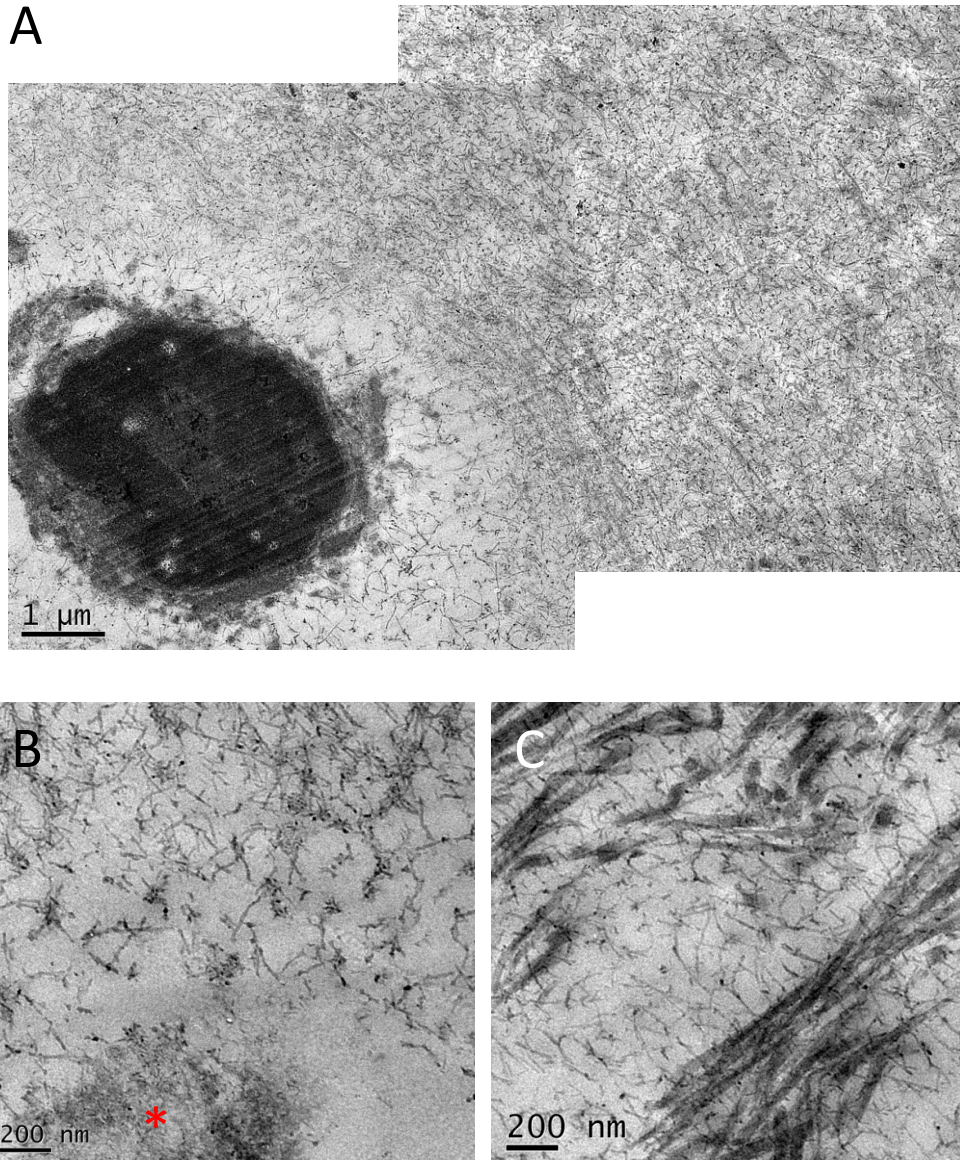


Figure 3.67. Chondrocyte ultrastructure in the superficial and deep zones of cartilage following moderate mechanical degradation in Ringer's solution lubricant. Stained with Cupromeronic blue **A.** A chondrocyte in the superficial zone of the tissue. **B.** A chondrocyte and its nucleus (partially shown ; asterisk) in the deep zone of the tissue. **C.** The transitional zone between the chondrocyte environment and the territorial region of the tissue in the deep zone.

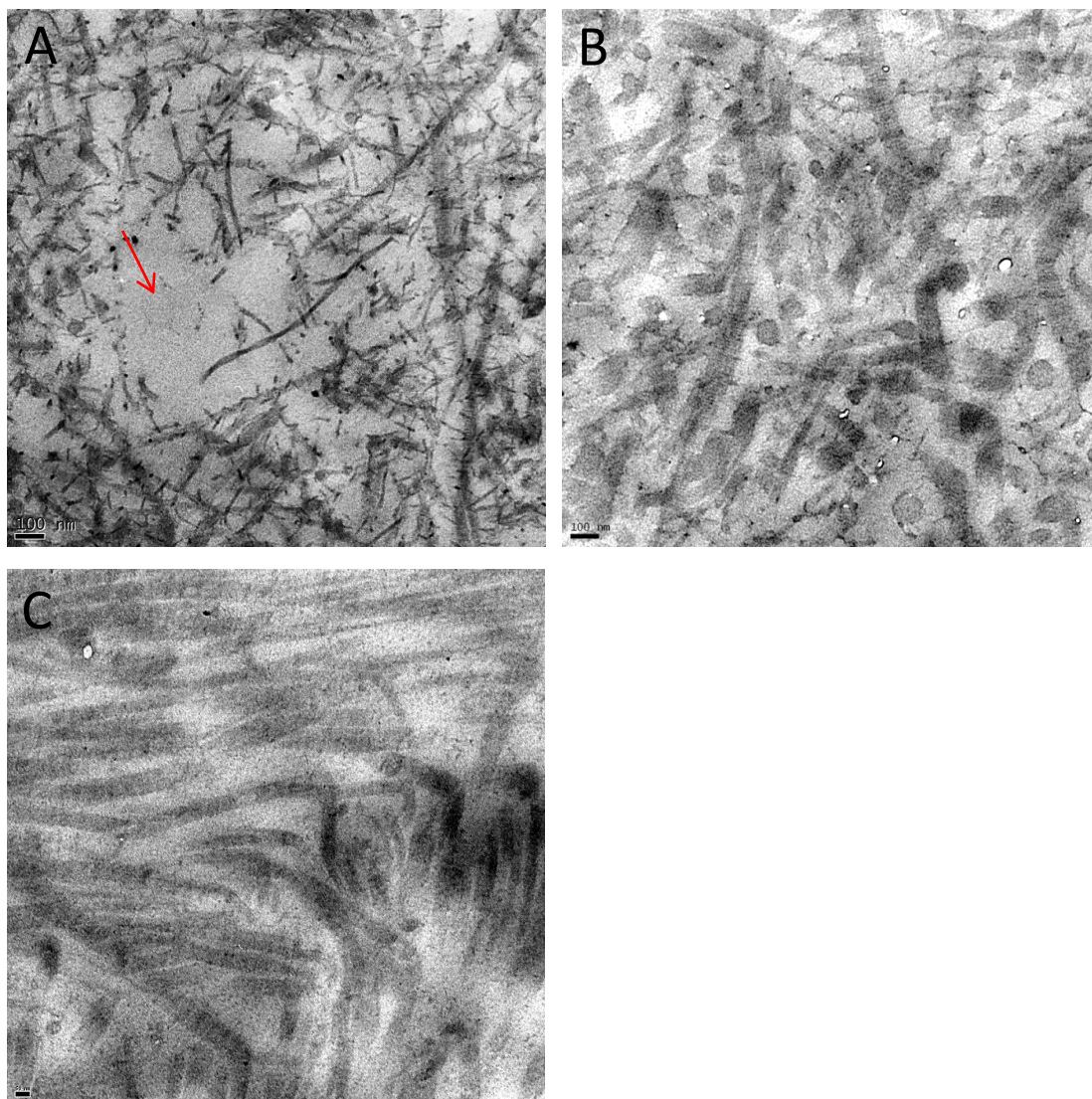


Figure 3.68. Tissues following moderate condition mechanical degradation with serum solution lubricant stained with Cupromeronic blue dye for proteoglycans. A. The superficial zone of the tissue showing gaps in the collagen network (arrow). **B.** The middle zone of the tissue. **C.** The deep zone of the tissue.

3.5.13 Quantitative assessment of collagen and glycosaminoglycan content of cartilage tissues

3.5.13.1 Collagen content of undegraded and mechanically degraded cartilage tissues.

The hydroxyproline assay was used to provide a measure of the collagen content of specimens. Six specimens were analysed for each condition. Standard concentrations were used allowing the hydroxyproline content of specimens to be interpolated from a standard curve (Figure

3.69). Results for the hydroxyproline assay were calculated using the dry weight of the tissue. The collagen content of the undegraded control cartilage was approximately 621 $\mu\text{g}\cdot\text{mg}$ (Figure 3.70). The tissue treated under mild mechanical degradation conditions had a collagen content of 591 $\mu\text{g}\cdot\text{mg}^{-1}$. Moderately mechanically degraded specimens treated with Ringer's solution and serum lubricant had collagen contents of 688 $\mu\text{g}\cdot\text{mg}^{-1}$ and 797 $\mu\text{g}\cdot\text{mg}^{-1}$ respectively (Figure 3.70). There was no significant difference in the collagen content between any of the degraded tissues and the undegraded control tissues. However, the collagen content of the tissue degraded under mild conditions in Ringer's solution was significantly lower than the tissue degraded under moderate conditions in serum based lubricant (Figure 3.70).

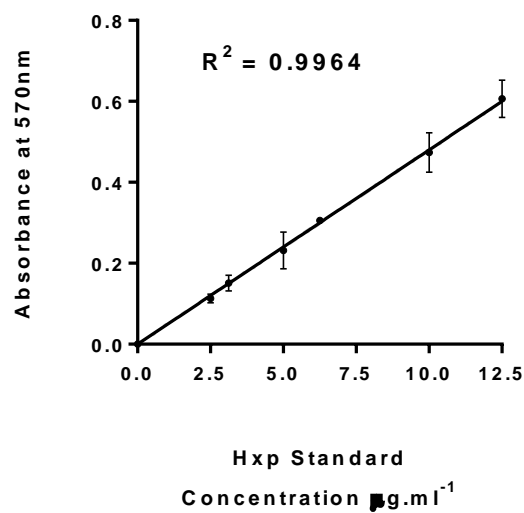


Figure 3.69. The relationship between absorbance at 570nm and the concentration of trans-4-hydroxy-L-proline ($\text{mg}\cdot\text{ml}^{-1}$). Data is presented as the mean ($n=3$) $\pm 95\%$ confidence limits.

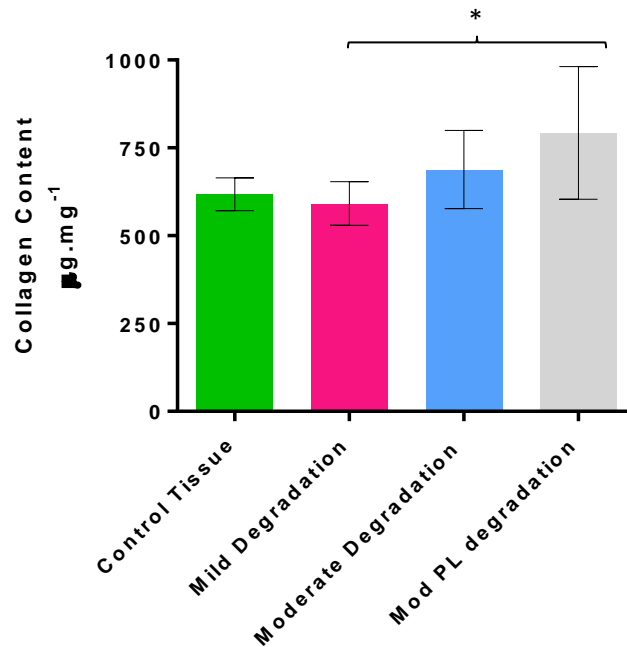


Figure 3.70. The collagen content of control cartilage and mechanically degraded cartilage. Data is presented as the mean (n=6) \pm 95% confidence limits. The data was analysed using one way analysis of variance followed by determination of significant differences between groups using a Tukey post test; * equates $P \leq 0.05$.

3.5.13.2 Glycosaminoglycan content of undegraded and mechanically degraded cartilage tissues.

The glycosaminoglycan (GAG) assay was used to assess the GAG content of the cartilage tissue. Standard chondroitin sulphate concentrations were used allowing the GAG content of specimens to be interpolated from the standard curve (Figure 3.71). The GAG content of the undegraded tissue was $334 \mu\text{g.mg}^{-1}$ of the dry weight of the tissue. The tissue degraded under mild mechanical degradation conditions contained a GAG content of $145.6 \mu\text{g.mg}^{-1}$, while tissues degraded under moderate mechanical conditions in Ringers's solution and serum lubricants contained $125 \mu\text{g.mg}^{-1}$ and $111 \mu\text{g.mg}^{-1}$, respectively. The GAG content of undegraded control tissues was significantly greater than the GAG content of the mechanically degraded tissues (Figure 3.72)

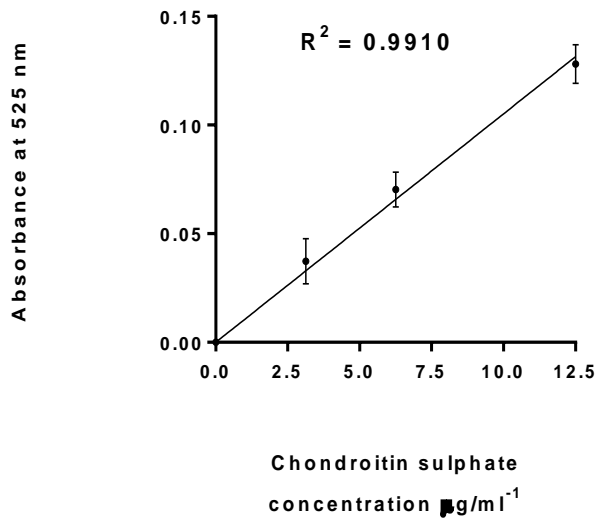


Figure 3.71. The relationship between absorbance at 525nm and the concentration of chondroitin sulphate B (mg.ml⁻¹). Data is presented as the mean (n=3) ±95% confidence limits.

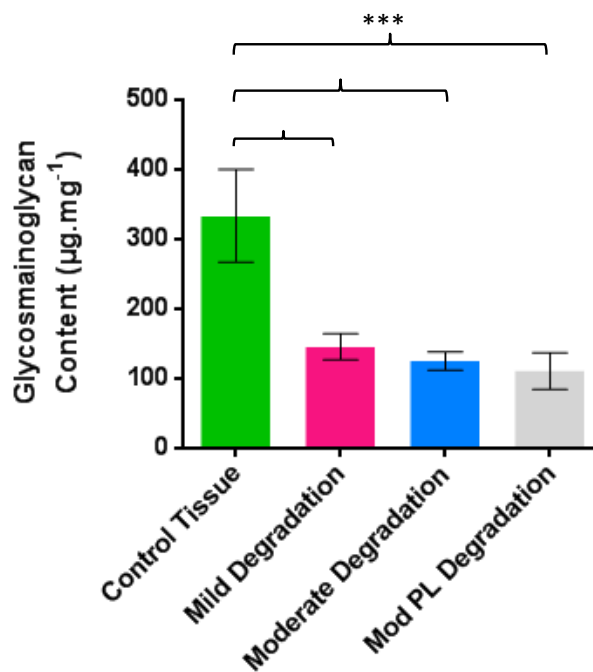


Figure 3.72. The GAG content of control cartilage and mechanically degraded cartilage. Data is presented as the mean (n=6) ±95% confidence limits. The data was analysed using one way analysis of variance followed by determination of significant differences between groups using a Tukey post test; *** equates $P \leq 0.001$.

3.5.14 Quantitative assessment of collagen and glycosaminoglycan content of lubricants recovered from mechanical degradation protocols

3.5.14.1 Collagen content of lubricant recovered from mechanical degradation protocols

The hydroxyproline assay was used to provide a measure of the collagen content of the lubricants recovered after mechanical degradation testing had been completed. The original protocol for detecting collagen in tissue specimens was adapted for lubricants (Section 3.4.10). The mean hydroxyproline concentration detected in the mild lubricant was $6.6 \mu\text{g}\cdot\text{ml}^{-1}$ or $47 \mu\text{g}\cdot\text{ml}^{-1}$ collagen, whereas the moderate lubricant contained $12.9 \mu\text{g}\cdot\text{ml}^{-1}$ of hydroxyproline or $92 \mu\text{g}\cdot\text{ml}^{-1}$ of collagen. The average hydroxyproline concentration in the Ringer's solution control was $1.4 \mu\text{g}\cdot\text{ml}^{-1}$ or $10 \mu\text{g}\cdot\text{ml}^{-1}$ of collagen (Figure 3.73). The collagen content of the Ringer's solution control was significantly lower than the collagen content of the lubricant recovered from the moderate condition degradation protocol.

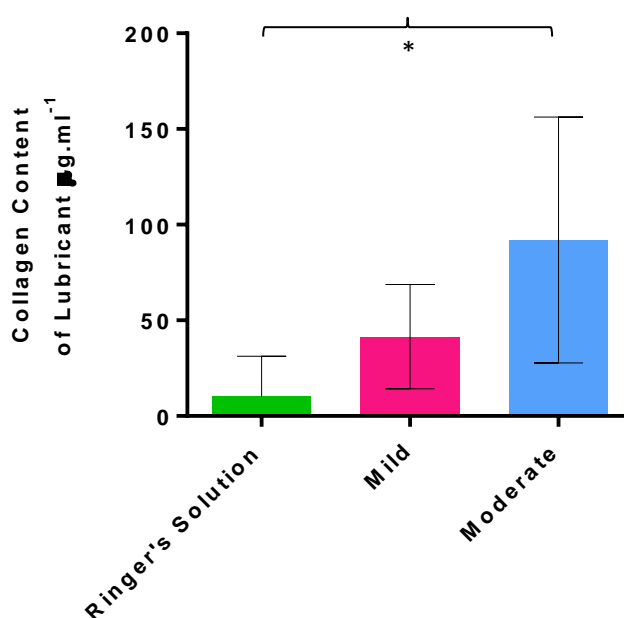


Figure 3.73. The collagen content of lubricants recovered after mechanical degradation protocols. Data is presented as the mean ($n=6$) $\pm 95\%$ confidence limits. The data was analysed using one way analysis of variance followed by determination of significant differences between groups using a Tukey post test; * equates $P \leq 0.05$.

3.5.14.2 Glycosaminoglycan content of lubricant recovered from mechanical degradation protocols

The glycosaminoglycan (GAG) assay was used to provide a measure of the GAG content of the lubricants recovered after mechanical degradation testing had been completed. The original protocol for detecting GAGs in tissue specimens was adapted for lubricants (Section 3.4.11). The concentration of GAGs in the mild lubricant was $11.9 \mu\text{g}\cdot\text{ml}^{-1}$, while the concentration of GAGs in the moderate condition lubricant in Ringers solution and the moderate condition lubricant in serum lubricant was $39.2 \mu\text{g}\cdot\text{ml}^{-1}$ and $45 \mu\text{g}\cdot\text{ml}^{-1}$, respectively. There was a significant difference between the Ringer's solution control and both Ringer's solution and serum lubricants under the moderate condition (Figure 3.74). The results showed that mechanical degradation increased the GAG concentration in the lubricants.

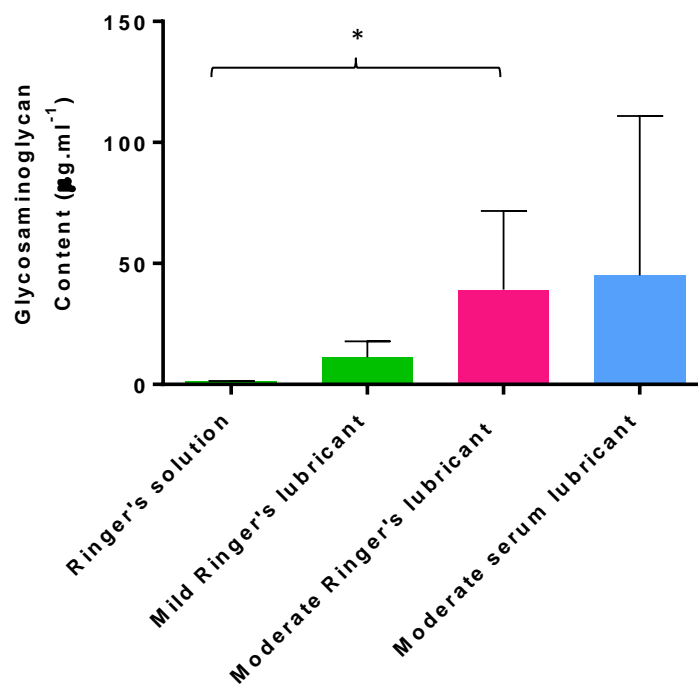


Figure 3.74. The GAG content of lubricants recovered from mechanical degradation protocols. Data is presented as the mean ($n=6$) \pm 95% confidence limits. The data was analysed using one way analysis of variance followed by determination of significant differences between groups using a Tukey post test; * equates $P \leq 0.05$.

3.6 Summary of results

The following table provides a summary of the results that were obtained during analysis of the cartilage specimens that underwent mechanical degradation conditions.

	Friction	Surface Roughness	Height loss	Histo-architecture	Qualitative GAG analysis	Minor component presence			Surface morphology	Ultrastructural analysis		HXP Tissue ($\mu\text{g.mg}^{-1}$)	GAG Tissue ($\mu\text{g.mg}^{-1}$)	HXP Lubricant ($\mu\text{g.ml}^{-1}$)	GAG Lubricant ($\mu\text{g.ml}^{-1}$)
						Biglycan	COMP	Collagen VI		Collagen network disruption	Aggrecan Disruption				
Undegraded control	N/A	Smooth	N/A	Smooth	Intense +++	+++	+++	+++	Smoothest	---	---	87	334	1.4	1.1
Mild degradation with Ringer's solution	Low	Smooth	No	Smooth/ cracks/ internal tear	++	+++	+++	+++	Rough	+	+	82.8	145.6	6.6	11.9
Moderate degradation with Ringer's solution	Low	Rough	No	Cracks/ tissue loss/ cartilage detaching	-	+	+++	+++	Roughest	++	++	96.4	125	12.9	39.2
Moderate degradation with serum lubricant	Low	Smooth/ Rough	No	Cracks/ tissue loss	--	+	+++	++	Smooth	++	++	111	111	N/A	45.0

Figure 3.75. A summary of the results obtained using a range of methods to characterise cartilage mechanical degradation models. Key: *** indicates strong presence of the feature, ** indicates Presence, * indicates slight presence, - indicates reduction in presence of feature, -- indicates strong reduction, --- indicates complete absence of a feature.

In summary, the surface roughness of cartilage specimens was increased in specimens as the load on the tissue was increased. However, some of the specimens articulated in serum lubricant retained a smooth surface. The surface roughness results correlated with the degradative changes that were observed in the cartilage histoarchitecture. The GAG content of the specimens that were mechanically degraded was reduced when compared with the control tissue. The collagen content of specimens was not altered significantly by the mechanical degradation. The collagen VI content did not appear to be altered in the specimens articulated in Ringer's solution, however, a reduction was observed in specimens degraded in serum lubricant. Biglycan staining was reduced in specimens degraded under moderate conditions. COMP staining was not altered by mechanical degradation.

3.7 Discussion

The aim of this study was to develop and characterise mechanical degradation models that replicated the tribological conditions of degenerate cartilage tissue. Three degradation models were developed using Ringer's solution and serum in PBS as lubricants.

Two models of degradation were chosen to investigate the effect of contact stress on tissues. The contact stresses that were chosen reflected physiological values and produced tissues with some features that were similar to degraded cartilage tissue as seen in the Modified International Cartilage Repair Society Chondral Injury Classification System and the microscopic histologic histochemical grading system developed by Mankin *et al* (1971).

Ringer's solution was chosen as a lubricant because of its osmotic properties which allowed the cartilage tissue to remain hydrated during mechanical degradation. Ringer's solution was also chosen for its simplicity, which facilitated the analysis of cartilage components released into the lubricant during testing. Calf serum was used as an alternative to synovial fluid as a lubricant. The calf serum lubricant contained glycoproteins and lipids which are important molecules implicated in boundary lubrication between cartilage tissues.

An extensive range of complementary qualitative and quantitative methods were used to thoroughly characterise the degraded cartilage tissues. The methods were chosen so that the scope of changes to the tissue that were anticipated would be detectable. For example, established methods such as alcian blue staining and a glycosaminoglycan assay were used in conjunction with cupromeronic blue staining. This allowed detailed information about the macroscopic and ultrastructural condition of GAGs and proteoglycans in the tissue to be determined which was reinforced with quantitative data.

The major findings of this chapter were that lubricant and contact stress had a profound effect on the degradation of tissue specimens during mechanical degradation. As contact stress was increased in the moderate condition, a large volume of GAGs were lost from the tissue and the collagen and aggrecan networks were disrupted. Tissue was lost from the surface of the specimens and the surface became rougher. However under "mild" conditions a large proportion of GAGs remained in the tissue and there was a reduction in tissue loss from the specimen surface. The surfaces of the mild specimens also remained relatively smooth. Collagen VI and COMP remained relatively unchanged in the degraded tissues under both mild and moderate conditions, whereas biglycan was reduced under both conditions. However, in some cases the results were largely variable.

From the results that were obtained it was clear that both the contact stress and the lubricant chosen for the mechanical degradation protocol had an effect on the changes that occurred in the cartilage tissue. The increasing contact stress from the mild to moderate condition led to a significant increase in tissue loss, damage to the cartilage surface, destruction of the aggrecan network, loss of GAGs and collagen fibre networks.

It was evident that the type of lubrication employed during mechanical degradation had an effect on extent of damage that was observed in the cartilage specimens. Ringer's solution offered lower protection from damage at the higher contact stress used in the moderate condition, but was sufficient for the mild loading condition, as the data showed that in the mild condition the cartilage was similar in comparison to the undegraded control tissue, aside from a loss of GAGs. The data from the moderate condition tests in serum lubricant had the largest level of variance, with some specimens having little damage to their ultrastructure and a smooth superficial layer, whereas other specimens were severely damaged in a manner that replicated the moderate condition specimens that were articulated in Ringer's solution. This may have been because of the pin geometry. The serum may have been able to prevent severe damage to pins that were congruent with the plate surface via boundary lubrication. However, if the pin and plate were not congruent the serum may not have been able to prevent damage occurring that was similar to that seen in some of the specimens degraded under moderate conditions in Ringer's solution. The serum also seemed to exacerbate GAG loss from the cartilage tissue. This may have been due to the electrochemical characteristics of the lubricant which was not isotonic with the tissue as the Ringer's solution was, possibly causing GAGs to leach out.

The changes in cartilage height measured using the shadowgraph showed that there was no loss of cartilage height during any of the degradation protocols. However, the method that was used successfully to measure statically loaded pins may not have been appropriate for pins following dynamic loading conditions since the macroscopic images of the tissues showed that the edges of the pin remained the same height despite tissue loss within the central region of the pin. In future a vernier height gauge should be used to take readings in the centre of the pin which would allow height changes in this region to be recorded. The loss of height in the centre of the pin that was observed macroscopically may not have correlated with loss of height on the edge of the cartilage pins due to an edge effect. Edge effects are caused by the different response of tissue that is unrestrained at the circumference of the pin to those in the central region of the pin which are restrained by the surrounding tissue. The large load on the cartilage pin may have resulted in the edges of the pin spreading outwards during loading which may have resulted in a lower exposure of the pin edge to abrasion

against the opposing plate. This result showed that it would be better to use large tissue specimens because this may reduce the influence of edge effects on tissue specimens. A reduction in edge effects is desirable because edge effects equate to an occurrence of non-physiological conditions.

The H & E images of the specimens reflected the extent of changes that were seen with the other characterisation techniques. When the load was increased there was an increase in cracking of the tissue which may have been due to the contact stress on the tissue. There was also a tissue loss from the cartilage surface which would have been exacerbated by the multidirectional motion used during the degradation protocol.

The ESEM images of the cartilage surface and the surface roughness data were used in a complementary manner. The results showed that the surface of the tissue became rougher as an increased load was applied when specimens were articulated in Ringer's solution. However the surface roughness of the tissue articulated with serum solution was variable, with some specimens remaining fairly smooth while others became very rough. The results from the two techniques were found to be in agreement for all specimens. One of the drawbacks of using the surface profilometry method for assessing cartilage surface roughness was that the surface roughness readings did not take into account the whole tissue surface. Traces were taken across the surface and an average roughness was calculated, however it would have been more accurate if the surface roughness of the whole surface could have been determined.

The biggest ultrastructural change brought about by the mechanical degradation regimes was the loss of aggrecan from the tissue, shown in the TEM images. This was interesting because there appeared to be a significant amount of biglycan remaining in the tissue after mechanical degradation had occurred, shown by the immunohistochemistry results. This may be due to differences in the way that these two different types of proteoglycan are anchored into the matrix. Biglycan is associated with collagen II and collagen VI in the ECM, whereas the large aggrecan core is attached to hyaluronan via one link protein, which may make aggrecan easier to disrupt (Watanabe *et al.*, 1997 ; Wiberg *et al.*, 2003). The results showed that loss of aggrecan in the cartilage tissue in patients with degenerative diseases such as osteoarthritis may also be lost through kinematic degradation rather than enzymatic digestion alone. It would be interesting to conduct further experiments on the aggrecan fragments in the lubricant collected after mechanical degradation using atomic force microscopy. This is because the atomic force microscopy would make it possible to visually determine the changes that may have occurred to aggrecan. The collagen network was

disrupted by the mechanical degradation especially in the superficial zone of the tissue. The deep zone of the tissue in the specimens examined appeared to remain in a tight network.

A limitation of the TEM technique was that imaging of cartilage zones was inconsistent. This was due to the small size of the specimen which meant it was not possible to take sections in precise areas of the tissue. This may have led to some middle zone sections being taken in closer proximity to either the superficial or deep zones which may have had an effect on the structure of the tissue that was observed. Some of the deep zone sections may have also been closer to the calcified zone which could have had an effect on the tissue structure seen in the images. This could also explain why in some repeats, collagen fibres were not identical in size despite being from the same zone in the tissue.

The largest loss of aggrecan was seen in tissues degraded under moderate loading conditions. These results correlated with the alcian blue staining in which specimens loaded under moderate conditions with either lubricant showed the largest amount of GAG loss.

The antibody labelling of cartilage oligomeric protein (COMP) and collagen VI showed that these two components were not significantly depleted by the mechanical degradation regimes. COMP is found in the synovial fluid and serum of osteoarthritis patients. Therefore these results imply that during cartilage degeneration, COMP is lost from the tissue via biological means (Clark *et al.*, 1999 ; Song *et al.*, 2012). Similar staining to that seen in this study for collagen VI has been observed previously in human tissues (Pullig *et al.*, 1999). However in the tissues observed in the Pullig study, collagen VI staining was increased within the tissue. It was also observed in the deep zone of the tissue as tissue became increasingly degraded, which was not observed during this study. This infers that collagen VI is altered through biological processes during *in vivo* cartilage degeneration.

The concentration of collagen and GAG in cartilage have been determined in human tissues, where approximately 64% of the dry weight of cartilage is collagen, while 21% of the dry weight is proteoglycan, leaving approximately 15% of the tissue remaining, which is taken up by cells and other minor cartilage components (Maroudas *et al.*, 1980). In this study the collagen content and GAG content were 621 $\mu\text{g}\cdot\text{mg}^{-1}$ and 334 $\mu\text{g}\cdot\text{mg}^{-1}$ respectively. Therefore these two components account for approximately 95.5% of the bovine cartilage composition. The slight differences seen in comparison in the results of the human study may be due to inter-species variation and may also be due to the different locations from which the tissue was taken.

The collagen content of the tissues did not change due to mechanical degradation when compared to the undegraded tissue. However, there was an apparent increase in the collagen content of the tissue degraded under moderate conditions with serum lubricant. This may have been due to the large loss of GAGs from the tissue which would effectively increase the collagen content of the tissue. Despite there being no apparent loss in collagen from the tissue, hydroxyproline residues were detected in the lubricants. This implied that there were cartilage wear particles being removed from the bulk of the tissue, but that collagen was not leaching from the tissue. One limitation was that the hydroxyproline assay is optimised to detect total collagen levels, therefore it was not possible to say whether other collagen types, such as collagen IX, were leaching from the tissue.

Unfortunately it was not possible to determine the collagen content of the serum lubricant due to time constraints. However when observing the results for the hydroxyproline assay on tissues and lubricants with Ringer's solution it could be predicted that collagen was not lost from the tissue mass but that it may have been present in the lubricant due to cartilage wear particles that had been worn from some of the rougher specimens.

There was a significant loss of GAGs from the tissue under all of the mechanical degradation conditions however the highest loss was in the tissue that was more heavily loaded. In line with this, higher GAG concentrations were found in the lubricants that were taken from the specimens degraded under moderate conditions.

Despite the differences seen in the specimens that were degraded under the varying conditions, there was no significant difference between the friction values taken for any of the conditions. The friction coefficient measured during all of the conditions was at a relatively low level and rose slightly. The only slight difference that was seen was between the friction values of the mild and moderate conditions. The mild specimen eventually reached a plateau where friction remained relatively constant whereas the friction between the specimens under the moderate conditions continued to rise throughout the test. This may have been because the specimens under mild loading conditions reached an equilibrium, while the friction between the specimens under moderate conditions may have continued to increase as the GAGs were removed from the specimens.

3.8 Conclusion

Both the mild and moderate mechanical degradation protocols resulted in degeneration of cartilage specimens. Loading was the most important factor in terms of causing the most damage to the cartilage tissue. The tissues loaded under moderate conditions became rougher, they had increased damage to the cartilage surface, increased GAG loss, and greater wear. The lubricant type also had an effect on specimens. Ringer's solution lubricant was suitable for maintaining the tissue at mild level of loading but did not protect the tissue from severe degradation at moderate loading levels. The serum lubricant appeared to protect some specimens from severe degradation however other specimens appeared as damaged as those under moderate loading conditions with Ringer's solution, which produced a large variability in the results for this lubricant.

Chapter 4

Development and Characterisation of an Enzymatic Model of Cartilage Degradation

4.1 Introduction

During degeneration, cartilage tissue is degraded through mechanical and biological means. Matrix metalloproteases (MMPs) produced by chondrocytes are found in healthy cartilage tissue and help to maintain cartilage homeostasis (Aigner and Stove, 2003). Cartilage degeneration of a biological nature, rather than a mechanical nature, begins to occur when the rate of extracellular matrix degradation by catabolic enzymes in the tissue is greater than the rate of anabolic activity (Mueller and Tuan, 2011). One of the main components of the cartilage tissue that are lost during enzymatic digestion are the proteoglycans and their associated glycosaminoglycans (Thompson and Oegema, 1979).

Proteoglycans with their associated GAGs are integral for optimal cartilage function because GAGs attract water into the tissue, which causes the cartilage to swell (Mow and Huijskes, 2005). Swelling caused by interstitial fluid pressurisation in the cartilage is fundamental for maintaining low friction in joints. Therefore when GAGs are depleted from the tissue it has a major effect on the biotribological properties of the tissue (Katta *et al.*, 2007). A reduction in GAGs has been shown to reduce the ability of cartilage to resist loading on the solid phase of the tissue which can lead to cartilage damage (Mow and Huijskes, 2005). Therefore it was hypothesised that enzymatic treatment of cartilage tissue to remove GAGs would provide a model of cartilage degradation representative of the biotribological state of cartilage tissue following biological degradation as compared to the previous model of mechanical degradation.

A variety of enzymes have been used to investigate changes to cartilage tissue structure and properties caused by biological degradation. Previous studies have included the use of collagenases, hyaluronidase and chondroitinase ABC (Katta *et al.*, 2007; Park *et al.*, 2008; June and Fyhrie, 2009; Lee *et al.*, 2013). All of these studies aimed to determine the effects of removal or alteration of the individual components on the cartilage tissue, to increase knowledge of the relationship between the structure and function of cartilage tissue in more detail.

June and Fyhrie, (2009) used collagenase and hyaluronidase to digest bovine cartilage samples. The study investigated the ability of models of polymer dynamics to predict the contributions of matrix components to the flow independent viscoelastic properties of cartilage tissue. The theory of polymer dynamics is used to describe the motions and interactions of polymeric molecules in a quantitative manner. In cartilage this includes the collagen network and the aggrecan network. Flow independent viscoelastic properties are

caused by the interactions between the solid components of the tissue and cannot be distinguished from fluid dependent viscoelastic properties experimentally, hence the assessment of polymer dynamics in this study for use in distinguishing these two factors. Since polymer dynamics are affected by the length of the polymers in the tissue, collagenase and hyaluronidase were used to decrease the length of the polymers in the tissue. The use of collagenase and hyaluronidase allowed the authors to determine how collagen and hyaluronidase networks contributed to a faster stress-relaxation rate in the tissue. The authors also confirmed their hypothesis; that polymer dynamics are able to give a greater understanding of how individual cartilage components contribute to the properties of cartilage tissue.

Chondroitinase ABC, collagenase and hyaluronidase have been used to investigate the effects of degradation of the specific matrix components on the friction of porcine cartilage tissues (Lee *et al.*, 2013). Each enzyme was used to treat cartilage samples followed by reciprocation of the treated samples against each other in a rig under variable loads and sliding speeds. In this study the cartilage was cut from the bone and glued to glass slides before articulation. Removing the cartilage from the bone was likely to have had an effect on the results and the glue used may have leached into the tissue, which was only approximately 3mm thick. The removal of bone or use of glue could have affected the deformation properties of the tissue or altered fluid flow through the tissue, which is also likely to have affected friction readings. The authors reported that treatment with any of the enzymes increased the friction between specimens, with chondroitinase ABC treatment causing the greatest increase. Treatment with chondroitinase ABC and hyaluronidase also modified the stick slip conditions recorded during articulation, which were related to increased wear of the cartilage surface.

Katta *et al.* (2007) investigated the effects of chondroitinase ABC treatment on the friction and deformation characteristics of cartilage tissue. The rationale for conducting this study was that contradictory results had been found in relation to the link between GAG loss and an increase in friction between cartilage tissues. This study found via indentation testing that depletion of GAGs from the cartilage resulted in a loss in compressive stiffness in the cartilage. The elastic modulus of the cartilage was decreased by the enzyme treatment and permeability was increased. An increase in friction was seen in treated specimens under dynamic loading conditions. The study confirmed GAG loss using a quantitative biochemical assay and the surface was examined using surface profilometry and scanning electron microscopy. Further characterisation of the tissues was, however, not conducted. Histological analysis would have allowed the changes to the tissue architecture and components of the

tissue to be qualitatively analysed. Transmission electron microscopy of the tissue may also have given an insight into any ultrastructural changes in the tissues.

The studies described above indicate that selective digestion of cartilage components can be useful for revealing how the different components of the cartilage tissue influence the cartilage properties. Chondroitinase ABC is a particularly interesting enzyme due to its substantial effect on the GAGs in the cartilage tissue, which are responsible for the ability of the cartilage to resist loading, and prevent damage to the tissue during articulation via biphasic lubrication.

The enzyme chosen in the present study to digest GAGs in the cartilage tissue, was chondroitinase ABC. Chondroitinase ABC carries out an elimination reaction with chondroitin-4-sulphate (chondroitin sulphate A), chondroitin-6-sulphate (chondroitin sulphate C) and dermatan sulphate (formerly known as chondroitin sulphate B) which yields 4,5-unsaturated disaccharides. As a result the GAGs are removed from the aggrecan core protein to which they are attached. After chondroitinase ABC treatment has occurred other components of the tissue such as collagen remain intact (Yamagata *et al.*, 1968; Lyyra *et al.*, 1999).

As described in Chapter 3, in which mechanical degradation of cartilage was investigated, in this part of the study histological techniques were used to assess changes to the tissue structure and alterations in the components of the tissue after chondroitinase ABC treatment. GAG and hydroxyproline assays were used to determine changes in the amount of the two major components of the cartilage tissue, GAGs and collagen, respectively. Transmission electron microscopy was used to determine how the removal of GAGs from the tissue changed the appearance of the tissue on an ultrastructural scale. The GAG content of cartilage tissue has been reported to be related to the compressive resistance of the tissue (Mow and Huiskes, 2005). To investigate these changes indentation testing was performed before and after chondroitinase ABC treatment. Indentation analysis of chondroitinase ABC treated cartilage tissue has been conducted in previous studies and is an established method for investigating changes to cartilage stiffness properties caused by enzymatic treatment (Stolz *et al.*, 2004; Katta *et al.*, 2007; Hall *et al.*, 2009).

4.2 Aims and objectives

The aim of the studies described in this chapter was to compare native bovine control cartilage tissue to bovine cartilage tissues that had undergone treatment with chondroitinase ABC. The tissues were compared comprehensively using quantitative and qualitative methods.

Objectives:

- To develop an enzymatic degradation method for bovine cartilage tissue using chondroitinase ABC to remove glycosaminoglycans from the cartilage tissue.
- To use histological staining to assess the normal histoarchitecture and staining patterns of glycosaminoglycans in chondroitinase ABC treated bovine cartilage tissue using haematoxylin and eosin staining and alcian blue staining, respectively.
- To determine the distribution of biglycan, cartilage oligomeric matrix protein (COMP) and collagen VI qualitatively in chondroitinase ABC treated bovine cartilage tissues using immunohistochemistry.
- To determine the deformation properties of the cartilage tissue before and after chondroitinase ABC treatment using indentation testing.
- To use transmission electron microscopy with cupromeronic blue dye to examine the bovine cartilage ultrastructure and GAG interactions in enzymatically degraded a tissue.
- To quantitatively determine the glycosaminoglycan and collagen content of chondroitinase ABC treated bovine cartilage tissue.

4.3 Experimental approach

The experimental approach taken during this part of the study is shown in Figure 4.1. The diagram shows the various steps that were undertaken in the enzyme treatment of the cartilage specimens and the subsequent steps taken to characterise the treated tissues, including sample numbers.

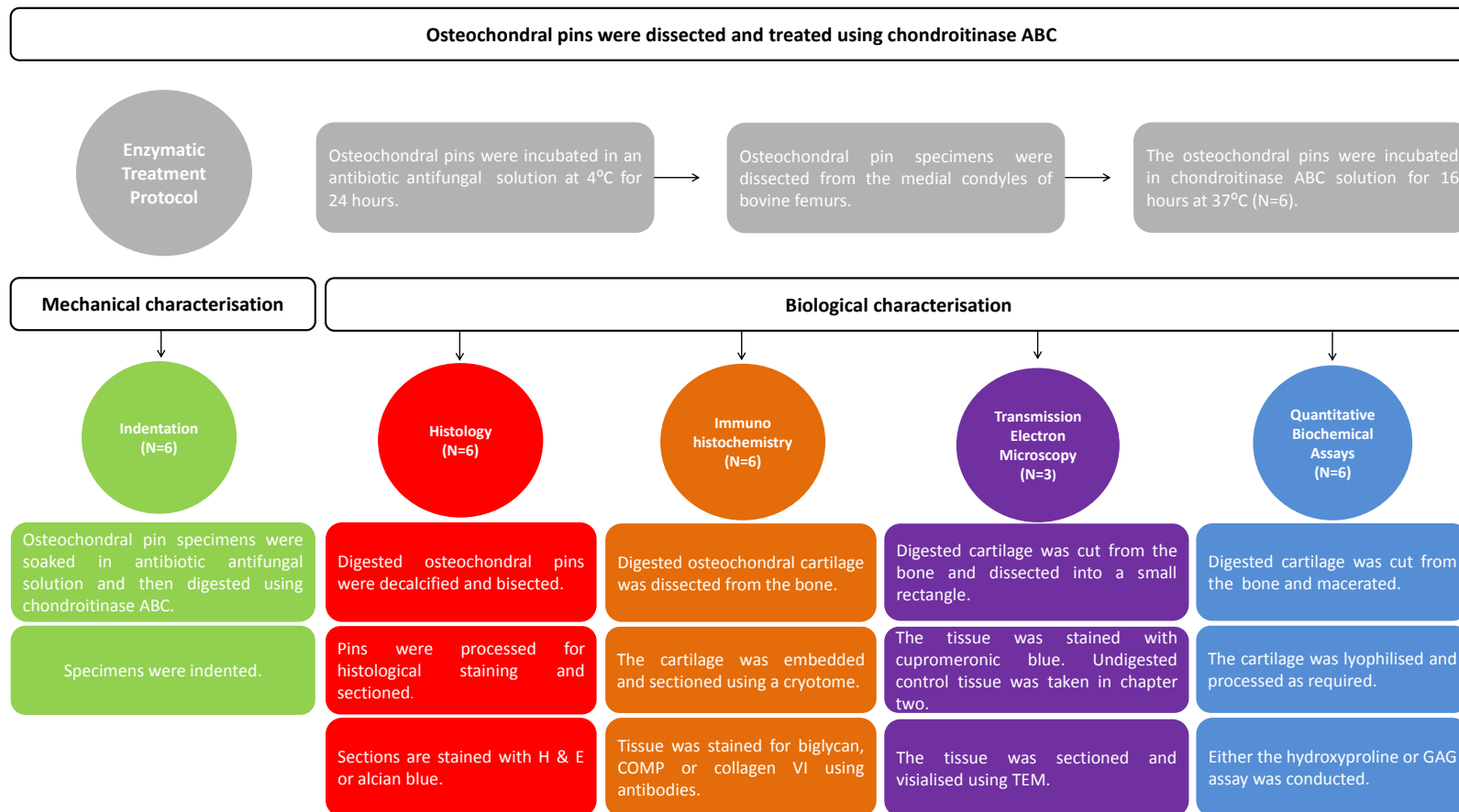


Figure 4.1. The experimental approach taken in the research described in chapter 4 in which specimens were treated with chondroitinase ABC. The image includes the characterisation techniques that were used to analyse specimens and the number of replicates.

4.4 Methods

A number of the methods that were used in this chapter have been described previously in Chapter 2. These methods include histological staining using haematoxylin and eosin (Section 2.6.1) and alcian blue staining (Section 2.6.2), immunohistochemical analysis of biglycan, COMP and collagen VI (Section 2.6.3), TEM with cupromeronic blue dye to examine cartilage ultrastructure (Section 2.7.2) and quantitative biochemical assays for GAGs and collagen (Sections 2.8.1 and 2.8.2).

4.4.1 Chondroitinase ABC treatment of cartilage tissue

Chondroitinase ABC was used to deplete GAGs from the cartilage tissue. The chondroitinase ABC was suspended in a buffer solution at pH 8, as recommended by the supplier. The enzyme solution, which also contained bovine serum albumin (BSA), was incubated at 37°C during treatment of the cartilage. The temperature conditions and addition of BSA put the solution at risk of bacterial growth. Therefore the cartilage pin specimens were soaked in a solution of antibiotics in PBS for 24 h before enzymatic treatment. Antibiotics were also added to the chondroitinase ABC treatment solution.

4.4.1.1 Extensive chondroitinase ABC treatment of cartilage tissue

The protocol described below was also used to create positive control tissues for the cupromeronic blue staining protocol (described in section 2.7.2). However, rather than one 16 hour incubation, specimens were incubated extensively for two consecutive 24 hour periods in the chondroitinase ABC solution with the solution being refreshed at the 24 hour time point.

4.4.1.2 Antibiotic solution

The antibiotic solution was prepared by adding one PBS tablet and the antibiotics listed in Table 4.1 to 30 ml of distilled water. The solution was stirred using a magnetic stirrer bar until all of the antibiotics were dissolved. The pH of the solution was adjusted to pH 7 using sodium hydroxide solution (1 M) or hydrochloric acid (1 M). The volume of the solution was increased to 100 ml using distilled water

4.4.1.3 Chondroitinase ABC treatment solution

Tris (0.605 g), 0.82 g of sodium acetate and 0.02 g of BSA were added to 10 ml of distilled water. The antibiotics listed in Table 4.1 were also added to the solution. The solution was adjusted to pH 8 using sodium hydroxide solution (1 M) and chondroitinase ABC was added to

the solution to produce a final concentration of 0.1U.ml^{-1} . The solution volume was increased to 100 ml using distilled water. For chondroitinase ABC treatment, osteochondral pins were dissected (Section 2.4) and each pin was placed into 5 ml of antibiotic solution for 24 h at 4°C on a shaker at 100 rpm. The osteochondral pins were then placed into 5 ml of the chondroitinase ABC treatment solution for 16 hours at 37°C .

Table 4.1 Antibiotic concentrations in the antibiotic solution.

Component	Description	Final concentration
Nystatin	Antifungal	2500 U.ml^{-1}
Gentamicin	Broad spectrum aminoglycoside antibiotic	$20\text{ }\mu\text{g.ml}^{-1}$
Polymixin B	Antibiotic active against Gram negative rod bacteria	$200\text{ }\mu\text{g.ml}^{-1}$
Vancomycin	Antibiotic active against Gram positive bacteria	$50\text{ }\mu\text{g.ml}^{-1}$
Imipenem	Broad spectrum beta lactam antibacterial	0.2 mg.ml^{-1}
Amphotericin B	Antifungal	$25\text{ }\mu\text{g.ml}^{-1}$
Aprotonin	Protease inhibitor	10 KIU.ml^{-1}

After 16 h incubation, the specimens were removed from the chondroitinase ABC treatment solution and rinsed in PBS to remove the enzyme. Specimens that were chosen for histological assessment were placed into 10% (v/v) NBF and processed accordingly (Section 2.5.3). For the specimens chosen for immunohistochemical analysis, the cartilage disk was cut from the bone and processed as described in Section 2.6.3. Cartilage specimens for TEM were removed from the bone and processed as detailed in Section 2.7.2. Specimens used for indentation testing were stored at -20°C for a maximum of 31 days in a sterile bijou containing tissue paper soaked in Ringer's solution before being defrosted overnight at 4°C .

4.4.2 Histological assessment of chondroitinase ABC treated cartilage tissues

Sections were stained using H & E and alcian blue as described in Sections 2.6.1 and 2.6.2, respectively.

4.4.3 Immunohistological assessment of chondroitinase ABC treated cartilage tissues

Immunohistochemical staining for biglycan, collagen VI and cartilage oligomeric matrix protein was carried out as described in Section 2.6.3.

4.4.4 Transmission electron microscopy analysis of chondroitinase ABC treated cartilage tissue

Ultrastructural changes to the cartilage tissue were assessed using cupromeronic blue staining with transmission electron microscopy previously described in Section 2.7.2.

4.4.5 Quantitative biochemical analysis of chondroitinase ABC treated cartilage tissue

Quantitative biochemical assays for glycosaminoglycans (Section 2.8.2) and collagen (Section 2.8.1) were carried out to assess whether loss of either of these components from the tissue had occurred during enzyme treatment.

4.4.6 Indentation testing of chondroitinase ABC treated cartilage tissues to derive cartilage deformation properties

To investigate the changes to the deformation properties of the cartilage after treatment with chondroitinase ABC, an indentation rig was used (Figure 4.2). The rig was manufactured in house, in the School of Mechanical Engineering, University of Leeds. Before indentation testing, cartilage specimens were defrosted overnight at 4°C. Specimens that were used for indentation testing were not kept frozen for more than 28 days after dissection. This was because it was not known if freezing specimens for over one month had an effect on the biomechanical properties of the tissue.

Each osteochondral specimen was fastened into a collet using an allen key. The collet was slotted into the specimen cup which was filled with Ringer's solution. A 3 mm diameter flat bottomed indenter tip was screwed into the tip holder. The specimen cup, which was screwed into the base of the indenter was adjusted vertically via screwing and unscrewing of the cup so that the cartilage surface was approximately 1 mm from the indenter tip. The indenter was allowed to indent the tissue surface continuously for 60 min.

A linear variable differential transformer (LVDT) was attached to the shaft at the top of the indenter to measure displacement of the shaft. A piezoelectric force transducer was fitted

to the rig above the indenter attachment. The data from the LVDT and the force sensor was relayed to a computer via an analogue to digital converter. Labview 9 software was used to automatically record data and to specify test conditions.

Weights were not added to the rig during indentation, as a result a total of 70 g was loaded onto pin specimens through the weight of the rig components. The sampling frequency of the digital measurements was 5 Hertz.

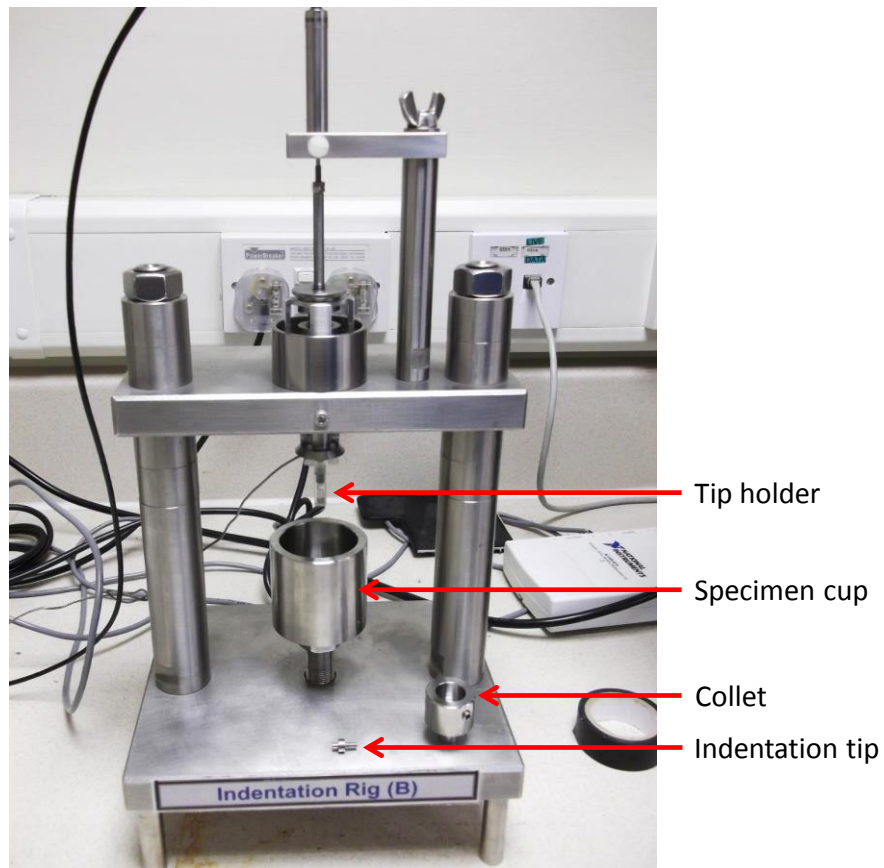


Figure 4.2. The indentation apparatus used to indent untreated control and chondroitinase ABC treated cartilage specimens. Image shows the indenter rig and components of the rig required for indentation testing.

4.5 Results

Histological staining was used to examine the architecture of the tissue (H&E) and the distribution of GAGs (alcian blue) after chondroitinase ABC treatment.

4.5.1 Histological evaluation of chondroitinase ABC treated cartilage specimens

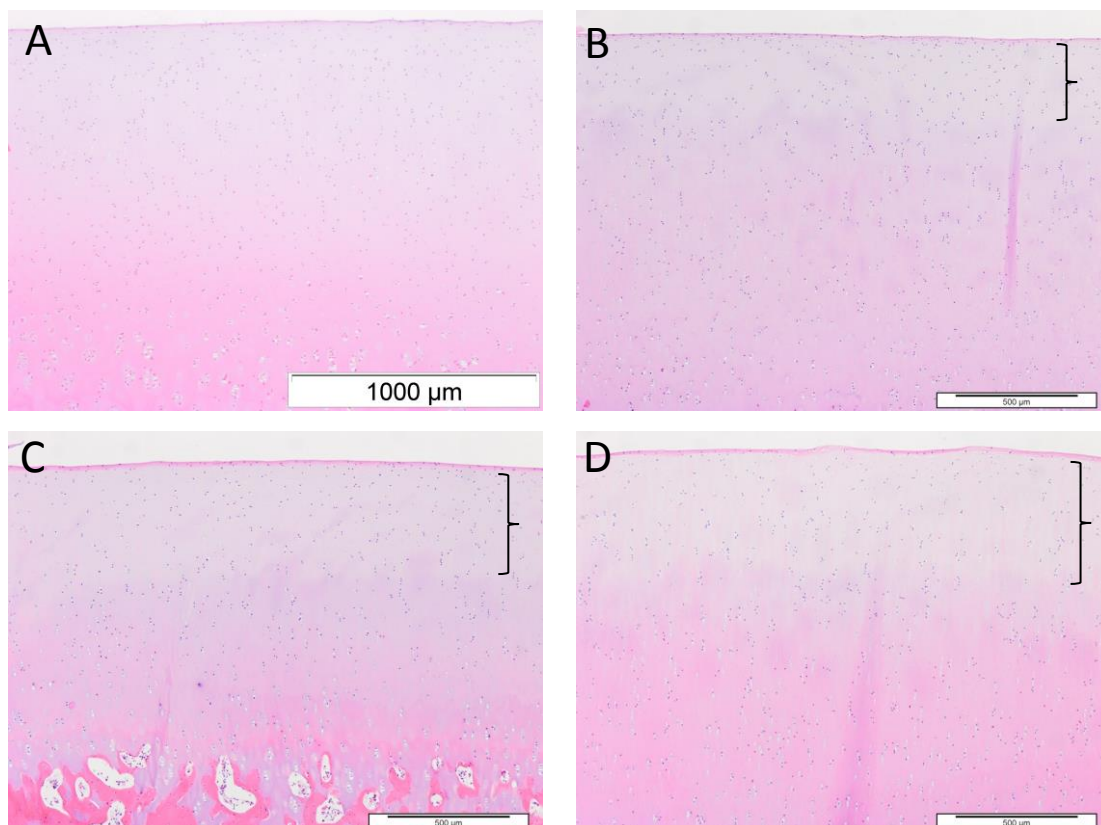


Figure 4.3. Representative images of haematoxylin and eosin stained sections of cartilage pin tissue treated with chondroitinase ABC. A. The untreated control. B,C,D. The chondroitinase ABC treated specimens. The pale band of staining has been highlighted (Braces ; N=6).

The enzymatic treatment of the cartilage specimens with chondroitinase ABC did not have a significant effect on the tissue structure (Figure 4.3). The appearance of the tissue was very similar to the untreated control specimens, however there was a band of pale staining in the superficial to upper middle zone in which eosin staining was lighter due possibly due to the removal of GAGs from the tissue by the chondroitinase ABC (Figure 4.3B, C and D).

4.5.2 Qualitative evaluation of GAGs in chondroitinase ABC treated cartilage

Alcian blue was used to stain for GAGs in the tissue. This stain was of particular interest in this part of the study because the purpose of the chondroitinase ABC treatment was to deplete GAGs in the tissue. Therefore alcian blue staining provided qualitative assessment of the changes to the GAG staining pattern caused by the chondroitinase ABC treatment (Figure 4.4).

Following chondroitinase ABC treatment there was a distinctive pale band in the superficial and upper middle zones of the sections of the specimens where a large amount of GAGs had been lost from the tissue (Figure 4.4B, and D).

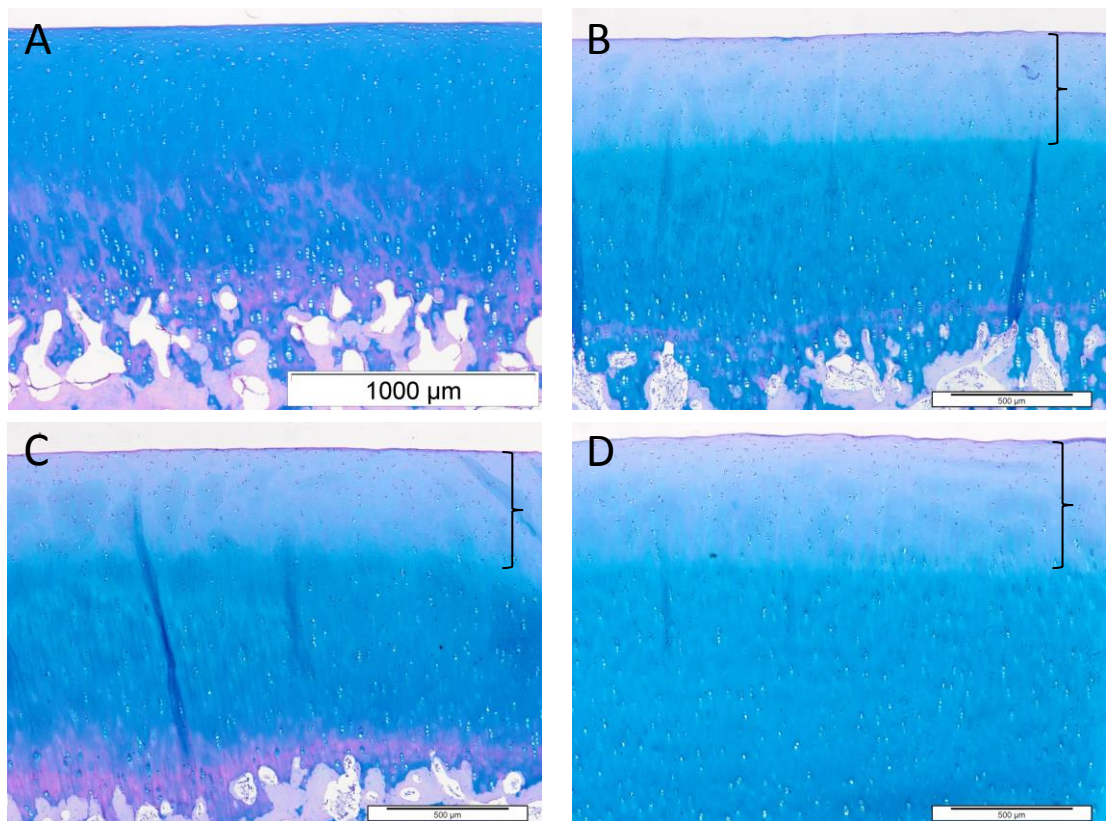


Figure 4.4. Representative images of alcian blue stained sections of cartilage pin specimens treated with chondroitinase ABC. A. The untreated control B,C,D. The chondroitinase ABC treated specimens. The pale band of staining has been highlighted (Braces ; N=6).

Alcian blue staining at the cartilage surface was weak, which led to the appearance of a thin purple band. Staining in the lower middle and deep zones of the treated tissue remained as intense as the untreated control specimens (Figure 4.4A).

4.5.3 Qualitative evaluation of biglycan in chondroitinase ABC treated cartilage specimens

Biglycan staining was used to assess the effects of chondroitinase ABC treatment on this small proteoglycan. A representative image of a section of the untreated control tissue is shown in Figure 4.5A. After the chondroitinase ABC treatment there was a reduction in biglycan staining in the superficial zone of the tissue, despite some artifactual staining, observed in some specimens, such as a strong band of staining in the superficial zone (Figure 4.5B). There was a reduction in haematoxylin staining in the sections in the superficial to upper middle zones of the tissue (Figure 4.5B and C). All specimens also had a reduction in staining in the middle and deep zones of the tissue. However, staining was still visible in the deep zone of the tissue (Figure 4.5D and E).

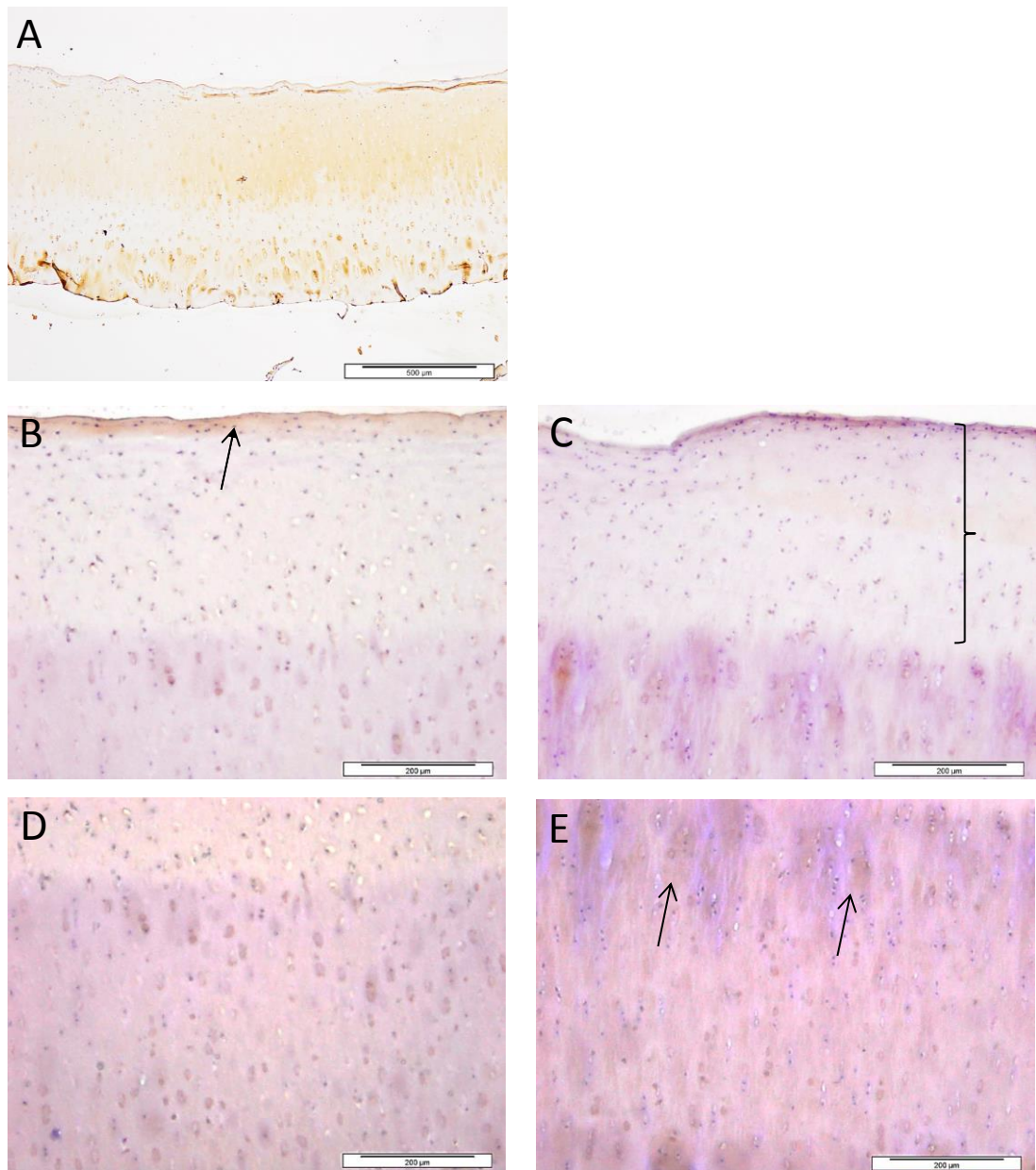


Figure 4.5. Representative images of chondroitinase ABC treated cartilage pin sections labelled with a biglycan antibody (N=6). **A.** Untreated control tissue **B.** The surface and upper middle zone of the treated tissue. The arrow shows artifactual staining. **C.** The surface and upper middle zone of the treated tissue, which showed a reduction in haematoxylin staining (brace). **D.** The middle to deep zones of the tissue. **E.** The middle to deep zones of the treated tissue in which some staining was observed (arrows).

4.5.4 Qualitative evaluation of cartilage oligomeric matrix protein in chondroitinase ABC treated cartilage tissue

Six specimens were prepared for staining with COMP. The COMP staining that was observed in the chondroitinase treated specimens was much paler than in the control tissue, however on closer inspection it was observed that staining was present across the superficial and middle zones of the tissue, as it was in untreated control tissues (Figure 4.6A). In areas of COMP staining, the stain was evenly distributed. Two of the six specimens had COMP staining in the calcified zones, however, the staining was likely to be artifactual (Figure 4.6D and E).

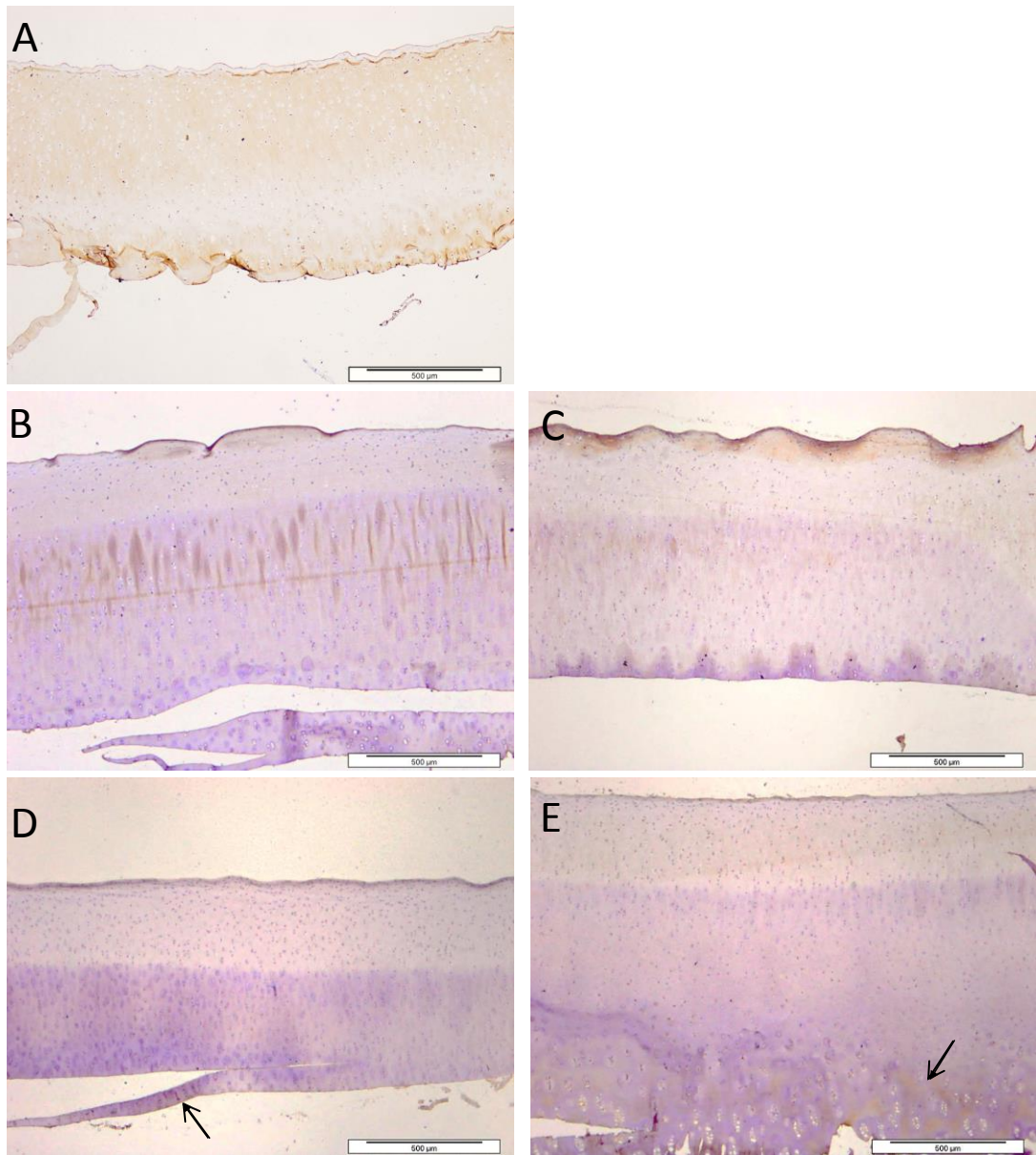


Figure 4.6. Chondroitinase ABC treated cartilage pin sections stained with a cartilage oligomeric matrix protein antibody A. The untreated control tissue. **B-E.** Chondroitinase ABC treated specimens with arrows highlighting artefact staining in the calcified zone of specimens D and E (N=6).

4.5.5 Qualitative evaluation of collagen VI in chondroitinase ABC treated cartilage tissue

Chondroitinase ABC treated specimens stained for collagen VI had the same staining pattern and intensity as the untreated controls (Figure 4.7A). Staining was strong in the pericellular

regions of chondrocytes. Some specimens showed a more intense band of staining in the middle zone of the tissue (Figure 4.7C). There was also visible staining of collagen VI in the interterritorial regions of the tissue (Figure 4.7E).

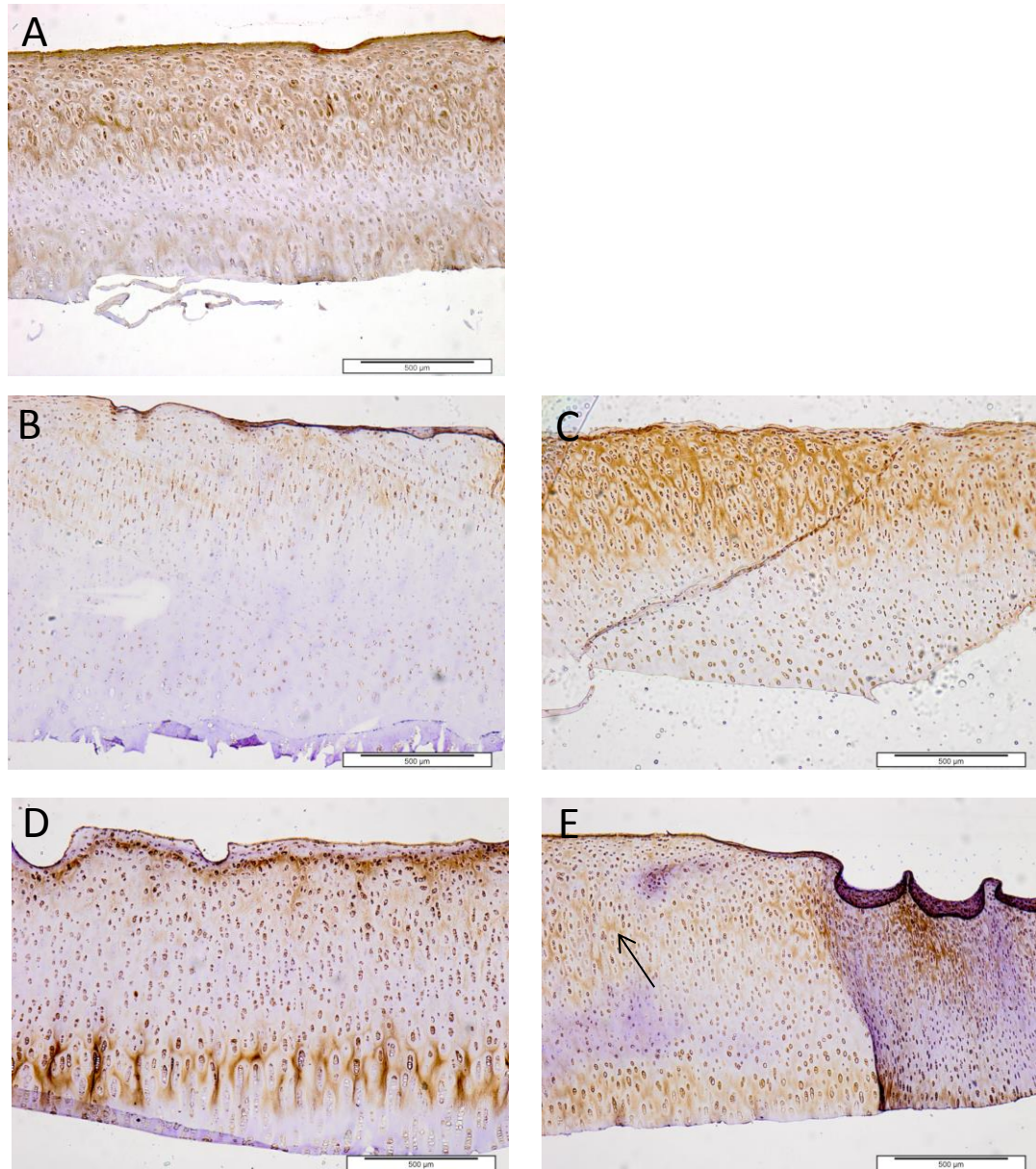


Figure 4.7. Chondroitinase ABC treated cartilage sections labelled with a collagen VI antibody (N=6). A. The untreated control tissue. B-E. The chondroitinase ABC treated specimens (N=6). Interterritorial staining is highlighted (arrow).

4.5.6 Qualitative evaluation of proteoglycans in cartilage tissues stained with cupromeronic blue dye

Transmission electron microscopy in combination with Cupromeronic blue stain was used to investigate the ultrastructural changes to the cartilage tissue with a focus on the GAGs, which were stained using Cupromeronic blue. In addition to this, a positive control was developed through extensive treatment of cartilage tissues with chondroitinase ABC (Section 4.4.1.1).

At the surface of the chondroitinase ABC treated tissue, there was an obvious change in the cartilage appearance (Figure 4.8A). The surface of the tissue was no longer smooth and defined. The structure of the tissue was also less defined and had a cloudy amorphous appearance, collagen fibres were not clearly visible, as they were in the untreated negative control (Figure 4.8B). In the middle zone of one of the three chondroitinase ABC treated tissue specimens, the aggrecan network was disrupted and there was a reduction in aggrecan staining (Figure 4.9A). In two of the specimens the links between the aggrecan were disrupted, however there was visible GAG staining. The structure of the chondroitinase ABC treated tissues was less clearly defined than the untreated negative control tissues. In the deep zone of the treated tissue a dark amorphous cloud of staining was observed in the treated specimen inferring that GAGs were still present (4.10A), as was seen in the deep zone of untreated negative control tissue (4.10B). The aggrecan network was similar to the network seen in the untreated control suggesting that the GAG aggrecan complex was intact. However, the ultrastructure of the tissue in the treated specimens was less well defined.

These results inferred that the chondroitinase ABC enzyme cleaved the chondroitin sulphate in the superficial zone and the chondroitin sulphate subsequently leached out of the tissue. The chondroitinase ABC also reached the middle zone of the tissue and partially depleted the GAGs in this zone however, the GAGs did not completely leach out. From the analysis it appeared that the chondroitinase ABC did not penetrate into the deep zone, as GAGs remained present and the aggrecan network remained intact.

In order to confirm that the cupromeronic blue dye was specifically staining GAGs in the tissue, positive control cartilage tissue created through extensive chondroitinase ABC treatment, was analysed (Section 4.4.1.1; Figure 4.11). The superficial zone was free from GAG staining and appeared lighter than the control images (Figure 4.11A). In the upper middle zone of the tissue, no small proteoglycans or aggrecan were visible. The extensive chondroitinase treatment protocol increased collagen fibre visibility in the sections and allowed another component of the tissue, which was assumed to be hyaluronan to become more easily

observed (Figure 4.11B). The extensive chondroitinase ABC treatment completely removed the aggrecan network from the deep and middle zones of the tissue (Figure 4.11C/D).

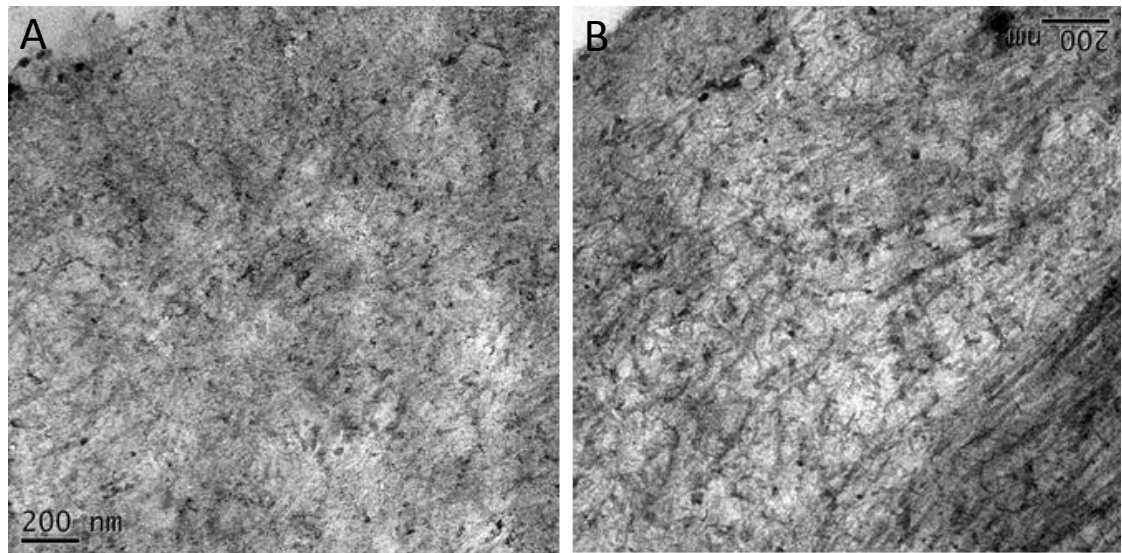


Figure 4.8. Chondroitinase ABC treated and untreated control cartilage specimens stained with Cupromeronic blue dye viewed with TEM. A. The superficial zone of the chondroitinase ABC treated tissue showing the cartilage surface in the top left corner. **B.** The superficial zone of the untreated negative control cartilage tissue showing the cartilage surface in the top left corner.

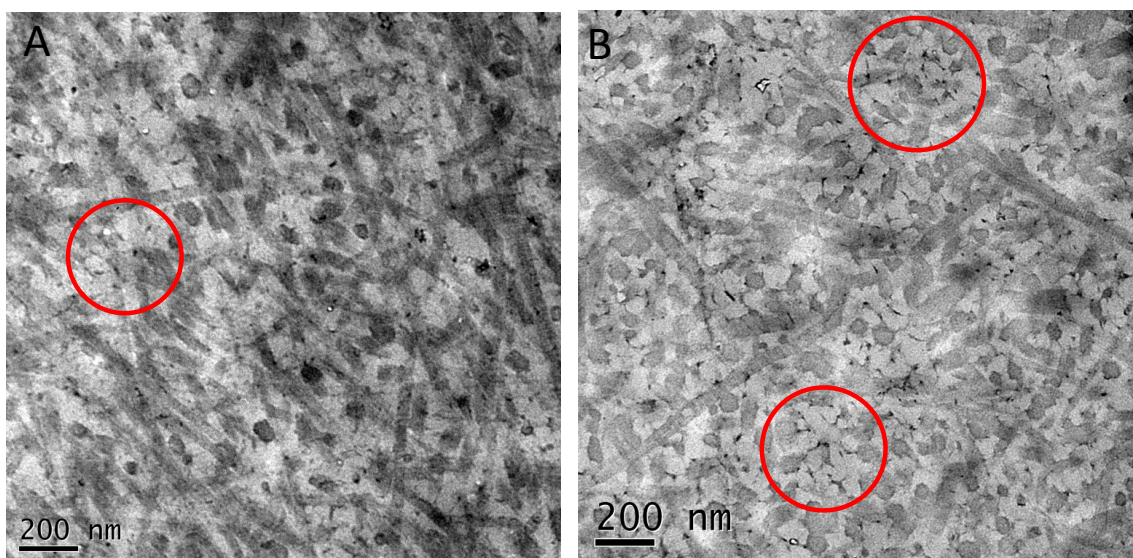


Figure 4.9. Chondroitinase ABC treated and untreated control cartilage specimens stained with Cupromeronic blue dye viewed with TEM. A. The middle zone of the chondroitinase ABC treated tissue where the aggrecan network has been disrupted (circle). **B.** The middle zone of the untreated negative control cartilage tissue with examples of intact areas of the aggrecan network (circles).

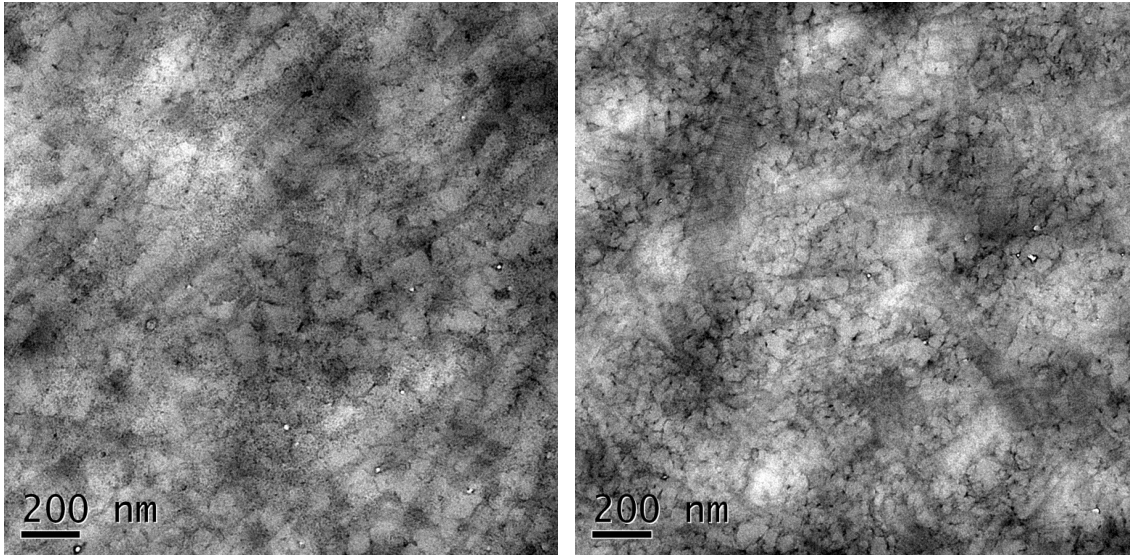


Figure 4.10. Chondroitinase ABC treated and untreated control cartilage specimens stained with Cupromeronic blue dye viewed with TEM. A. The deep zone of the chondroitinase ABC treated tissue. B. The deep zone of the untreated negative control cartilage tissue.

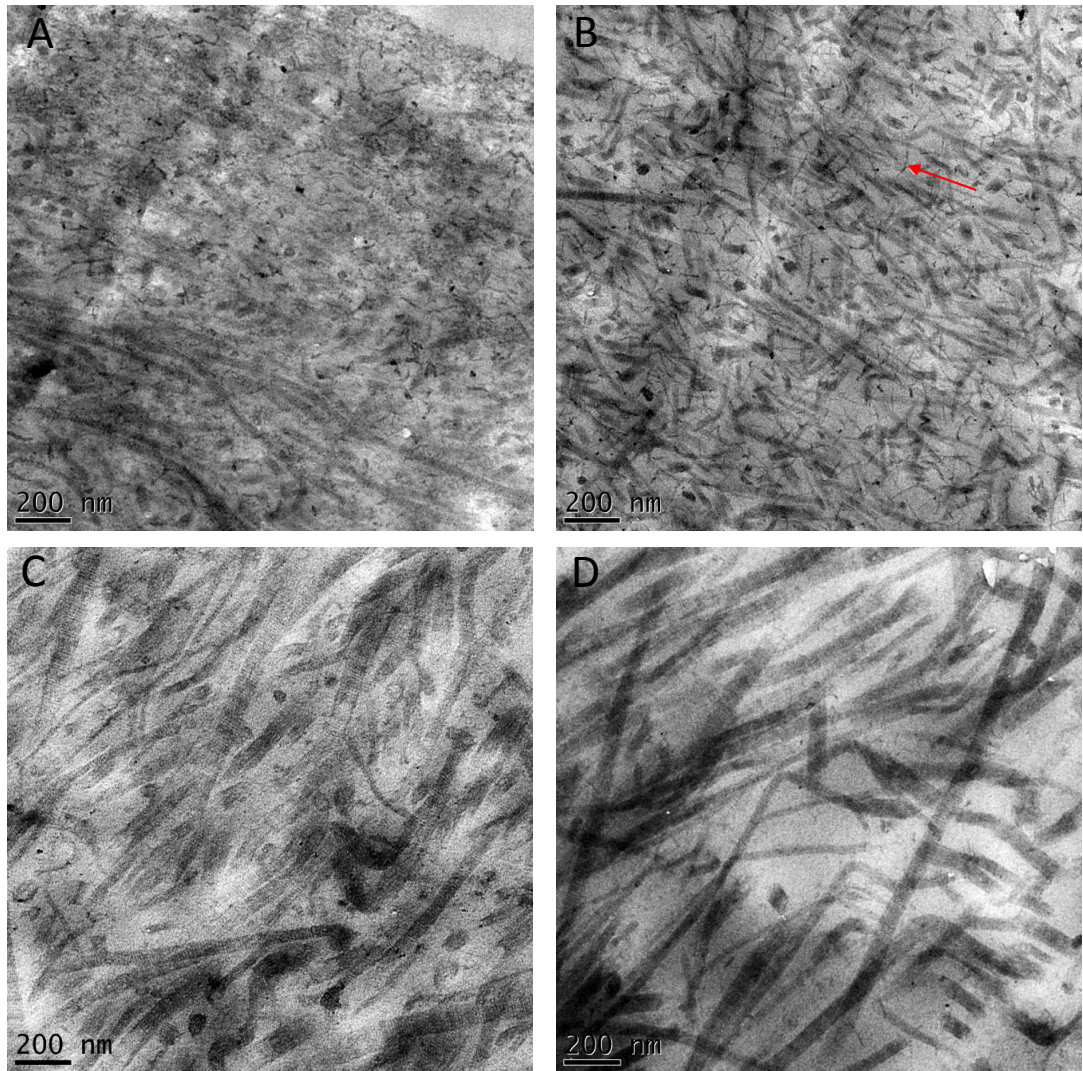


Figure 4.11. TEM images of cartilage tissue treated with chondroitinase ABC and stained with Cupromeronic blue dye to act as negative control images. A. The superficial zone of the tissue; the surface of the tissue is visible in the top right hand side of the image. **B.** The upper middle zone of the tissue. Hyaluronan was observed in the extensively treated specimens (arrow) **C.** The middle zone of the tissue. **D.** The deep zone of the tissue.

4.5.7 Quantitative assessment of the collagen and glycosaminoglycan content of untreated control tissue and chondroitinase ABC treated cartilage tissue

The collagen and glycosaminoglycan (GAG) content of the chondroitinase treated cartilage tissues was quantified using colorimetric assays. These two assays have been previously used

in this study to investigate the changes in collagen and GAG content of mechanically degraded tissues (Section 3.5.13). Six chondroitinase ABC treated specimens were assessed for collagen and GAG content.

4.5.7.1 Collagen content of chondroitinase ABC treated cartilage tissues

The unknown concentrations of collagen in the chondroitinase ABC treated cartilage tissues were determined using standards read from a standard curve. The average collagen content of untreated control cartilage tissue was $618 \mu\text{g}\cdot\text{mg}^{-1}$ of the dry weight of the tissue. The average collagen content of the chondroitinase ABC treated tissue was $706 \mu\text{g}\cdot\text{mg}^{-1}$. There was no significant difference between the collagen contents of the treated tissue and the untreated control tissue ($p > 0.05$; Student's t-test; Figure 4.12). It was concluded that the chondroitinase ABC treatment did not reduce the collagen content of the tissue.

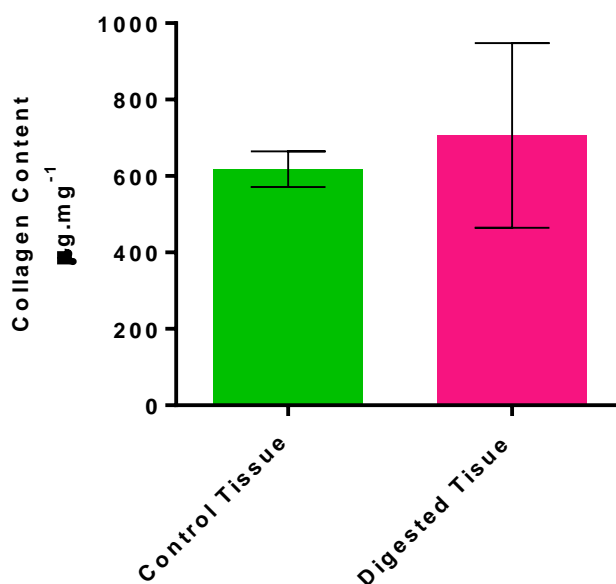


Figure 4.12. The collagen content of untreated control cartilage and cartilage treated using chondroitinase ABC at a concentration of $0.1\text{U}\cdot\text{ml}^{-1}$ for 16 hours. No significant difference was found between the two values. Data is presented as the mean ($n=6$) $\pm 95\%$ confidence limits.

4.5.7.2 Glycosaminoglycan content of chondroitinase ABC treated cartilage tissues

Six specimens were analysed for GAG content. The assay quantified the concentration of GAGs lost during the chondroitinase ABC treatment. Unknown concentrations of GAGs were

determined using standards read from a standard curve. The untreated control tissue had a GAG content of $328 \mu\text{g}\cdot\text{mg}^{-1}$, whereas the chondroitinase ABC treated tissue had a GAG content of $108.4 \mu\text{g}\cdot\text{mg}^{-1}$ (Figure 4.13). There was a highly significant difference between the two values ($P < 0.0001$; Student's t-test). The chondroitinase ABC treatment removed GAGs from the tissue resulting in a significantly lower concentration of GAGs post treatment.

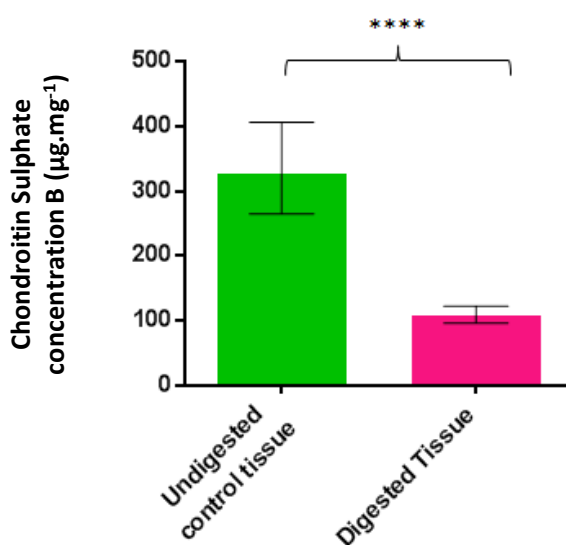


Figure 4.13. The glycosaminoglycan content of untreated control cartilage and cartilage treated using chondroitinase ABC. A significant difference was found between the two values. Data is presented as the mean ($n=6$) $\pm 95\%$ confidence limits. The data was analysed using a Student's t-test; **** equates $P \leq 0.0001$.

4.5.8 Indentation analysis of chondroitinase ABC treated cartilage specimens

Six chondroitinase ABC treated specimens were indented in addition to six untreated controls. The specimens were indented while submerged in Ringer's solution, as previously described in Section 4.4.6.

There was no significant difference between the displacement of the non-treated and treated tissues at the early time points ranging from time point zero up to one minute (Figure 4.14B ; $P > 0.05$; Student's t-test). At the two minute time point and at all of the time points subsequent to this, there was a significant difference between the non-treated control tissue and the chondroitinase ABC treated tissue ($P < 0.05$; Student's t-test; Figure 4.14A). These

results implied that chondroitinase ABC treatment affected the displacement of the cartilage, resulting in an increase in the displacement of the tissue and a reduction in stiffness.

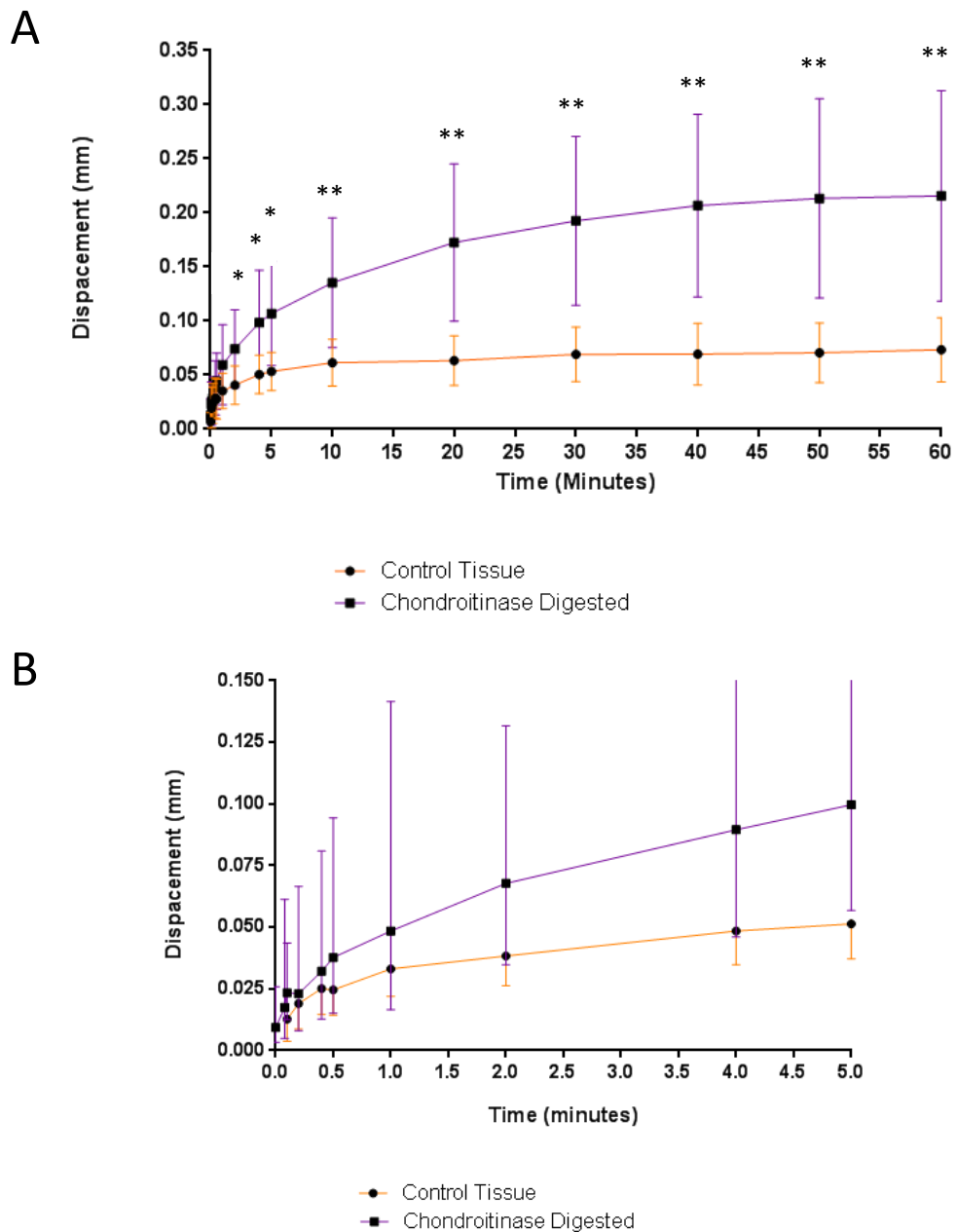


Figure 4.14. The displacement of untreated control tissue and chondroitinase ABC treated cartilage tissue during a 60 minute indentation test. A The purple line marks the deformation of the chondroitinase ABC treated tissue. The orange line marks the deformation of the untreated control tissue. A significant difference was found between the values at several time points. Data is presented as the mean (n=6) \pm 95% confidence limits. The data was analysed using a Student’s t-test; * $P \leq 0.05$, ** $P \leq 0.01$. **B.** The early elastic response region which showed no significant differences between displacement of control and digested tissues.

4.6 Discussion

The purpose of this part of the study was to treat cartilage tissue using chondroitinase ABC to remove GAGs and to investigate the changes caused by GAG removal from the tissues using a variety of techniques; histological, antibody labelling, TEM, quantitative assays and indentation analysis. This was in order to determine the effects that treatment had on the tissue structure, ultrastructure, properties and matrix components, to provide insight into the biotribological performance of the tissues.

The H & E staining of the chondroitinase ABC cartilage specimens showed that there was no significant difference between the appearance of the treated and untreated tissues. However, there was a clear difference in the images stained with alcian blue. The treated tissues showed a pale band in the superficial and upper middle zones of the tissue caused by the removal of GAGs by the chondroitinase ABC. This result correlated with the significant loss of GAGs, detected using the quantitative GAG assay. The GAG assay showed that chondroitinase ABC treatment reduced the GAG content of the tissue from $328.2 \mu\text{g}\cdot\text{mg}^{-1}$ to $108.4 \mu\text{g}\cdot\text{mg}^{-1}$. The results obtained agree with previous studies in which chondroitinase ABC has been used to remove GAGs from cartilage tissues (Katta *et al.*, 2007). Treating the cartilage tissue with chondroitinase ABC did not have an effect on the collagen content of the tissue, which can be explained by the fact that chondroitinase ABC does not interact with collagen.

The major change seen in the immunohistochemical analysis of the treated and untreated control tissues, was in the distribution of biglycan. Staining for biglycan was lighter in the treated tissues. This was most likely due to the fact that the antibody stained for a specific region on the two chondroitin sulphate chains of biglycan, which were removed via chondroitinase ABC treatment (Iozzo, 1999). The results were in line with the hypothesis that chondroitinase ABC would reduce the biglycan staining in the tissues. Collagen VI was of interest because it resides in the pericellular environment of cartilage tissues. Therefore the loss of this component may have given an indication about the changes that occur in the environment immediately adjacent to the chondrocyte. It also gave more information about an alternative collagen to type II collagen. The collagen VI distribution was not affected by the chondroitinase ABC treatment, however COMP staining appeared to be lighter. It is not clear why COMP staining would be lighter as COMP does not contain any GAG chains. The changes in staining may have been due to a technical error or could be down to an increase in the permeability of the cartilage, which may have led to an indirect effect on COMP loss.

In the previous chapter it was shown that mechanical degradation of the tissue altered both the GAG concentration and the aggrecan network in the tissue. It was hypothesised that

chondroitinase ABC would deplete the GAGs from the tissue which would disrupt the aggrecan network and deplete the GAGs attached to the small leucine rich proteoglycans from the tissue. The results of the Cupromeronic blue staining visualised using TEM showed that chondroitinase ABC had removed GAGs from the superficial zone of the cartilage tissue and had led to the partial digestion and removal of GAGs from the middle zone of the tissue. The aggrecan network in the middle zone of the tissue appeared disrupted due to GAG removal. The deep zone was minimally affected, which may have been due to the short amount of time that the tissues were exposed to chondroitinase ABC. The results suggest that the enzyme did not penetrate the deep zone of the tissue. The structure of the chondroitinase ABC treated tissue was less well defined than that of the untreated control. This may be due to a decrease in the stiffness of the tissue, making it more difficult to section. The cartilage tissue that was treated extensively with chondroitinase ABC, which acted as a positive control, did not show evidence of GAG staining. This implied that the cupromeronic blue staining was specific for GAGS.

Indentation analysis can be used to determine the displacement of a material such as cartilage. Displacement analysis was used because GAGs are known to increase the stiffness of cartilage, therefore it was proposed that GAG removal with chondroitinase ABC treatment would reduce the compressive stiffness of the tissue, resulting in increased displacement. A significant difference was seen between the indentation profile of the untreated control and chondroitinase ABC treated cartilage tissue after several minutes of indentation. The untreated control tissue reached a plateau of deformation that remained at a constant level after 10 minutes, whereas the treated tissue continued to deform throughout the test. There was no significant difference between the displacement values measured on the early region of the curve. The early region of the curve represents the elastic stage of the viscoelastic response of cartilage, which is observed when cartilage tissue is under deformation. This result suggests that the elastic properties of the tissue were not affected by chondroitinase ABC digestion. The results of this study agree with the results in a similar study (Katta *et al.*, 2007). It is likely that the increased deformation of the tissue is linked to the loss of GAGs from the surface and middle zones of the tissue. It can be postulated that the loss of GAGs reduced the interstitial fluid pressurisation in the tissue reducing the ability of the tissue to resist compressive forces. If more time was available, it would have been possible to use the indentation data with a finite element model to derive further information about the treated tissues, such as permeability and elastic modulus (Pawaskar *et al.*, 2010).

During cartilage degradation a spectrum of changes take place and the degradation observed in the model presented in this work represents one part of that spectrum. Chondroitinase ABC is suitable for use in creating degradation models because GAG loss is a

major part of cartilage degradation. However, it would improve the model if the model complexity was increased. For example, it could be useful to use additional enzymes such as a collagenase to break down the collagen matrix, which would further replicate cartilage in a degenerated state. Further work could include digestion of tissue components with alternative enzymes alongside articulation in a friction rig to assess the changes to the tribological properties of the tissues after digestion. In future the model could be used to investigate the biotribology of degenerated cartilage via friction rig testing under various conditions such as variable loads or sliding speeds.

4.7 Conclusion

The chondroitinase ABC removed GAGs from the cartilage tissue. This was demonstrated both qualitatively and quantitatively using histology, TEM and biochemical assays. The treated cartilage tissue showed an increase in deformation under load compared to untreated tissue. The chondroitinase ABC treated tissue may be used as a model for investigation of novel cartilage substitution materials or biomaterials. Because the model did not have an altered structure or loss of any of the components besides GAGs it may be useful for investigating methodologies that aim to re-incorporate GAGs back into the matrix.

Chapter 5

Characterisation of cartilage wear particles
generated during mechanical degradation
protocols.

5.1 Introduction

Wear is used to describe the damage, erosion or destruction of a material as a result of friction or motion. As with surfaces in engines for example, the surfaces of joints in the body also experience friction and wear which causes damage to the surface of cartilage tissue. The damage can be in the form of wear particles which are a result of tissue loss from the surface of the tissue. Wear particles have predominantly been studied in relation to joint replacement materials, such as ultra high molecular weight polyethylene (UHMWPE), ceramics, and cobalt chrome (Catelas *et al.*, 2003; Tipper *et al.*, 2006; Brown *et al.*, 2007; Richards *et al.*, 2008; Dressler *et al.*, 2011; Ellison *et al.*, 2012; Behl *et al.*, 2013). It has been recognised that wear of these materials may be the cause of osteolytic loosening of implants, as it has been determined that particles of a certain size range can be phagocytosed by macrophages which causes inflammation and bone resorption around the implant (Beck *et al.*, 2012).

Cartilage wear particles have been observed in the synovial fluid of patients with osteoarthritis (Kuster *et al.*, 1998). More recently, interest in cartilage wear particles has increased which is due in part to advances in technology that have made isolation and analysis of the particles more feasible. One of the earliest studies on cartilage wear particles was conducted using sheep joints. Synovial fluid containing wear particles was extracted from the cavity in the joint, separated using ferrography and analysed using SEM (Stachowiak and Podsiadlo, 1997). The problem with imaging cartilage particles using SEM, is that the techniques used in the preparation of the particles for SEM imaging may have altered the features of the particles such as the size or surface topography. Following on from the initial study, human cartilage wear particles were obtained and analysed using numerical particle shape predictors. The study concluded that the shape of cartilage wear particles from osteoarthritic joints was altered in comparison to wear particles extracted from healthy knees (Podsiadlo *et al.*, 1997; Kuster *et al.*, 1998).

Following these early studies, Peng (2007) used a mechanical rig to generate cartilage wear particles in sheep joints, to investigate the 2D and 3D parameters of wear particles. This study also aimed to correlate particle features with the worn surfaces of the cartilage in the joint which was done successfully. The study stated that in future, this type of analysis may lead to an alternative method for diagnosis of degenerative diseases such as osteoarthritis as the particles may be linked to degradative stages of the disease. However, the study disregarded particles under 5 μm in size, which may have had important implications. In addition to this, particles were treated with chemicals such as gluteraldehyde which may have affected the features of the particles, such as size.

Mendel *et al.* (2010) adapted a technique known as ferrography, to allow them to isolate cartilage wear particles from human synovial fluid by labelling cartilage particles with nanometric paramagnetic beads. One of the issues with the method used in this study was that the synovial fluid was mixed with saline solution and centrifuged. This was performed to make the synovial fluid suitable for use with the ferrographer. However, the diluted synovial fluid was removed after centrifugation which may have resulted in the loss of some wear particles from the solution. In addition to this, the particles were coated in a layer of copper approximately 15–20 nm thick before visualisation, which may have altered the surface topography features of the particles; this could be particularly problematic in future studies in which the surface topography of particles is to be investigated. The use of ferrography is also associated with overlapping of particles during detection by the ferrographer. The bioferrography technique was used in a follow up study that investigated the effects of hyaluronan injections on the characteristics of cartilage wear particles (Hakshur *et al.*, 2011). The study found that while hyaluronan injections appeared to slow the rate of wear, they did not prevent joint degradation overall.

Most recently Tian *et al.* (2012) used feature parameters such as “hill and valley recognition” and field parameters defined in ISO standard ISO/FDIS 25178-2 alongside laser scanning confocal microscopy to study the surface topography of ovine cartilage wear particles for the first time. The particles were isolated using filtration. The results may have the potential to complement current diagnostic procedures for osteoarthritis. The same group also used atomic force microscopy to study the nanomechanical properties of human cartilage wear particles (Wang *et al.*, 2013). An issue with the methodology used in the study, was that particles were imaged in either air or water. The authors postulated that the particles imaged in air may have lost moisture by evaporation and which may have affected their size giving rise to an underestimation of particle size. To overcome this, particles were imaged in water. However, the water used may have caused the cartilage particles to swell artificially, increasing particle size and masking surface features. Both the dry and hydrated environments may have had an effect on the surface topography, size and mechanical properties of the particles that were being assessed.

It is clear therefore that further investigation of cartilage wear particles is important because the investigation of changes in particles during degenerative diseases, which include changes in size distribution and mechanical properties, may help to provide a deeper understanding of degenerative diseases such as osteoarthritis. It is also clear that despite some early studies that showed interesting results, the field of cartilage wear particles is still in its infancy and that the quality of the methodologies used to isolate and characterise wear particles must be improved if physiologically relevant results are to be obtained.

5.1.1 Rationale

The wear particle isolation procedures developed within the IMBE have been successfully optimised for UHMWPE and metal particles. The processes rely on recovery of particles by filtration, involve several steps that are not suitable for cartilage particle analysis, including digestion of particles with enzymes or strong alkali for several days (Tipper *et al.*, 2000; Brown *et al.*, 2007). Therefore a new isolation method suitable for cartilage wear particles was developed. To observe the particles in their natural state, environmental electron scanning microscopy (ESEM) was used to visualise the particles. The use of ESEM allowed the direct visualisation of untreated, hydrated cartilage wear particles for the first time, to the author's knowledge. Mendel *et al.* (2010) previously used ESEM coupled with energy dispersive X-ray spectroscopy to characterise the chemical composition of cartilage wear particles, but did not publish images of the cartilage particles taken using ESEM. Imaging of the cartilage wear particles with ESEM presented several problems, which included difficulty observing cartilage particles at high magnifications. Therefore the procedure for imaging particles developed in the IMBE was adapted for the cartilage particles.

5.2 Aims and Objectives

The aim of this chapter was to isolate and characterise the cartilage wear particles that were generated during mechanical degradation protocols described previously in Chapter 3.

Objectives

- To develop a method for isolation of cartilage wear particles from Ringer's solution lubricants recovered from mechanical degradation tests.
- To use environmental scanning electron microscopy to take images of cartilage wear particles in a natural hydrated state.
- To develop a method for identifying the differences in the quantity and features of cartilage wear particles generated from the mild and moderate mechanical degradation regimes.

5.3 Methods

Cartilage wear particles were generated under mild (3.1 MPa/ 200 N) and moderate (7.5 MPa/ 478 N) mechanical degradation regimes, described previously in Chapter three (Section 3.4.2). During the mechanical degradation protocols, an osteochondral pin was articulated against an osteochondral plate for six hours in Ringer's solution lubricant. At the end of the test the lubricant was collected, the total volume was quantified and then aliquoted into 2 ml eppendorfs. The eppendorfs were stored at -20°C. To create a control for this part of the study, three repeats of the mechanical degradation protocol were conducted without cartilage tissue in the rig. This helped to determine whether particles in the lubricant had come from the tissue or the surrounding environment during the test.

5.3.1 Particle Isolation

Before the particles were isolated from the lubricant, the lubricant was defrosted at room temperature for 10 minutes. A 15 ml vacuum filter (Millipore) was clamped onto a 125 ml filter flask (Millipore; Figure 5.1A). A 10 µm pore sized filter was carefully placed into the vacuum filter using tweezers, so as not to damage the filter (Figure 5.1B). The filter flask was attached to an electric pump (Figure 5.1C).

The following procedure was performed in a class I laminar flow cabinet to minimise airborne contamination of filters. When the lubricant had defrosted the eppendorf was shaken by hand to redistribute the particles. A syringe was used to remove 1 ml of lubricant from the eppendorf. The lubricant was added onto the filter. The syringe was then refilled with Ringer's solution twice which was used to flush any particles from the inside of the syringe. A volume of 15 ml of Ringer's solution was then added into the measuring cylinder clamped to the filtration flask and allowed to run through. The electric pump was set to the lowest setting and attached to the filter flask to speed up the filtration process when necessary. Following this, a further 15 ml of Ringer's solution was added to the measuring cylinder and allowed to run through the filter into the filtration flask. As soon as the lubricant had passed through the filter, the filter was then placed onto Ringer's solution soaked tissue paper in a petri dish for transport to the environmental electron microscope.

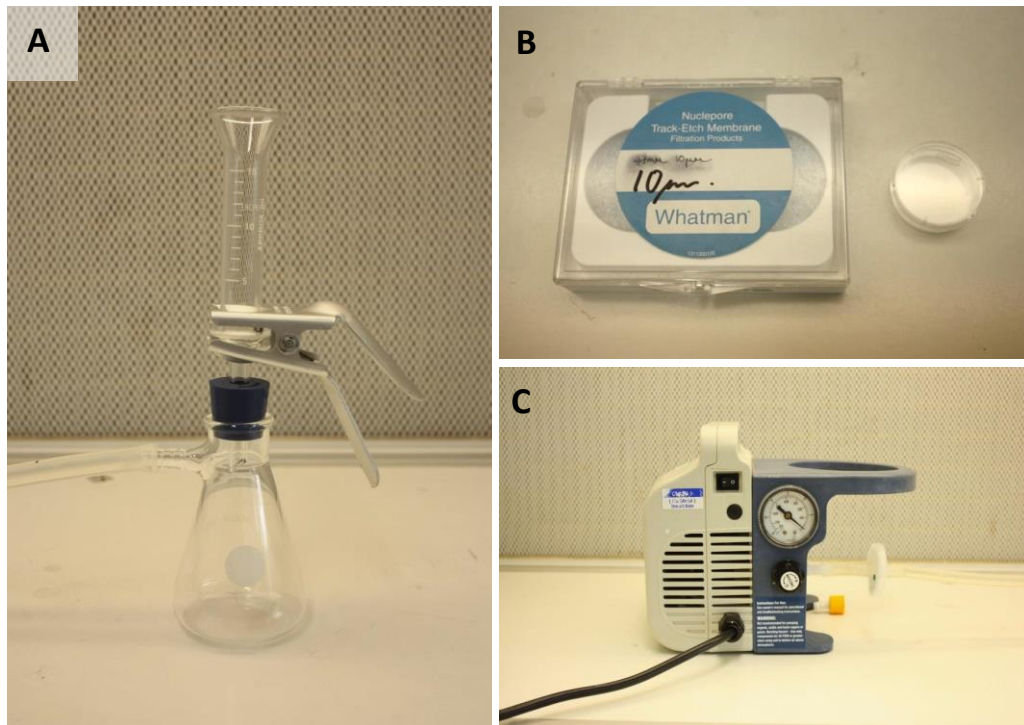


Figure 5.1. Apparatus for cartilage wear particle isolation. **A.** The vacuum filter holder (composed of a measuring cylinder and filter holder with bung), and filter flask components. The measuring cylinder and filter holder were held together with a clamp. **B.** The case containing 45 mm diameter 10 µm pore filters and the petri dish. **C.** The electric pump.

5.3.2. Investigation into the effects of humidity on particle appearance

To determine how a decrease in humidity affected the appearance of the cartilage particles, an area of the filter with several particles was selected. An image of the particles was captured at 96% humidity. From there, the humidity was decreased in 9 to 10 % increments down to 46 % and an image was captured of the particles at each humidity.

5.3.3 Imaging of cartilage wear particles using environmental scanning electron microscopy (ESEM)

A section of each filter was taken just within the perimeter of the area covered in particles using a 6 mm biopsy punch (Figure 5.2). The filter sample was placed onto the Peltier-cooled specimen stage in an FEI Quanta 200F environmental scanning electron microscope as previously described (Section 2.7.1).

Images of the particles on the filter were captured between 8 and 14 kV at 87-90% humidity. To prevent particles being sampled more than once, images were taken at specific

co-ordinates which were selected via the ESEM computer programme (Table 5.1). This resulted in 49 images being captured from each filter. The magnification used to image the particles was 1500x. If a particle was only partially visible at any of the selected co-ordinates, the co-ordinate was slightly altered so that the particle could be included. This was done as long as the change in-co-ordinates did not result in an intrusion of the surrounding co-ordinate points. If a particle was too large to fit the screen it was not included in the particle count.

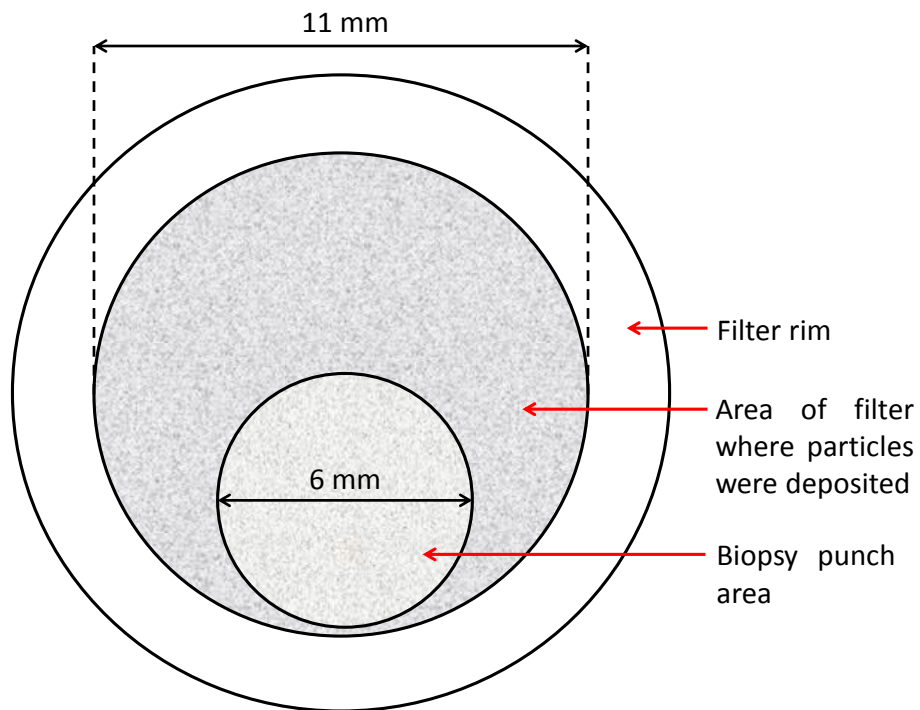


Figure 5.2. A schematic of the filter post filtration, including the area of the filter which was removed using a 6mm diameter biopsy punch for imaging using ESEM.

Image Pro-plus 6 imaging software was used to manually draw around and record the number of particles that were observed at each co-ordinate on the filter. The total percentage area of the filter that was observed was determined (Figure 5.3). This allowed the total number of particles on the filter to be estimated by extrapolating to estimate the number of particles on the unobserved area of the filter. The number of particles was also normalised to account for the variation in the volumes of lubricant that were retrieved from the bath after mechanical testing had been conducted.

Table 5.1. The Co-ordinates used when taking images of particles on the filter.

X-axis co-ordinate	Y-axis co-ordinate
-1.8	-1.8, -1.2, -0.6, 0, 0.6, 1.2, 1.8
-1.2	-1.8, -1.2, -0.6, 0, 0.6, 1.2, 1.8
-0.6	-1.8, -1.2, -0.6, 0, 0.6, 1.2, 1.8
0	-1.8, -1.2, -0.6, 0, 0.6, 1.2, 1.8
0.6	-1.8, -1.2, -0.6, 0, 0.6, 1.2, 1.8
1.2	-1.8, -1.2, -0.6, 0, 0.6, 1.2, 1.8
1.8	-1.8, -1.2, -0.6, 0, 0.6, 1.2, 1.8

Total area of the filter observed during imaging

The average area of the filter that was observed per image taken was **0.034 mm²** and the number of images taken for each filter was **49**.

Therefore the total area observed during imaging of each filter

$$= 1.69 \text{ mm}^2 (49 \times 0.034 \text{ mm}^2)$$

Calculation of the total filter size

The diameter of the total filtration area, not including the filter rim was **11 mm**. The equation for determining the area of a circle is:

$$(\text{radius}^2) \pi$$

Therefore the total filtration area where particles could have been captured on the filter

$$= 95.03 \text{ mm}^2$$

Percentage of the filter observed during particle imaging

The area actually imaged was **1.69 mm²** while the total filter area was **95.03 mm²**.

Therefore the percentage of filter that was imaged

$$= (1.69/95.03) \times 100 = 1.77 \%$$

Figure 5.3. Calculation of the percentage area of the filter observed during imaging.

5.4 Results

A total of five lubricant specimens from each loading condition were filtered and analysed by ESEM imaging.

5.4.1 Study into the effect of humidity on particle appearance

To determine how changes to the humidity in the ESEM chamber affected the appearance of the cartilage particles, a short investigation was completed. As the humidity in the ESEM chamber was reduced, the appearance of the particles was altered (Figure 5.4). The surface of the cartilage particles was featureless at the highest humidity (96%). As the humidity was reduced more features became visible on the surface of the particles and Ringer's salts were seen to be precipitating on the surface of the particles. When comparing the image captured at 96% humidity to the image captured at 46% humidity, it was observed that all of the major features visible on the image at low humidity could also be observed at the highest humidity, with the exception of one feature (Figure 5.4). It was concluded that cartilage particles should be imaged at a humidity of approximately 87 to 90 %. This was to maximise the information that could be obtained from the images, while maintaining a high humidity in the chamber to prevent alterations in particle appearance, caused by drying.

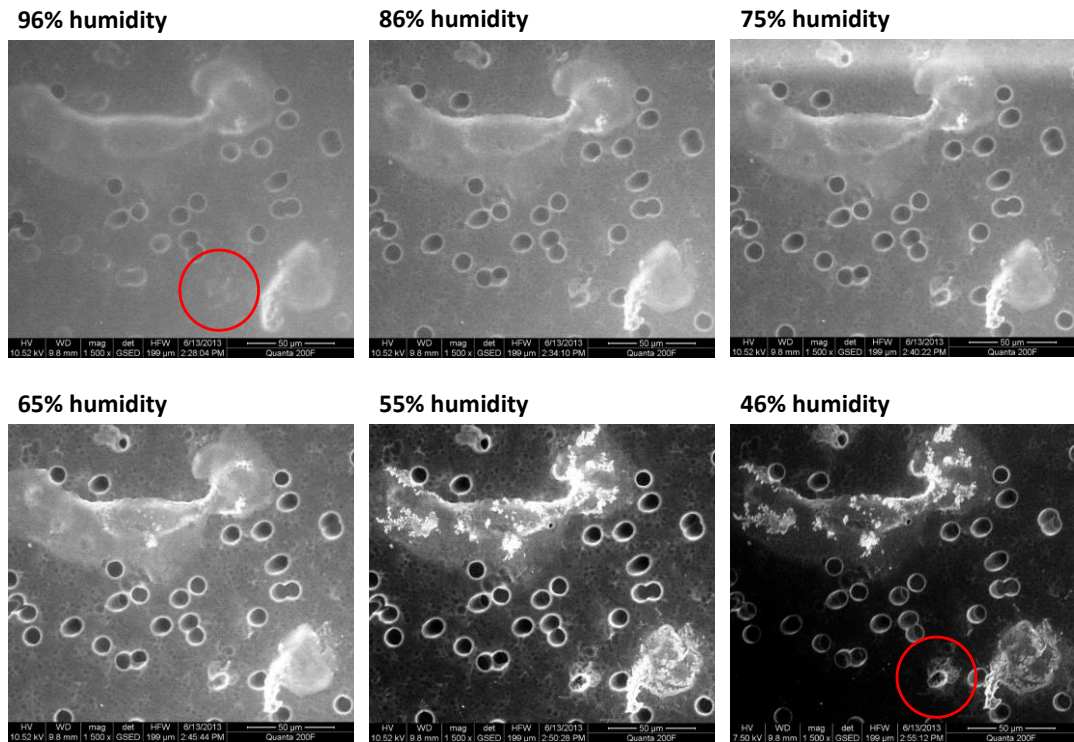


Figure 5.4. The appearances of the cartilage wear particles at a range of humidities. As the humidity dropped the clarity of the images was improved. Precipitated salt crystals from the Ringer’s solution could be seen clearly on the surface of the largest particle in the images taken at 55 and 45 % humidity. There was only one feature that was visible on the lowest humidity image that was not also clearly visible on the highest humidity image (circled).

A greater number of particles were released into the lubricant during the moderate mechanical degradation regime as compared to the mild degradation regime. On average 5581 particles were released into each ml of the lubricant during the mild degradation regime, whereas 8886 were released during the moderate degradation regime. The control, which did not include osteochondral tissue was found to contain 301 particles per ml of lubricant. The number of particles in the mild condition lubricant was significantly higher than the number detected in the control lubricant (Figure 5.5). The number of particles in the moderate lubricant was also significantly higher than the number in the control lubricant (Figure 5.5).

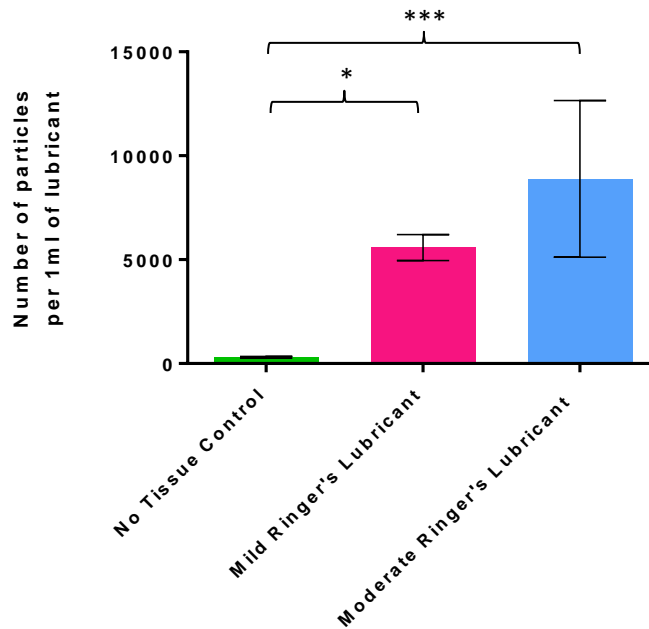


Figure 5.5. The average number of particles found in 1 ml of lubricant recovered from mild and moderate mechanical degradation protocols. The values were normalised to each ml of lubricant. Data is presented as the mean (n=5) \pm 95% confidence limits. The data was analysed using one way analysis of variance followed by determination of significant differences between groups using a Tukey post test; * equates to $P \leq 0.05$; *** equates to $P \leq 0.001$.

5.4.2 Imaging of cartilage wear particles from lubricants using ESEM

Examples of the particles observed in the Ringer's solution lubricants after mild and moderate mechanical degradation protocols are shown in Figures 5.6 and 5.7, respectively. Many of the particles that were observed were clearly defined, however some particles were semi-amorphous (Figure 5.6G-I). The particles generated under both degradation conditions did not appear to have a dominant size or shape. A range of particle shapes were seen in both of the lubricants and it was possible to observe different types of particle in the same image. Four different types of particle, fibrous, spherical, granular and smooth flake are shown in Figure 5.6A. Fibrillar particles were observed in the images shown in Figures 5.6B and 5.6C. In Figure 5.6D a smooth flake like particle could be observed in the image while in Figure 5.6E a particle that appeared to have a cross between a granular and globular appearance was observed. Globular particles with an irregular shape and smooth edges were observed (Figure 5.6F). Finally, the amorphous particles shown in the images in Figures 5.6G-I had a flake like or diffuse globular appearance with smooth edges.

There were several images taken of the moderate condition lubricant that showed irregular globular rough particles (Figures 5.7 A-C). Smooth irregular globular particles were also observed (Figures 5.7D-F). As was observed in the mild condition lubricant, diffuse globular particles were observed in the moderate condition lubricant (Figure 5.7G). Particles that appeared diffuse but did not appear to be globular due to their amorphous nature were observed alongside globular rough particles (Figure 5.7H). Globular smooth particles were also observed in moderate condition lubricants (Figure 5.7I).

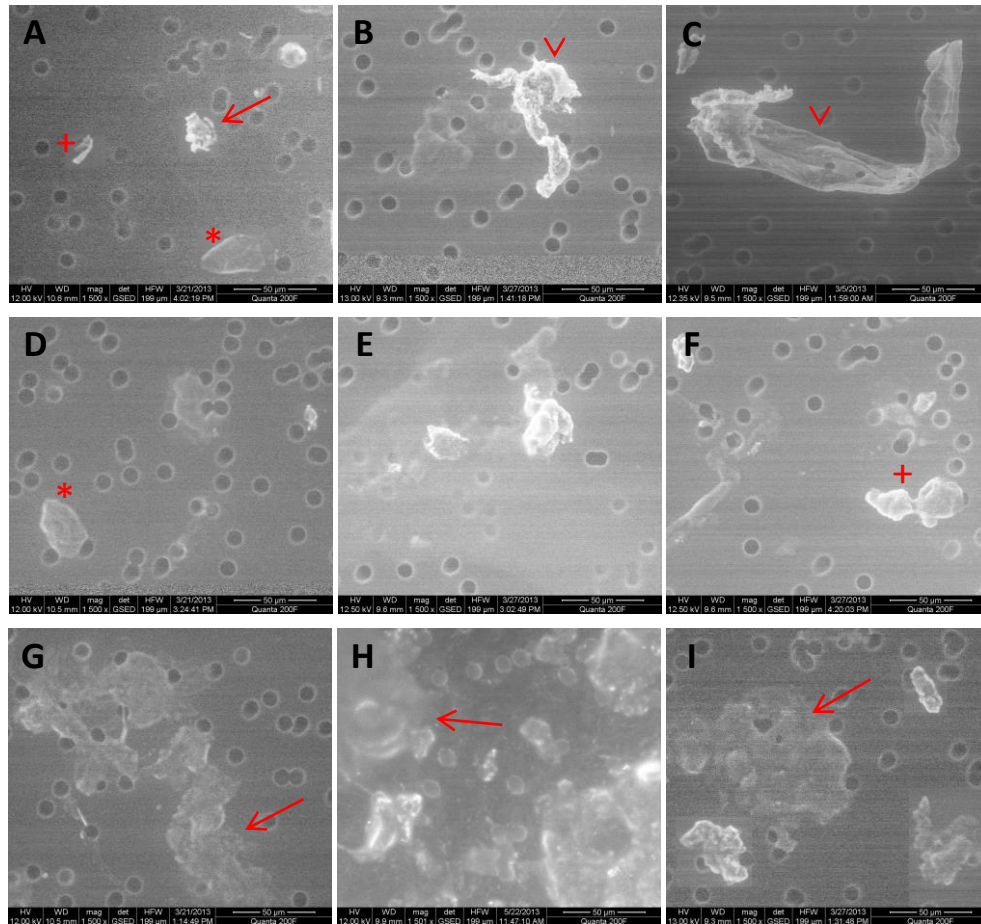


Figure 5.6. A range of images taken of cartilage wear particles in Ringer’s solution lubricant recovered from mild condition mechanical degradation using ESEM. A-F. Typical images of cartilage particles which were clearly defined. Globular particles with smooth edges (asterisks) were observed alongside fibrillar particles (arrow heads), irregular particles with rough edges (arrow) and irregular shaped particles (crosses). **G-I.** Examples of images that included particles with semi-amorphous boundaries (arrows). Scale bar represents 50 µm. Magnification 1500X.

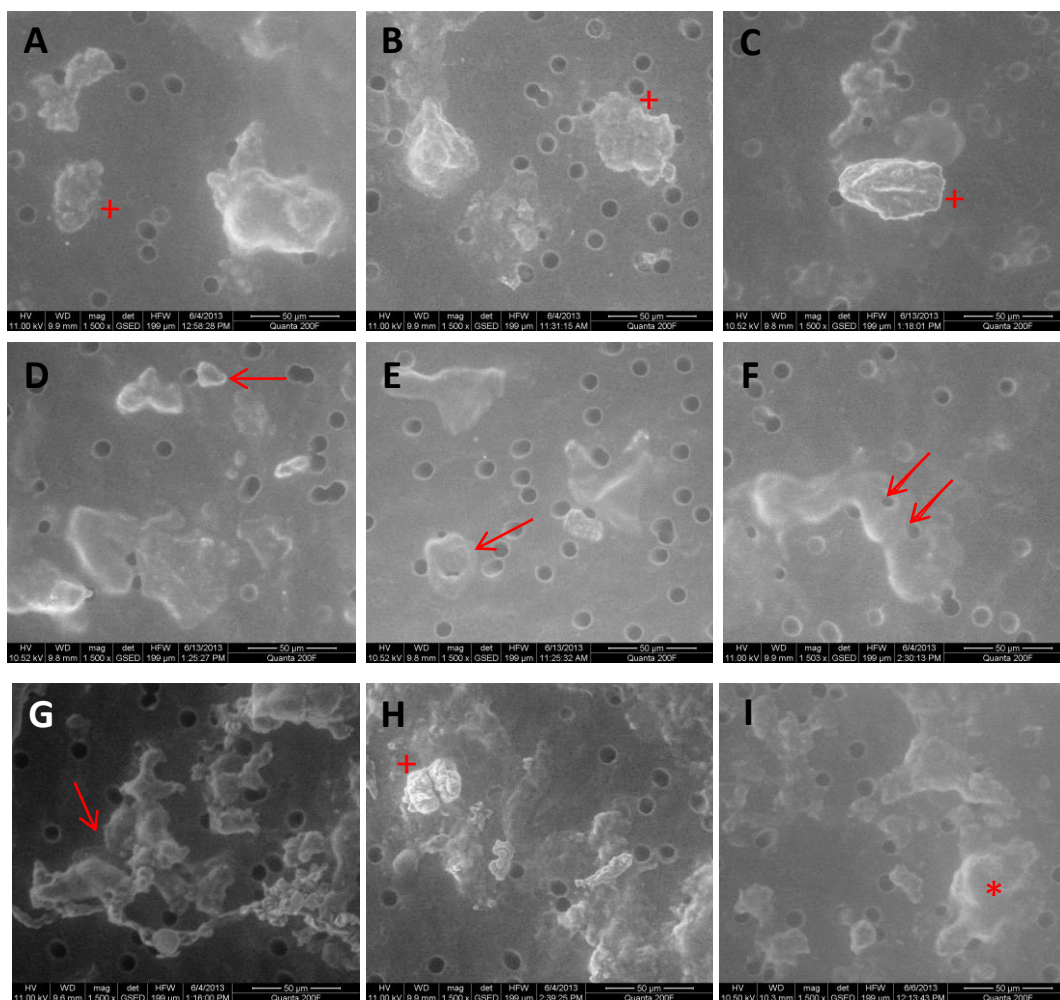


Figure 5.7. A range of images taken of cartilage wear particles in Ringer's solution lubricant recovered from moderate condition mechanical degradation taken using ESEM. A-E. Typical screenshots showing particles recovered from moderate condition lubricant including globular particles with both smooth (arrow) and rough edges (crosses). **F.** An amorphous globular particle is shown with pores of the filter visible through part of the particle (arrows). **G-I.** Images show screenshots that include examples of diffuse (arrow), globular (cross) and amorphous particles (asterisk). Scale bar represents 50 µm. Magnification 1500X.

Particles that were observed in the control solutions are shown in Figure 5.8. The particles observed in the control lubricant did appear to have different characteristics to those found in the lubricants recovered after degradation although some globular particles were observed

(Figure 5.8A.) In addition to globular particles, straight fibrillar, spherical and irregular granular particles were observed (Figures 5.8B-D).

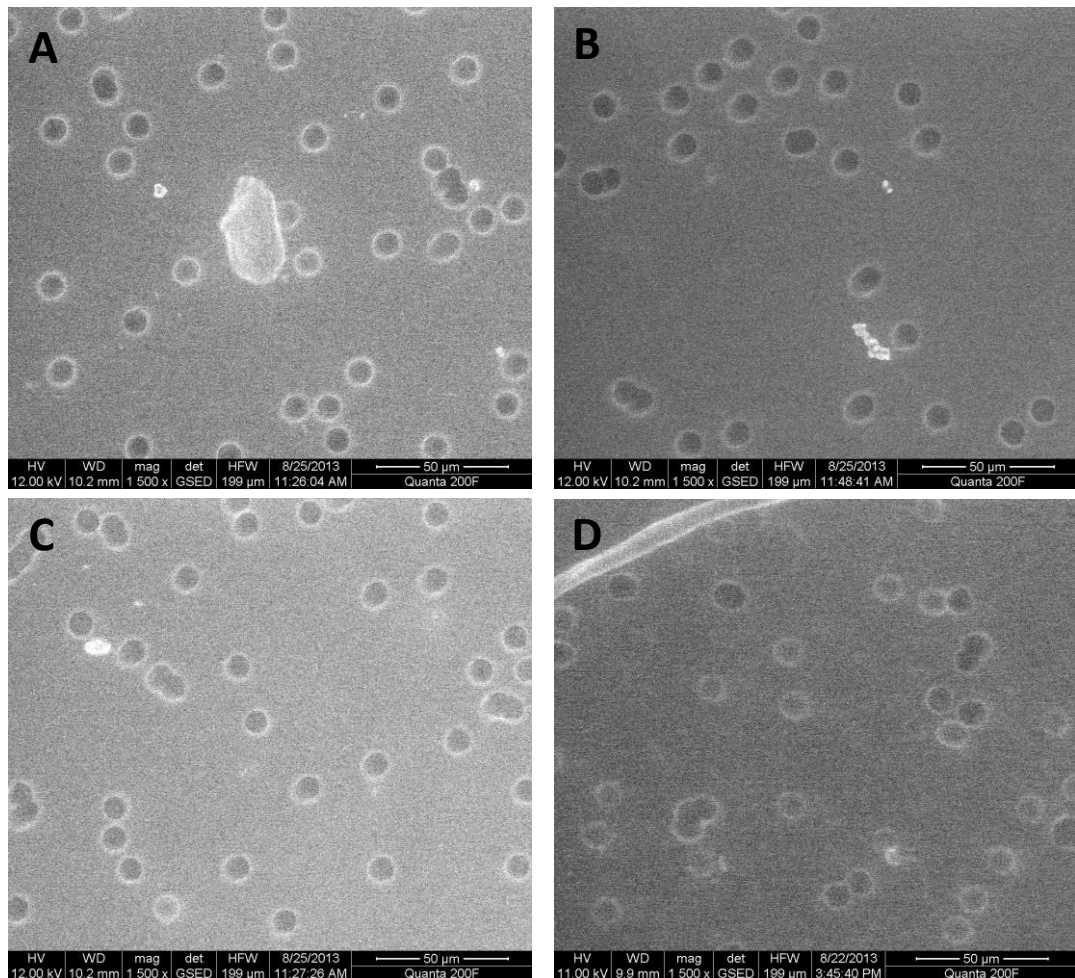


Figure 5.8 Images showing typical contaminants in the control lubricant taken using ESEM. **A.** Occasionally, granular particles that appeared similar to the cartilage particles found in the recovered lubricants were observed in the control solutions. **B.** A sharp granular particle. **C.** A small spherical contaminant particle **D.** A straight fibrous hair like particle was observed. Scale bar represents 50 µm. Magnification 1500X.

5.5 Discussion

Particle isolation and analysis revealed that the moderate degradation condition produced more wear particles than the mild degradation condition and the control. This implied that an increase in the wear of the cartilage under the heavier load had occurred. However, it was not possible to say conclusively that an increased volume of wear was observed under moderate conditions since the size of the particles was not determined due to time constraints and difficulties measuring amorphous particles. It was not possible to say if the particles were removed predominantly from the osteochondral pins or plates as damage was observed on both components after mechanical loading (Chapter 3). However, the protocol developed in this part of the study was suitable for visualising and analysing hydrated cartilage wear particles.

While other studies in the literature have not investigated the effect of variable load on particle numbers generated *in vitro*, Peng (2007) showed that an increase in the length of the loading cycle, resulted in an increased number of wear particles in the lubricant as determined by filtration. The increase in the length of the loading cycle also resulted in an increase in degradation to the cartilage tissue. Mendel *et al.* (2010) found that in synovial fluid samples extracted from human hip, knee and ankle joints, there was a higher number of particles in the synovial fluid from the most severely degraded joints compared to the samples from joints with lower grades of degradation and the control samples.

The major drawback of using the ESEM in a hydrated mode to image cartilage wear particles was that a number of the cartilage wear particles appeared to be semi-amorphous, which made drawing around the boundary of the particles during image analysis difficult. The humidity of the ESEM chamber was reduced from 100% during imaging to increase the resolution of the particles. However, it was observed that dropping the humidity below 84% resulted in the appearance of Ringer's solution salt crystals, which implied that the particles were beginning to dry out at a humidity of 84% and below. This was supported by the study of the effect of humidity which showed that it was not necessary to capture images at low humidity values to complete effective analysis of the particles. The majority of the particles were visible at the highest humidity. In addition to this, the increased number of features and sharper boundaries observed on the particles at a low humidity may not accurately reflect the appearance of the particles in a hydrated state. In future studies a humidity ranging between 86 % and 90 % should allow adequate visualisation of all the particles on the filter while preventing a change in the size and morphology of the particles due to drying.

Observation of a very low number of particles in the control lubricants led to the conclusion that the majority of particles imaged in the lubricants recovered from mechanical degradation studies were cartilage wear particles removed from the surface of the cartilage tissue, rather than environmental contaminants. However, it is clear that low level environmental contaminants were present in the recovered lubricant solutions. Approximately 5.4% of particles in the mild condition lubricant were contaminant, while approximately 3.4% of the particles found in the lubricant recovered from moderate conditions were contaminants. The particles that were observed in the control lubricant often had a different shape to those found in the lubricants recovered from the degradation.

To reduce contamination, a closed cabinet could be used during the mechanical degradation protocol to prevent contamination entering the lubricant. It was also observed that some particles in the controls may have been cartilage particles, which were left on the filtration equipment after washing. Therefore a more thorough washing procedure would be required in future. It would also have been interesting to use an energy dispersive X-ray spectroscopy (EDS) detector to identify the composition of the wear particles. A high carbon and sulphur content would have indicated that the particles were composed of cartilage, whereas detection of calcium would have indicated that particles of bone were also present in the lubricant (Hakshur *et al.*, 2011).

Future work would include examining an increased number of the particle features such as particle length and area. It would have also been interesting to investigate smaller particles using filters with smaller pores sizes, to provide a more complete picture of the size range of the wear particles. Determining the size of the wear particles may have shown a difference in the average particle size under the two different loading conditions. It would also have been interesting to examine the particles that were generated in serum lubricant under moderate conditions. However, alterations to the protocol would have been required to effectively remove the serum from the lubricant to enable visualisation of the particles.

5.6 Conclusion

An increase in loading led to an increase in the number of cartilage wear particles released into the lubricant during mechanical degradation. The protocol that was devised, was suitable for visualising and analysing cartilage wear particles in a hydrated state.

Chapter 6

General Discussion

6.1 Discussion

Due to a lack of suitable methods for the tribological assessment of cartilage substitution materials, there is a requirement for the development of systems that can be used to determine the tribological properties of these novel therapeutics. The aims of this project were to develop methodologies for the production of models of cartilage degeneration. These models of cartilage degeneration can be used to assess the tribological properties of novel cartilage substitution materials in an environment that mimics the biotribological conditions of degraded cartilage. To facilitate this, mechanical and biological cartilage degradation methodologies were developed which represented the two axis of cartilage degradation seen *in vivo*.

The mechanical degradation models aimed to represent the tribological condition of degraded cartilage tissues observed *in vivo*. The models were found to accurately replicate several features of degraded tissues seen in stages of cartilage degradation that are observed in osteoarthritic tissues, such as roughening of the cartilage surface and disruption of the collagen fibril network. The biological model was developed through the use of chondroitinase ABC, which removed large numbers of GAGs from the tissue. This accurately represented the large GAG loss seen in degraded cartilage tissues *in vivo*. However, the chondroitinase ABC enzyme had a substantial effect on the GAG content of the cartilage tissues. The use of more subtle degradative enzymes, such as cathepsins, in the future would increase the sophistication of the model. The wear of the cartilage degradation models was assessed via observation of cartilage wear particles taken from the lubricants used in the mechanical degradation protocols. The protocol that was developed for isolating and imaging the particles was successful in allowing visualisation and quantitation of cartilage wear in the lubricant.

Degradation models for tribological assessment of novel cartilage substitution materials solve a variety of problems associated with novel treatment strategies that are being developed for degraded cartilage tissues. There are a range of problems with early stage pharmacological treatments and end stage treatments for degenerative joint diseases such as osteoarthritis. For example, pharmacological treatments do not prevent cartilage degeneration and joint replacements are not suitable for young patients as they can fail due to the adverse effects of wear particles (Ingham and Fisher, 2000). Therefore, there is a gap to be bridged between early and end-stage treatment that involves novel cartilage substitution and regenerative therapies. Cartilage substitution materials can range from tissue engineered constructs to biomaterials (Johnstone *et al.*, 2013), which can include polyurethanes (Santerre *et al.*, 2005) and hydrogels (Cheung *et al.*, 2007). Many of these materials do not closely mimic

the cartilage ultrastructure, or consist of a homogeneous structure. One of the major barriers to successful development and application of cartilage substitution and regenerative treatments is the limitations of methods for assessment of the functional biotribology of novel materials (Butler *et al.*, 2000). Often studies focus heavily on only the physical, biological and biochemical properties (Guilak *et al.*, 2001).

Therefore it is clear that there is a need for the development of models that replicate degenerated cartilage biotribology which can be used to investigate cartilage biotribology and its interaction with novel substitution materials, which includes detailed investigations into the characteristics of degraded tissues. This will result in improved *in vitro* pre-clinical test methods, for example a whole natural joint simulator for thorough assessment of novel substitution materials. A detailed understanding of the cartilage ECM and biotribology after degradation will assist in understanding how the tissue responds to different conditions which can also help to tailor the successful development of suitable novel materials. Improvements in *in vitro* testing will lead to improved assessment of materials long term, this will accelerate the translation of therapies to the patient. Essentially: further understanding of cartilage biotribology will result in a move towards earlier functional interventions and approaches to preserving tissues using regenerative solutions.

A major objective of this study was to develop mechanical degradation methodologies for cartilage tissue. The purpose of the degradation models was to produce cartilage tissue that replicated the biotribological condition of cartilage at stages along the spectrum of cartilage degeneration. These models of degradation could be used to investigate cartilage biotribology or to investigate how degraded tissues respond to novel substitution materials. The development of the models also provided a set of parameters that can be used to produce cartilage degradation in future whole joint studies. This study built on previous *in vitro* studies that have been used to investigate cartilage biotribology under various conditions (Pickard *et al.*, 1998; Pickard *et al.*, 2000; Katta *et al.*, 2007; Lizhang *et al.*, 2011).

A simple configuration pin on plate rig was used to produce the cartilage on cartilage degradation models. The rig was chosen because its simplicity would facilitate the investigation of the biotribology of the degradation models and cartilage specimens in future studies with potential substitution materials. In addition, as this was a preliminary study, the simplicity of the rig was important to avoid over complication at the first stage. Despite its simplicity, the use of the rig produced a range of cartilage degradation states, and the conditions reproduced some features of the cartilage degradation process observed in degraded human cartilage tissues *in vivo* at a greatly increased rate. The study attempted to follow conditions found *in-vivo* in humans more closely than other studies through steps that

included cartilage on cartilage articulation, which produced degradation that could be corroborated with several published grading systems (International Cartilage Research Society grading system and Pritzker *et al.*, 2006) for osteoarthritis at both a macroscopic and ultrastructural level. Many previous *in vitro* degradation studies have used conditions that do not represent those observed *in vivo* such as abnormal loading conditions and non-physiological wear of cartilage tissues with sand paper (Tanaka *et al.*, 2005; Wilson *et al.*, 2006). There are also several studies that have attempted to assess the tribological properties of cartilage substitution materials. However, many of these studies articulate potential cartilage substitution materials against metal and glass which does not accurately represent the tribological conditions found *in vivo* (Freeman *et al.*, 2000 ; Covert, *et al.*, 2003 ; Pan *et al.*, 2007 ; Blum *et al.*, 2013).

The major findings of this part of the study were that loading had a significant effect on the rate of degradation of cartilage tissue. It was observed that the increase in load applied under the moderate condition (478N) significantly increased the damage to the osteochondral specimens compared with the mild condition (200N). Mechanical loading did not appear to have a significant effect on the total collagen (w/w) and COMP content of cartilage. However, it did alter the aggrecan network and led to a reduction in the GAG content (w/w) of the tissue. An increase in load during mechanical tests also significantly increased the surface roughness of cartilage specimens. Static loading did not result in a permanent decrease in the cartilage height. GAGs were lost from the tissue during mechanical degradation however the levels of collagen in the tissue remained at a similar level as a percentage of tissue weight. It was also shown that GAGs and collagen were present in the lubricant recovered after mechanical tests. This indicated that collagen was not leaching from the tissues as a reduction in the percentage of collagen per unit of tissue weight would have been observed. Rather the collagen detected in the lubricant must have been a result of cartilage wear particles.

The major limitation of the mechanical study was the diameter of the osteochondral pins, which were relatively small (9 mm). This resulted in an increased influence of edge effects on the tissue specimens. However, the small size of the specimens did facilitate the degradation process. To improve the study, osteochondral pins with a larger diameter could have been used to reduce the influence of edge effects on specimens. The results obtained with serum lubricant also highlighted a problem with the test regime due to the variability in the results that were obtained. In some cases the serum lubricant appeared to protect the cartilage from degradation, however, other specimens appeared to have degradation that was similar to the degradation observed on pins that had been subject to moderate loading degradation in Ringer's solution. This may have been due to the geometry of the specimens, as certain specimen pairs may have had increased congruity which in combination with the serum

lubricant may have protected specimens from damage. Some specimens may have been extracted from the condyles at a slight angle which could have resulted in uneven loading of the pin edge on the osteochondral plate resulting in abrasive wear. To try and investigate this further, it would be useful for a greater number of replicates to be completed in addition to investigating the congruency of specimens which may be possible using surface profilometry techniques.

Aggrecan is a large proteoglycan that forms aggregates in the cartilage tissue. The structure of aggrecan was effectively observed using TEM alongside cupromeronic blue staining. This part of the study represented one of the first examples of comprehensive characterisation of mechanically degraded cartilage specimens. Cupromeronic blue has been used previously to investigate the ultrastructure of articular cartilage (Orford and Gardner, 1985). However, it has not been used to investigate the alterations observed in the tissue caused by *in vitro* mechanical degradation regimes. In one study by Orford *et al.*, (1985) it was observed that in canine tissues that had been degraded *in vivo* via a division of the anterior cruciate ligament, the collagen network became disrupted and GAGs were lost from the superficial zone of the tissue, which correlated with findings of this study.

The results of the immunohistochemical staining were also novel as staining for biglycan, COMP and collagen VI had not previously been studied in relation to mechanical degradation models, to the author's knowledge. It was observed that COMP and collagen VI staining were not greatly altered by either the mild or moderate mechanical degradation regime, which may indicate that these components are lost through biological degradation of cartilage tissues. However, biglycan was reduced in tissues that had undergone loading under the moderate degradation protocol. The study also considered both biological and mechanical evaluation methodologies during tissue characterisation which facilitated a more complete understanding of how the tissues were affected during degradation.

The use of Ringer's solution lubricant under low level loads did not produce a significant level of damage to the cartilage tissue during articulation. This may have partly been due to the salt concentration of the Ringer's solution. The salt concentration may have allowed the cartilage to continue maintenance of fluid phase loading, which forms part of the biphasic loading capabilities of cartilage tissue. This therefore, may have protected the tissue from damage. It is also likely that boundary lubrication may have occurred via a layer of phospholipids and glycoproteins on the surface of the tissue. Under the moderate loading condition it appears that Ringer's solution did not have a protective effect on the cartilage tissue. However, in serum lubricant half of the specimens appeared to be protected from severe wear on the surface of the tissues. The serum may have provided additional boundary lubrication to protect the tissue surface preventing it from becoming rough (Forsey *et al.*,

2006; Bryan *et al.*, 2010). In future tests, it may be useful to add hyaluronan to the serum lubricant to make the lubricant more physiologically relevant, as hyaluronan regulates the viscosity of the synovial fluid (Laurent *et al.*, 1996).

The methodology that was used to treat cartilage specimens with chondroitinase ABC was developed at Leeds and has previously been utilised in a study that determined the effects of GAG loss on cartilage tribology (Katta *et al.*, 2007). Therefore the novel aspect of this part of the study was in the extensive characterisation of the tissue that was carried out after enzyme treatment of the cartilage. The large range of techniques that was used to characterise the tissues provided a way of determining the most suitable methodologies for assessing changes to the cartilage tissues caused by enzyme digestion. Chondroitinase ABC was used to digest GAGs from the cartilage tissue as they are a major component of, and are integral to the correct functioning of biphasic lubrication in the tissue. As degraded cartilage tissues are found to have a reduced GAG content it was appropriate to use chondroitinase ABC. In future studies GAG depleted tissue will be useful for mimicking degraded cartilage tissues when assessing the tribology and characteristics of cartilage substitution materials.

The major findings in this part of the study were that biglycan staining was reduced in the treated tissue. There appeared to be a slight reduction in COMP staining and collagen VI was not affected significantly by chondroitinase ABC treatment. The aggrecan network in the tissue was disrupted and in some cases was no longer visible and the structure of the cartilage observed in the tissue sections became more amorphous after chondroitinase ABC treatment. This correlated with the reduction in GAG staining quantified in the biochemical assay and the reduction in GAG staining seen in the alcian blue images. In addition to this, the deformation of the cartilage was increased during indentation when the tissue had been treated with chondroitinase ABC. The increase in deformation may be because the compressive stiffness of cartilage is regulated by the GAGs in the extracellular matrix (Mow and Huiskes, 2005). The results for the indentation study and the quantitative GAG analysis correlated with the previous study by Katta *et al.*, (2007). Cupromeronic blue staining has been used previously to investigate the ultrastructure of articular cartilage however it has not been used to investigate the alterations observed in the tissue caused by enzymatic degradation (Orford and Gardner, 1985; Scott and Stockwell, 2006).

Limitations of this part of the study were that the process of chondroitinase digestion was started at the surface and progressed linearly through the tissue to the middle zone whereas *in vivo* GAG loss has been shown to begin around chondrocytes in the pericellular environment (Loeser *et al.*, 2003). Additionally chondroitinase ABC is not an enzyme that is produced by chondrocytes *in vivo*. Enzymes that promote the catabolic destruction of cartilage tissue in a physiologically relevant way such as collagenases (Salminen *et al.*, 2002) are

commercially available; however, they are prohibitively expensive for use on a large scale. Use of physiologically relevant enzymes may have made the study more representative of the scenario occurring *in vivo* during cartilage degradation. For example, the use of a collagenase (MMP-13) would have initiated cleavage of collagen in the tissue which alongside use of the chondroitinase ABC could have represented biologically based cartilage degradation in a more physiologically relevant way (Ehrlich *et al.*, 1978). Despite the chondroitinase ABC treatment removing a large volume of GAGs from the cartilage surface, the model remains useful as it reflects the large reduction in GAGs that is observed in degraded cartilage tissues.

The methodology that was used for isolating cartilage wear particles was based on a method previously developed at Leeds for polymeric particles. However, due to the low volume of lubricant filtered compared with lubricants containing polymeric particles, particle isolation equipment for smaller volumes was used. The method worked well for isolating the cartilage wear particles in the Ringer's solution lubricant with some adaptations to the methodology. The number of particles in each lubricant was successfully determined revealing that a higher number of particles were released into the lubricant under moderate loading conditions compared with mild loading conditions. The increased wear observed under the higher loading condition correlated with an increase in the surface roughness of the cartilage tissue which was also confirmed quantitatively using histology.

The wear particles observed in the lubricant in this study may have been a result of fatigue wear in the cartilage tissue. The collagen and aggrecan networks in the tissue were disrupted which would weaken the tissue structure resulting in particles of tissue being removed from the cartilage surface. The production of the wear particles through fatigue wear may have also led to the occurrence of adhesive wear, in the form of three body wear, which may have aggravated wear of the cartilage surface (Nordin & Frankel, 2001).

The shape of the cartilage wear particles was assessed quantitatively using the American Society for Testing and Materials (ASTM; ASTM *Standards*, 2005) guide to standard practice for characterisation of particles. Many of the particles did fit with the particle shapes observed and described in the standard. However, it was clear that not all of the cartilage wear particles could be described accurately using the standards. This was especially true for the amorphous particles that were observed which did not fit any of the particle descriptions fully. This may be because the standard has not been developed for assessment of wear particles from biological tissues. In future, it would be useful to develop additional guidelines that can be used alongside the ASTM guide to effectively characterise cartilage wear. For example, a semi-quantitative way of recording amorphous particles could be developed through indication of the presence or absence of amorphous particles on the image.

A major limitation that was encountered while imaging the cartilage wear particles was the time taken to capture images using the ESEM. This drastically reduced the number of images that could be taken during each session. One way to overcome this would be to filter a larger volume of lubricant onto the filter so that a greater concentration of particles could be observed in the same amount of time. However, this may lead to issues with particles clumping together, which was not an issue with the methodology used in the current study.

This study is the first in which cartilage wear particles have been studied in an unaltered state using ESEM. Mendel *et al.* (2010) used ESEM to image particles coupled with SEM imaging, but it was not clear to what extent the ESEM imaging was used in the final results and no images taken using ESEM were published. Previous studies have used SEM imaging; which involves coating the particles, laser scanning confocal microscopy or atomic force microscopy to study cartilage wear particles (Podisadlo *et al.*, 1997; Kuster *et al.*, 1998; Peng, 2007; Hakshur *et al.*, 2011; Wang *et al.*, 2013). Laser scanning confocal microscopy requires the particles to be dyed and is also not suitable for imaging particles of a small size due to issues with resolution ($\leq 2 \mu\text{m}$). Some studies have used ferrography to isolate particles rather than filtering. It is difficult to say which methodology is superior without a direct comparison between the methods being available. In addition, drawing around particles by hand on images using image analysis software may lead to errors and the methodology is also highly time consuming. However, it is also possible during ferrographical analysis for particles to overlap each other, which lead to errors in the particle sizes and the number of particles that are recorded during SEM.

In future the mechanical degradation protocol could be used to generate cartilage wear particles for further studies. It would be interesting to compare the cartilage particles generated by the mechanical degradation protocol to particles recovered from human synovial fluid samples that have been generated *in vivo*. This could give an indication of the comparability of the wear produced by an *in vitro* model and the wear seen *in vivo*.

6.1.1 Future work

Future work could include testing of novel cartilage substitution materials such as tissue engineered constructs with the mechanical and enzyme degradation models. For example, the degraded cartilage tissue models could be articulated with substitution materials in the pin-on-plate rig, followed by analysis and characterisation of the tissue (Figure 6.1). Eventually, the simple configuration pin-on-plate model can be developed for use with whole joints via the application of the mechanical test conditions used in this study, to large joint components using a simulator. It may also be possible to combine the mechanical and enzymatic models in whole joints via the use of more subtle degradative enzymes such as cathepsins. Following degradation of the large joint components using the conditions defined in this study, plugs of cartilage substitution materials could be fitted into the tissue, in the condyles, for example and articulated in a simulator. Following an appropriate number of loading cycles, the joint tissues could be analysed using the large range of appropriate characterisation methodologies, which were determined in this study.

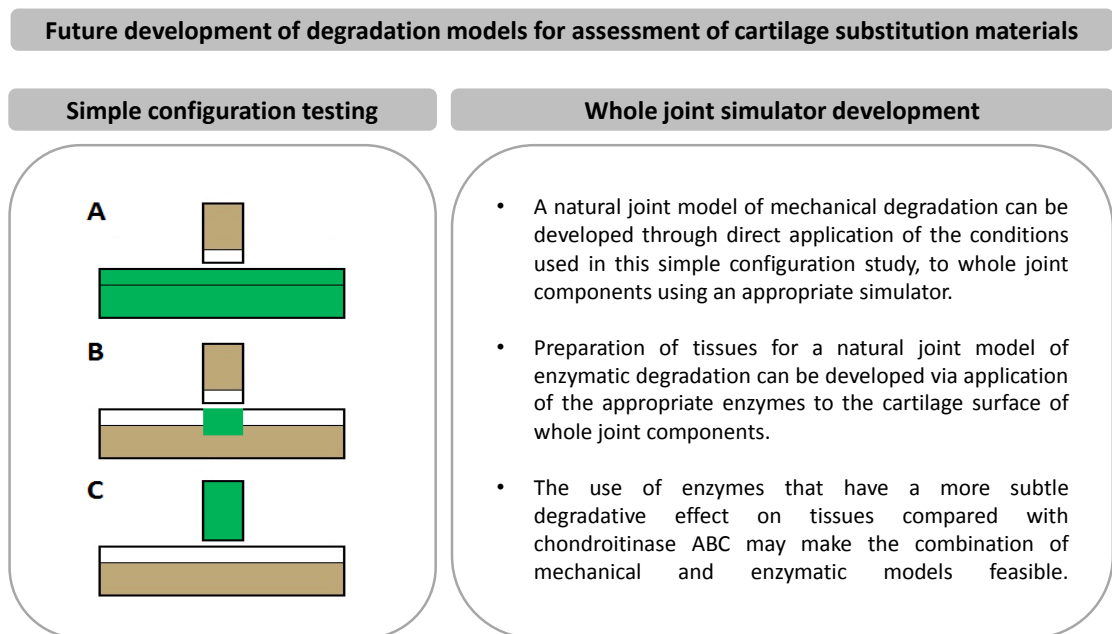


Figure 6.1. Future development of degradation models for assessment of cartilage substitution materials. It will be possible to use the simple configuration degradation models for assessment of cartilage substitution in a range of formats. **A.** Osteochondral pin against cartilage substitution plate. **B.** Osteochondral pin against osteochondral plate with cartilage substitution material insert. **C.** Cartilage substitution material pin against osteochondral plate.

Further testing of the lubricants using antibody based assays for specific proteins such as enzyme linked immunosorbent assays (ELISA) would also be very interesting because such methods could be developed for assessing levels of cartilage tissue damage by solely examining lubricants. Good targets for ELISA would include aggrecan and small leucine rich proteoglycans. Additionally, in a future study it may be possible to quantitatively assess the levels of minor cartilage components through fluorescence labelling of components such as COMP and biglycan.

Another protocol that requires development is a method for collagen detection in serum lubricants. Currently, an acid hydrolysis step is used in the collagen detection assay. When serum lubricants with cartilage particles were acid hydrolysed, a large volume of caramelisation was observed which was a result of a reaction between proteins and sugars in the solution via a process known as the Maillard reaction. This made analysis of the collagen in the serum unfeasible. To overcome this issue, an investigation into removal of GAGs from the lubricant to prevent caramelisation, using guanidine hydrochloride extraction was undertaken. However, there was not enough time to complete the study. Part of the problem in the development of the protocol was that guanidine hydrochloride must be thoroughly washed from specimens to allow the collagen assay to work correctly. However, during the wash step, test tubes containing the guanidine extracted samples were firstly centrifuged before supernatant containing the GAGs was removed. This could have meant some particles containing collagen may have been removed. One way of assessing whether the centrifugation step was sufficiently effective, could be via mass spectroscopy of the extracted supernatant, to assess whether any peaks indicative of cartilage or collagen were observed. It could also be possible to use chondroitinase ABC instead of guanidine hydrochloride to extract the GAGs from the tissue and into the supernatant, which may not require such an extensive number of washing steps.

To obtain further information about the biomechanical properties of the chondroitinase ABC treated tissue, finite element analysis of the tissue could be performed on tissues. This would have allowed further tissue properties to be derived, for example the permeability and elastic modulus of the tissue.

It would be interesting to investigate the macrophage response to cartilage wear particles to examine if there is a link between cartilage wear particles and inflammation. Previously, biomaterial particles of certain sizes and certain topographical features have been shown to initiate an inflammatory response in cells (Sieving *et al.*, 2003; Papageorgiou *et al.*, 2007). In addition to this, features of particles from osteoarthritic joints and control joints have been shown to alter (Podsiadlo *et al.*, 1997). Therefore it would also be useful to complete a

more thorough investigation of the particle features, such as size and surface topography. This may allow a link between the type of particle observed and the level of damage to the tissue to be established. It would also be interesting to determine the size distribution of particles using filters with smaller pore sizes. This could lead to the establishment of a link between contact stress and the average size of wear particle produced from the tissue. In addition it may be possible to determine whether a certain particle shape or size is produced from a specific zone of the tissue. It would be useful to develop a protocol for imaging of particles in serum lubricant. However, it would be necessary to give some thought as to what defines a particle, as some particles were very amorphous and appeared more as gel like deposits than particles, despite their amorphous appearance remaining as the humidity in the ESEM was dropped.

In future it will be possible for the degradation models developed in this study to be used for *in vitro* analysis of novel cartilage substitution materials such as tissue engineered constructs or biomaterials. It will also be possible for the models to be developed into whole full joint simulators with living tissue which could be used as a precursor to pre-clinical testing. This may reduce the number of animals used for testing novel materials. In addition, the range of characterisation methods that were developed and adapted for use in the study will be useful for comprehensive analysis of degraded cartilage tissues generated by different degradation regimes.

The study has also highlighted which methods require further development to give an even greater understanding of the processes occurring in mechanically and enzymatically degraded tissues. For example, in future height measurements should be taken using alternative equipment such as a Vernier height gauge as readings at the edge of the pin do not accurately detect the tissue loss occurring in the centre of the pin.

6.1.2 Conclusion

The mechanical degradation models that were developed in this study represent two stages of cartilage degeneration which can be used to investigate the tribological properties of novel cartilage substitution materials. The enzyme model may also be used to assess novel substitution materials or may be further developed via the use of additional degradative enzymes. The enzyme model may also be useful for assessment of therapies which aim to restore GAGs to degraded cartilage tissues.

The investigation of cartilage wear has provided an interesting insight into a relatively novel area. The protocol developed for investigating cartilage wear could be used to further study cartilage wear particles and their features. This may reveal more about potential links between cartilage wear particles and the cartilage degeneration process.

Chapter 7

7.1 References

Accardi, M.A., and Dini, D., and Cann, P.M., 2011. Experimental and numerical investigation of the behaviour of articular cartilage under shear loading—Interstitial fluid pressurisation and lubrication mechanisms. *Tribology International*, 44(5) pp. 565–578.

Aigner, T., Stöß, H., Weseloh, G., Zeiler, G., von der Mark, K., 1992. Activation of collagen type II expression in osteoarthritic and rheumatoid cartilage. *Virchows Archiv B*, 62(1) pp. 337-345.

Aigner, T., Bertling, W., Stöss, H., Weseloh, G., and von der Mark, K., 1993. Independent expression of fibril-forming collagens I, II, and III in chondrocytes of human osteoarthritic cartilage. *The Journal of Clinical Investigation*, 91(3) pp. 829-37.

Aigner, T., and Dudhia, J., 1997. Phenotypic modulation of chondrocytes as a potential therapeutic target in osteoarthritis: A hypothesis. *Annals of the Rheumatic Diseases*, 56 pp. 287-291.

Aigner, T., Zien, A., Gehrsitz, A., Gebhard, P.M., and McKenna, L., 2001. Anabolic and catabolic gene expression pattern analysis in normal versus osteoarthritic cartilage using complementary DNA-array technology. *Arthritis Rheumatism*, 44 pp. 2777-89.

Aigner, T., and Stove, J., 2003. Collagens- major component of the physiological cartilage matrix, major target of cartilage degeneration, major tool in cartilage repair. *Advanced Drug Delivery Reviews*, 55(12) pp.1569-1593.

Alaaeddine, N., Di Battista, J.A., Pelletier, J-P., Kiansa, K., Cloutier, J-M., and Martel-Pelletier, J., 1997. Osteoarthritic synovial fibroblasts possess an increased level of tumor necrosis factor-receptor 55 (TNF-R55) that mediates biological activation by TNF α . *The Journal of Rheumatology*, 24 pp. 1985–1994.

Alaaeddine, N., Di Battista, J.A., Pelletier, J.P., Kiansa, K., Cloutier, J.M., and Martel-Pelletier, J., 1999. Differential effects of IL-8, LIF (pro-inflammatory) and IL-11 (anti-inflammatory) on TNF-alpha-induced PGE(2) release and on signalling pathways in human OA synovial fibroblasts. *Cytokine*, 11(12) pp.1020-30.

Alexopoulos, L.G., Williams, G.M., Upton, M.L., Setton, L.A., and Guilak, F., 2005. Osteoarthritic changes in the biphasic mechanical properties of the chondrocyte pericellular matrix in articular cartilage. *Journal of Biomechanics*, 38(3) pp. 509-17.

Alonzi, T., Fattori, E., Lazzaro, D., Costa, P., Probert, L., Kollias, G., De Benedetti, F., Poli, V., and Ciliberto, G., 1998. Interleukin 6 is required for the development of collagen-induced arthritis. *The Journal of Experimental Medicine*, 187 pp.461-468.

Amour, A., Slocombe, P.M., Webster, A., Butler, M., Graham Knight, C., Smith, B.J., Stephens, P.E., Shelley, C., Hutton, M., Knäuper, V., Docherty, A.J.P., and Murphy, G., 1998. TNF- α converting enzyme (TACE) is inhibited by TIMP-3. *FEBS Letters*, 435 pp.39-44.

Arend, W.P., Malyak, M., Guthridge, C.J., Gabay, C., 1998. Interleukin-1 receptor antagonist: role in biology. *Annual Review of Immunology*, 16:27-55.

Armstrong, C.G., and V.C. Mow. 1982. Variations in the intrinsic mechanical properties of human articular cartilage with age, degeneration, and water content. *Journal of Bone and Joint Surgery; American Edition*, 64 pp. 88-94.

ASTM *Standards*: American Society for Testing and Materials 2005. Standard Practice for Characterization of Particles. Designation: F 1877 – 05.

Attur, M.G., Patel, I.R., Patel, R.N., Abramson, S.B., Amin, A.R., 1998. Autocrine production of IL-1 β by human osteoarthritis-affected cartilage and differential regulation of endogenous nitric oxide, IL-6, prostaglandin E₂, and IL-8. *Proceedings of the Association of American Physicians*, 110(1) pp.65-72.

Bader, D.L., Kempson, G.E., Barrett, A.J., and Webb, W., 1981. The Effects of Leukocyte Elastase on the Mechanical-Properties of Adult Human Articular-Cartilage in Tension. *Biochimica et Biophysica Acta*, 677 pp. 103-108.

Bader, D.L., Kempson, G.E., Egan, J., Gilbey, W., and Barrett, A.J., 1992. The effects of selective matrix degradation on the short term compressive properties of adult human articular cartilage. *Biochimica et Biophysica Acta*, 1116(2) pp.147-154.

Baeurle, S.A., Kiselev, M.G., Makarova, E.S., and Nogovitsin., E.A., 2009. Effect of the counterion behavior on the frictional–compressive properties of chondroitin sulphate solutions. *Polymer*, 50 (7) pp.1805-1813.

Bakker, A.C., Joosten, L.A.B., Arntz, O., Helsen, M.M.A., Bendele, A.M., Van De Loo, F.A.J., and Van Den Berg, W.B., 1997. Prevention of murine collagen-induced arthritis in the knee and ipsilateral paw antagonist protein in the knee by local expression of human interleukin-1 receptor. *Arthritis & Rheumatism*, 40(5) pp. 893-900.

Baragi, V.M., Renkiewicz, R.R., Jordan,H., Bonadio, J., Hartman, J.W., and Roessler, B.J., 1995. Transplantation of Transduced Chondrocytes Protects Articular Cartilage from Interleukin 1-Induced Extracellular Matrix Degradation. *The Journal of Clinical Investigation*, 96 pp.2454-60.

Bayliss, M.T., Osborne, D., Woodhouse, S., and Davidson. D., 1999. Sulfation of chondroitin sulfate in human articular cartilage - The effect of age, topographical position, and zone of cartilage on tissue composition. *Journal of Biological Chemistry*, 274 pp. 15892-15900.

Bayliss, M.T., Hutton, S., Hayward, J., and Maciewicz, R.A., 2001. Distribution of aggrecanase (ADAMTs 4/5) cleavage products in normal and osteoarthritic human articular cartilage: the influence of age, topography and zone of tissue. *Osteoarthritis and Cartilage* 9(6) pp.553–560.

Beck, R.T., Illingworth, K.D., Saleh, K.J., 2012. Review of periprosthetic osteolysis in total joint arthroplasty: an emphasis on host factors and future directions. *Journal of Orthopaedic Research*, 30(4) pp.541-6.

Behl, B., Papageorgiou, I., Brown, C., Hall, R., Tipper, J.L., Fisher, J., and Ingham, E., 2013. Biological effects of cobalt-chromium nanoparticles and ions on dural fibroblasts and dural epithelial cells. *Biomaterials*, 34(14) pp. 3547-3558.

Bendele, A.M., and Hulman, J.F., 1988. Spontaneous cartilage degeneration in guinea pigs. *Arthritis & Rheumatism*, 31(4) pp. 561-5.

Bendele, A.M., 2001. Animal models of osteoarthritis. *Journal of Musculoskeletal and Neuronal Interactions*, 1(4) pp. 363-376.

Benderdour, M., Tardif, G., Pelletier, J.P., Di Battista, J.A., Reboul, P., Ranger, P., Martel-Pelletier, J., 2002. Interleukin 17 (IL-17) induces collagenase-3 production in human osteoarthritic chondrocytes via AP-1 dependent activation: differential activation of AP-1 members by IL-17 and IL-1 β . *Journal of Rheumatology*, 29(6) pp. 1262-72.

Bhala, N., Emberson, J., Merhi, A., Abramson, S., Arber, N., Baron, J.A., Bombardier, C., Cannon, C., Farkouh, M.E., FitzGerald, G.A., Goss, P., Halls, H., Hawk, E., Hawkey, C., Hennekens, C., Hochberg, M., Holland, L.E., Kearney, P.M., Laine, L., Lanus, A., Lance, P., Laupacis, A., Oates, J., Patrono, C., Schnitzer, T.J., Solomon, S., Tugwell, P., Wilson, K., Wittes, J., Baigent, C., Adelowo, O., Aisen, P., Al-Quorain, A., Altman, R., Bakris, G., Baumgartner, H., Bresee, C., Carducci, M., Chang, D.M., Chou, C.T., Clegg, D., Cudkowicz, M., Doody, L., El Miedany, Y., Falandry, C., Farley, J., Ford, L., García-Losa, M., González-Ortiz, M., Haghghi, M., Hála, M., Iwama, T., Jajić, Z., Kerr, D., Kim, H.S., Köhne, C., Koo, B.K., Martin, B., Meinert, C., Müller, N., Myklebust, G., Neustadt, D., Omdal, R., Ozgocmen, S., Papas, A., Patrignani, P., Pelliccia, F., Roy, V., Schlegelmilch, I., Umar, A., Wahlström, O., Wollheim, F., Yocum, S., Zhang, X.Y., 2013. Vascular and upper gastrointestinal effects of non-steroidal anti-inflammatory drugs: meta-analyses of individual participant data from randomised trials. *The Lancet*.

Bidanset, D.J., Guidry, C., Rosenberg, L.C., Choi, H.U., Timpl, R., and Hook, M., 1992. Binding of the proteoglycan decorin to collagen type VI. *The Journal of Biological Chemistry*, 267(8) pp. 5250-6.

Blanco, F.J., Ochs, R.L., Schwarz, H., and Lotz, M., 1995. Chondrocyte apoptosis induced by nitric oxide. *American Journal of Pathology*, 146(1) pp.75–85.

Blaschke, U.K., Eikenberry, E.F., Hulmes, D., Gallai, H.J and Bruckner, P., 2000. Collagen XI Nucleates Self-assembly and Limits Lateral Growth of Cartilage Fibrils. *The Journal of Biological Chemistry*, 275(14) pp.10370–10378.

Blum, M.M., and Ovaert, T.C., 2013. Low friction hydrogel for articular cartilage repair: Evaluation of mechanical and tribological properties in comparison with natural cartilage tissue. *Materials Science and Engineering C: Materials for Biological Applications*, 33(7) pp. 4377-83.

Blumenfeld, I., Livne, E., 1999. The role of transforming growth factor (TGF- β), insulin like growth factor (IGF)-1 and interleukin (IL)-1 in osteoarthritis and aging of joints. *Experimental Gerontology*, 31 pp. 821-829.

Bogdan, C., Thuring, H., Dlaska, M., Rollinghoff, M., and Weisst, C., 1997. Mechanism of Suppression of Macrophage Nitric Oxide Release by IL-13: Influence of the Macrophage Population. *Journal of Immunology*, 159 pp. 4506-4513.

Bonassar, L.J., Stinn, J.L., Paguio, C.G., Frank, E.H., Moore, V.L., Lark, M.W., Sandy, J.D., Hollander, A.P., Poole, A.R., Grodzinsky, A.J., 1996. Activation and inhibition of endogenous matrix metalloproteinases in articular cartilage: effects on composition and biophysical properties. *Archives of Biochemistry and Biophysics*, 333(2) pp. 359-67.

Boschetti, F., and Peretti, G.M., 2008. Tensile and compressive properties of healthy and osteoarthritic human articular cartilage. *Biorheology*, 45(3-4) pp. 337-44.

Bourne, R.B., 1990. Unicompartmental Knee Replacement. *Current Orthopaedics*, 4(2) pp. 95-98.

Brass, A., Kadler, K.E., Thomas, J.T., Grant, M.E., Boot-Handford, R.P., 1992. The fibrillar collagens, collagen VIII, collagen X and the C1q complement proteins share a similar domain in their C-terminal non-collagenous regions. *FEBS Letters*, 303(2-3) pp. 126-8.

Brew, K., Dinakarpanian, D., and Nagase, H., 2000. Tissue inhibitors of metalloproteinases: evolution, structure and function. *Biochimica et Biophysica Acta*, 1477(1-2) pp. 267-283.

Brew, K., and Nagase, H., 2010. The tissue inhibitors of metalloproteinases (TIMPS): an ancient family with structural and functional diversity. *Biochimica et Biophysica Acta*, 1803(1) pp. 55-71.

Brown, C., Williams, S., Tipper, J.L., Fisher, J., and Ingham, E., 2007. Characterisation of wear particles produced by metal on metal and ceramic on metal hip prostheses under standard and microseparation simulation. *Journal of Materials Science: Materials in Medicine*, 18(5) pp. 819-827.

Bruckner P, van der Rest M., 1994. Structure and function of cartilage collagens. *Microscopy Research and Technique*, 28(5) pp. 378-84.

Bryan, N., Andrews, K.D., Loughran, M.J., Rhodes, N.P., and Hunt, J.A., 2010. Elucidating the Contribution of the Elemental Composition of Fetal Calf Serum Towards Antigenic Expression of Primary Human Umbilical Vein Endothelial Cells In Vitro. *Bioscience Reports*, 31(3) pp. 199-210.

Buckwalter, J.A., 1998. Articular cartilage: injuries and potential for healing. *Journal of Orthopaedic & Sports Physical Therapy*, 28 pp. 192-202.

Butler, D.L., Goldstein, S.A., Guilak, F., 2000. Functional tissue engineering: the role of biomechanics. *Journal of Biomechanical Engineering*, 122(6) pp. 570-5.

Caligaris, M., Canal, C.E., Ahmad, C.S., Gardner, T.R., and Ateshian G.A., 2009. Investigation of the frictional response of osteoarthritic human tibiofemoral joints and the potential beneficial tribological effect of healthy synovial fluid. *Osteoarthritis Cartilage*, 17(10) pp. 1327-32.

Campbell, I.K., Piccoli, D.S., Butler, D.M., Singleton, D.K., and Hamilton, J.A., 1988. Recombinant human interleukin-1 stimulates human articular cartilage to undergo resorption and human chondrocytes to produce both tissue- and urokinase-type plasminogen activator. *Biochimica et Biophysica Acta*, 967 pp. 183-94.

Carroll, G.J., and Bell, M.C., 1993. Leukaemia inhibitory factor stimulates proteoglycan resorption in porcine articular cartilage. *Rheumatology International*, 13 pp. 5-8.

Catelas, I., Bobyn, J.D., Medley, J.B., Krygier, J.J., Zukor, D.J., Huk, O.L., 2003. Size, shape, and composition of wear particles from metal-metal hip simulator testing: effects of alloy and number of loading cycles. *Journal of biomedical materials research Part A*, 67(1) pp. 312-27.

Chakraborti, S., Mandal, M., Das, S., Mandal, A., and Chakraborti, T., 2003. Regulation of Matrix Metalloproteinases: An overview." *Molecular and cellular biochemistry*, 253 pp.296-285.

Chakravarti, S., Magnuson, T., Lass, J.H., Jepsen, K.J., LaMantia, C., Carroll, H., 1998. Lumican regulates collagen fibril assembly: skin fragility and corneal opacity in the absence of lumican. *Journal of Cell Biology*, 141 pp. 1277–1286.

Chen, Q., Gibney, E., Fitch, J.M., Linsenmayer, C., Schmid, T.M., and Linsenmayer, T.F., 1990. Long-Range Movement and Fibril Association of Type-X Collagen within Embryonic Cartilage Matrix. *Proceedings of the National Academy of Sciences of the United States of America*, 87 pp. 8046-8050.

Chen, C., Burton-Wurster, N., Lust, G., Bank, R.A., and Tekoppele, J.M., 1999. Compositional and metabolic changes in damaged cartilage are peak-stress, stress-rate, and loading-duration dependent. *Journal of Orthopaedic Research*, 17(6) pp. 870–879.

Cheung, H.Y., Lau, K.T., Lu, T.P., and Hui, D., 2007. A critical review on polymer-based bio-engineered materials for scaffold development. *Composites Part B: Engineering*, 38(3) pp. 291-300.

Chomarat, P., Vannier, E., Dechanet, J., Rissoan, M.C., Banchereau, J., Dinarello, C.A., and Miossec, P., 1995. Balance of IL-1 receptor antagonist/IL-1 β in rheumatoid synovium and its regulation by IL-4 and IL-10. *The Journal of Immunology*, 154(3) pp.1432-1439.

Chung, C., and Burdick, J.A., 2008. Engineering Cartilage Tissue. *Advanced Drug Delivery Reviews*, 60(2) pp. 243–262.

Claassen, H., and Tschirner, T., 2003. Topographical and histological examination of osteophytes taken from arthrotic femoral heads. *Annals of Anatomy*, 185 pp. 67-71.

Clark, A.G., Jordan, J.M., Vilim, V., Renner, J.B., Dragomir, A.D., Luta, G., and Kraus, V.B., 1999. Serum cartilage oligomeric matrix protein reflects osteoarthritis presence and severity: the Johnston County Osteoarthritis Project. *Arthritis & Rheumatism*, 42(11) pp. 2356-64.

Covert, R.J., Ott, R.D., and Ku, D.N., 2003. Friction characteristics of a potential articular cartilage biomaterial. *Wear* 255, pp. 1064–8.

Cremer, M.A., Rosloniec, E.F., and Kang, A.H., 1998. The cartilage collagens: a review of their

structure, organization, and role in the pathogenesis of experimental arthritis in animals and in human rheumatic disease. *Journal of Molecular Medicine*, 76 pp. 275-288.

Crockett, R., Roos, S., Rossbach, P., Dora, C., Born, W., and Troxler, H., 2005. Imaging of the surface of human and bovine articular cartilage with ESEM and AFM. *Tribology Letters*, 19(4) pp. 311–317.

Daheshia, M., and Yao, J.Q., 2008. The Interleukin 1 β Pathway in the Pathogenesis of Osteoarthritis. *The Journal of Rheumatology*, 35(12) pp. 31226-32.

Danielson, K.G., H. Baribault, D.F. Holmes, H. Graham, K.E. Kadler, and R.V. Iozzo. 1997. Targeted disruption of decorin leads to abnormal collagen fibril morphology and skin fragility. *Journal of Cell Biology*, 136 pp. 729-43.

de Hooge, A.S., van de Loo, F.A., Bennink, M.B., Arntz, O.J., de Hooge, P., and van den Berg, W.B., 2005. Male IL-6 gene knockout mice developed more advanced osteoarthritis upon aging. *Osteoarthritis Cartilage*, 13(1) pp. 66–73.

Dechanet, J., Taupin, J.L., Chomaratham, P., Rissoan, M.C., Moreau, J.F., Banchereau, J., and Miossec, P., 1994. Interleukin-4 but not interleukin-10 inhibits the production of leukemia inhibitory factor by rheumatoid synovium and synoviocytes. *European Journal of Immunology*, 24 pp. 3222-3228.

Dean, D.D., Martel-Pelletier, J., Pelletier, J.P., Howell, D.S., and Woessner, J.F., 1989. Evidence for metalloproteinases and metalloproteinase inhibitor imbalance in human osteoarthritic cartilage. *The Journal of Clinical Investigation*, 84 pp. 678-685.

Dejica, V.M., Mort, J.S., Laverty, S., Percival, M.D., Antoniou, J., Zukor, D.J., and Poole, R., 2008. Cleavage of type II collagen by cathepsin K in human osteoarthritic cartilage. *American Journal of Pathology*, 173(1) pp.161-169.

Di Cesare, P.E., Chen, F.S., Moergelin, M., Carlson, C.S., Leslie, M.P., Perris, R., and Fang, C., 2002. Matrix–matrix interaction of cartilage oligomeric matrix protein and fibronectin. *Matrix Biology*, 21(5), pp. 461-470.

Doherty, T.M., Kastelein, R., Menon, S., Andrade, S., and Coffman, R.L., 1993. Modulation of Murine Macrophage Function by 1L-13. *Journal of Immunology*, 151 pp. 7151-7160.

Dore, S., Pelletier, J.P., Di Battista, J.A., Tardif, G., Brazeau, P., and Martel-Pelletier, J., 1994. Human osteoarthritic chondrocytes possess an increased number of insulinlike growth factor 1 binding sites but are unresponsive to its stimulation. Possible role of IGF-1-binding proteins. *Arthritis & Rheumatism*, 37 pp. 253–263.

Dorotka, R., Windberger, U., Macfelda, K., Bindreiter, U., Toma, C., and Nehrer, S., 2005. Repair of articular cartilage defects treated by microfracture and a three-dimensional collagen matrix. *Biomaterials*, 26: pp. 617-3629.

Dressler, M.R., Strickland, M.A., Taylor, M., Render, T.D., and Ernsberger, C. N., 2011. Predicting wear of UHMWPE: decreasing wear rate following a change in direction. *Wear*, 271(11-12), 2879-2883.

Dripps, D.J., Branduber, B.J., Thompson, R.C., and Eisenberg, S.P., 1991. IL-1 receptor antagonist binds to the 80 kDa IL-1 receptor but does not initiate signal transduction. *Journal of Biological Chemistry*, 266 pp. 10331-10336.

Duda, G.N., Eilers, M., Loh, L., Hoffman, J.E., Kääh, M., Schaser, K., 2001. Chondrocyte Death Precedes Structural Damage in Blunt Impact Trauma. *Clinical Orthopaedics and Related Research*, 393 pp. 302-309.

Echtermeyer, F., Bertrand, J., Dreier, R., Meinecke, I., Neugebauer, K., Fuerst, M., Lee, Y.J., Song, Y.W., Herzog, C., Theilmeier, G., and Pap, T., 2009. Syndecan-4 regulates ADAMTS-5 activation and cartilage breakdown in osteoarthritis. *Nature Medicine*, 15(9) pp. 1072-6.

Economides, A.N., Carpenter, L.R., Rudge, J.S., Wong, V., Koehler-Stec, E.M., Hartnett, C., Pyles, E.A., Xu X., Daly, T.J., Young, M.R., Fandl, J.P., Lee, F., Carver, S., McNay, J., Bailey, K., Ramakanth, S., Hutabarat, R., Huang, T.T., Radziejewski, C., Yancopoulos, G.D., and Stahl, N., 2003. Cytokine traps: multi-component, high-affinity blockers of cytokine action. *Nature Medicine*, 9 pp. 47-52.

Eeckhout, Y., and Vaes, G., 1977. Effects of lysosomal cathepsin B, plasmin and and kallikrein, and spontaneous activation. *The Biochemical Journal*, 166 pp. 21-31.

Ehrlich, M.G., Houle, P.A., Vigliani, G., Mankin, H.J., 1978. Correlation between articular cartilage collagenase activity and osteoarthritis. *Arthritis & Rheumatism*, 21(7) pp. 761–766.

Ellison, P., Tipper, J.L., Jennings, L.M., and Fisher, J., 2012. Biological activity of polyethylene wear debris produced in the patellofemoral joint. *Proceedings of the Institution of Mechanical Engineers, Part H: Journal of Engineering in Medicine*, 226(5) pp.377-83.

Farquhar, T., Xia, Y., Mann, K., Bertram, J., Burton-Wurster, N., Jelinski, L., and Lust, G., 1996. Swelling and fibronectin accumulation in articular cartilage explants after cyclical impact. *Journal of Orthopaedic Research*, 14(3) pp. 417-23.

Felson, D.T., Gale, D.R., Elon Gale, M., Niu, J., Hunter, D.J., Goggins, J., and LaValley, M.P., 2005. Osteophytes and progression of knee osteoarthritis. *Rheumatology*, 44(1) pp.100-104.

Fernandes, J.C., Martel-Pelletier, J., Lascau-Coman, V., Moldovan, F., Jovanovic, D., Raynauld, J.P., and Pelletier, J.P., 1998. Collagenase-1 and collagenase-3 synthesis in normal and early experimental osteoarthritic canine cartilage: an immunohistochemical study. *Journal of Rheumatology*, 25 pp. 1585-94.

Flannery, C.R., Lark, M.W., and Sandy, J.D., 1992. Identification of a stromelysin cleavage site within the interglobular domain of human aggrecan. Evidence for proteolysis at this site in vivo in human articular cartilage. *Journal of Biological Chemistry*, 267 pp. 1008-14.

Flannery, C.R., Hughes, C. E., Schumacher, B.L., Tudor, D., Aydelotte, M.B., Kuettner, K.E., and Caterson, B., 1999. Articular cartilage superficial zone protein (SZP) is homologous to megakaryocyte stimulating factor precursor and is a multifunctional proteoglycan with potential growth-promoting, cytoprotective, and lubricating properties in cartilage metabolism. *Biochemical and Biophysical Research Communications*, 254 pp. 535-541.

Flannelly, J., Chambers, M.G., Dudhia, J., Hembry, R.M., Murphy, G., Mason, R.M., Bayliss, M.T., 2002. Metalloproteinase and tissue inhibitor of metalloproteinase expression in the murine STR/ort model of osteoarthritis. *Osteoarthritis Cartilage*, 10(9) pp. 722-33.

Flechtenmacher, J., Huch, K., Thonar, E.J., Mollenhauer, J.A., Davies, S.R., Schmid, T.M., Puhl, W.,

Sampath, T.K., Aydelotte, M.B., Kuettner, K.E., 1996. Recombinant human osteogenic protein 1 is a potent stimulator of the synthesis of cartilage proteoglycans and collagens by human articular chondrocytes. *Arthritis & Rheumatism*, 39(11) pp.1896-904.

Forsey, R.W., Fisher, J., Thompson, J., Stone, M.H., Bell, C., and Ingham, E., 2006. The effect of hyaluronic acid and phospholipid based lubricants on friction within a human cartilage damage model. *Biomaterials*, 27(26) pp. 4581-90.

Forster, H., and Fisher, J., 1999. The influence of continuous sliding and subsequent surface wear on the friction of articular cartilage. *Proceedings of the Institution of Mechanical Engineers, Part H: Journal of Engineering in Medicine*, 213(4) pp. 329-45.

Forster, H., and Fisher, J., 1996. The influence of loading time and lubricant on the friction of articular cartilage. *Proceedings of the Institution of Mechanical Engineers, Part H: Journal of Engineering in Medicine*, 210(2) pp. 109-19.

Fox, A.J.S., Bedi, A., and Rodeo, S.A., 2009. The Basic Science of Articular Cartilage: Structure, Composition, and Function. *Sports Health: A Multidisciplinary Approach*, 1(6) pp. 461-468.

Freemont, A. J., Hampson, V., Tilman, R., Goupille, P., Taiwo, Y., Hoyland, J.A., 1997. Gene expression of matrix metalloproteinases 1, 3 and 9 by chondrocytes in osteoarthritic human knee articular cartilage is zone and grade specific. *Annals of the Rheumatic Diseases*, 56 pp. 542-548.

Freeman, M.E., Furey, M.J., Love, B.J., and Hampton, J.M., 2000. Friction, wear, and lubrication of hydrogels as synthetic articular cartilage. *Wear*, 241 pp. 129–35.

Furukawa, T., Ito, K., Nuka, S., Hashimoto, J., Takeji, H., Takahara, M., Ogino, T., Young, M.F., and Shinomura, T., 2009. Absence of biglycan accelerates the degenerative process in mouse intervertebral disc. *Spine (Phila Pa 1976)*, 34(25) pp. E911–E917.

Gannon, J.M., Walker, G., Fischer, M., Carpenter, R., Thompson Jr., R.C., and Oegema Jr, T.R., 1991. Localization of type X collagen in canine growth plate and adult canine articular cartilage. *Journal of Orthopaedic Research*, 9 pp. 485-494.

Ganu, V., Ronald Goldberg, R., Peppard, J., Rediske, J., Melton, R., Hu, S.I., Wang, W., Duvander, C., Heinegård, D., 1998. Inhibition of interleukin-1-alpha-induced cartilage oligomeric matrix protein degradation in bovine articular cartilage by matrix metalloproteinase inhibitors: Potential role for matrix metalloproteinases in the generation of cartilage oligomeric matrix protein fragments in arthritic synovial fluid. *Arthritis & Rheumatism*, 41(12) pp. 2143-2151.

Geng, Y., McQuillan, D., and Roughley, P.J., 2006. SLRP interaction can protect collagen fibrils from cleavage by collagenases. *Matrix Biology*, 25 pp. 484-491.

Getgood, A., Bhullar, T.P.S., Rushton, N., 2009. Current concepts in articular cartilage repair. *Orthopaedics and Trauma*, 23(3), pp. 189-200.

Gibson, G.J., and M.H. Flint. 1985. Type-X Collagen-Synthesis by Chick Sternal Cartilage and Its Relationship to Endochondral Development. *Journal of Cell Biology*, 101 pp. 277-284.

Goldring, M.B., 2000. The role of the chondrocyte in osteoarthritis. *Arthritis & Rheumatism*, 43(9) pp. 1916-1926.

Glasson, S.S., Askew, R., Sheppard, B., Carito, B., Blanchet, T., Ma, H.L., Flannery, C.R., Peluso, D., Kanki, K., Yang, Z., Majumdar, M.K., and Morris, E.A., 2005. Deletion of active ADAMTS5 prevents cartilage degradation in a murine model of osteoarthritis. *Nature*, 434 pp. 644-8.

Gleghorn, J.P., Jones, A.R., Flannery, C.R., and Bonassar, L.J., 2009. Boundary mode lubrication of articular cartilage by recombinant human lubricin. *Journal of Orthopaedic Research*, 27(6) pp. 771-7.

Gordon, M.K., and Hahn, R.A., 2010. Collagens. *Cell and Tissue research*, 339(1) pp.247-257.

Gründer, T., Gaissmaier, C., Fritz, J., Stoop, R., Hortschansky, P., Mollenhauer, J., and Aicher, W.K., 2004. Bone morphogenetic protein (BMP)-2 enhances the expression of type II collagen and aggrecan in chondrocytes embedded in alginate beads. *Osteoarthritis Cartilage*, 12(7) pp. 559-67.

Graindorge, S.L., and Stachowiak, G.W., 2000. Changes occurring in the surface morphology of articular cartilage during wear. *Wear*, 241 pp. 134-150.

Graindorge, S., Ferrandez, W., Jin, J., Ingham, E., Grant, C., Twigg, P., and Fisher, J. 2005. Biphasic surface amorphous layer lubrication of articular cartilage. *Medical Engineering and Physics*, 27(10) pp. 836-844.

Graindorge, S., Ferrandez, W., Ingham, E., Jin, J., Twigg, P., and Fisher. 2006. The role of the surface amorphous layer of Articular Cartilage in Joint Lubrication. *Proceedings of the Institute of Mechanical Engineers Part H: Journal of Engineering in Medicine*, 220(5) pp. 597-607.

Gratz, K.R., Wong, B.L., Bae, W.C., and Sah, R.L., 2009. The Effects of Focal Articular Defects on Cartilage Contact Mechanics. *Journal of Orthopaedic Research*, 27(5) pp. 584–592.

Greenwald, A.S., and O'Connor, J.J., 1971. The transmission of load through the human hip joint. *Journal of Biomechanics*, 4(6) pp. 507–528.

Grimmer, C., Balbus, N., Lang, U., Aigner, T., Cramer, T., Müller, L., Swoboda, B., and Pfander, D., 2006. Regulation of Type II Collagen Synthesis during Osteoarthritis by Prolyl-4-Hydroxylases: Possible Influence of Low Oxygen Levels. *The American journal of pathology*, 169(2) pp. 491–502.

Gründer, T., Gaissmaier, C., Fritz, J., Stoop, R., Hortschansky, P., Mollenhauer, J., Aicher, W.K., 2004. Bone morphogenetic protein (BMP)-2 enhances the expression of type II collagen and aggrecan in chondrocytes embedded in alginate beads. *Osteoarthritis and Cartilage*, 12(7) pp.559-567.

Guenther, H. L., Guenther, H.E., Froesch. E.R., and Fleisch, H., 1982. Effect of insulin-like growth factor on collagen and glycosaminoglycan synthesis by rabbit articular chondrocytes in culture. *Cellular and Molecular Life Sciences*, 38(8) pp. 979-981.

Guilak, F., Butler, D.L., and Goldstein, S.A., 2001. Functional tissue engineering: the role of biomechanics in articular cartilage repair. *Clinical Orthopaedics and Related Research*, 391(Suppl) pp. S295-305.

Guingamp, C., Gegout-Pottie, P., Philippe, L., Terlain, B., Netter, P., and Gillet, P., 1997. Monoiodoacetate-induced experimental osteoarthritis: a dose-response study of loss of mobility, morphology, and biochemistry. *Arthritis & Rheumatism*, 40(9) pp. 1670-9.

Guler, H.P., Caldwell, J., Littlejohn, T., McIlwain, H., Offenber, H., Stahl, N., 2001. A phase 1, single dose escalation study of IL-1 trap in patients with rheumatoid arthritis. *Arthritis & Rheumatism*, 44, pp. S370.

Hakshur, K., Benhar, I., Bar-Ziv, Y., Halperin, N., Segal, D., Eliaz, N., 2011. The effect of hyaluronan injections into human knees on the number of bone and cartilage wear particles captured by bio-ferrography, *Acta Biomaterialia*, 7(2), pp. 848-857.

Hall, M.L., Krawczak, D.A., Simha, N.K., and Lewis, K.L., 2009. Effect of Dermatan Sulfate on the indentation and Tensile Properties of Articular Cartilage. *Osteoarthritis Cartilage*, 17(5) pp.655–661.

Hamblin, A.S. (1993). *Cytokines and cytokine receptors*. New York: Oxford University Press Inc.

Hedbom, E., and Heinegard, D., 1993. Binding of fibromodulin and decorin to separate sites on fibrillar collagens. *Journal of Biological Chemistry*, 268(27) pp. 307–12.

Hangody, L., Dobos, J., Baló, E., Pánics, G., Hangody, L.R., and Berkes, I., 2010.

Clinical experiences with autologous osteochondral mosaicplasty in an athletic population: a 17-year prospective multicenter study. *The American Journal of Sports Medicine*, 38(6) pp. 1125-33.

Heim, M., Römer, L., and Scheibel, T., 2010. Hierarchical structures made of proteins. The complex architecture of spider webs and their constituent silk proteins. *Chemical Society Reviews*, 39 pp. 156-164.

Henkelsa, K.M., Frondorfa, K., Gonzalez-Mejia, M.E., Doseff, A.L., and Gomez-Cambronero, J., 2011. IL-8-induced neutrophil chemotaxis is mediated by Janus kinase 3 (JAK3). *Febs letters*, 585(1) pp. 159–166.

Henrotin, Y.E., De Groote, D.D., Labasse, A.H., Gaspar, S.E., Zheng, S.X., Geenen, V.G., and Reginster, J.Y.L., 1996. Effects of exogenous IL-1 β , TNF α , IL-6, IL-8 and LIF on cytokine production by human articular chondrocytes. *Osteoarthritis and Cartilage* 4(3) pp. 163-173.

Hermann, J.A., Hall, M.A., Maini, R.N., Feidmann, M., and Brennan, F.M., 1998. Important immunoregulatory role of Interleukin-11 in the inflammatory process in rheumatoid arthritis. *Arthritis & Rheumatism*, 41(8) pp. 1388-1397

Hildebrand, A., Romaris, M., Rasmussen, L.M., Heinegard, D., Twardzik, D.R., Border, W.A., and Ruoslahti, E., 1994. Interaction of the small interstitial proteoglycans biglycan, decorin and fibromodulin with transforming growth factor beta. *The Biochemical Journal.*, 302(2) pp. 527–534.

Hodge, W.A., Fijan, R.S., Carlson, K.L., Burgess, R.G., Harris, W.H., and Mann, R.W., 1986. Contact pressures in the human hip joint measured in vivo. *Proceedings of the National Academy of Sciences*, 83(9).

Hoemann, C. D., 2004. Molecular and Biochemical Assays of Cartilage Components In De Ceuninck, F., Sabatini, M., Pastoureau, P. Eds. 2004. *Methods in Molecular Medicine. Cartilage and Osteoarthritis. Volume 2, Structure and In Vivo Analysis.* New Jersey: Humana Press, Chapter 8 127-152.

Holden, P., Meadows, R.S., Chapman, K.L., Grant, M.E., Kadler, K.E., and Briggs, M.D., 2001. Cartilage oligomeric matrix protein interacts with type IX collagen, and disruptions to these interactions identify a pathogenetic mechanism in a bone dysplasia family. *Journal of Biological Chemistry*, 276(8) pp. 6046-55.

Hollander, A.P., Pidoux, I., Reiner, A., Rorabeck, C., Bourne, R., Poole, A.R., 1995. Damage to Type II Collagen in Aging and Osteoarthritis Starts at the Articular Surface, Originates Around Chondrocytes, and Extends into the Cartilage with Progressive Degeneration. *The Journal of Clinical Investigation*, 96, pp. 2859-2869

Homandberg, G.A., R. Meyers, and D.L. Xie. 1992. Fibronectin fragments cause chondrolysis of bovine articular cartilage slices in culture. *Journal of Biological Chemistry*, 267 pp. 3597-604.

Hooper, N, M. (1996). *Zinc Metalloproteinases in Health and Disease.* London: Taylor & Francis. 158-160.

Huang, W., Li, W.Q., Dehnade, F., and Zafarullah, M., 2002. Tissue inhibitor of metalloproteinases-4 (TIMP-4) gene expression is increased in human osteoarthritic femoral head cartilage. *Journal of Cellular Biochemistry*, 85(2) pp. 295-303.

Hui, W., Bell, M.C., Carroll, G.J., and Layton, M.J., 1998. Modulation of cartilage proteoglycan metabolism by LIF binding protein. *Cytokine*, 10(3) pp. 220-226.

Hwang, S.Y., Kim, J.Y., Kim, K.W., Park, M.K., Moon, Y., Kim, Y.U., and Kim, H.Y., 2004. IL-17 induces production of IL-6 and IL-8 in rheumatoid arthritis synovial fibroblasts via NF- κ B- and PI3-kinase/Akt dependent pathways. *Arthritis Research & Therapy*, 6(2) pp. R120–R128.

Ingham, E., and Fisher, J., 2000. Biological reactions to wear debris in total joint replacement. *Proceedings of the Institution of Mechanical Engineers, Part H: Journal of Engineering in Medicine*, 214(1) pp. 21-37.

Iozzo R.V., 1997. The family of the small leucine-rich proteoglycans: key regulators of matrix assembly and cellular growth. *Critical Reviews in Biochemistry and Molecular Biology*, 32 pp.141–174.

Isenberg, D A. (2004). *Oxford Textbook of Rheumatology*. 3rd ed. Oxford: Oxford. Page 330.

Iwanaga, H., Matsumoto, T., Enomoto, H., Okano, K., Hishikawa, Y., Shindo, H., and Koji, T., 2005. Enhanced expression of insulin-like growth factor-binding proteins in human osteoarthritic cartilage detected by immunohistochemistry and in situ hybridization. *Osteoarthritis and Cartilage*, 13 pp. 439-448.

Jiang, H., Peterson, R.S., Wang, W.H., Bartnik, E., Knudson, C.B., and Knudson, W., 2002. A requirement for the CD44 cytoplasmic domain for hyaluronan binding, pericellular matrix assembly, and receptor-mediated endocytosis in COS-7 cells. *Journal of Biological Chemistry*. 277:10531-10538.

Jin, Z.M., M. Stone, E. Ingham, and J. Fisher. 2006. Biotribology. *Current Orthopaedics*, 20 pp. 32-40.

Johnson, M.D., Hyeong-Reh Choi Kim , Chesler, L., Tsao-Wu, G., Polverini , P.J., Bouck, N., 2005. Inhibition of angiogenesis by tissue inhibitor of metalloproteinase. *Journal of Cellular Physiology*, 160(1) pp. 194-202.

Johnson, K , Farley, D., Hu, S.I., Terkeltaub, R., 2003. One of two chondrocyte-expressed isoforms of

cartilage intermediate-layer protein functions as an insulin-like growth factor 1 antagonist. *Arthritis & Rheumatism*, 48(5) pp. 1302-1314.

Johnstone, B., Alini, M., Cucchiaroni, M., Dodge, G.R., Eglin, D., Guilak, F., Madry, H., Mata, A., Mauck, R.L., Semino, C.E., Stoddart, M.J., 2013. Tissue engineering for articular cartilage repair – the state of the art. *European Cells and Materials*, 25 pp. 248-267.

Jones, G.C., and G.P. Riley. 2005. ADAMTS proteinases: a multi-domain, multi-functional family with roles in extracellular matrix turnover and arthritis. *Arthritis Research and Therapy*, 7 pp. 160-9.

Joosten, L.A., Helsen, M.M., Saxne, T., van De Loo, F.A., Heinegard, D., van Den Berg, W.B., 1999. IL-1 α/β Blockade Prevents Cartilage and Bone Destruction in Murine Type II Collagen-Induced Arthritis, Whereas TNF- α Blockade Only Ameliorates Joint Inflammation. *The Journal of Immunology*, 163 pp. 5049-5055.

Jovanovic, D., Pelletier, J.P., Alaaeddine, N., Mineau, F., Geng, C., Ranger, P., and Martel-Pelletier, J., 1997. Effect of IL-13 on cytokines, cytokine receptors and inhibitors on human osteoarthritis synovium and synovial fibroblasts. *Osteoarthritis and Cartilage*, 6(1) pp. 40-49.

Jovanovic, D.V., Di Battista, J.A., Martel-Pelletier, J., Jolicoeur, F.C., He, Y., Zhang, M., Mineau, F., and Pelletier, J.P., 1998. IL-17 Stimulates the Production and Expression of Proinflammatory Cytokines, IL- β and TNF- α by Human Macrophages. *The Journal of Immunology*, 160 pp. 3513-3521.

Julkunen, P., Wilson, W., Jurvelin, J.S., and Korhonen, R.K., 2009. Composition of the pericellular matrix modulates the deformation behaviour of chondrocytes in articular cartilage under static loading. *Medical and Biological Engineering and Computing*, 47(12) pp. 1281-90.

June, R.K., and Fyhrie, D.P., 2009. Enzymatic digestion of articular cartilage results in viscoelasticity changes that are consistent with polymer dynamics mechanisms. *BioMedical Engineering Online*, 8(32).

Kaneko, S., Satoh, T., Chiba, J., Ju, C., Inoue, K., and Kagawa, J., 2000. Interleukin-6 and interleukin-8 levels in serum and synovial fluid of patients with osteoarthritis. *Cytokines, Cellular & Molecular Therapy*, 6 (2) pp. 71–79.

Kashiwagi, M., Tortorella, M., Nagase, H., Brew, K., 2001. TIMP-3 is a potent inhibitor of aggrecanase-1 (ADAM-TS4) and aggrecanase-2 (ADAM-TS5). *Journal of Biological Chemistry*, 276(16) pp. 12501-12504.

Katta, J., Stapleton, T., Ingham, E., Jin, Z.M., Fisher, J., 2007. Engineering in Medicine The effect of glycosaminoglycan depletion on the friction and deformation of articular cartilage. *Proceedings of the Institution of Mechanical Engineers, Part H: Journal of Engineering in Medicine*, 222(1) pp. 1-11.

Katta, J., Jin, Z., Ingham, E., and Fisher, J., 2009. Chondroitin sulphate: an effective joint lubricant? *Osteoarthritis Cartilage*, 17(8) pp. 1001-8.

Katz, E.P., Wachtel, E.J., Maroudas, A., 1986. Extracellular proteoglycans osmotically regulate the molecular packing of collagen in cartilage. *Biochimica et Biophysica Acta*, 882(1) pp. 136-9.

Keene, D.R., Engvall, E., Glanville, R.W., 1988. Ultrastructure of type VI collagen in human skin and cartilage suggests an anchoring function for this filamentous network. *Journal of Cell Biology*, 107(5) pp. 1995–2006.

Keene, D.R., and Tufa, S. Reichert T.M., *Methods In Cell Biology; Transmission Electron Microscopy of Cartilage and Bone*. 2010

Kheir, E., and Shaw, D., 2009. Hyaline articular cartilage. *Orthopaedics and Trauma*, 23(6) pp. 450–455.

Kiansa, K., Cloutier, J.M., Martel-Pelletier, J., 1999. PGE2 release and on signalling pathways in human OA synovial fibroblasts. *Cytokine*, 11(12) pp. 1020-1030.

Kim, H.A., Cho, M.L., Choi, H.Y., Yoon, C.S., Jhun, J.Y., Oh, H.J., and Kim H.Y., 2006. The catabolic pathway mediated by Toll-like receptors in human osteoarthritic chondrocytes. *Arthritis & Rheumatism*, 54(7) pp. 2152-63.

Kim, K.S., Lee, Y.A., Choi, H.M., Yoo, M.C., and Yang, H.I., 2012. Implication of MMP-9 and urokinase plasminogen activator (uPA) in the activation of pro-matrix metalloproteinase (MMP)-13. *Rheumatology International*, 32(10) pp. 3069-75.

Kishimoto, T., 2006. Interleukin-6: discovery of a pleiotropic cytokine. *Arthritis Research & Therapy*, 8(Suppl 2) S2.

Kleemann, R.U., Krockner, D., Cedraro, A., Tuischer, J., and Duda, G.N., 2005. Altered cartilage mechanics and histology in knee osteoarthritis: relation to clinical assessment (ICRS Grade). *Osteoarthritis and Cartilage*, 13(11) pp. 958-963.

Knauper, V., Wilhelm, S.M., Seperack, P.K., De Clerck, Y.A., Langley K.E., Osthues, A., and Tschesche, H., 1993. Direct activation of human neutrophil procollagenase by recombinant stromelysin. *Biochemical Journal*, 295 pp. 581-586.

Knudson, W., and C.B. Knudson. 1991. Assembly of a Chondrocyte-Like Pericellular Matrix on Non-Chondrogenic Cells - Role of the Cell-Surface Hyaluronan Receptors in the Assembly of a Pericellular Matrix. *Journal of Cell Science*, 99 pp. 227-235.

Knudson, C.B., 1993. Hyaluronan Receptor-Directed Assembly of Chondrocyte Pericellular Matrix. *Journal of Cell Biology*, 120 pp. 825-834.

Koopman, W.J and Moreland, L.W., (2005). *Arthritis and Allied Conditions*. 15th ed. Philadelphia: Lippincott Williams & Wilkins. 2204-2206.

Kuo A.C., Rodrigo, J.J., Reddi, A.H., Curtiss, S., Grotkopp, A.S., and Chiu, M., 2006. Microfracture and bone morphogenetic protein 7 (BMP-7) synergistically stimulate articular cartilage repair. *Osteoarthritis and Cartilage*, 14(11) pp. 1126-1135.

Kuster, M.S., Podsiadlo, P., Stachowiak, G.W., 1998. Shape of wear particles found in human knee joints and their relationship to osteoarthritis. *British Journal of Rheumatology*, 37(9) pp. 978-84.

Kwan, A.P., Cummings, C.E., Chapman, J.A., and Grant, M.E., 1991. Macromolecular organization of chicken type X collagen in vitro. *Journal of Cell Biology*, 114(3) pp. 597-604.

Lampe, A.K., and Bushby, K.M.D., 2005. Collagen VI related muscle disorders. *Journal of medical genetics*, 42 pp. 673-685.

Laupattarakasem, W., Laopaiboon, M., Laupattarakasem, P., Sumananont, C., 2008. Arthroscopic debridement for knee osteoarthritis. *Cochrane Database of Systematic Reviews*, 23(1) pp. CD005118.

Laurent T.C., Laurent U.B.G., and Fraser, J.R.E., 1996. The structure and function of hyaluronan: An overview. *Immunology and Cell Biology*, 74 pp. A1-A7.

Lee, D.W., Banquy, X., and Israelachvili, J.N., 2013. Stick-slip friction and wear of articular joints. *Proceedings of the National Academy of Sciences of the United States of America*, 110(7) pp. E567–E574.

Lee, S-S., Duong, C-T., Park, S-H., Cho, Y., Park, S., and Park, S., 2013. Frictional response of normal and osteoarthritic articular cartilage in human femoral head. *Proceedings of the Institution of Mechanical Engineers, Part H: Journal of Engineering in Medicine*, 227(2) pp. 129-37.

L'Hermette, M.F., Tournay-Chollet, C., Polle, G., and Dujardin, F.H., 2006. Articular Cartilage, Degenerative Process, and Repair: Current Progress. *International Journal of Sports Medicine*, 27 pp. 738-744.

Linn, F.C., and Sokoloff, L., 1965. Movement and composition of interstitial fluid of cartilage. *Arthritis and Rheumatism*, 8(4) pp.481-494.

Liu, Y.E., Wang, M., Greene, J., Su, J., Ullrich, S., Li, H., Shengi, S., Alexander, P., Sang, Q.A., and Shi, Y.E., 1997. Preparation and Characterization of Recombinant Tissue Inhibitor of Metalloproteinase 4 (TIMP-4). *Journal of Biological Chemistry*, 272(33) pp. 20479-20483.

Liu, H., McKenna, L.A., Dean, M.F., 2000. An N-Terminal Peptide from Link Protein Can Stimulate Biosynthesis of Collagen by Human Articular Cartilage. *Archives of Biochemistry and Biophysics*, 378(1), pp. 116–122

Lizhang, J., Fisher, J., Jin, Z., Burton, A., and Williams, S., 2011. The effect of contact stress on cartilage friction, deformation and wear. *Proceedings of the Institute of Mechanical Engineers Part H: engineering in medicine*, 225(5) pp. 461-475.

Loening, A.M., James, I.E., Levenstonc, M.E., Badger, A.M., Frank, E.H., Kurz, B., Nuttall, M.E., Hung, H., Blake, S.M., Grodzinsky, A.J., and Lark, M.W., 2000. Injurious Mechanical Compression of Bovine Articular Cartilage Induces Chondrocyte Apoptosis. *Archives of Biochemistry and Biophysics*, 381(2) pp. 205–212.

Loeser, R.F., Pacione, C.A., and Chubinskaya, S., 2003. The Combination of Insulin-Like Growth Factor 1 and Osteogenic Protein 1 Promotes Increased Survival of and Matrix Synthesis by Normal and Osteoarthritic Human Articular Chondrocytes. *Arthritis & Rheumatism* 48(8) pp. 2188-2196.

Lorenz, H., and W. Richter. 2006. Osteoarthritis: cellular and molecular changes in degenerating cartilage. *Progress in histochemistry and cytochemistry*, 40 pp. 135-63.

Lorenzo, P., Bayliss, M.T., and Heinegård, D., 1998. A novel cartilage protein (CILP) present in the mid-zone of human articulate cartilage increases with age. *Journal of Biological Chemistry*, 273 pp. 23463-23468.

Loulakis, P., Shrikhande, A., Davis, G., and Maniglia, C.A., 1992. N-terminal sequence of proteoglycan fragments isolated from medium of interleukin-1-treated articular-cartilage cultures. Putative site(s) of enzymic cleavage. *Biochemical Journal*, 284(Pt 2) pp. 589-93.

Lotz, M., and Guerne, P.A., 1991. Interleukin-6 induces the synthesis of tissue inhibitor of metalloproteinases-1/erythroid potentiating activity. *Journal of Biological Chemistry*, 266, pp. 2017-20.

Lubberts, E., Joosten, L.A., van de Loo, F.A., van den Gersselaar, L.A., and van den Berg, W.B., 2000. Reduction of interleukin-17-induced inhibition of chondrocyte proteoglycan synthesis in intact murine articular cartilage by interleukin-4. *Arthritis & Rheumatism*, 43(6) pp. 1300-6.

Lufti, A.M., 1975. The bone and joint journal. Morphological changes in the articular cartilage after meniscectomy. *The Bone and Joint Journal (British Volume)*, 57(4) pp. 525-8.

Lukić, I.K., Jelusić-Dražić, M., Kovacić, N., and Grcević, D., 2009. Damage associated molecular patterns- emerging targets for biological therapy of childhood arthritides. *Inflammation and Allergy Drug Targets*. 8(2) pp. 139-45.

Lyyra, T., Arokoski, J.P.A., Oksala, N., Vihko, A., Hyttinen, M., Jurvelin, J.S., and Kiviranta, I., 1999. Experimental validation of arthroscopic cartilage stiffness measurement using enzymatically degraded cartilage samples. *Physics in Medicine and Biology*, (44) pp. 525–535.

Maier, R., Ganun, V., and Lotz, 1993. Interleukin-11, an Inducible Cytokine in Human Articular Chondrocytes and Synoviocytes, Stimulates the Production of the Tissue Inhibitor of Metalloproteinases. *Journal of Biological Chemistry*, 268(29) pp. 21527-21532.

Mankin, H.J., Dorfman, H., Lippiello, L., and Zarins, A., 1971. Biochemical and metabolic abnormalities in articular cartilage from osteo-arthritic human hips. II. Correlation of morphology with biochemical and metabolic data. *Journal of Bone and Joint Surgery American Edition*. 53(3) pp. 523-37.

Mann, H.H., Ozbek, S., Engel, J., Paulsson, M., and Wagener, R., 2004. Interactions between the cartilage oligomeric matrix protein and matrilins. Implications for matrix assembly and the pathogenesis of chondrodysplasias. *Journal of Biological Chemistry*, 279(24) pp. 25294-8.

Marcelino, J., and McDevitt, C.A., 1995. Attachment of articular cartilage chondrocytes to the tissue form of type VI collagen. *Biochimica et Biophysica Acta - Protein Structure and Molecular Enzymology*, 1249(2) pp. 180–188.

March, C.J., Mosley, B., Larsen, A., Cerretti, D.P., Braedt, G., Price, V., Gillis, S., Henney, C.S., Kronheim, S.R., Grabstein, K., Conlon, P.J., Hopp, T.P., and Cosman, D., 1985. Cloning, sequence and expression of two distinct human interleukin-1 complementary DNAs. *Nature*, 315 pp. 641-647.

Maroudas, A., Bayliss, M.T., and Venn, M.F., 1980. Further studies on the composition of human femoral head cartilage. *Annals of the Rheumatic Diseases*, 39 pp. 514-523.

Martel-Pelletier, J., Mineau, F., Jovanovic, D., Di Battista, J.A., Pelletier, J.P., 1999. Mitogen-activated protein kinase and nuclear factor kappaB together regulate interleukin-17-induced nitric oxide production in human osteoarthritic chondrocytes: possible role of transactivating factor mitogen-activated protein kinase-activated protein kinase (MAPKAPK). *Arthritis & Rheumatism*, 42(11) pp. 2399-409.

Marticke, J.K., Hösselbarth, A., Hoffmeier, K.L., Marintschev, I., Otto, S., Lange, M., Plettenberg, H.K.W., Spahn, G., Hofmann, and G.O., 2010. How do visual, spectroscopic and biomechanical changes of cartilage correlate in osteoarthritic knee joints? *Clinical Biomechanics*, 25(4), pp. 332-340.

Martin, J.A and Buckwalter, J.A., 2002. Aging, articular cartilage chondrocyte senescence and osteoarthritis. *Biogerontology*, 3 pp. 257–264.

Matyas, J.R., Adams, M.E., Huang, D., Sandell, L.J., 1997. Major role of collagen IIB in the elevation of total type II procollagen messenger RNA in the hypertrophic phase of experimental osteoarthritis. *Arthritis & Rheumatism*, 40(6) pp. 1046–1049.

McCann, L., Ingham, E., Jin, Z., and Fisher, J., 2009. An investigation of the effect of conformity of knee hemiarthroplasty designs on contact stress, friction and degeneration of articular cartilage: a tribological study. *Journal of Biomechanics*, 42(9) pp. 1326-31.

McCutchen, C. W., 1966. Boundary lubrication by synovial fluid: demonstration and possible osmotic explanation. *Federation Proceedings*, 25 pp. 1061 (1966).

McGloughlin, T. M., and Kavanagh, A.G., 2000. Wear of ultra-high molecular weight polyethylene (UHMWPE) in total knee prostheses: a review of key influences. *Proceedings of the Institution of Mechanical Engineers, Part H: Journal of Engineering in Medicine*, 214 pp. 349-359.

Melrose, J., Fuller, E.S., Roughley, P.J., Smith, M.M., Kerr, B., Hughes, C.E., Caterson, B., and Little, C.B., 2008. Fragmentation of decorin, biglycan, lumican and keratocan is elevated in degenerate human meniscus, knee and hip articular cartilages compared with age-matched macroscopically normal and control tissues. *Arthritis Research & Therapy*, 10(4) R79.

Mendel, K., Eliaz, N., Benhar, I., Hendel, D., and Halperin, N., 2010. Magnetic isolation of particles suspended in synovial fluid for diagnostics of natural joint chondropathies. *Acta Biomaterialia*, 6(11) pp. 4430-8.

Mendler, M., Eich-Bender, S.G., Vaughan, L., Winterhalter, K.H. and Bruckner, P., 1989. Cartilage contains mixed fibrils of collagen types II, IX and XI. *Journal of Cell Biology*, 108 pp. 191-197.

Mengshol, J. A., Vincenti, M.P., Coon, C.I., Barchowsky, A., and Brinckerhoff, C.E., 2000. Interleukin-1 induction of collagenase 3 (Matrix Metalloproteinase 13) Gene Expression in Chondrocytes requires p38, c-JUN N-Terminal Kinase and Nuclear Factor kB. *Arthritis & Rheumatism*, 43(4) pp. 801–811.

Merline, R., Schaefer, R.M., and Schaefer, L., 2009. The matricellular functions of small leucine-rich proteoglycans (SLRPs). *The Journal of Cell Communication and Signaling*, 3 pp. 323–335.

Milner, J.M., Elliott, S.F., and Cawston, T.E., 2001. Activation of procollagenases is a key control point in cartilage collagen degradation: Interaction of serine and metalloproteinase pathways. *Arthritis & Rheumatism*, 44(9) pp. 2084-2096.

Milner, J.M., Rowan, A.D., Elliott, S.F., and Cawston, T.E., 2003. Inhibition of furin-like enzymes blocks interleukin-1 alpha/oncostatin M-stimulated cartilage degradation. *Arthritis & Rheumatism*, 48(4) pp.1057-1066.

Miosge, N., Hartmann, M., Maelicke, C., and Herken, R., 2004. Expression of collagen type I and type II in consecutive stages of human osteoarthritis. *Histochemistry and Cell Biology*, 122 pp. 229-36.

Miosge, N., Waletzko, K., Bode, C., Quondamatteo, F., Schultz, W., and Herken, R., 1998. Light and electron microscopic in-situ hybridization of collagen type I and type II mRNA in the fibrocartilaginous tissue of late-stage osteoarthritis. *Osteoarthritis Cartilage*, 6 pp. 278-85.

Mitchell, P.G., Magna, H.A., Reeves, L.M., Lopresti-Morrow, L.L., Yocum, S.A., Rosner, P.J., Geoghegan, K.F., and Hambor, J.E., 1996. Cloning, expression, and type II collagenolytic activity of matrix metalloproteinase-13 from human osteoarthritic cartilage. *The Journal of Clinical Investigation*, 97(3) pp. 761–768.

Miossec, P., 2004. An update on the cytokine network in rheumatoid arthritis. *Current Opinion in Rheumatology*, 16 pp. 218-222.

Morel, V., and Quinn, T.M., 2004. Cartilage injury by ramp compression near the gel diffusion rate. *Journal of Orthopaedic Research*, 22(1) pp. 145-51.

Morgelin, M., Paulsson, M., Hardingham, T.E., Heinegård, D., and Engel, J., 1988. Cartilage proteoglycans. Assembly with hyaluronate and link protein as studied by electron microscopy. *Biochemical Journal*, 253 pp. 175-185.

Mort, J.S., and Billington, C.J., 2001. Articular cartilage and changes in arthritis Matrix Degradation. *Arthritis Research and Therapy*, 3 pp. 337-341.

Mort, J.S., Dodge, G.R., Roughley, P.J., Liu, J., Finch, S.J., DiPasquale, G., and Poole, A.R., 1993. Direct evidence for active metalloproteinases mediating matrix degradation in interleukin 1 -stimulated human articular cartilage. *Matrix*, 13 pp. 95-102.

Mow, V.C., and Lai, W.M., 1979. Mechanics of animal joints. *Annual Review of Fluid Mechanics*, 11 pp.247-288.

Mow, V.C., , C.C., and Hung, C.T., 1999. The extracellular matrix, interstitial fluid and ions as a mechanical signal transducer in articular cartilage. *Osteoarthritis Cartilage*, 7(1) pp.41-58.

Mow, VC. & Huiskes, R. (2005). *Basic Orthopaedic Biomechanics and Mechano-Biology*. Philadelphia: Lippincott Williams & Wilkins.

Mueller, M.B., and Tuan, R.S., 2011. Anabolic/Catabolic Balance in Pathogenesis of Osteoarthritis: Identifying Molecular Targets. *American Academy of Physical Medicine and Rehabilitation*, 3(6), pp. S3-S11.

Muragaki, Y., Mariman, E.C., van Beersum, S.E., Perälä, M., van Mourik, J.B., Warman, M.L, Olsen, B.R., and Hamel, B.C., 1996. A mutation in the gene encoding the $\alpha 2$ chain of the fibril-associated collagen IX, COL9A2, causes multiple epiphyseal dysplasia (EDM2). *Nature Genetics*, 12 pp.103-105.

Murphy, G., Cockett, M.I., Stephens, P.E., Smith, B.J., and Docherty, A.J., 1987. Stromelysin is an activator of procollagenase A study with natural and recombinant enzymes. *The Biochemical Journal*, 248 pp. 265-268.

Murphy, G., Houbrechts, A., Cockett, M.I., Williamson, R.A., O'Shea, M., and Docherty, A.J., 1991. The N-terminal domain of tissue inhibitor of metalloproteinases retains metalloproteinase inhibitory activity. *Biochemistry*, 30(33) pp. 8097-102.

Murphy, A.N., Unsworth, E.J., and Stetler-Stevenson, W.G., 1993. Tissue inhibitor of metalloproteinases-2 inhibits bFGF-induced human microvascular endothelial cell proliferation. *Journal of Cellular Physiology*, 157 pp. 351-358.

Murphy, G., 2011. Tissue inhibitors of metalloproteinases. *Genome Biology*, 12(11) pp. 233.

Murphy, G., and Lee, M.H., 2005. What are the roles of metalloproteinases in cartilage and bone damage? *Annals of Rheumatic Diseases*, 64 pp. iv44-iv47.

Murphy-Ullrich, J.E., Pallero, M.A., Boerth, N., Greenwood, J.A., Lincoln, T.M., and Cornwell, T.L., 1996. Cyclic GMP-dependent protein kinase is required for thrombospondin and tenascin mediated focal adhesion disassembly. *Journal of Cell Science*, 109(10) pp. 2499-508.

Myllyharju, J., and Kivirikko, K.I., 2001. Collagens and collagen-related diseases. *Annals of Medicine*. 33(1) pp. 7-21.

Naka, M.H., Y. Morita, and K. Ikeuchi. 2005. Influence of proteoglycan contents and of tissue hydration on the frictional characteristics of articular cartilage. *Proceedings of the Institution of Mechanical Engineers Part H-Journal of Engineering in Medicine*. 219 pp. 175-182.

Nakase, T., Miyaji, T., Tomita, T., Kaneko, M., Kuriyama, K., Myoui A., Sugamoto, K., Ochi, T., and Yoshikawa, H., 2003. Localization of bone morphogenetic protein-2 in human osteoarthritic cartilage and osteophyte. *Osteoarthritis and Cartilage*, 11 pp. 278-284.

National institute for Health and Clinical Excellence (NICE) Guidelines. Cartilage injury - autologous chondrocyte implantation (ACI) (review) (TA89). 2005.

National institute for Health and Clinical Excellence (NICE). IPG162 Mosaicplasty for knee cartilage defects - information for the public. 2006.

Nietfeld, J.J., Wilbrink, B., Helle, M., Van Roy, J.L., Den Otter, W., Swaak, A.J., and Huber-Bruning, O., 1990. Interleukin-1-induced interleukin-6 is required for the inhibition of proteoglycan synthesis by interleukin-1 in human articular cartilage. *Arthritis and Rheumatism*, 33(11) pp. 1695-1701.

Newman J.H., 2000. Unicompartmental knee replacement. *The Knee*, 7(2) pp. 63-70.

Nerlich, A.G., Wiest, I., von der Mark, K., 1993. Immunohistochemical analysis of interstitial collagens in cartilage of different stages of osteoarthritis. *Virchows Archive. B, Cell pathology including molecular pathology*, 63(4) pp. 249-55.

Northwood, E., Fisher, J., and Kowalski, R., 2007. Investigation of the friction and surface degradation of innovative chondroplasty materials against articular cartilage. *Proceedings of the Institution of Mechanical Engineers, Part H: Journal of Engineering in Medicine*, 221(3) pp. 263-279.

Nordin, M., and Frankel, V.H., 2001. *Basic Biomechanics of the Musculoskeletal system*. 3rd ed. Philadelphia: Lippincott Williams and Wilkins.

Nugent, A.E., Speicher, D.M., Gradisar, I., McBurney, D.L., Baraga, A., Doane, K.J., and Horton, Jr., W.E., 2009. Advanced Osteoarthritis in Humans Is Associated with Altered Collagen VI Expression and Upregulation of ER-stress Markers Grp78 and Bag-1. *Journal of Histochemistry and Cytochemistry*, 57(10) pp. 923–931.

Okamura, H., Tsutsui, H., Komatsu, T., Yutsudo, M., Hakura, A., Tanimoto, T., Torigoe, K., Okura, T., Nukada, Y., Hattori, K., Akita, K., Namba, M., Tanabe, F., Konishi, K., Fukuda, S., and Kurimoto, M., 1995. Cloning of a new cytokine that induces IFN- γ production by T cells. *Nature*, 378 pp. 88-91.

Olee, T., Hashimoto, S., Quach, J., and Lotz, M., 1999. IL-18 Is Produced by Articular Chondrocytes

and Induces Proinflammatory and Catabolic Responses. *The Journal of Immunology*, 162 pp. 1096-1100.

Orford, C.R., and Gardner, D.L., 1985. Ultrastructural histochemistry of the surface lamina of normal articular cartilage. *Histochemical Journal*, 17(2) pp. 223-33.

Ostergaard, K., Salter, D.M., Andersen, C.B., Petersen, J., and Bendtzen, K., 1997. CD44 expression is up-regulated in the deep zone of osteoarthritic cartilage from human femoral heads. *Histopathology*, 31 pp. 451-9.

Otani, K., Nita, I., Macaulay, W., Georgescu, H.I., Robbins, P.D., and Evans, C.H., 1996. Suppression of antigen-induced arthritis in rabbits by ex vivo gene therapy. *The Journal of Immunology*, 156 pp. 3558-3562.

Outerbridge, R.E., 1961. The Etiology of Chondromalacia Patellae. *Journal of Bone and Joint Surgery*, 43-B pp. 752-757.

Overall, C.M., Wrana, J.L., and Sodek, J., 1989. Independent Regulation of Collagenase, 72-kDa Progelatinase, and Metalloendoproteinase Inhibitor Expression In Human Fibroblasts by Transforming Growth Factor- β . *Journal of Biological Chemistry* 264(3) pp.1860-1869.

Overall, C.M., Wrana, J.L., and Sodek, J., 1991. Transcriptional and Post-transcriptional Regulation of 72-kDa Gelatinase/Type IV Collagenase by Transforming Growth Factor- β I in Human Fibroblasts; comparisons with collagenase and tissue inhibitor of matrix metalloproteinase gene expression. *Journal of Biological Chemistry*. 266(21) pp.14064-14071.

Paasilta, P., Lohiniva, J., Göring, H.H., Perälä, M., Räänä, S.S., Karppinen, J., Hakala, M., Palm, T., Kröger, H., Kaitila, I., Vanharanta, H., Ott, J., and Ala-Kokko, L., 2001. Identification of a novel common genetic risk factor for lumbar disc disease. *The Journal of the American Medical Association*, 285 pp. 1843-1849.

Pan, Y.S, Xiong, D.S, and Ma, R.Y., 2007. A study on the friction properties of poly (vinyl alcohol) hydrogel as articular cartilage against titanium alloy. *Wear* 262 pp. 1021-5.

Papageorgiou, I., Brown, C., Schins, R., Singh, S., Newson, R., Davis, S., Fisher, J., Ingham, E., Case, C.P., 2007. The effect of nano- and micron-sized particles of cobalt–chromium alloy on human fibroblasts in vitro. *Biomaterials*, 28(19) pp. 2946–2958.

Park, S., Nicoll, S.B, Mauck, R.L, Ateshian, G.A., 2008. Cartilage mechanical response under dynamic compression at physiological stress levels following collagenase digestion. *Annals of Biomedical Engineering*, 36(3) pp. 425-34.

Patterson, M.L., Atkinson, S.J., Knäuper, V., and Murphy, G., 2001. Specific collagenolysis by gelatinase A, MMP-2, is determined by the hemopexin domain and not the fibronectin-like domain. *FEBS Letters*, 503 pp. 58-162.

Patwari, P., Fay, J., Cook, M.N., Badger, A.M., Kerin, A.J., Lark, M.W., and Grodzinsky, A.J., 2001. In Vitro Models for Investigation of the Effects of Acute Mechanical Injury on Cartilage. *Clinical Orthopaedics and Related Research*, 391S pp. S61–S71.

Patwari, P., Cook, M.N., DiMicco, M.A., Blake, S.M., James, I.E., Kumar, S., Cole, A.A., Lark, M.W., and Grodzinsky, A.J., 2003. Proteoglycan degradation after injurious compression of bovine and human articular cartilage in vitro: Interaction with exogenous cytokines. *Arthritis & Rheumatism*, 48(5) pp. 1292–1301.

Pawaskar, S.S., Fisher, J., and Jin, Z., 2010. Robust and general method for determining surface fluid flow boundary conditions in articular cartilage contact mechanics modeling. *Journal of Biomechanical Engineering*, 132(3) pp. 031001.

Pei, D., and Weiss, S.J., 1995. Furin dependent intracellular activation of the human stromelysin-3 zymogen. *Nature*, 375 pp.2 44-247.

Peichl, P., Ceska, M., Effenberger, F., Haberhauer, G., Broell, H., and Lindley, I.J., 1991. Presence of NAP-1/IL-8 in Synovial Fluids Indicates a Possible Pathogenic Role in Rheumatoid Arthritis. *Scandinavian Journal of Immunology*, 34(3) pp. 333-339.

Pelletier, J-P., Martel-Pelletier, J., Ghandur-Mnaymneh, L., Howell, J.S., and Frederick Woessner Jr, J., 1985. Role of synovial membrane inflammation in cartilage matrix breakdown in the Pond-Nuki dog model of osteoarthritis. *Arthritis & Rheumatism*, 28(5), pp. 554–561.

Peng, Z., 2007. Osteoarthritis diagnosis using wear particle analysis technique: Investigation of correlation between particle and cartilage surface in walking process. *Wear*, 262(5–6) pp. 630-640.

Peterson, L., Brittberg, M., Kiviranta, I., Åkerlund, E.L., and Lindahl, A., 2002. Autologous Chondrocyte Transplantation Biomechanics and Long-Term Durability. *American Journal of Sports Medicine*, 30(1) pp. 2-12.

Pfaff, M., Aumailley, M., Specks, U., Knolle, J., Zerwes, H.G., Timpl, R., 1993. Integrin and Arg-Gly-Asp Dependence of Cell Adhesion to the Native and Unfolded Triple Helix of Collagen Type VI. *Experimental cell research*, 206(1) pp. 167–176.

Pfander, D., Heinz, N., Rothe, P., Carl, H-D., and Swoboda, B., 2004. Tenascin and aggrecan expression by articular chondrocytes is influenced by interleukin 1b: a possible explanation for the changes in matrix synthesis during osteoarthritis. *Annals of the Rheumatic Diseases*, 63 pp. 240–244.

Pickard, J., Ingham, E., Egan, J., Fisher, J., 1998. Investigation into the effect of proteoglycan molecules on the tribological properties of cartilage joint tissues. *Proceedings of the Institute of Mechanical Engineers Part H: engineering in medicine*, 212(3) pp. 177-82.

Pickard, J., Fisher, J., Ingham, E., Egan, J., Hallett, J., 2000. Investigation into the tribological condition of acetabular tissue after bipolar joint replacement hip surgery. *Proceedings of the Institute of Mechanical Engineers Part H: engineering in medicine*, 214(4) pp. 361-70.

Plumb, M.S., Treon, K., and Aspden, R.M., 2006. Competing regulation of matrix biosynthesis by mechanical and IGF-1 signalling in elderly human articular cartilage in vitro. *Biochimica et Biophysica Acta*, 1760 pp. 762-767.

Podsiadlo, P., Kuster, M., and Stachowiak, G.W., 1997. Numerical analysis of wear particles from non-arthritic and osteoarthritic human knee joints. *Wear*, 210(1–2) pp. 318-325.

Polster, J., and Recht, M., 2005. Postoperative MR evaluation of chondral repair in the knee. *European Journal of Radiology* 54(2) pp. 206-213.

Pond, M.J., and Nuki, G., 1973. Experimentally-induced osteoarthritis in the dog. *Annals of the Rheumatic Diseases*, 32 pp. 387-388.

Poole, C.A., 1997. Articular cartilage chondrons: Form, function and failure. *Journal of Anatomy* 191 pp. 1-13.

Poole, R., 1999. An introduction to the pathophysiology of osteoarthritis. *Frontiers in Bioscience*, 4 pp. d662-670.

Poole, A. R., Rosenberg, L.C., Reiner, A., Ionescu, M., Bogoch, E., and Roughley, P.J., 1996. Contents and Distributions of the Proteoglycans Decorin and Biglycan in Normal and Osteoarthritic Human Articular Cartilage. *Journal of Orthopaedic Research*, 14(5) pp. 681-689.

Poole, A.R., Toshi, K., Tadashi, Y., Fackson, M., Masahiko, K., and Lavery, S., 2001. Composition and Structure of Articular Cartilage: A Template for Tissue Repair. *Clinical Orthopaedics & Related Research*, 391 pp.S26-S33.

Porter, S., Clark, I.M., Kevorkian, L., and Edwards, D.R., 2005. The ADAMTs metalloproteinases. *The Biochemical Journal*, 386 pp. 15-27.

Pritzker, K.P.H., Gay, S., Jimenez, S.A., Ostergaard, K., Pelletier, J.P., Revell, P.A., Salter, D., and van den Berg, W.B., 2006. Osteoarthritis cartilage histopathology: grading and staging. *Osteoarthritis and Cartilage*, 14 pp. 13-29.

Pullig, O., Weseloh, G., and Swoboda, B., 1999. Expression of type VI collagen in normal and osteoarthritic human cartilage. *Osteoarthritis and Cartilage*, 7(2) pp. 191–202.

Quinn, T.M., Allen, R.G., Schalet, B.J., Perumbuli, P., Hunziker, E.B., 2001. Matrix and cell injury due to sub-impact loading of adult bovine articular cartilage explants: effects of strain rate and peak stress. *Journal of Orthopaedic Research*, 19 pp. 242-219.

Ratner, M., 2008. IL-1 trap go-ahead. *Nature Biotechnology*, 26 pp. 485.

Richards, L., Brown, C., Stone, M.H., Fisher, J., Ingham, E., and Tipper, J.L., 2008. Identification of nanometre-sized ultra-high molecular weight polyethylene wear particles in samples retrieved in vivo. *Journal of Bone and Joint Surgery (British Volume)*, 90-B pp. 1106-1113.

Rose, T.M., and Bruce, A.G., 1991. Oncostatin M is a Member of a Cytokine Family that Includes Leukemia-Inhibitory Factor, Granulocyte Colony-Stimulating Factor, and Interleukin-6. *Proceedings of the National Academy of Sciences*, 88(19) pp. 8641-8645.

Roughley, P.J., 2006. The structure and function of cartilage proteoglycans. *European Cells and Materials*, 12 pp. 92-101.

Ryan, M.C., and Sandell, L.J., 1990. Differential expression of a cysteine-rich domain in the amino-terminal propeptide of type II (cartilage) procollagen by alternative splicing of mRNA. *The Journal of Biological Chemistry*, 265 pp. 10334-10339.

Saarakkala, S., Julkunen, P., Kiviranta, P., Mäkitalo, J., Jurvelin, J.S., and Korhonen, R.K., 2010. Depth-wise progression of osteoarthritis in human articular cartilage: investigation of composition, structure and biomechanics. *Osteoarthritis Cartilage*, 18(1) pp. 73-81.

Saha, N., Moldovan, F., Tardif, G., Pelletier, J.P., Cloutier, J.M., and Martel-Pelletier, J., 1999. Localization and Role in the Maturation of Interleukin-1beta and Interleukin-18. *Arthritis & Rheumatism*, 42(8) pp. 1563-1784.

Saklatvala, J., 1986. Tumour necrosis factor stimulates resorption and inhibits synthesis of proteoglycan in cartilage. *Nature* 322 pp.547-9.

Saklatvala, J. Nagase, E. and Salvesen, G. (B)(2003). *Proteases and the Regulation of Biological Processes*. London: Portland Press.

Salminen, H. J., Säämänen, A.M., Vankemmelbeke, M.N., Auho, P.K., Perälä, M.P., Vuorio, E.I., 2002. Differential expression patterns of matrix metalloproteinases and their inhibitors during

development of osteoarthritis in a transgenic mouse model. *Annals of the Rheumatic Diseases*, 61 pp. 591-597.

Sandell, L.J., Morris, N., Robbins, J.R., and Goldring, M.B., 1991. Alternatively Spliced Type 11 Procollagen mRNAs Define Distinct Populations of Cells during Vertebral Development: Differential Expression of the Amino-Propeptide. *The Journal of Cell Biology*, 114(6) pp. 1307-1319.

Sandell, L.J., and T. Aigner. 2001. Articular cartilage and changes in arthritis - An introduction: Cell biology of osteoarthritis. *Arthritis Research*, 3 pp. 107-113.

Sandy, J.D., Flannery, C.R., Neame, P.J., and Lohmander, L.S., 1992. The structure of aggrecan fragments in human synovial fluid. Evidence for the involvement in osteoarthritis of a novel proteinase which cleaves the Glu 373-Ala 374 bond of the interglobular domain. *Journal of Clinical Investigation*, 89 pp. 1512-6.

Santerre, J.P., Woodhouse, K., Laroche, G., and Labrow, R.S., 2005. Understanding the biodegradation of polyurethanes: From classic implants to tissue engineering materials. *Biomaterials*, 26 pp. 7457-7470.

Sato, H., and Takino, T., 2010. Coordinate action of membrane-type matrix metalloproteinase-1 (MT1-MMP) and MMP-2 enhances pericellular proteolysis and invasion. *Cancer Science*, 101 (4) pp. 843-847.

Scanzello, C.R., Plaas, A., and Crow, M.K., 2008. Innate immune system activation in osteoarthritis: is osteoarthritis a chronic wound? *Current Opinion in Rheumatology*, 20(5) pp. 565-72.

Schalkwijk, J., Joosten, L.A., Van Den Berg, W., Van Wyk, J.J., De VanPutte, L.A., 1989. Insulin-like growth factor stimulation of chondrocyte proteoglycan synthesis by human synovial fluid. *Arthritis & Rheumatism*, 32(1), pp. 66 – 71.

Schmid, T.M., R.G. Popp, and Linsenmayer, T.F., 1990. Hypertrophic Cartilage Matrix - Type-X Collagen, Supramolecular Assembly, and Calcification. *Annals of the New York Academy of Sciences*, 580 pp. 64-73.

Schmidt-Rohlfing, B., Gavenis, K., Kippels, M., and Schneider, U., 2002. New potential markers for cartilage degradation of the knee joint. *Scandinavian Journal of Rheumatology*, 31 pp. 151-7.

Schmidt, T.A., Gastelum, N.S., Nguyen, Q.T., Schumacher, B.L., and Sah, R.L., 2007. Boundary Lubrication of Articular Cartilage: Role of Synovial Fluid Constituents. *Arthritis & Rheumatism*, 56(3) pp. 882–891.

Schwarz, I.M., Hills, B.A., 1998. Surface-active phospholipid as the lubricating component of lubricin. *British Journal of Rheumatology*, 37(1) pp. 21-6.

Scott, J.E, and Stockwell, R.A., 2006. Cartilage elasticity resides in shape module decoran and aggrecan sumps of damping fluid: implications in osteoarthritis. *Journal of Physiology*, 574(3) pp. 643-50.

Séguin, C.A., and Bernier, S.M., 2003. TNF α suppresses link protein and type II collagen expression in chondrocytes: Role of MEK1/2 and NF- κ B signaling pathways. *Journal of Cellular Physiology*, 197 pp. 356–369.

Sieving, A., Wu, B., Mayton, L., Nasser, S., Wooley, P.H., 2003. Morphological characteristics of total joint arthroplasty-derived ultra-high molecular weight polyethylene (UHMWPE) wear debris that provoke inflammation in a murine model of inflammation. *Journal of Biomedical Materials Research Part A*, 64A(3) pp. 457–464.

Silver, F.H., Bradica, G and Tria, A., 2001. Viscoelastic behaviour of osteoarthritic cartilage. *Connective tissue research*, 42(3) pp. 223-233.

Sirko-Osadsa, D.A., Murray, M.A., Scott, J.A., Lavery, M.A., Warman, M.L., and Robin, N.H., 1998. Stickler syndrome without eye involvement is caused by mutations in COL11A2, the gene encoding the α_2 (XI) chain of type XI collagen. *The Journal of Pediatrics*, 132(2) pp. 368-371.

Skaalure, S.C., Milligan, I.L., and Bryant, S.J., 2012. Age impacts extracellular matrix metabolism in chondrocytes encapsulated in degradable hydrogels. *Journal of Biomedical Materials*, 7(2) pp. 024111.

Smith, R.J., Chin, J.E., Sam, L.M., and Justen, J.M., 1991. Biologic effects of an interleukin-1 receptor antagonist protein on interleukin-1-stimulated cartilage erosion and chondrocyte responsiveness. *Arthritis and Rheumatism*, 34(1) pp. 78-83.

Smith, R.L., Carter, D.R., and Schurman, D.J., 2004. Pressure and Shear Differentially Alter Human Articular Chondrocyte Metabolism. *Clinical Orthopaedics and Related Research*, 427S, pp. S89–S95.

Smith, M.M., Little, C.B., Moskowitz, R.W., Altman, R.D., Hochberg, M.C., Buckwalter, J.A., Goldberg, V.M. Experimental models of osteoarthritis. In: osteoarthritis. Diagnosis and Medical/Surgical Management. fourth Edition. Philadelphia, London, New York, St. Louis, Sydney, Toronto: WB Saunders Company; 2007, pp. 107-125.

Söder, S., Hambach, L., Lissner, R., Kirchner, T., and Aigner, T., 2002. Ultrastructural localization of type VI collagen in normal adult and osteoarthritic human articular cartilage. *Osteoarthritis Cartilage*, 10(6) pp. 464-70.

Solovieva, S., Lohiniva, J., Leino-Arjas, P., Raininko, R., Luoma, K., Ala-Kokko, L., and Riihimäki, H., 2002. COL9A3 gene polymorphism and obesity in intervertebral disc degeneration of the lumbar spine: evidence of gene-environment interaction. *Spine*, 27 pp. 2692-2696.

Song, S.Y., Han, Y.D., Hong, S.Y., Kim, K., Yang, S.S., Min, B.H., and Yoon, H.C., 2012. Chip-based cartilage oligomeric matrix protein detection in serum and synovial fluid for osteoarthritis diagnosis. *Analytical Biochemistry*, 420(2) pp. 139-46.

Stachowiak, G.W., and Podsiadlo, P., 1997. Analysis of wear particle boundaries found in sheep knee joints during in vitro wear tests without muscle compensation. *Journal of Biomechanics*, 30(4), pp. 415-419.

Stachowiak, G.P., Stachowiak, G.W., and Podsiadlo, P., 2006. Automated classification of articular cartilage surfaces based on surface texture. *Proceedings of the Institution of Mechanical Engineers, Part H: Journal of Engineering in Medicine*, 220(8) pp. 831-43.

Stanton, H., and Fosang, A.J., 2002. Matrix metalloproteinases are active following guanidine hydrochloride extraction of cartilage: generation of DIPEN neoepitope during dialysis. *Matrix Biology*, 21(5), pp. 425–428.

Sternlicht, M. D., and Werb, Z., 2001. How matrix metalloproteinases regulate cell behaviour. *Annual Review of Cell and Developmental Biology*, 17 pp. 463–516.

Stolz, M., Raiteri, R., Daniels, A.U., VanLandingham, M.R., Baschong, W., and Aebi, U., 2004. Dynamic Elastic Modulus of Porcine Articular Cartilage Determined at Two Different Levels of Tissue Organization by Indentation-Type Atomic Force Microscopy. *Biophysical Journal*, 86(5) pp. 3269–3283.

Sugiyama, E., Kuroda, A., Taki, H., Ikemoto, M., Hori, T., Yamashita, N., Maruyama, M., and Kobayashi, M., 1995. Interleukin 10 cooperates with interleukin 4 to suppress inflammatory cytokine production by freshly prepared adherent rheumatoid synovial cells. *Journal of Rheumatology*, 22(11) pp. 2020-6.

Sui, Y., Lee, J.H., DiMicco, M.A., Vanderploeg, E.J., Blake, S.M., Hung, H.H., Plaas, A.H., James, I.E., Song, X.Y., Lark, M.W., Grodzinsky, A.J., 2009. Mechanical injury potentiates proteoglycan catabolism induced by interleukin-6 with soluble interleukin-6 receptor and tumor necrosis factor alpha in immature bovine and adult human articular cartilage. *Arthritis and Rheumatism*, 60(10) pp. 2985-96.

Sumer, E.U., Sondergaard, B.C., Madsen, S.H., Qvist, P., and Karsdal, M.A., 2006. Interleukin-1-alpha in comparison to interleukin-1-beta is a more potent stimulator of aggrecanase mediated aggrecan degradation in human articular cartilage. *Osteoarthritis and Cartilage*, 14 (supplement 2) pp. S58.

Svensson, L., Aszodi, A., Reinholt, F.P., Fassler, R., Heinegard, D., and Oldberg, A., 1999. Fibromodulin-null mice have abnormal collagen fibrils, tissue organization, and altered lumican deposition in tendon. *Journal of Biological Chemistry*, 274 pp. 9636–9647.

Swann, D.A., Slayter, H.S., and Silver, F.H., 1981. The molecular structure of lubricating glycoprotein-I, the boundary lubricant for articular cartilage. *Journal of Biological Chemistry*, 256(11) pp. 5921-5.

Tanaka, E., Iwabe, T., Dalla-Bona, D.A., Kawai, N., van Eijden, T., Tanaka, M., Kitagawa, S., Takata, T., and Tanne, K., 2005. The effect of experimental cartilage damage and impairment and restoration of synovial lubrication on friction in the temporomandibular joint. *Journal of Orofacial Pain*. 19(4) pp. 331-6.

Tardif, G., Reboul, P., Pelletier, J.P., Geng, C., Cloutier, J.M., Martel Pelletier, J., 1996. Normal expression of type 1 insulin-like growth factor receptor by human osteoarthritic chondrocytes with increased expression and synthesis of insulin like growth factor binding proteins. *Arthritis & Rheumatism*, 39 pp. 968-978.

Tardif, G., Pelletier, J.P., Dupuis, M., Geng, M., Cloutier, J.M., and Martel-Pelletier, J., 1999. Collagenase 3 production by human osteoarthritic chondrocytes in response to growth factors and cytokines is a function of the physiologic state of the cells. *Arthritis & Rheumatism*, 42(6), pp. 1147-1158.

Taskiran, D., Stefanovicracic, M., Georgescu, H., and Evans, C., 1994. Nitric-Oxide Mediates Suppression of Cartilage Proteoglycan Synthesis by Interleukin-1. *Biochemical and Biophysical Research Communications*, 200(1) pp. 142-148.

Teeple, E., Fleming, B.C., Mechrefe, A.P., Crisco, J.J., Brady, M.F., and Jay, G.D., 2007. Frictional properties of Hartley guinea pig knees with and without proteolytic disruption of the articular surfaces. *Osteoarthritis and cartilage*, 15 pp. 309-15.

Temple-Wong, M.M., W.C. Bae, M.Q. Chen, W.D. Bugbee, D. Amiel, R.D. Coutts, M. Lotz, and R.L. Sah. 2009. Biomechanical, structural, and biochemical indices of degenerative and osteoarthritic deterioration of adult human articular cartilage of the femoral condyle. *Osteoarthritis and Cartilage*, 17 pp. 1469-1476.

Tesche, F., and Miosge N., 2004. Perlecan in late stages of osteoarthritis of the human knee joint. *Osteoarthritis Cartilage*, 12(11) pp. 852-62.

Tetlow, L.C., Adlam, D.J., and Woolley, D.E., 2001. Matrix Metalloproteinase and Proinflammatory Cytokine Production by Chondrocytes of Human Osteoarthritic Cartilage Associations With Degenerative Changes. *Arthritis & Rheumatism*, 44(3) pp. 585–594.

Thambyah, A., Goh, J.C., and De, S.D., 2005. Contact stresses in the knee joint in deep flexion. *Medical Engineering and Physics*, 27(4) pp.329-35.

Thibault, M., Poole, A.R., and Buschmann, M.D., 2002. Cyclic compression of cartilage bone explants in vitro leads to physical weakening, mechanical breakdown of collagen and release of matrix fragments. *Journal of Orthopaedic Research*, 20 pp. 1265-1273.

Thompson Jr, R.C., and Oegema, Jr, T.R., 1979. Metabolic activity of articular cartilage in osteoarthritis. An in vitro study. *The Journal of Bone and Joint Surgery; American Volume*, 61(3) pp. 407-416.

Thompson, A., 1998a. *The Cytokine Handbook*. 3rd ed. London: Academic Press Ltd.

Thur, J., Rosenberg, K., Nitsche, D.P., Pihlajamaa, T., Ala-Kokko, L., Heinegård, D., Paulsson, M., and Maurer, P., 2001. Mutations in cartilage oligomeric matrix protein causing pseudoachondroplasia and multiple epiphyseal dysplasia affect binding of calcium and collagen I, II, and IX. *Journal of Biological Chemistry*, 276(9) pp. 6083-92.

Tian, Y., Wang, J., Peng, Z., Jiang, X., 2011. Numerical analysis of cartilage surfaces for osteoarthritis diagnosis using field and feature parameters. *Wear*, 271(9–10), pp. 2370-2378.

Tian., Y., Wang, J., Peng, Z., and Jiang, X., 2012. A new approach to numerical characterisation of wear particle surfaces in three-dimensions for wear study. *Wear*, 282-283 pp. 59-68.

Tilwani, R.K., Bader D.L., and Chowdhury, T.T., 2012. Biomechanical Conditioning Enhanced Matrix Synthesis in Nucleus Pulposus Cells Cultured in Agarose Constructs with TGF β . *Journal of Functional Biomaterials*, 3(1) pp. 23-36

Tipper, J.L., Ingham, E., Hailey, J.L., Besong, A.A., Fisher, J., Wroblewski, B.M., and Stone, M.H., 2000. Quantitative analysis of polyethylene wear debris, wear rate and head damage in retrieved Charnley hip prostheses. *Journal of Materials Science: Materials in Medicine*, 11(2) pp. 117-124.

Tipper, J.L., Galvin, A.L., Williams, S., McEwen, H.M.J., Stone, M.H., Ingham, E., and Fisher, J., 2006. Isolation and characterization of UHMWPE wear particles down to ten nanometers in size from in vitro hip and knee joint simulators. *Journal of Biomedical Materials Research Part A*, 78A(3), pp. 473–480.

Tortorella, M.D., Pratta, M., Liu, R.Q., Austin, J., Ross, H., Abbaszade, I., Burn, T., and Arner, E., 2000. Sites of Aggrecan Cleavage by Recombinant Human Aggrecanase-1 (ADAMTS-4). *Journal of Biological Chemistry*, 275 pp. 18566-18573.

Tortorella, M.D., Malfait, A.M., Deccico, C., and Arner, E., 2001. The role of ADAM-TS4 (aggrecanase-1) and ADAM-TS5 (aggrecanase-2) in a model of cartilage degradation. *Osteoarthritis and Cartilage*, 9 pp. 539–552.

Torzilli, P.A., 1988. Water content and equilibrium water partition in immature cartilage. *Journal of Orthopaedic Research*, 6(5) pp.766-769.

Trowbridge, J.M., and R.L. Gallo. 2002. Dermatan sulfate: new functions from an old glycosaminoglycan. *Glycobiology*, 12 pp. 117r-125r.

Tyler, J.A., 1989. Insulin-like growth factor 1 can decrease degradation and promote synthesis of proteoglycan in cartilage exposed to cytokines. *Biochemical Journal*, 260 pp. 543-548.

Upadhyay, A., Sharma, G., Kivivuori, S., Raye, W.S., Zabihi, E., Carroll, G.J., and Jazayeri, J.A., 2009. Role of a LIF antagonist in LIF and OSM induced MMP-1, MMP-3, and TIMP-1 expression by primary articular chondrocytes. *Cytokine*, 46(3) pp. 332-338.

Van Beuningen, H.M., Glansbeek, H.L., van der Kraan, P.M., and van den Berg, W.B., 2000. Osteoarthritis-like changes in the murine knee joint resulting from intra-articular transforming growth factor- β injections. *Osteoarthritis and Cartilage*, 8(1), pp. 25-33.

Van de Loo, F.A., Kuiper, S., van Enkevort, F.H., Arntz, O.J., and van den Berg, W.B., 1997. Interleukin-6 reduces cartilage destruction during experimental arthritis. A study in interleukin-6-deficient mice. *American Journal of Pathology*, 151(1) pp. 177-91.

Van den Berg, W., 1999. The role of cytokines and growth factors in cartilage destruction in osteoarthritis and rheumatoid arthritis. *Zeitschrift für Rheumatologie*, 58 pp.136-141.

van der Kraan, P.M., Blaney Davidson, E.N., and van den Berg, W.B., 2010. Bone morphogenetic proteins and articular cartilage: To serve and protect or a wolf in sheep clothing's? *Osteoarthritis Cartilage*, 18(6) pp. 735-41.

Vankemmelbeke, M., 1998. Characterization of helical cleavages in type II collagen generated by Matrixins. *Biochemical Journal*, 330, pp. 633-640.

Van Roon, J.A., van Roy, J.L., Duits, A., Lafeber, F.P., and Bijlsma, J.W. , 1995. Proinflammatory cytokine production and cartilage damage due to rheumatoid synovial T helper-1 activation is inhibited by interleukin-4. *Annals of Rheumatic Diseases*, 54 pp. 836-840.

Vaughan, L., Mendler, M., Huber, S., Bruckner, P., Winterhalter, K.H., Irwin, M.I., and Mayne, R., 1988. D-periodic distribution of collagen type IX along cartilage fibrils. *The Journal of Cell Biology*, 106(3) pp. 991-997.

Veje, K., Hyllested-Winge, J.L., and Ostergaard, K., 2003. Topographic and zonal distribution of tenascin in human articular cartilage from femoral heads: normal versus mild and severe osteoarthritis. *Osteoarthritis Cartilage*, 11 pp. 217-27.

Vikkula, M., Mariman, E.C., Lui, V.C., Zhidkova, N.I., Tiller, G.E., Goldring, M.B., van Beersum, S.E., de Waal Malefit, M.C., van den Hoogen, F.H., Ropers, H.H., Mayne. R., Cheah, K.S., Olsen, B.R., Warman, M.L., and Brunner, H.G., 1995. Autosomal dominant and recessive osteochondrodysplasias associated with the COL11A2 locus. *Cell*, 80 pp. 431-437.

Villiger, P.M., Geng, Y., and Lotz, M., 1993. Induction of cytokine expression by leukemia inhibitory factor." *The Journal of Clinical Investigation*, 91(4) pp. 1575–1581.

Volck, B., Ostergaard, K., Johansen, J.S., Garbarsch, C., and Price, P.A., 1999. The distribution of YKL-40 in osteoarthritic and normal human articular cartilage. *Scandanavian Journal of Rheumatology*, 28 pp. 171-9.

Wagener, R., Harald, W.A., Ehlen, Ko, Y.P., Kobbe, B., Mann, H.H., Sengle, G., and Paulsson, M., 2005. The matrilins – adaptor proteins in the extracellular matrix. *Febs Letters*, 579(15), pp. 3323-3329.

Wang, M., Liu, Y.E., Greene, J., Sheng, S., Fuchs, A., Rosen, E.M., and Shi, Y.E., 1997. Inhibition of tumor growth and metastasis of human breast cancer cells transfected with tissue inhibitor of metalloproteinase 4. *Oncogene*, 14 pp. 2767-2774.

Wang, J., Verdonk, P., Elewaut, D., Veys, E.M., and Verbruggen, G., 2003. Homeostasis of the extracellular matrix of normal and osteoarthritic human articular cartilage chondrocytes in vitro. *Osteoarthritis Cartilage*, 11(11) pp. 801-9.

Wang, M., Peng, Z., Watson, J.A., Watson, G.S., and Yin, L., 2012. Nanoscale study of cartilage surfaces using atomic force microscopy. *Proceedings of the Institution of Mechanical Engineers, Part H: Journal of Engineering in Medicine*. 226 pp. 899-910.

Wang, M., Peng, Z., Vasilev, K., and Ketheesan, N., 2013. Investigation of Wear Particles Generated in Human Knee Joints Using Atomic Force Microscopy. *Tribology Letters*, 51(1) pp. 161-170.

Watanabe, H., Cheung, S.C., Itano, N., Kimata, K., and Yamada, Y., 1997. Identification of Hyaluronan-binding Domains of Aggrecan. *The Journal of Biological Chemistry*, 272 pp. 28057-28065.

Wen, C-Y., Wu, C-B., Tang, B., Wang, T., Yan, C-H., Lu, W.W., Pan, H., Hu, Y., Chiu, K-Y., 2012. Collagen fibril stiffening in osteoarthritic cartilage of human beings revealed by atomic force microscopy. *Osteoarthritis and Cartilage*, 20(8) pp. 916–922.

Westling, J., Fosang, A.J., Last, K., Thompson, V.P., Tomkinson, K.N., Hebert, T., McDonagh, T., Collins-Racie, L.A., LaVallie, E.R., Morris, E.A., and Sandy, J.D., 2002. ADAMTS4 Cleaves at the Aggrecanase Site (Glu³⁷³-Ala³⁷⁴) and Secondarily at the Matrix Metalloproteinase Site (Asn³⁴¹-Phe³⁴²) in the Aggrecan Interglobular Domain. *The Journal of Biological Chemistry*, 277 pp. 16059-16066.

Wiberg, C., Heinegård, D., Wenglén, C., Timpl, R., and Mörgelin, M., 2002. Biglycan Organizes

Collagen VI into Hexagonal-like Networks Resembling Tissue Structures. *The Journal of Biological Chemistry*, 277 pp. 49120-49126.

Wiberg, C., Klatt, A.R., Wagener, R., Paulsson, M., Bateman, J.F., Heinegård, D., and Mörgelin, M., 2003. Complexes of Matrilin-1 and Biglycan or Decorin Connect Collagen VI Microfibrils to Both Collagen II and Aggrecan. *The Journal of Biological Chemistry*, 278 pp. 37698-37704.

Williams, R.O., Marinova-Mutafchieva, L., Feldmann, M., and Maini, R.N., 2000. Evaluation of TNF-alpha and IL-1 Blockade in Collagen-Induced Arthritis and Comparison with Combined Anti-TNF-alpha/Anti-CD4 Therapy. *The Journal of Immunology*, 165 pp. 7240-7245.

Wilson, W., van Burken, C., van Donkelaar, C., Buma, P., van Rietbergen, B., and Huiskes, R., 2006. Causes of Mechanically Induced Collagen Damage in Articular Cartilage. *Journal of Orthopaedic Research*, 24(2), pp. 220–228.

Wilson, R., Diseberg, A.F., Gordon, L., Zivkovic, S., Tatarczuch, L., Mackie, E.J., Gorman, J.J., and Bateman, J.F., 2010. Comprehensive Profiling of Cartilage Extracellular Matrix Formation and Maturation Using Sequential Extraction and Label-free Quantitative Proteomics. *Molecular & Cellular Proteomics*, 9 pp. 1296-1313.

Wong, B.L., Bae, W.C., Chun, J., Gratz, K.R., Lotz, M., and Sah, R.L., 2008. Biomechanics of Cartilage Articulation. Effects of Lubrication and Degeneration on Shear Deformation. *Arthritis & Rheumatism*, 58(7), pp. 2065–2074.

Wong, B.L., and Sah, R.L., 2010. Effect of a focal articular defect on cartilage deformation during patello-femoral articulation. *Journal of Orthopaedic Research*. 28(12), pp. 1554–1561.

Wu, J. Z. and Herzog, W., 2002. Elastic anisotropy of articular cartilage is associated with the microstructures of collagen fibers and chondrocytes. *Journal of Biomechanics* 35(7) pp. 931-942.

Xiao, Y.T., Xiang, L.X., and Shao, J.Z., 2007. Bone morphogenetic protein. *Biochemical and Biophysical Research Communications*, 362(3), pp. 550-555

Yamagata, T., Saito, H., Habuchi, O., and Suzuki, S., 1968. Purification and Properties of Bacterial Chondroitinases and Chondrosulfatases. *The Journal of Biological Chemistry*, (243) pp. 1523-1535.

Yamaguchi, Y., Mann, D.M. and Ruoslahti, E., 1990. Negative regulation of transforming growth factor-beta by the proteoglycan decorin. *Nature*, 346 pp. 281-284.

Yasuda, T., Tchetina, E., Ohsawa, K., Roughley, P.J., Wu, W., Mousa, A., Ionescu, M., Pidoux, I., and Poole, A.R., 2006. Peptides of type II collagen can induce the cleavage of type II collagen and aggrecan in articular cartilage. *Matrix Biology*, 25 pp. 419-29.

Yoshida, H., Faust, A., Wilckens J., Kitagawa, M., Fetto, J., Chaoa, E, Y, S, 2006. Three-dimensional dynamic hip contact area and pressure distribution during activities of daily living. *Journal of Biomechanics*, 39(11) pp. 1996–2004.

Yu, W.H., Yu, S., Meng, Q., Brew, K., and Woessner J.F. Jr., 2000. TIMP-3 Binds to Sulphated Glycosaminoglycans of the Extracellular Matrix. *The Journal of Biological Chemistry*, 275(40) pp. 31226–31232.

Zafarullah, M., and Su, S., 1996. Tissue Inhibitor of Metalloproteinase-2 (TIMP-2) mRNA Is Constitutively Expressed in Bovine, Human Normal, and Osteoarthritic Articular Chondrocytes. *Journal of Cellular Biochemistry*, 60 pp. 211-217.

Zhang, D., Johnson, L.J., Hsu, H.P., and Spector, M., 2007. Cartilaginous deposits in subchondral bone in regions of exposed bone in osteoarthritis of the human knee: histomorphometric study of PRG4 distribution in osteoarthritic cartilage. *Journal of Orthopaedic Research*, 25 pp. 873-83.

Zwerina, J., Redlich, K., Polzer, K., Joosten, L., Kroenke, G., Distler, J., Hess, A., Pundt, N., Pap, T., Hoffmann, O., Gasser, J., Scheinecker, C., Smolen, J.S., Van Den Berg, W., and Schett, G., 2007. TNF-induced structural joint damage is mediated by IL-1. *Proceedings of the National Academy of Sciences*, 104(28) pp. 11742–11747.

